Dynamic Analysis of Actin Protrusion Assembly and Function During *Drosophila* Dorsal Closure

Sarah Woolner

A Thesis Submitted for the Degree of

Doctor of Philosophy

University of London

2005

Department of Anatomy and Developmental Biology

University College London

ProQuest LLC
789 East Eisenhower Parkway
P.O. Box 1346
Ann Arbor, MI 48106-1346

Abstract

The coordinated migration and fusion of epithelial sheets is employed on numerous occasions to shape the developing embryo and to repair tissues as part of the wound healing response. The morphogenetic episode of dorsal closure, whereby a large hole in the dorsal epithelium of the *Drosophila* embryo is drawn closed, provides a powerful model for the study of such cell movements because of its amenability to live imaging and the outstanding genetic tractability of *Drosophila.*

During dorsal closure, the leading edge epithelial cells surrounding the hole extend dynamic actin protrusions – filopodia and lamellipodia – which reach across the exposed amnioserosa layer and help to zip the epithelial edges together. In this thesis I have employed live imaging to investigate the assembly of these protrusions and to explore their roles during the closure process. I have carried out a detailed live analysis of wild type dorsal closure, which has provided a valuable staging framework with which to compare defective closure in mutant embryos. To begin to understand more about how actin protrusions are assembled by the epithelial leading edge, I have investigated the function of the small GTPase, Rac, by ectopic expression of constitutively active and dominant negative forms of *Rac1* and also using a triple *Rac* loss-of-function mutant.

The phenotypes I see in *Rac* mutant cells, where assembly of actin protrusions is either increased or reduced from wild type levels, suggest three roles for the actin protrusions during dorsal closure. Two of these are sensory, enabling leading edge cells to "find" their correct partner on the opposing epithelium, and to "read" contact inhibition cues once the two edges have met. The third is to function in priming cell-cell adhesion events as the two epithelial surfaces fuse. To begin to assess how the filopodia may fulfil these functions I have focused on a subset of unconventional myosins, which in other systems have been found to localise to filopodial tips. I show that one such myosin, Myo10A, localises to the tips of filopodia in cultured *Drosophila* cells, whilst its knockdown by RNA interference leads to intriguing dorsal closure defects, including segmental mismatching along the midline seam.

Table of Contents

Accompanying CD attached to back cover

Table of Figures

Commonly Used Abbreviations

AEL	After egg laying
bsk	*basket* – encodes *Drosophila* JNK
cDNA	Complementary deoxyribonucleic acid
Ck	Crinkled – *Drosophila* Myosin VIIa
DIG	Digoxigenin
DNA	Deoxyribonuceic acid
Dpp	Decapentaplegic
dsRNA	Double stranded ribonucleic acid
FERM	"Band 4.1, Ezrin, Radixin, Moesin" domain
FGF	Fibroblast growth factor
GFP	Green fluorescent protein
GTPase	Guanosine triphosphatase
hep	*hempiterous* – encodes *Drosophila* JNKK
Hep^{CA}	Constitutively active *Drosophila hemipterous*
JNK	Jun N-terminal kinase
Mad	*Mothers against dpp*
MAPK	Mitogen-activated protein kinase
mbc	*myoblast city* – encodes *Drosophila* DOCK180
Med	*Medea*
mRNA	Messenger ribonucleic acid
msn	*misshapen*
Myo10A	Myosin 10A – *Drosophila* Myosin XV
Myo28B1	Myosin 28B1 – *Drosophila* Myosin VIIb
MyTH4	"Myosin Tail Homology 4" domain
PAK	p21 activated kinase
PCR	Polymerase chain reaction
PI3K	Phosphoinositide 3-kinase
PIP_2	Phosphoinositide-4,5-biphosphate
PIP_3	Phosphoinositide-3,4,5-triphosphate
Pkn	*Drosophila* "protein kinase related to protein kinase N"
puc	*puckered*
put	*punt*
$Rac1^{N17}$	Dominant negative *Drosophila Rac1*
$Rac1^{V12}$	Constitutively active *Drosophila Rac1*
Rac^{J10}	Hypomorphic triple *Rac* mutant: $Rac1^{J10}$, *Rac2Δ, MtlΔ*
Rac^{J11}	Triple *Rac* mutant: $Rac1^{J11}$, *Rac2Δ, MtlΔ*
RNA	Ribonucleic acid
RNAi	Ribonucleic acid interference
SEM	Scanning electron microscopy
slpr	*slipper* – encodes *Drosophila* JNKKK
TEM	Transmission electron microscopy
tkv	*thickvein*
TGFβ	Transforming growth factor beta

Acknowledgements

First and foremost I'd like to say a huge thank-you to my supervisor, Paul Martin. He's been a fantastic boss, constantly supportive and enthusiastic, and has made my PhD a fun and fulfilling experience. I'd also like to thank all the members of the Martin Lab, past and present, for being such wonderful friends and colleagues; particular thanks to Antonio, who got me started on dorsal closure and taught me so much in a short time; Will, my fellow fly person at UCL and Brian, who has done an amazing job at getting the fly lab functioning in Bristol. Also thanks to Brian, Tom and Shirin for sparing their time to proof read parts of this thesis. Whilst in Bristol I've also received a great deal of support from Kate Nobes and her lab, and I'm really grateful for this.

There have been numerous occasions during my PhD when I've needed technical support and two people have been especially helpful: Mark Turmaine, in the UCL Anatomy EM suite, who taught me everything I needed to know about SEM and Sérgio Simões in the Jacinto lab, at the IMM in Lisbon, who helped me to get some lovely *dpp in situs*.

My PhD was based at the MRC LMCB, and I'd like to thank everyone involved in the Graduate programme there for running such an excellent course that I am very proud to have been a part of. Special thanks to my committee members at the LMCB: Stephen Nurrish, Nathalie Franc and Louise Cramer, who have offered me superb guidance and advice. I'd also like to thank my course-mates, Sarah, Charly, Tim and Ann for being such good friends right from the outset. Also, many thanks to the Medical Research Council, who funded this work.

During my PhD, I was fortunate enough to have the opportunity to spend some time in Susan Parkhurst's lab at the Fred Hutchinson Cancer Research Center in Seattle. I want to thank Susan for welcoming me into her lab and for teaching me so much, I am very grateful for all the wonderful opportunities she gave me. Also, thanks to Alicia, Craig and James in the Parkhurst lab for all their help, advice and friendship. The Hutch is an exceptionally friendly place, and I'd just like to thank everyone there who made me feel so at home and looked after me during stressful times.

Finally, I'd like to thank all my friends and family, whom I have neglected even more than usual whilst writing this thesis. In particular, I want to thank my Mum and Dad for just being the best parents ever.

CHAPTER 1

General Introduction

The development of any embryo is characterised by the sculpting, morphogenetic tissue movements that are used to shape it. One such event in *Drosophila* embryogenesis is dorsal closure, which involves the sealing of a large hole in the dorsal epidermis of the embryo. As this morphogenetic episode happens superficially, rather than deep within the embryo, it provides a powerful paradigm with which to study the cell biology and genetics of morphogenesis, allowing the amazing genetic tractability of *Drosophila* to be combined with dynamic live imaging. Dorsal closure also provides a bounty of key cellular behaviours which can be assessed *in vivo* during the process; including cell contractions, shape changes and the use of actin based protrusions to sense and seal two epithelial sheets together. Moreover, the cellular mechanisms underlying the movements involved in dorsal closure bear startling similarities with those used to heal wounds in embryonic and adult tissue, allowing us to learn more about the crucial process of tissue repair from the study of this morphogenetic episode (Jacinto et al., 2001).

1.1 SHAPING A DROSOPHILA EMBRYO

1.1.1 *Drosophila* embryonic development is punctuated by morphogenetic events

At the time of laying, a *Drosophila* egg is essentially a sack of cytoplasm contained and protected within two extra-embryonic cell layers, the vitelline membrane and the chorion. Over the course of about 14 hours (at 25°C) this "sack of cytoplasm" develops into a complex multicellular organism – the *Drosophila* larvae. *Drosophila* embryonic development, although fast, involves many co-ordinated events whose study provides us with enormous insight into the cell biology and genetics of the crucial developmental processes which generate an organism.

Drosophila embryogenesis begins with cleavage, in which the fertilised egg undergoes a series of 13 highly synchronous nuclear divisions, a process that takes just over 2

hours to complete at 25°C (Hartenstein, 1993; Weigmann et al., 2003). At this point the early embryo consists of a syncytial blastoderm of uncellularized nuclei, which congregate in a single layer at the surface of the egg. During the next phase of embryogenesis – cellularisation – miniature curtains of plasma membrane drop down from the outer membrane of the embryo to create pockets that will ultimately encapsulate each nucleus and give rise to an epithelial sheet of cells from which the embryo will develop.

Soon after cellularisation is complete, about 3 hours after egg laying (AEL, at 25°C), the embryo undergoes a series of shaping, morphogenetic events, tissue movements that are driven by cell shape changes, which in turn are largely dependent on reorganisation of the actin cytoskeleton. Morphogenesis initiates with gastrulation, whereby a subset of cells along the ventral midline of the embryo undergo a concerted constriction of their apical surfaces, leading to a local invagination of the epithelium called the "ventral furrow". As a consequence of this infolding, a patch of cells, which will later become the embryonic mesoderm, is internalised and coats the inside surface of the embryo. Beginning at about 3.5 hours AEL, the embryo is further sculpted by a back-to-back pair of morphogenetic events called germ-band extension and retraction (Hartenstein, 1993; Weigmann et al., 2003). During germ-band extension the presumptive germ-band is pushed along the dorsal side of the embryo towards the anterior end. Once it approaches the head, the germ-band goes into reverse and is drawn back to its ultimate position at the posterior of the embryo. The retraction of the germ-band leaves a large hole in the dorsal epidermis of the embryo and this hole is sealed closed by the next morphogenetic event in *Drosophila* embryogenesis, dorsal closure (see Figure 1.1).

1.1.2 Dorsal closure involves the co-ordinated efforts of three groups of cells

Dorsal closure is one of the final tissue movements in the development of the *Drosophila* embryo, but its proper completion is required for the embryo to hatch into a larvae (reviewed in Harden, 2002; Jacinto et al., 2002b). The process begins at about 10 hours AEL, just as the germ band reaches its position at the posterior, and takes around 2-3 hours to complete at room temperature. The hole left by germ-band retraction is elliptical or "eye-shaped" and its closure proceeds from the most anterior and posterior ends (or canthi) towards the centre. At the completion of closure the tight fusion seam resolves and vanishes, leaving a perfect, segmentally aligned, epithelial surface at the midline seam (see Figure 1.1).

Covering the eye-shaped hole is a monolayer of large flat cells called the amnioserosa, over which the epithelial edges must eventually travel to seal the hole. Dorsal closure requires the integrated efforts of three groups of cells: the exposed amnioserosa, the epithelial leading edge cells and the ventral epithelial cells. From the very start of closure the large cells of the amnioserosa begin to contract, pulling the attached epithelial edges towards each other. Conversely, the ventral epithelial cells elongate in a dorso-ventral direction helping to push the epithelium dorsally. The epithelial leading edge cells also elongate and, in addition, assemble specialised actin machineries which are crucial to the closure process.

1.1.3 Leading edge cells assemble an actin cable and actin protrusions

From early in dorsal closure F-actin (filamentous actin) accumulates along the dorsal side of all leading edge cells. The accumulated actin is associated with myosin and forms a contractile cable which runs around the circumference of the hole, connected between cells at anchor points provided by cell-cell adherens junctions (Jacinto et al., 2002a; Young et al., 1993). The cable has contractile properties and is thought to act as a "purse-string" helping to pull the two epithelial surfaces together (Hutson et al.,

2003; Kiehart, 1999; Kiehart et al., 2000). The leading edge cells also assemble actin protrusions, finger-shaped filopodia and web-like lamellipodia. These protrusions reach out across the amnioserosa and interact with the opposing epithelial edge and appear to help zip the epithelium shut from the "zipping canthi" at the most anterior and posterior ends of the hole (Jacinto et al., 2000).

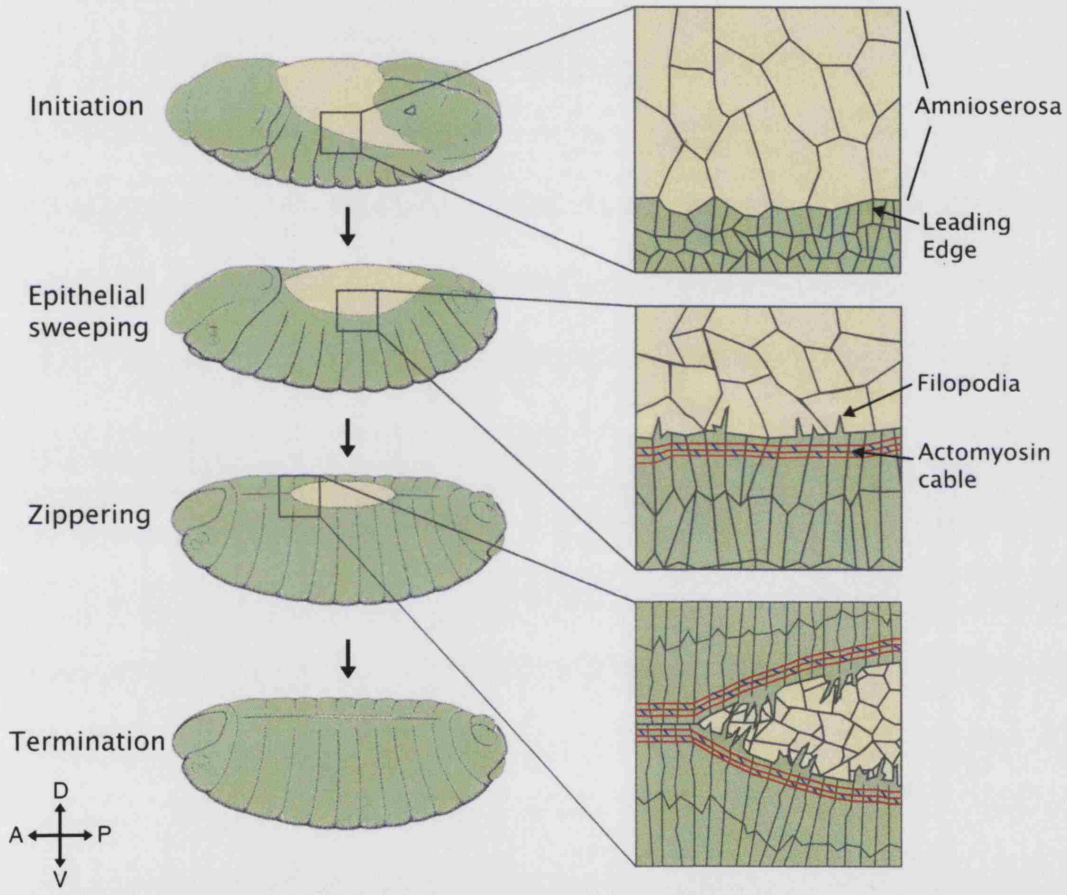

Figure 1.1 Schematic diagram of dorsal closure

Dorsal closure is represented as a 4 phase process (see Chapter 3) with the epithelium shown in green and amnioserosa in yellow. Embryo cartoons (left) display the progressive stages of the process. Boxed regions (right) show "zoom ins" of the epithelial leading edge. Dorsal closure begins as the germ band approaches its ultimate position at the posterior. Early in the process the large cells of the amnioserosa (yellow) contract and the epithelial cells (green) begin to elongate in a dorso-ventral direction (axis compass in bottom left). Slightly later in closure the epithelial leading edge begins to assemble an actomyosin cable (red and blue) and starts to extend actin protrusions across the amnioserosa (embryo drawings adapted from Hartenstein, 1993)

1.1.4 Dorsal closure provides an excellent model system for epithelial migration and fusion

Epithelial migration and fusion events are crucial tools used throughout development to shape the embryo. Examples in vertebrates include the zipping closure of the neural tube and the fusion of the secondary palette (see section 1.7.2, reviewed in Jacinto et al., 2001; Martin and Wood, 2002). Furthermore, similar mechanisms are re-activated in order to close wounds in epithelial tissue both in embryos and adults (see Section 1.7.3). Dorsal closure provides an exceptional system to study the genetics and mechanics of such epithelial movements both because of the amazing genetic tractability of *Drosophila* and also the relative ease with which dorsal closure can be imaged live.

The large forward genetic screens carried out in the 1980s by Nüsslein-Volhard, Weischaus and colleagues provided a huge base of genetic information about the development of *Drosophila*, and led to an explosion in the use of the fly as a genetic model organism (Nusslein-Volhard and Wieschaus, 1980). Many genes were subsequently revealed as playing crucial roles in dorsal closure and a selection of these are described in the following sections. The publication of the *Drosophila* genome in 2000 obviously expanded the possibilities for research in this model organism even more (Adams et al., 2000). Besides its genetic tractability, *Drosophila* offers other advantages in the study of morphogenetic episodes. One very important tool is the UAS/GAL4 system, which uses the yeast transcription factor GAL4 and its enhancer UAS sites to drive the expression of *Drosophila* genes or gene-constructs in specific tissues (Brand and Perrimon, 1993) (see Figure 1.2). For example, a transgene can be constructed to carry a dominant inhibitory version of a *Drosophila* gene along with upstream UAS enhancer elements. Flies with this construct can then be crossed to "driver" fly lines which carry GAL4 linked to a tissue specific promoter. In

the resulting embryos the dominant inhibitory transcript will only be expressed in the tissue specified by the driver line, allowing the function of the gene product to be assessed in this tissue alone, a particularly useful tool if a null mutation leads to early lethality.

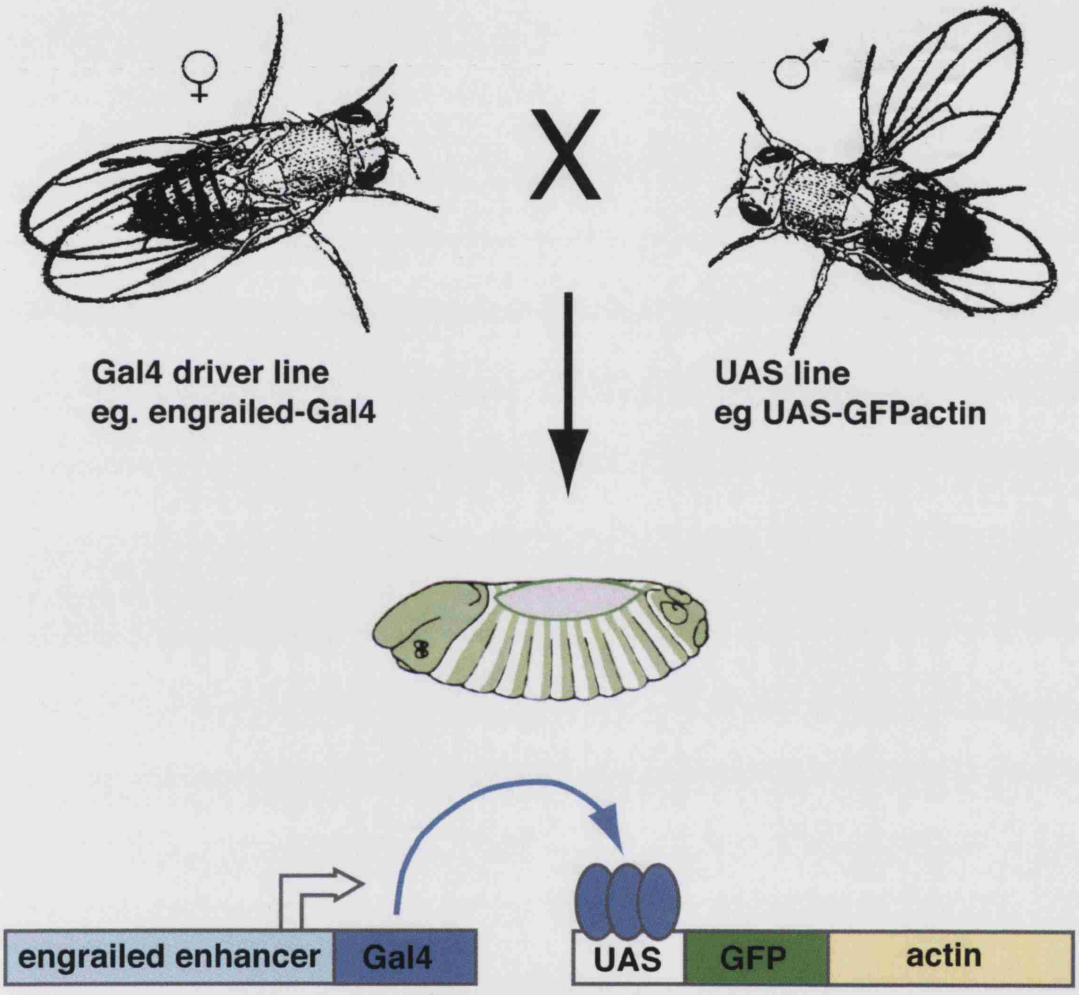

Figure 1.2 The UAS/GAL4 System

The UAS/GAL4 system can be used to express specific transgenes in particular tissues of the fly embryo. GAL4 driver line flies, in which tissue specific enhancer elements are linked to the GAL4 gene (e.g. *engrailed-GAL4*), are crossed to a line carrying UAS promoter upstream of the trangene to be expressed (e.g. GFP-actin). In the resulting embryo, GAL4 is expressed only in the cells/tissue specified by the driver line, and in turn GAL4 drives expression of the transgene via the UAS promoter (e.g. GFP-actin is expressed in the posterior of each segment of the embryonic epithelium during dorsal closure) (adapted from Brand and Perrimon, 1993).

The UAS/GAL4 system can also be used to drive tissue specific expression of fluorescent fusion proteins, where a *Drosophila* gene product is tagged with a fluorescing protein such as GFP (green fluorescent protein), allowing fluorescent confocal imaging to be carried out on live samples. The use of GFP-fusions, such as GFP-actin and GFP-moesin, has furthered the study of dorsal closure a great deal as it allows the dynamic cell shape changes and actin cytoskeletal machineries to be followed live throughout the process (Dutta et al., 2002; Jacinto et al., 2000; Jacinto et al., 2002a; Kiehart et al., 2000). Dorsal closure is a relatively simple process to image live as it takes place on the very surface of the embryo with no tissues above it (except the thin vitelline membrane) to obscure the imaging. This accessibility, together with the genetic tools available in *Drosophila* combine to make dorsal closure an excellent model from which to learn more about epithelial tissue movements.

1.2 SIGNALLING PATHWAYS USED IN DORSAL CLOSURE

1.2.1 The JNK cascade

The large genetic screens carried out with *Drosophila* identified a group of dorsal closure genes that where selected by their "dorsal open" cuticle phenotypes, where a failure in dorsal closure leaves a hole in the epidermis which is not covered by cuticle at the end of embryogenesis (Jürgens et al., 1984; Nüsslein-Volhard, 1984; Wieschaus, 1984). The names given to some of these dorsal closure genes, such as *basket* (*bsk*) and *kayak* (*kay*), reflect the phenotypes seen in their cuticles. Molecular characterisation of the dorsal closure genes began to reveal that a mitogen-activated protein kinase (MAPK) cascade was involved in the process (Glise et al., 1995; Hou et al., 1997; Kockel et al., 1997; Riesgo-Escovar and Hafen, 1997b; Riesgo-Escovar et al., 1996; Sluss et al., 1996). MAPK cascades are crucial signalling pathways involved in many vital cellular processes, which end with the activation of transcription factors (reviewed in Widmann et al., 1999). At the top of the cascade is a MAPK kinase kinase (MAPKKK) which, when activated, phosphorylates and activates a MAPK kinase which

in turn phosphorylates a MAPK and this then phosphorylates and activates specific transcription factors. In mammalian cells five MAPK families have been established which are determined by the identity of the final MAPK and therefore the transcription factors which are subsequently activated.

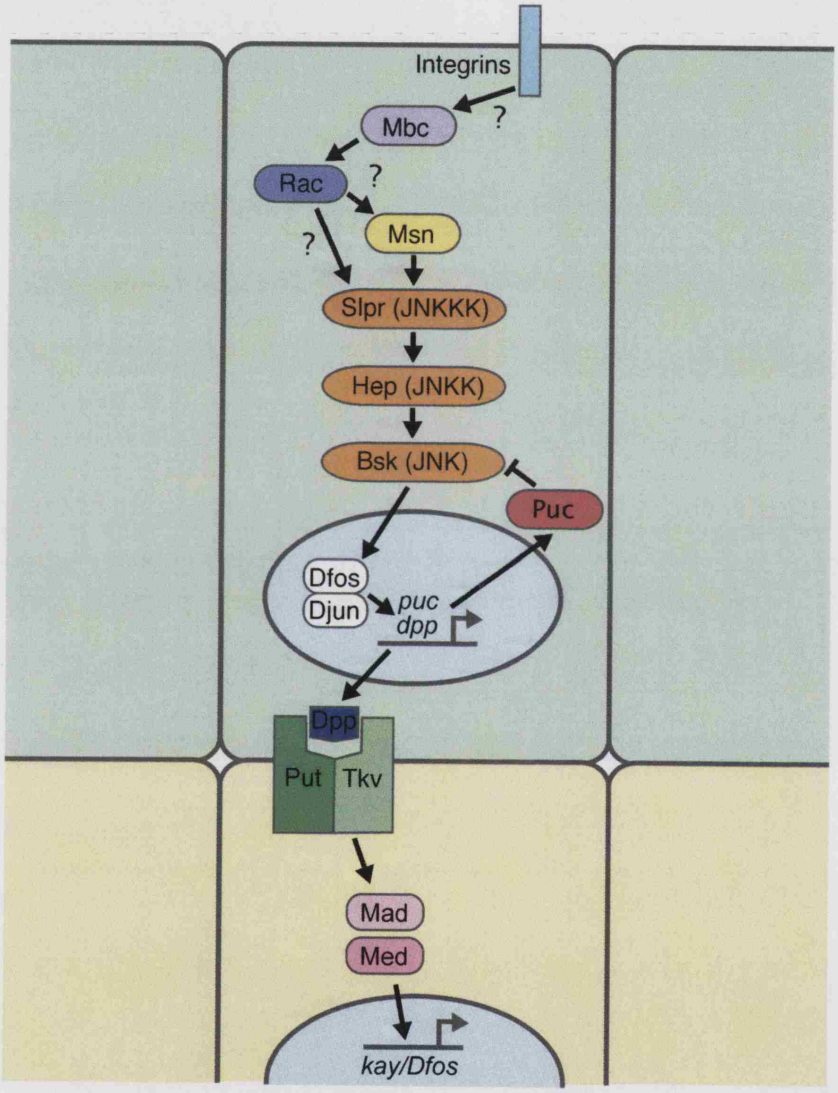

Figure 1.3 The dorsal closure JNK pathway

Early in dorsal closure a JNK pathway is activated in the epithelial leading edge cells (green). A series of Jun N-terminal kinases (orange ovals) are successively phosphorylated and activated, ultimately resulting in the translocation of the AP-1 transcriptional complex (Dfos and Djun) to the nucleus and the expression of specific downstream genes. One transcriptional target is Dpp whose release appears to act on cells ventral to the leading edge (yellow). A simplified version of the dorsal closure JNK cascade is shown with question marks indicating relationships that have not been conclusively proven. Collated with information from Harden 2002.

The first implication that a MAPK cascade was involved in dorsal closure came when the dorsal closure gene *hemipterous* (*hep*) was cloned. It was found to encode a MAPKK similar to mammalian Jun N-terminal kinase kinase (JNKK), a member of the JNK cascade family (Glise et al., 1995). JNK cascades end with the activation of the leucine zipper transcription factor, Jun, which then usually teams up with another leucine zipper protein, Fos, to form the transcriptionally active AP1 complex. Further cloning of the dorsal closure genes uncovered more members of the JNK pathway, for example *bsk* was found to encode *Drosophila* JNK (Riesgo-Escovar and Hafen, 1997b; Riesgo-Escovar et al., 1996; Sluss et al., 1996) whilst *kay* encodes *Drosophila* Fos (Riesgo-Escovar and Hafen, 1997a; Zeitlinger et al., 1997), and most recently the aptly named dorsal closure gene, *slipper* (*slpr*), was found to encode a JNKKK (Stronach and Perrimon, 2002) (Figure 1.3). All members of the JNK pathway exhibit similar phenotypes: the cells of the leading edge fail to maintain their dorso-ventral elongated state, appearing polygonal rather than rectangular in shape, and they also exhibit disruptions in leading edge actin and myosin assemblies, and ultimately the embryos fail to close their dorsal hole.

Further genetic analysis has uncovered two key genes which sit downstream of the JNK pathway and whose expression is therefore dependent on the activation of this cascade. Firstly, *decapentaplegic* (*dpp*), which encodes a member of the Transforming growth factor-β (TGF-β) superfamily, is expressed in the leading edge early in dorsal closure and JNK mutants show a consistent loss of this expression (Glise and Noselli, 1997; Hou et al., 1997; Riesgo-Escovar and Hafen, 1997b; Sluss and Davis, 1997; Stronach and Perrimon, 2002; Zeitlinger et al., 1997). Further corroborating evidence of a role for Dpp in dorsal closure came when members of a Dpp pathway were identified as dorsal closure genes and these are discussed in the following section. A second gene found downstream of JNK is *puckered* (*puc*), it encodes a dual-specificity

MAPK phosphatase and is expressed strongly in the leading edge. Puc targets Bsk for dephosphorylation suggesting that it provides a negative feedback loop on the JNK pathway (Martin-Blanco et al., 1998). Indeed, Puc appears to act as a brake during closure as *puc* mutants display an over contracted or "puckered" phenotype (Ring and Martinez Arias, 1993).

1.2.2 Dpp – a TGF-β signalling pathway in dorsal closure

As described in the previous section, the TGF-β family member, Dpp, has been implicated as being a downstream target of the JNK pathway during dorsal closure. This provides an interesting parallel to signalling in wound closure where TGF-β is a key player in the healing process (see section 1.7.3). The role of Dpp in dorsal closure was further strengthened with the discovery that mutations in genes encoding for two components of the TGF-β receptor complex, *thick veins* (*tkv*) and *punt* (*put*) cause dorsal closure defects also (Affolter et al., 1994; Brummel et al., 1994; Childs et al., 1993; Letsou et al., 1995; Nellen et al., 1994; Ruberte et al., 1995). Moreover, overexpression of *dpp* or an activated form of *tkv* can rescue, to a large extent, phenotypes caused by loss of JNK activity, providing convincing evidence that a Dpp pathway does sit downstream of the JNK cascade (Hou et al., 1997; Penton et al., 1994; Riesgo-Escovar and Hafen, 1997b; Sluss and Davis, 1997).

However, the dorsal closure phenotypes caused by mutations in members of the Dpp pathway are different from JNK cascade mutants. It appears that the Dpp pathway is not required for the dorso-ventral elongation or actin accumulation seen in leading edge cells, as these aspects are not affected in *tkv* or *put* mutants. In contrast, a major anomaly seen with these mutants is that the epithelial cells ventral to the leading edge fail to elongate as normal (Glise and Noselli, 1997; Riesgo-Escovar and Hafen, 1997a). One simple explanation for this phenotype is that Dpp acts in a paracrine fashion on

cells behind the leading edge instructing them to actively elongate or be passively stretched by the leading edge. Alternatively, Dpp may target the leading edge itself, because even though these cells do elongate in *tkv* and *put* mutants, the edge later develops constricted bunches and these may impede dorsal closure and prevent the elongation of ventral epithelial cells (Ricos et al., 1999). However, it is known that cells receiving the Dpp signal respond by translocating the *Drosophila* Smad protein, Mothers against Dpp (Mad), to the nucleus along with another Smad, Medea (Med), which together mediate the transcriptional effects of Dpp (Affolter et al., 2001) (see Figure 1.3).

1.2.3 Other signalling pathways in dorsal closure

A number of other signalling pathways have been uncovered in dorsal closure which feed into the JNK cascade or Dpp pathway. In this section, two major contributors, the Wnt/Wingless (Wg) pathway and Notch are considered (reviewed in Harden, 2002). Wg belongs to the Wnt family of secreted ligands which provide key pathways for cell fate decisions in vertebrates and insects. In *Drosophila* the canonical Wg pathway begins with secretion of Wg which binds to the Frizzled 2 (Fz2) receptor. This leads to activation of the Dishevelled (Dsh) protein and in turn prevents the degradation of Armadillo (Arm/β-catenin), which accumulates in the cytoplasm. Arm can then go on to promote the transcription of Wg-responsive genes by acting as a co-activator for the transcription factor dTCF. There is growing evidence of a role for Wg in dorsal closure as *wg* mutants display dorsal closure defects and reductions in leading edge expression of *dpp* and the reporter construct *puc-lacZ* (McEwen et al., 2000). Furthermore, ectopic activation of Wg away from the leading edge leads to expression of *dpp,* although such expression is dependant on JNK pathway activity as it does not occur in *kay* mutants (McEwen et al., 2000). It therefore appears that the Wg pathway feeds into the JNK cascade although it is not clear whether this might occur at the level

of Dsh activation or instead slightly later via the dTCF transcription factors. The dorsal closure phenotypes of *wg* mutants are less severe than JNK pathway members, with closure completing, albeit in a distorted manner, suggesting that the Wg pathway may not be a major activator of this morphogenetic episode, but rather acts as a modulator of *dpp* expression.

The receptor Notch plays crucial roles in cell fate decisions throughout development. *Notch* mutants have been found to possess dorsal holes and leading edge levels of *dpp* expression are higher than normal (Zecchini et al., 1999). Loss of Notch activity also suppresses the dorsal closure defects seen in JNK mutants. Together these results suggest that Notch can act as a brake on JNK signalling. However, it appears that the common mode for Notch function, involving the Notch ligand, Delta, cleavage of the Notch receptor and the transcriptional co-activator, Suppressor of Hairless (Su(H)), is not used in Notch's negative regulation of JNK in dorsal closure. One possibility is that Notch acts through Wg, as previous studies have shown that Notch is capable of inhibiting Wg in other cell types (Brennan et al., 1999a; Brennan et al., 1999b).

1.3 JUNCTIONS AND CELL ADHESION IN DORSAL CLOSURE

1.3.1 Cell-cell adhesions

Adherens junctions are a major form of cell-cell adhesion that mediate the fusion and maintenance of epithelial sheets. During dorsal closure the epithelial leading edge is decorated with spots of phosphotyrosine staining which have been found to contain known components of adherens junctions, suggesting that these junctions are functioning in closure (Harden et al., 1996). *Drosophila* adherens junctions are composed of E-cadherin, α-catenin, β-catenin and p120ctn. E-cadherin (encoded by the *shotgun* gene) forms the transmembrane core of the adherens junction, and its

extracellular domain interacts with E-cadherins on the surfaces of opposing cells, whilst intracellularly E-cadherin binds to β-catenin and p120ctn. α-catenin interacts with β-catenin and acts to link the cadherin-catenin complex to the actin cytoskeleton (reviewed in Tepass et al., 2001) (see Figure 1.4).

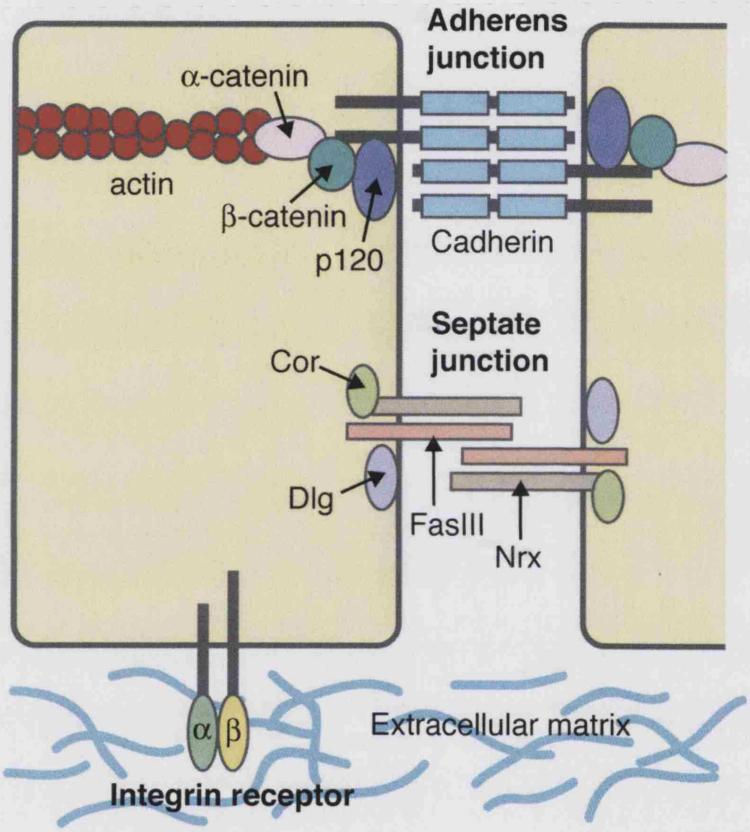

Figure 1.4 *Drosophila* cell adhesions

The three major forms of epithelial cell adhesion in *Drosophila* are shown. Adherens junctions are found most apically and consist of a cadherin-catenin complex which connects to the cell's actin cytoskeleton. The *Drosophila* septate junction has not yet been well described at the molecular level and the representation here just includes components that have been found to be involved in dorsal closure, but in reality it is likely to contain many more players. Integrins are generally located on the basal surface of epithelial cells where they mediate interactions with the extracellular matrix (collated using information from (Brown et al., 2000; Tepass et al., 2001).

Investigating the requirement for adherens junctions in dorsal closure has not been entirely straight forward due to the crucial roles of these structures early in development. E-cadherin, for example, cannot be completely eradicated from the embryo because it is needed in oogenesis (Tepass et al., 1996). However, germ line clones of weak *shotgun* (*shg*) alleles do exhibit a loss of dorsal cuticle although it is not clear whether this is actually due to a defect in dorsal closure, or other epithelial disruptions (Tepass et al., 1996). *β-catenin* (*arm*) mutants do possess large dorsal holes, although the interpretation of this phenotype is complicated by the fact that β-catenin also plays a key role in Wg signalling in dorsal closure (as described above in section 1.2.3) (McEwen et al., 2000). The dorsal holes in these mutant embryos are much larger than those seen in *wg* mutants suggesting that β-catenin is playing an additional role to Wg signalling and, presumably, this is in the assembly of adherens junctions.

Adherens junctions are likely to be fulfilling a number of functions in dorsal closure. Firstly, their position along the leading edge and their structural link to the actin cytoskeleton makes it likely that they provide strong anchoring points for intracellular segments of the actin cable, linking the cable between neighbouring cells and contributing to the mechanics of cable contraction, just as is seen in purse-string driven wound healing (Danjo and Gipson, 1998; Young et al., 1993). A second role for adherens junctions comes as the two epithelial surfaces begin to zip together by interdigitation of actin protrusions assembled by the leading edge cells. This filopodial interdigitation primes initial adhesions between the two epithelial surfaces, which then resolve to form mature junctions at the fusion seam (Jacinto et al., 2000). A similar process is used by cultured keratinocytes when they are induced to form epithelial sheets, and in this case it is known that interdigitated filopodia contain clusters of

adheren junction components which can mediate the initial adhesion and resolve to form mature adherens junctions (Vasioukhin et al., 2000) (see Figure 1.5).

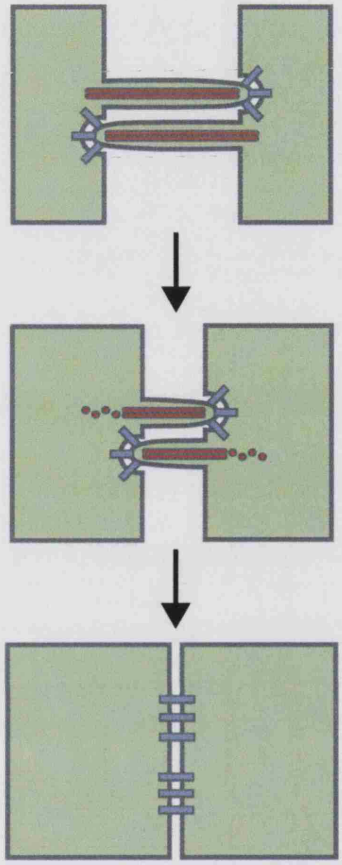

Figure 1.5 A filopodial interdigitation model for epithelial cell adhesion
In a number of different systems, including dorsal closure, fusion of epithelial cells is preceded by the assembly of filopodia. These actin (red) protrusions interdigitate and provide initial points of contact between two cells and sites for cell-cell adhesion (blue). The cells can then pull closer together and over time the initial contacts will develop into mature adherens junctions, forming a fused epithelial surface. Adapted from (Jacinto et al., 2002b).

However, adherens junctions appear to not only perform adhesive and structural roles in dorsal closure but may also contribute to both the assembly of leading edge actin structures and signalling during the closure process. The nonreceptor tyrosine kinase, Abelson (Abl) and its target Ena, a modulator of actin dynamics (see section 1.5.5), both localise to adherens junctions during dorsal closure. *Abl* mutants show defects in dorsal closure including a lack of coordinated cell shape change in the epithelium and an uneven distribution of actin along the leading edge. Ena is mis-localised in *abl* mutants and the pattern of Ena disruption mirrors F-actin defects in these mutants (Grevengoed et al., 2001). The mis-localisation of Ena may well be the fundamental

defect in *abl* mutants, as work in follicular epithelial cells has found that Ena mediates correct junction assembly and actin polymerisation at adherens junctions (Baum and Perrimon, 2001). A final role for adherens junctions in dorsal closure seems to be to provide sites for specialised signalling complexes in the leading edge. The two PDZ domain proteins, Canoe (Cno) and ZO-1 have been found to localise to adherens junctions along the leading edge and interact genetically with each other (Takahashi et al., 1998). Cno is known to be an activator of the JNK pathway in dorsal closure, as *cno* mutants have a large dorsal hole and show decreased leading edge expression of *dpp* and *puc-lacZ*. It therefore seems probable that Cno and ZO-1 form a signalling scaffold at adherens junctions which can help direct JNK signalling in the leading edge during the closure process.

Another form of cell-cell adhesion in *Drosophila* is the septate junction, which is analogous to the vertebrate tight junction (see Figure 1.4, reviewed in Tepass et al., 2001). These junctions do not appear to play such a broad role throughout dorsal closure as the adherens junctions do, but instead seem important for the final fusion of the two epithelial edges. The mutants of two components of septate junctions, *coracle* (*cor*) and *neurexin IV* (*nrx*) exhibit small holes at the dorsal midline, suggesting that dorsal closure can initiate and progress a considerable way before failing (Baumgartner et al., 1996; Fehon et al., 1994; Lamb et al., 1998). Further evidence that septate junctions come into play later in dorsal closure comes from analysis of the localisation of Fasciclin III (Fas III), an adhesion protein known to be associated with septate junctions (Snow et al., 1989). Fas III is specifically excluded from the dorsal surface of leading edge cells until the two epithelial edges meet, at which point Fas III becomes localised to the fusion seam (Harden et al., 1995; Magie et al., 1999). The formation of septate junctions along the leading edge could well be linked to adherens junctions, as the Lgl complex, a group of proteins crucial for adherens junction integrity,

also interact with septate junction components and may act as a scaffold upon which proteins such as Cor and Nrx can assemble (Tepass et al., 2001).

1.3.2 Integrins and extracellular matrix

Integrins, which mediate adhesion between cells and the extracellular matrix, also appear to have important functions in dorsal closure, as mutations in both the integrin β subunit, *myospheroid,* and an α subunit, encoded by the *scab* locus, lead to dorsal holes (Brown, 1994; Stark et al., 1997). Timelapse analysis of these mutants indicates that integrins might play a role in final fusion at the midline, much as septate junctions seem to, because the embryos initially appear to close, but subsequently rupture (Roote and Zusman, 1995). However, some evidence seems to contradict this conclusion as there is no strong expression of β-subunit containing integrins along the midline and also embryos lacking both maternal and zygotic β-integrin fail before the start of dorsal closure, in germ band retraction, indicating a role for integrins earlier in the process.

Cross-sectional analysis of embryos undergoing dorsal closure revealed some alternative roles for integrins during this process. This approach also uncovered an additional cellular player in dorsal closure – the yolk cell (Narasimha and Brown, 2004). The large yolk cell sits beneath the amnioserosa and strong integrin staining was found where the amnioserosa contacted the yolk cell membrane. Another site of strong integrin localisation was found at the interface between the amnioserosa and cells of the leading edge. Furthermore, at both of these locations, the integrin ligand and extracellular matrix component, laminin, was found to colocalise with integrins. Embryos lacking integrin showed detachment of the amnioserosa from the yolk cell and the cells of the amnioserosa now failed in their usual contraction. In addition, a loss of adhesion was seen at the interface between epithelial leading edge and

amnioserosa (Narasimha and Brown, 2004). It therefore appears that integrins play a number of adhesive roles during the dorsal closure process.

1.4 CYTOSKELETON AND RHO GTPASES IN DORSAL CLOSURE

1.4.1 Myosin

The first dorsal closure gene to be analysed in detail was *zipper* (*zip*), which encodes the heavy chain of *Drosophila* myosin II, a conventional non-muscle myosin (Nüsslein-Volhard, 1984). *Zip* mutant embryos display dorsal closure phenotypes, which vary from dorsal open through to slightly aberrant completion, depending on the strength of individual alleles and genetic background (Jacinto et al., 2002a; Nüsslein-Volhard, 1984; Young et al., 1993). In wild type embryos, myosin II accumulates in the leading edge early in dorsal closure, forming a strong band around the circumference of the hole (Young et al., 1993). As described previously in section 1.1.3, actin colocalises with this band of myosin and is thought to form a cable capable of myosin based contraction.

Early in closure zygotic *zip* mutants appear reasonably normal, with maternally contributed myosin accumulated in the leading edge. However as the maternal levels diminish the leading edge becomes less taut and increasingly disorganised. In severe *zip* alleles the epithelial sheets buckle and fail to fuse at the midline. Individual cells of the leading edge also lose their rectangular, elongated shape and become polygonal and splayed (Young et al., 1993). The localisation of actin in *zip* mutants appears unaffected but live imaging has shown that as the actomyosin cable disintegrates in these embryos, the leading edge extends larger and more exuberant actin protrusions (Jacinto et al., 2002a). These results indicate that the presence of myosin II and the formation of an actomyosin cable during dorsal closure acts to restrain and organise the leading edge, maintaining a coherent surface which can be closed efficiently and precisely. Further evidence for the restraining, contractile nature of the cable comes

from laser ablation studies where small holes blasted in the leading edge cause cells at the margin of the wound to spring apart as tension is lost. Whilst these experiments also endorse the idea of the actomyosin cable acting as a purse-string directly aiding closure, it is clear that it does not provide the only force necessary for closure, as embryos in which the leading edge is repeatedly laser wounded still continue to close (Kiehart et al., 2000).

Myosin II is the only myosin, so far, to have a clearly defined role in dorsal closure. To date, 13 myosin heavy chain genes have been identified in the *Drosophila* genome and it seems likely that at least some of these will fulfil important functions during the closure process. Indeed, recent data indicate that the fly myosin VI, *jaguar* (*jag*), may play a role in dorsal closure as newly generated *jag* mutants fail in either germ-band retraction or dorsal closure. Furthermore, Jag is strongly expressed in the leading edge and the actin protrusions assembled by these cells, where it may be important for the correct localisation of E-cadherin (Millo et al., 2004). The potential functions of other myosin classes during dorsal closure are explored in Chapter 5.

1.4.2 Actin and Rho GTPases

As described above in section 1.1.3, during dorsal closure the leading edge assembles two key actin structures: a contractile actomyosin cable and actin protrusions, filopodia and lamellipodia. Actin also accumulates around the cortex of each amnioserosal cell where it is presumably involved in the dramatic contractions displayed by these cells. As actin is essential for cell viability, mutants in actin would not be useful for studying morphogenesis in the embryo. Instead, much of our understanding of the role that different actin structures play during dorsal closure has come from study of the family of key actin cytoskeletal regulators, the Rho family of small GTPases.

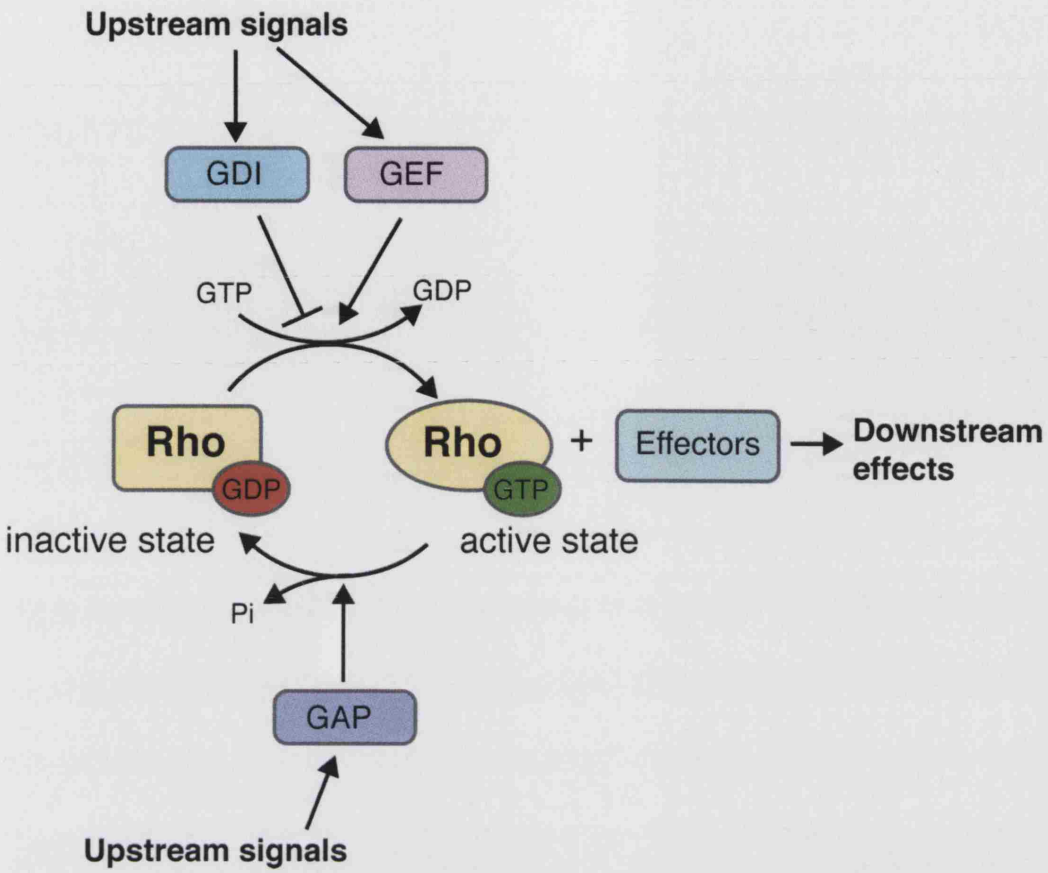

Figure 1.6 Cycling of Rho GTPases

The Rho family of small GTPases act as molecular switches, cycling between an inactive, GDP-bound form, and an active, GTP-bound form. Upstream signals feed into regulators of Rho GTPase activity – the GEFs, GAPs and GDIs – and so affect the balance of the cycle. When in the active form Rho GTPases can go on to activate numerous effectors leading to a variety of downstream effects (adapted from Raftopoulou and Hall, 2004).

Rho GTPases act as molecular switches to control signal transduction pathways, cycling between an active GTP-bound and inactive GDP-bound form (see Figure 1.6). When in their active GTP-bound state they can interact with a wide range of downstream effectors to drive various cellular responses (reviewed in Raftopoulou and Hall, 2004; Wennerberg and Der, 2004). The cycling of Rho GTPases between the active and inactive forms is tightly regulated by three groups of proteins (see Figure 1.6). Guanine nucleotide exchange factors (GEFs) activate the GTPase by promoting the exchange of GDP for GTP. In contrast, GTPase-activating proteins negatively

regulate the cycle by enhancing the GTPase activity of the Rho family member, whilst guanine nucleotide dissociation inhibitors are thought to block the cycle by sequestering the GDP-bound form (Moon and Zheng, 2003; Schmidt and Hall, 2002; Zheng, 2001). A great deal of the work carried out to investigate Rho GTPase function has used the expression of mutant forms of the GTPases which upset the usual cycling. Constitutively active forms of GTPases possess mutations that reduce their intrinsic GTPase activity and do not respond to GAPs, and so, in this way, remain active irrespective of upstream signalling. Conversely, mutations which give the Rho GTPase a preferential affinity for GDP lock the GTPase in the inactive state and are thought to act as dominant negatives by sequestering GEFs, preventing the activation of their wild type counterparts (Harden et al., 1995).

The most well studied downstream effect of the Rho GTPases is their regulation of the actin cytoskeleton, and it is this activity which will be concentrated on here. Work in cultured fibroblasts has indicated that different members of the Rho family are responsible for organising actin into specialised arrangements. Activation of Rho was found to regulate the formation of contractile actomyosin, which in cultured cells form stress fibres (Ridley and Hall, 1992). In contrast the Rho family members Rac and Cdc42 were found to be required for the assembly of lamellipodia and filopodia, respectively (Nobes and Hall, 1995; Ridley et al., 1992). How each of these members of the Rho GTPase family impact actin organisation during dorsal closure is under investigation and this work has uncovered striking similarities between their roles in this *in vivo* event and those attributed in tissue culture.

RhoA/Rho1

Eradicating *Drosophila* RhoA/Rho1 function either with loss-of-function mutations or expression of a dominant negative form of *Rho1* leads to defects in the dorsal cuticle, indicative of problems with dorsal closure (Harden et al., 1999; Lu and Settleman,

1999; Magie et al., 1999; Strutt et al., 1997). *Rho1* zygotic mutants do complete dorsal closure but have a highly disorganised leading edge, with uneven constriction of cells along the leading edge (Magie et al., 1999). Live imaging of *Rho1* zygotic mutants with expression of GFP-actin shows that, as the maternally contributed supply of Rho1 protein dies out during dorsal closure, the actin cable disintegrates and the leading edge becomes progressively more chaotic and disorganised. Concomitant with the loss of the actin cable in these mutants, the leading edge also begins to extend increased numbers of larger and more exuberant actin protrusions (Jacinto et al., 2002a). A similar phenotype is seen when dominant negative *Rho1* is expressed in *engrailed* stripes of the embryo during dorsal closure, as the expressing cells fail to assemble a cable and extend larger lamellipodial protrusions. Without the restraining action of the cable the *Rho1* dominant negative cells advance towards the midline faster, moving past their wild type neighbours to take over the leading edge (Jacinto et al., 2002a).

Together these results point to the importance of Rho1 in the assembly of the leading edge actomyosin cable during dorsal closure, a structure that bears similarities to the Rho controlled actin stress fibres found in cultured cells. The case for Rho1 involvement in the cable is further strengthened by the fact that *Rho1* and *zipper* interact genetically, so that as well as being integral in the reorganisation of the actin cytoskeleton into a cable structure, Rho1 may also be regulating myosin function during dorsal closure (Halsell et al., 2000). The path through which loss of Rho1 can lead to increased actin protrusion at the leading edge remains unclear, it could be just that the breakdown of the cable increases the amount of F-actin available to build protrusions or, alternatively, could indicate the Rho1 negatively regulates other members of the Rho family that are responsible for protrusion assembly.

Rac1, Rac2 and Mtl

Drosophila has three Rac-like genes, *Rac1*, *Rac2* and *Mtl* which all seem to be involved, to a greater or lesser degree, in dorsal closure (Hakeda-Suzuki et al., 2002). Expression of a dominant negative form of *Rac1* during dorsal closure leads to a loss of leading edge actin organisation and also a failure in leading edge cell elongation (Harden et al., 1995; Harden et al., 1999). Similarly, a triple *Rac* mutant, which lacks functional copies of all three *Rac* genes, fails in dorsal closure and exhibits a loss of actin accumulation at the leading edge (Hakeda-Suzuki et al., 2002). Together these findings certainly indicate that the Rac proteins are involved in regulating actin organisation at the leading edge. The cell elongation phenotype seen with expression of dominant negative *Rac1* also indicated that Rac may play a role in the JNK cascade, as JNK pathway mutants exhibit similar problems at the leading edge. This speculation was corroborated when experiments showed that the expression of a constitutively active version of Jun could partially rescue the dominant negative *Rac1* phenotype (Hou et al., 1997). However, this result has not yet been verified in the triple *Rac* mutant and I will return to this question in Chapter 4. In addition, our present knowledge of Rac function in dorsal closure has relied exclusively on fixed tissue analysis, which makes it difficult to determine the role of Rac in protrusion assembly as these fragile structures are mostly lost in the fixation process. Since tissue culture work has indicated that Rac is required for the formation of lamellipodia this is an important omission and will be addressed in Chapter 4.

Cdc42

Cdc42 zygotic loss of function mutant embryos display defects in dorsal closure and germ band retraction (Genova et al., 2000). However, detailed analysis of the actin cytoskeleton has not been carried out in these mutants. Instead much of our knowledge concerning the role of Cdc42 in actin regulation during dorsal closure has come from studies using expression of a dominant negative form of the GTPase. When

dominant negative *Cdc42* is expressed throughout the embryo at closure, a partial loss of leading edge actin is seen, although the affect on actin organisation does not seem as severe as that caused by the expression of dominant negative *Rac1* (Harden et al., 1999). Live imaging of embryos expressing dominant negative *Cdc42* in *engrailed* segmental stripes revealed that *Cdc42* is required for filopodial formation at the leading edge, as the transgene expressing cells no longer assemble these structures (Jacinto et al., 2000). Without filopodia these cells can not fuse properly at the midline and also often fail to find their correct segmental partners on the opposing epithelium, resulting in embryos that do not have the usual midline segmental alignment.

The mechanism by which Cdc42 may control filopodia assembly in dorsal closure remains largely unknown but clues can be gleaned from work in other systems, especially tissue culture. In the following section, I outline what is known about actin protrusion formation, focussing on investigations in single cells.

1.5 CONTROL OF ACTIN PROTRUSION FORMATION

1.5.1 The actin cytoskeleton

The actin cytoskeleton provides a crucial structural and transport network within a cell, but it is also key in driving cell shape change and cellular motility. Actin filaments are organised into a variety of dynamic networks to form structures such as stress fibres, cables and filopodial and lamellipodial protrusions. The actin in stress fibres and cables associates with myosin motors enabling it to generate tensile or contractile force, so for example, if a contractile cable forms at the apical edge of a cell, this edge will be tugged inwards giving the cell a wedge-like shape. Similarly, if a cable is formed at the edge of a sheet of cells it can be used to draw cells together by a "purse-string" contraction method, as occurs in wound healing or, to an extent, in dorsal closure (Kiehart, 1999; Martin and Lewis, 1992; McCluskey and Martin, 1995; Young et al., 1993).

Cell motility relies on the constant dynamic reorganisation of the actin cytoskeleton. The crawling motility of a single cell in culture requires a cycle of four steps: protrusion of the leading edge, adhesion to the substratum, retraction of the rear and de-adhesion (reviewed in Pollard and Borisy, 2003). This section will concentrate on what is known about the actin dynamics which drive the assembly of protrusive structures at the leading edge of a motile cell, hopefully providing an insight into how similar structures might be formed by the epithelial leading edge during dorsal closure.

1.5.2 Building filaments and actin treadmilling

Actin is a globular protein which cycles between monomeric and filamentous forms in the cell. Each actin filament is composed of a double helical arrangement of actin monomers, sitting head-to-tail to give the filament a molecular polarity, with one end being called the "barbed" end and the other the "pointed" end. Growth of actin filaments occurs preferentially at the barbed end and actin filaments are orientated with their growing, barbed ends towards the exterior of the cell (Small et al., 1978). The lamellipodium at the leading edge of a motile cell consists of a branched network of actin filaments and for the cell to move forwards this network must extend and push the leading edge membrane in the direction of movement. (see Figure 1.7) Thus, protrusive motility requires the polymerisation of actin at the barbed ends close to the leading edge.

The spontaneous assembly of actin monomers is kinetically unfavourable, as actin dimers and trimers are very unstable; however, once a filament is started, it will grow rapidly. Actin monomers bound to ATP are added preferentially to the barbed end, but over time the ATP is hydrolysed to ADP and ADP-actin then dissociates from the pointed end of the filament (Pollard and Borisy, 2003). The rapid growth of actin filaments means that the major rate-limiting step in protrusion extension is the

availability of new actin monomers. As a result, maintaining a pool of actin monomers to add to growing filaments is crucial to the assembly of actin protrusions. One means by which to deliver new actin monomers to barbed ends is to recycle them as they dissociate from the pointed, non-growing ends of the actin filaments, in a process called actin treadmilling. ADF/cofilins assist in this recycling by severing old, ADP rich, filaments and promoting the dissociation of ADP-actin from the ends of filaments (Zebda et al., 2000). However, to drive protrusive motility, filaments must be assembled rapidly and treadmilling alone is not sufficient to supply monomers as quickly as required. As a result the cell has developed a variety of ways to free up monomers and store them ready for polymerisation.

1.5.3 Maintaining an actin monomer pool

A major player in the maintenance of an actin monomer pool is a small actin binding protein called profilin. Profilin binds to the barbed end of actin monomers preventing them from associating with the pointed end of filaments and so further pushing the balance towards polymerisation at the barbed end (Kaiser et al., 1999; Pring et al., 1992). In addition, profilin also acts as a nucleotide exchange factor for actin, competing with ADF/cofilin for ADP-actin and then promoting the dissociation of ADP, ultimately recycling the actin to an ATP bound, polymerisation ready state (see Figure 1.7) (Rosenblatt et al., 1995). Another mechanism for maintaining a pool of monomeric actin is the association of WH2 domain containing protein, thymosin-β4, with ATP-actin monomers. The binding of thymosin-β4 to actin, prevents all actin assembly reactions, and so the balance of thymosin-β4 and profilin in the cell is crucial (De La Cruz et al., 2000; Safer and Nachmias, 1994). As profilin has greater affinity for actin than thymosin-β4 this allows profilin to provide a ready supply of polymerisation competent monomers whilst thymosin-β4 keeps a pool of monomers in reserve. It must be noted, however, that the *Drosophila* genome does not contain thymosin-β4 but does encode a

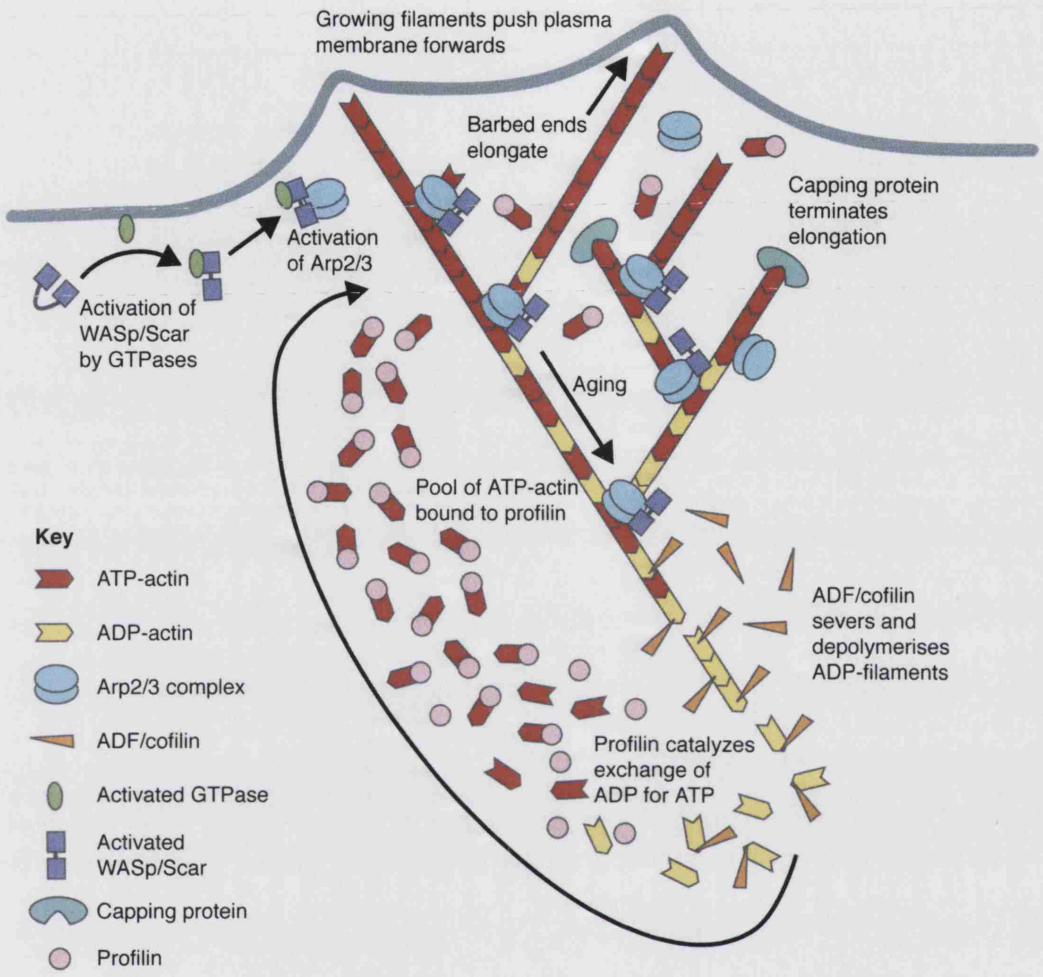

Figure 1.7 The actin treadmilling model of protrusion formation

The assembly of protrusions at the leading edge of a motile cell can be considered using the actin treadmilling model. In this, ATP-actin monomers (red darts) are added onto the growing barbed end of the branched network and ADP-actin (yellow darts) is removed at the pointed end of filaments. Addition of monomers at the barbed end pushes the plasma membrane forward and forms lamellipodial protrusions. A number of actin binding proteins play crucial roles in actin treadmilling: the Arp2/3 complex (blue ovals), once activated by WASp/Scar proteins (purple dumb-bell), nucleates new branched filaments of actin, whilst capping protein (green oval) binds to filament barbed ends and prevents further elongation. As the actin filaments age, ATP is hydrolysed to ADP, providing sites for ADF/cofilin (orange triangles) to attack and sever the older filaments. Profilin (pink circles) binds to ADP-actin and catalyses the exchange of ADP for ATP, maintaining a pool of polymerisation ready actin monomers (adapted from Pollard and Borisy, 2003) .

related WH2 domain containing protein called ciboulot (Paunola et al., 2002).

A further means by which actin protrusion can be regulated is by control of the length and quantity of actin filaments being generated. The further elongation of actin filaments can be inhibited by the binding of specialised capping proteins to their barbed ends; this not only prevents the draining of the monomer pool but the extent of capping seems to help determine whether filopodia or lamellae are assembled at the leading edge, as discussed further in Section 1.5.5. Another crucial element in actin dynamics is the formation of new barbed ends on which filaments can grow; this process of actin nucleation, is discussed in the following section.

1.5.4 Nucleating actin filaments

The primary nucleator of actin used by the cell to assemble actin protrusions appears to be the Arp2/3 complex (Machesky et al., 1994). This complex is able to bind to the pointed ends of actin and initiates the growth of new actin filaments at a 70° angle to the original filament. This generates the branched network of lamellipodial protrusions which can be elegantly visualised using specialist transmission electron microscopy (TEM) techniques. Immunogold labelling with antibodies to components of the Arp2/3 complex reveals the localisation of the complex at the Y-junctions between actin filament branches (Svitkina and Borisy, 1999). However, the Arp2/3 complex, alone, cannot drive actin nucleation but requires the input of further activators. The WASp/Scar family of proteins, when released from their autoinhibited state, have been found to be major activators of actin nucleation by Arp2/3 (Machesky and Insall, 1998), and these are discussed in greater detail in section 1.5.5

Another group of actin-binding proteins that have recently been found to nucleate actin are members of the Formin family. Once freed from autoinhibition by activated Rho

GTPases, formins are able to bind to the barbed end tips of actin filaments, where they can remain as the filament elongates (Higashida et al., 2004), blocking the access of capping proteins but allowing the incorporation of actin monomers (Zigmond et al., 2003). In this way, formins are able to drive the formation of long actin filaments. To date, formins have tended to be thought of as being most important for the assembly of actin cable structures, as members of the family have been found to be involved in stress fibre formation in cultured cells (Satoh and Tominaga, 2001) and for cable formation in yeast (Sagot et al., 2002). However, recent data suggest that formins may play a role in filopodia formation as tissue culture experiments have found that one mammalian formin, Drf3, is a downstream effector of Cdc42, the small GTPase that regulates filopodial assembly (Peng et al., 2003). Finally, very recent work has uncovered a new barbed end nucleator of actin, the *Drosophila* WH2 domain containing protein, Spire, although exactly which actin structures Spire contributes to remain to be defined (Baum and Kunda, 2005; Quinlan et al., 2005)

1.5.5 Building filopodia versus lamellipodia

The branched network formed by the nucleation of actin by Arp2/3 and its activators nicely explains how lamellipodia are assembled at the leading edge of cultured motile cells and also in *in vivo* situations such as dorsal closure. However, it does not so easily account for the formation of filopodia, as structural studies have shown that these protrusions consist of an unbranched bundle of aligned actin filaments. These filaments are rooted in the branched network but Arp2/3 is excluded from the length of the filopodium. An *in vitro* reconstitution assay sheds some light on how filopodia might be assembled. If WASP coated beads are added to a cytoplasmic extract various actin structures form around the bead, but the predominant arrangement is a "cloud" of actin assembled in a branched network analogous to a lamellipodia (Svitkina et al., 2003; Vignjevic et al., 2003). However, if capping protein is depleted from the extract this

arrangement switches and most beads are surrounded by a "star-like" array, which consists of bundled actin filaments similar to the structure of filopodia. In fact, if purified proteins are used, all that is needed to produce these "stars" is WASP, actin, Arp2/3 and fascin, which is thought to act to bundle the actin filaments (Vignjevic et al., 2003). It therefore appears that a branching actin network may be pushed towards forming filopodia if capping protein activity is reduced or antagonised. This is, at least in part, born out by some recent work in cultured cells where depletion of capping protein by short hairpin RNA caused an "explosive" increase in filopodia formation (Mejillano et al., 2004). However, generally, cells maintain high concentrations of capping protein so it is thought that rather than reducing these levels, cells instead may employ antagonists of capping action, such as the Ena/VASP family of proteins. Indeed, if capping protein levels are depleted in Ena/VASP deficient cells, no switch to filopodial production is seen (Mejillano et al., 2004).

The decision of whether to assemble filopodia or lamellipodia had been thought to run through two parallel pathways, although the model for filopodial formation described above does not necessarily require this. Key to both pathways are members of the WASP family of Arp2/3 activators. These can be organised into two subfamilies, one containing WASPs and the other containing Scar/WAVE proteins. The filopodial inducing small GTPase, Cdc42, was found to specifically activate WASPs (Higgs and Pollard, 2000; Rohatgi et al., 2000) whilst Scar/WAVE proteins were found to be downstream of Rac1 (Eden et al., 2002), the GTPase known to stimulate lamellipodial formation. Thus it appeared that two separate pathways controlled actin protrusion formation. However, this does not appear to be the case in *Drosophila* cells, which carry only a single *WASp* and single *SCAR* gene, as in this case, SCAR seems to be the major regulator for both lamellipodia and filopodia assembly, whilst WASp appears less important (Biyasheva et al., 2004; Rogers et al., 2003). The speculation is that, in

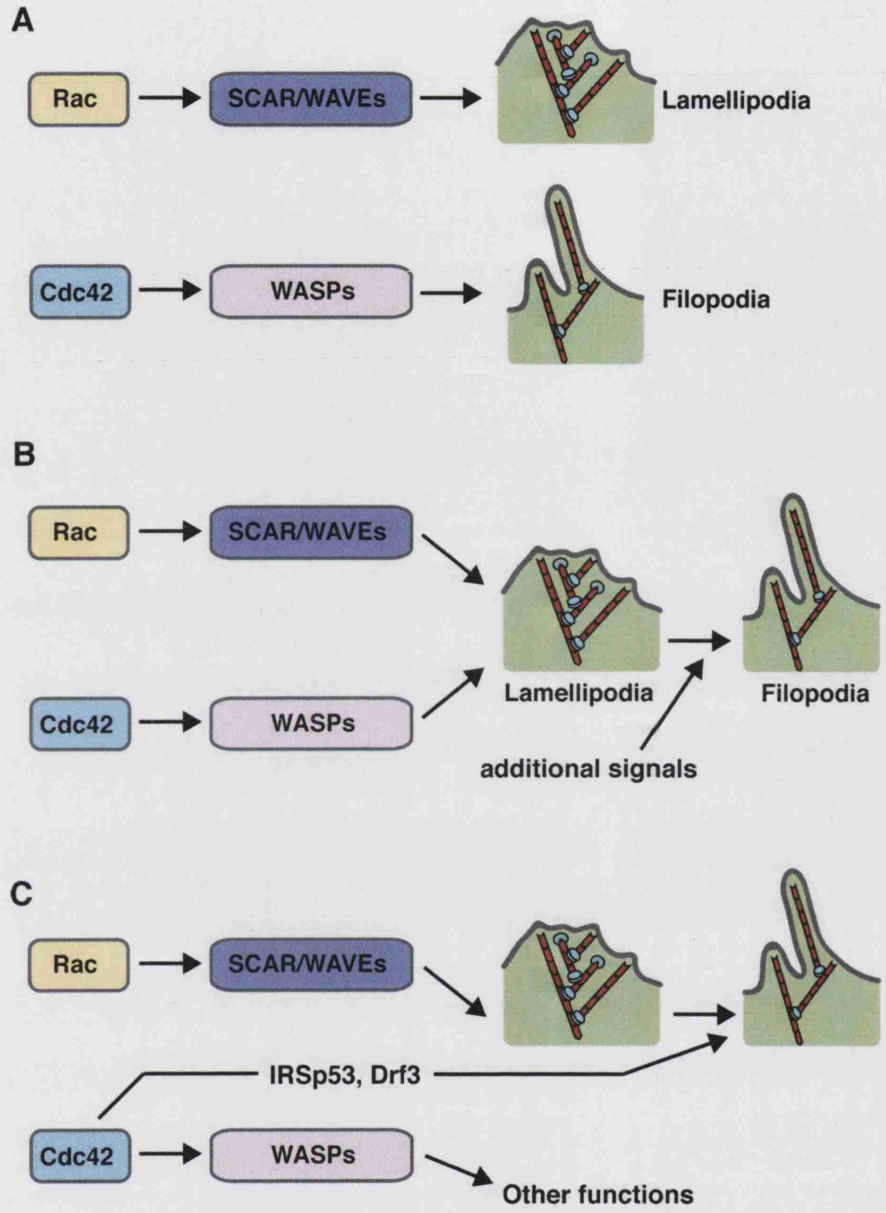

Figure 1.8 Alternative models for the control of actin protrusion assembly

Three different models have been suggested to explain the differential control of filopodial versus lamellipodial protrusion: (A) The Parallel pathways model. Lamellipodia and filopodia are regulated by two parallel pathways: lamellipodia via activation of Scar/WAVEs by Rac and filopodia through the activation of WASPs by Cdc42. (B) The Cascade pathways model. Rac and Cdc42 signal to Scar/WAVEs and WASPs to initiate lamellipodia assembly, which are subsequently transformed into filopodia by additional signals. (C) Refined cascade model. In cultured *Drosophila* cells Scar seems to be the major mediator of actin protrusion formation, suggesting a model whereby lamellipodia assembly is controlled by Rac and Scar and the subsequent transformation into filopodia occurs through Cdc42 and, perhaps, effectors such as IRSp53 and Drf3 (adapted from Biyasheva et al., 2004).

Drosophila cells at least, a cascade rather than parallel pathways are functioning (see Figure 1.8), with Rac activating SCAR leading to the assembly of lamellipodia, whilst the assembly of filopodia lies downstream of this and is controlled by the input of further factors, such as the recruitment of the anti-capping protein Ena/VASP by the Cdc42 effector IRSp53 (Krugmann et al., 2001), or even nucleation by members of the formin family (Peng et al., 2003).

1.6 FUNCTIONS OF ACTIN PROTRUSIONS IN DEVELOPMENT

Actin protrusions come in a variety of shapes and sizes, from the large web-like sheets of lamellipodia to the thin finger-like structures of filopodia and cytonemes. This section describes the diverse and expanding range of functions that actin protrusions have been found to carry out during development.

1.6.1 Cell migration and chemotaxis

The extension of actin protrusions is key to cell migration, providing mechanical pull and directionality for motility, whilst also giving cells a means to explore their environment during migration. Cell movements are used during development to shape the embryo in morphogenetic events such as dorsal closure, and also bring about the connections and interactions between cells, such as is seen during the wiring of the developing nervous system. Single cell migrations are necessary for the developmental dispersal of various cell lineages, such as hemocytes and germ cells, and later, rather similar cell migrations are pivotal in tissue repair and for the migration of inflammatory cells to sites of injury. Furthermore, the inappropriate activation of cell motility, such as during tumour cell metastasis or the recruitment of inflammatory cells in chronic inflammatory diseases such as arthritis can be extremely harmful to the individual and thus the study of cell migration has important clinical relevance. A great deal is known about the mechanics underlying the migration of single cells and the importance of actin protrusions in this motility, and these aspects will be explored below.

The migration of single cells is usually directional with the leading edge of a migrating cell extending a large lamellipodial sheet or pseudopodial process. In many cases cells find their way by following gradients of extracellular cues, a process called chemotaxis. The social amoeba, *Dictyostelium discoideum,* has proved a powerful model in which to unravel the mechanisms of chemotaxis, with *Dictyostelium* cells following various chemotactic signals during their life cycle. In particular, *Dictyostelium* cells secrete their own chemoattractant, cAMP, in order to bring individual cells together to participate in sexual or asexual developmental programmes (reviewed in Franca-Koh and Devreotes, 2004). Upon sensing a chemotactic gradient, a *Dictyostelium* amoeba switches from extending actin protrusions randomly around its circumference to assembling a large protrusion called a pseudopod at what will become the leading edge of the cell. To generate this polarisation the cell must restrict actin polymerisation to defined regions and this seems to be facilitated through the specific localisation of key signalling molecules to the front or rear of the cell.

Upon sensing a gradient, the earliest signs of asymmetry in a *Dictyostelium* cell is the complementary localisation of phosphoinositide-3 kinase (PI3K) and phosphatase and tensin homologue (PTEN). Stimulation with a chemoattractant leads to recruitment of PI3K from the cytosol to the plasma membrane, and this occurs where the cell is sensing the highest concentration of the attractant, and so defines the front, leading edge of the cell. Conversely, stimulation also leads to the dissociation of PTEN from the membrane, meaning that PTEN is restricted to the rear of the cell where the levels of chemoattractant are lower (see Figure 1.9). PI3K converts the lipid phosphoinositide-4,5-biphosphate (PIP_2) into phosphoinositide-3,4,5-triphosphate (PIP_3), whilst PTEN catalyses the reverse reaction, thus leading to much higher levels of PIP_3 at the leading edge of the migrating cell (Franca-Koh and Devreotes, 2004). It is then thought that PIP_3 acts to recruit PH domain containing proteins to the leading

edge. It certainly appears that the restriction of PIP_3 to the front of the cell helps determine the site of pseudopod extension as PTEN loss-of-function mutants in which PIP_3 levels are more generally elevated, assemble excessive actin protrusions often in directions other than towards the chemotactic gradient (Luo et al., 2003). However, the exact link between PIP_3 and actin protrusion assembly in pseudopod extension is not entirely understood, as, for example, it does not seem to act through WAVE/SCAR proteins as might be expected (Blagg et al., 2003). One suggestion is that PIP_3 helps to co-ordinate extension of the plasma membrane with actin polymerisation and pseudopod extension (Cox et al., 1999).

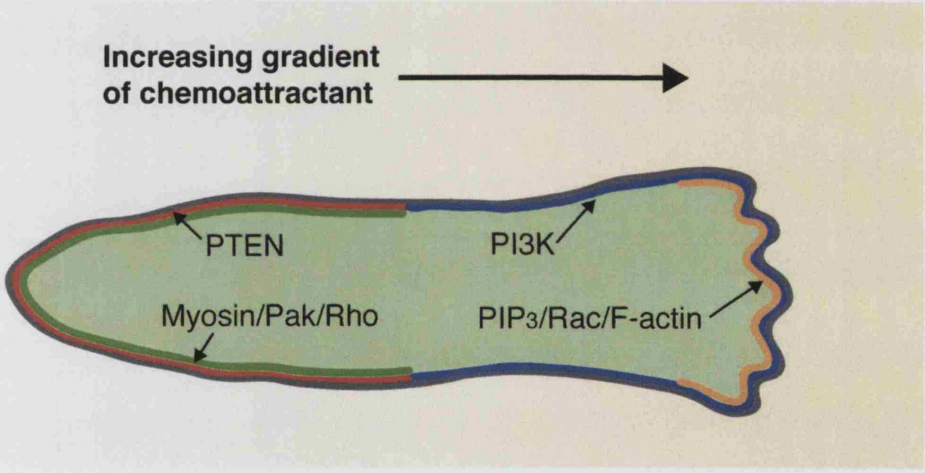

Figure 1.9 Localisation of key molecules during chemotaxis

The chemotaxis of *Dictyostelium* cells up a chemoattractant gradient correlates with the asymmetric localisation of various crucial molecules. PTEN (red) and Myosin, Pak and Rho (green) are restricted to the back half of the cell, whilst PI3K (blue) localises to the front, with PIP3, Rac and F-actin (orange) concentrated at the leading edge of the pseudopod (adapted from Franca-Koh and Devreotes, 2004).

Another connection between PIP_3 and pseudopod extension may run through the Rho small GTPases. Studies in cultured mammalian neutrophils, which migrate in a similar manner to *Dictyostelium* amoeba, have shown that active, GTP bound, Rac1 and Cdc42 concentrate at the leading edge during chemotaxis (see Figure 1.9). Expression of dominant negative versions of either of these GTPases leads to failures

in chemotaxis, with dominant negative Rac1 blocking chemoattractant induced actin polymerisation and dominant negative Cdc42 interfering with the persistence and direction of pseudopods (Srinivasan et al., 2003). Evidence is growing that PIP_3 sits upstream of the activation of these GTPases, restricting their activity to the leading edge of a migrating cell. Studies have shown that several Rac GEFs can be activated and recruited by PIP_3, and similarly the restricted activation of Cdc42 at the leading edge depends on the localisation of PIP_3 and the action of PI3K (Li et al., 2003b; Welch et al., 2002).

1.6.2 Inflammation and phagocytosis

Upon wounding or infection our bodies unleash a protective inflammatory response. Inflammatory signals released from the site of an injury draw specialised blood cells, neutrophils and macrophages, to the wound where they engulf cell and matrix debris, as well as microorganisms, and release signals that direct components of the wound healing process. An understanding of the mechanisms behind the chemotaxis of inflammatory cells has come from *in vitro* studies in *Dictyostelium* and cultured leukocytes, such as is described in the previous section. However, *in vivo* analysis of inflammation is shedding further light on this process, and *Drosophila* is proving a very useful system for such investigations due to its amenability to live imaging. These investigations show similarities to the *in vitro* data, but also reflect some crucial differences only seen when chemotaxis is studied in an *in vivo* setting (Stramer et al., 2005).

In *Drosophila,* the cellular equivalent to macrophages and neutrophils appears to be the hemocyte, as it travels through the adult fly or larvae, searching out and engulfing apoptotic debris and pathogens (Tepass et al., 1994). In embryos a single hemocyte lineage, the plasmatocytes, seem to fulfill this role. Live imaging of these hemocytes reveal that they extend large and dynamic lamellipodial sheets around their

circumference (Stramer et al., 2005). Laser wounding of embryonic epithelium late in development leads to the rapid recruitment of hemocytes to the site of injury. Hemocytes from up to 40μm away from the wound respond by polarising their lamellipodial protrusions to create a leading edge and then crawling towards the wound zone (Stramer et al., 2005).

Knocking out Rac activity, either by using a loss-of-function mutant or by expressing dominant negative *Rac1* in the hemocytes, leads to a dramatic reduction in the number of hemocytes recruited to wounds. Hemocytes lacking Rac produce much smaller lamellar protrusions compared to wild type and these hemocytes fail to disperse properly from their site of origin in the head, indicating the importance of the lamellipodia in the motility of these cells (Stramer et al., 2005). In contrast, hemocytes lacking Cdc42 still assemble lamellipodia and, in fact, appear more active than wild types, assembling more exuberant protrusions. These cells were found to be capable of chemotaxing to the wound although cell tracking studies indicated that they took a more tortuous route to the wound site than wild type cells (Stramer et al., 2005). This seems to suggest that Cdc42 is largely dispensable for hemocyte chemotaxis, although it does appear to play a role in maintaining the directionality of protrusion extension, and therefore motility, towards the wound. The fact that Cdc42 is not essential for inflammatory chemotaxis in the fly embryo seems at odds to work *in vitro* where this GTPase has been implicated in the sensing of chemotactic factors (Srinivasan et al., 2003), and perhaps shows the need for these movements to be studied *in vivo* as well as *in vitro.*

Once a hemocyte or macrophage has reached the wound it then begins its job of engulfing cell debris and pathogens. This process, called phagocytosis, is also carried out away from wounds as macrophages patrol normal tissues searching for, and

removing, apoptotic cells and other debris that are the consequence of the normal developmental programme. The assembly of action protrusions is essential to phagocytosis with engulfing cells seen to extend large cytoplasmic processes which wrap around the corpse or debris and drag it inside (Stramer et al., 2005).

1.6.3 Axon guidance

Another developmental process where actin protrusions play central role is in the wiring of the nervous system. In a wide range of animals the nervous system develops in the embryo via neurons sending out long projections called axons, which search out their specific targets to ultimately generate an intricate network of connections that innervate the body. Each axon must navigate the embryonic environment, following strict pathways to its target cell, and is guided along its route by a variety of molecular guidance cues (reviewed in Tessier-Lavigne and Goodman, 1996). At the growing tip of the axon is an actin-rich, hand-shaped structure called the growth cone. This highly dynamic structure consists of a number of filopodia joined by webs of lamellipodia and it is key to the ability of an axon to respond to guidance cues and navigate within embryonic tissues (Figure 1.10).

The growth cone is in a constant state of flux, extending and retracting filopodia and lamellipodia. Occasionally, the protrusions stabilise and when this happens the growth cone moves forward and axon is pulled along in its wake. Growth cone retraction appears to be driven by myosin II activity, and it seems to be the balance of myosin mediated retraction and actin polymerisation dependent extension which is key to the growth cone's function (Giniger, 2002); such that an attractant guidance molecule will push the balance towards actin polymerisation in the growth cone, and thus lead the axon towards the source, while a repellent cue favours retraction driving the growth cone to turn away. In a similar way, if a growth cone senses a repellent on one side, that portion of the structure will collapse causing the growth cone to turn in the opposite

direction (see Figure 1.10). Attractive and repulsive cues can be diffusible factors (as illustrated in Figure 1.10) or cell membrane tethered molecules. To date several key families of signalling molecules have been identified as pivotal in axon guidance; major players include: the semaphorin family of repulsive cues; netrins, which can mediate attraction or repulsion; ephrins, a family of cell surface bound cues; and slit, a repulsive midline cue that acts through its receptor, robo (Kidd et al., 1999; Tessier-Lavigne and Goodman, 1996).

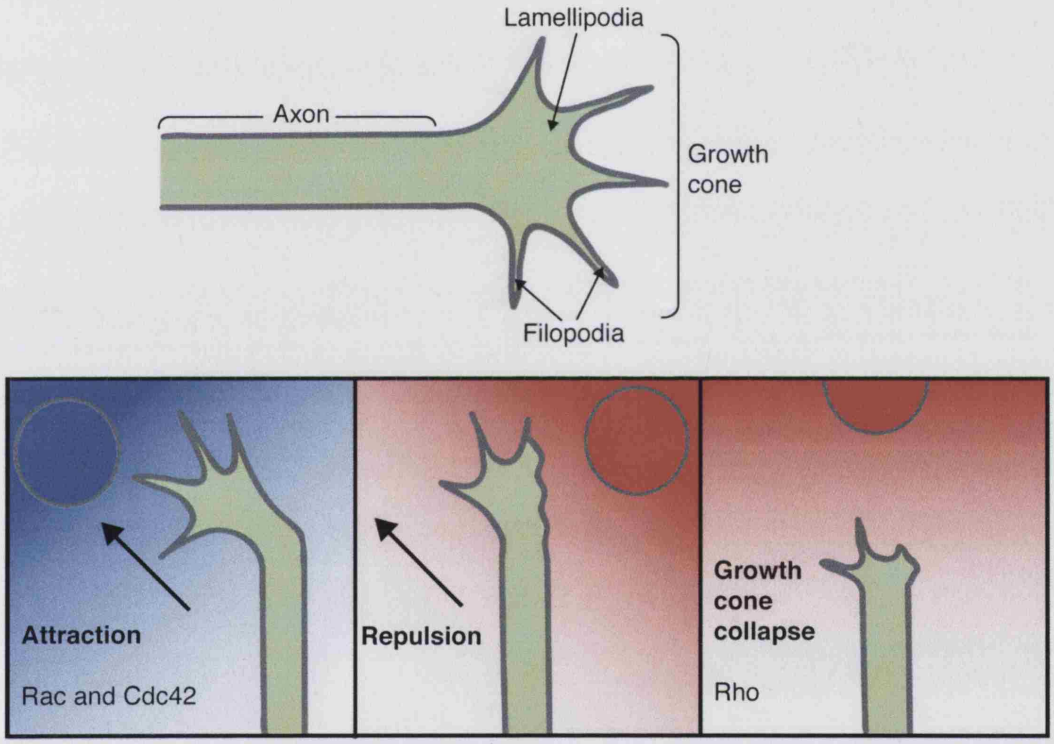

Figure 1.10 Control of actin dynamics in the growth cone of an axon

The growth cone of an axon is a "hand-shaped" structure which consists of lamellipodia and filopodia (top). During axon guidance the axon responds to guidance cues by altering the actin dynamics of the growth cone, such that an attractive cue (blue) leads to a stabilisation of actin protrusions causing the growth cone to move towards the source; whilst, a repulsive cue (red) leads to a collapse on one side of (centre), or the entire growth cone (right) causing the axon to turn away from that region. The Rho family of small GTPases have been implicated in the control of actin dynamics in the growth cone, with Rac and Cdc42 proving important for extension and stabilisation of the growth cone structures and Rho being involved in traction and collapse of the structure (collated with information from (Giniger, 2002).

With the clear importance of actin cytoskeleton dynamics in the axon guidance process it is, perhaps, unsurprising that the Rho family of small GTPases are implicated in this process. The speculation is that Cdc42 is involved in the extension of growth cone protrusions, with Rac acting to stabilise these structures, whilst Rho functions in the opposing action, driving myosin mediated retraction of the growth cone (Giniger, 2002). To endorse these ideas there is evidence that, at least some, axon guidance cues may feed into pathways containing the Rho GTPases. One example are the Plexins, a family of transmembrane receptors known to mediate the response of the growth cone to the Semaphorin family of repulsive axon guidance cues. Various experiments have implicated Rac and Rho as being effectors of Plexin. Both GTPases can bind the cytoplasmic domain of Plexin, Rac only when it is GTP-bound and active but Rho in either the GDP or GTP-bound form (Driessens et al., 2001; Hu et al., 2001). Genetic experiments in *Drosophila* indicate that Plexin is a positive regulator of Rho function, since reducing the dosage of Rho to half its usual amount rescues the axon misrouting phenotypes which are seen when Plexin is overexpressed in the embryo. In contrast, when the same experiment is carried out with Rac, reducing the levels of this GTPase increases the effects seen with overexpression of Plexin. These results suggest that Plexin has an inhibitory effect on Rac, maybe by binding and sequestering Rac-GTP and thus preventing its action. As Plexin can bind both the GTP and GDP-bound forms of Rho and, through genetic evidence appears to be a positive regulator of Rho function, it seems likely that Plexin is aiding the conversion of inactive, GDP-bound, to active, GTP-bound, Rho. Together these actions would mean that, in response to the presence of a Semaphorin, Plexin could mediate repulsion by simultaneously enhancing Rho activity and inhibiting Rac function, therefore switching the balance in the growth cone away from actin polymerisation and towards retraction.

1.6.4 Cell-cell communication and signalling

Recently, evidence has been growing that filopodia play a further intriguing role during development, in cell-cell communication and long-range signalling (reviewed in Bryant, 1999). Long thin filopodia, sometimes known as cytonemes, have been seen projecting long distances between cells in a variety of tissues. In sea urchin embryos filopodia 0.2-0.4μm in diameter and up to 80μm long are seen projecting across the blastocoel cavity from primary mesenchyme cells to ectoderm cells on the opposite side (Miller et al., 1995). It is thought that these protrusions may allow communication between the two cell types since, although the two populations are a large distance apart, it is known that the ectodermal cells exert influence over the development of the primary mesenchyme. Long, thin filopodia are also apparent during the development of the fly tracheal system, where terminal tracheal cells extend long processes to oxygen deprived cells as a precursor to the establishment of a mature network delivering air to internal tissues (Jarecki et al., 1999).

The best evidence that these protrusions may participate in long range signalling has come from the cytonemes observed in *Drosophila* imaginal discs (Ramirez-Weber and Kornberg, 1999). Imaginal discs are highly patterned sacks of epithelial cells that develop in the larvae and unfold during metamorphosis to generate the majority of adult structures, and have proved to be an excellent model in which to study patterning events. However, it was not until live imaging was carried out that imaginal disc cells were seen to extend long actin-rich cytoneme protrusions, as these fragile extensions are easily destroyed by fixation. A crucial aspect of patterning in the wing imaginal disc is that morphogenic signals appear to travel over large distances. For example, Dpp is expressed in a narrow stripe in the centre of the disc and is then thought to regulate the expression of various target genes in a concentration dependant manner, influencing cells even as far away as the very edge of the wing disc. However, a major

problem with this long distance gradient model of signalling is that some morphogenetic signals, including Dpp, are not thought capable of diffusing such distances. Possible alternative explanations for how long range signalling can occur in the wing disc are that morphogens may be are packaged up into small vesicles called argosomes (reviewed in Cadigan, 2002), or potentially delivered these distances by cytonemes, as discussed below.

Co-culturing different fragments of wing discs showed that cells from anterior or posterior regions of the disc could be induced to extend cytonemes if they were cultured next to cells taken from the central, *dpp* expressing, region of the disc. In these cases the anterior and posterior cells extended long protrusions, some as long as 700μm, which were all orientated towards the central region derived cells (Ramirez-Weber and Kornberg, 1999). With such definite directionality it seems likely that the cytonemes may be extending in response to a chemoattractant produced by the signalling centres found in the central region. Fibroblast growth factor (FGF) may be the chemoattractant which induces cytoneme assembly in the wing imaginal disc, as anterior cells cultured either with beads coated with FGF, or fly S2 cells expressing FGF, extend long protrusions towards the source of FGF (Ramirez-Weber and Kornberg, 1999). Coincidently, the chemoattractant signal that directs the growth of cell extensions towards oxygen deprived regions in the developing tracheal system of the fly also appears to be FGF (Metzger and Krasnow, 1999).

The evidence presented above suggests that long filopodial protrusions may play a role in mediating the dispersal of a morphogenic signal. However, one key question which still remains is how such a system could deliver a graded level of morphogen to cells depending on their location in the tissue undergoing patterning. Perhaps this could be explained by simple actin dynamics, in that cells closer to the source of

morphogen would need to form much shorter protrusions than those further away to come into contact with the signal, or possibly there could be a mechanism involving degradation of the morphogen or a second message as it travels back along the cytoneme towards the cell body.

1.6.5 Epithelial fusion

There are numerous stages in the development of a wide range of embryos, including dorsal closure in the *Drosophila* embryo, where a gap in an epithelial layer must be closed over and tightly sealed. In a similar way, holes caused by injury must be rapidly closed and fused to maintain the protective epidermal barrier. These movements are explored in more detail, and compared with dorsal closure, below (Section 1.7). There is growing evidence that actin protrusions play crucial roles in many diverse episodes of epithelial fusion. Actin protrusions can be used to help the two epithelial surfaces migrate towards one another, rather as occurs in the migration of single cells (described in section 1.6.1), except that in the case of epithelial migrations the leading edge involves the co-ordinated contribution of many cells, requiring extra levels of regulation to maintain coherent movement of the epithelium as a whole. Dorsal closure reveals another specialised role for actin protrusions in epithelial fusion. Here filopodia exhibit a sensing function, allowing cells of the leading edge to identify their correct segmental partner on the opposing epithelial sheet (Jacinto et al., 2000). Whilst, clearly, many epithelial fusion events do not involve the alignment of segments, this function in dorsal closure could indicate a more general sensing role for actin protrusions during epithelial fusions perhaps allowing cells to respond to "contact inhibition" type cues telling them when they have contacted the opposing epithelial edge. However, possibly the clearest role for actin protrusions in epithelial fusion events comes right at the end as the two sheets seal together.

Primary mouse keratinocytes grown in culture can be induced to form monolayers with the addition of Ca^{2+}. The keratinocytes extend numerous filopodia and when filopodia from opposing cells make contact they slide upon each other and "embed" themselves into the neighbouring cells (Vasioukhin et al., 2000). As described previously in section 1.3.1, E-cadherin-catenin complexes cluster at the tips of the keratinocyte filopodia and these complexes mature into strong cell-cell adhesions between the two cells (Vasioukhin et al., 2000). The interdigitation of filopodia to zip two sheets of cells together seems to be a well conserved mechanism in epithelial fusion events, visualised particularly clearly in dorsal closure and the related process of ventral enclosure in the *C.elegans* embryo, which is explored in the following section.

1.7 COMPARISONS BETWEEN DORSAL CLOSURE AND OTHER EPITHELIAL FUSION EVENTS

1.7.1 *C. elegans* ventral enclosure

The process of ventral enclosure in the nematode worm, *C. elegans,* shares many similarities with *Drosophila* dorsal closure (see Figure 1.11). Like dorsal closure, ventral enclosure involves the closure of a large hole in the epidermis of the embryo, in this case on the ventral surface. The process begins when four epithelial cells, so called "leading cells", positioned in pairs at the anterior end of the hole, begin to extend filopodia and move towards the ventral midline of the embryo. Like the filopodia assembled by the leading edge during dorsal closure, the protrusions are crucial for the fusion of these cells at the midline and so are ultimately required for the completion of ventral enclosure (Raich et al., 1999; Williams-Masson et al., 1997). Studies of ventral enclosure have elegantly shown that adherens junction components localise to the filopodia that are extended by leading cells, and that filopodial contact appears to prime cadherin mediated adhesion and junction formation (Raich et al., 1999). The movement of the leading cells pulls the epidermis around towards the ventral side of the embryo but completion of ventral enclosure requires the coordinated elongation

and contraction of a second population of cells, called "pocket cells", which line the edges of the hole posterior to the leading cells. Once the leading cells have fused they

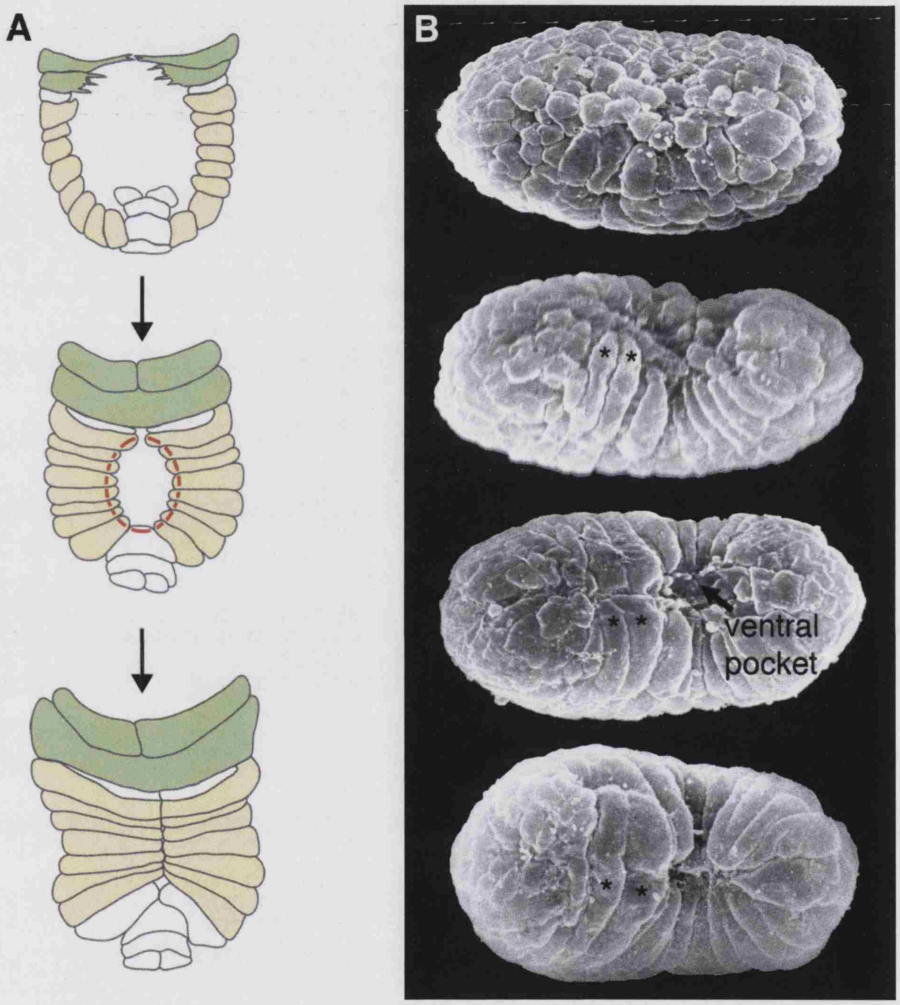

Figure 1.11 Ventral enclosure in the *C.elegans* embryo

C. elegans ventral enclosure is an epithelial fusion event which shares many similarities with dorsal closure. (A) Schematic diagrams illustrating ventral enclosure: the process starts as the four leading cells (green) assemble filopodia and begin to migrate ventrally. Once the leading cells have met at the midline, the pocket cells (yellow) assemble an actin cable and "purse-string" the hole closed (adapted from Williams-Masson et al., 1997). (B) A set of scanning electron micrographs of a *C. elegans* embryo undergoing ventral enclosure, leading cells are highlighted with asterisks (reproduced with permission from (Martin and Parkhurst, 2004).

begin to contract their apices and elongate along the dorsoventral axis, just as *Drosophila* leading edge cells elongate at the start of dorsal closure. In addition, actin accumulates at the apical edge of the pocket cells and is thought to form a cable that closes the hole by purse-string contraction. Laser ablation of regions along this edge release tension in the closing epithelium, just as is seen in similar cable ablation studies in dorsal closure (Kiehart et al., 2000; Williams-Masson et al., 1997).

1.7.2 Epithelial fusion events in vertebrate embryonic development

Development of the vertebrate embryo also involves a number of epithelial fusion events, including neural tube closure, palate fusion and mammalian eyelid closure. Strikingly, many of the mechanisms and signalling pathways underlying these fusions appear to be shared with *Drosophila* dorsal closure. The vertebrate neural tube is formed from an originally flat layer of neural plate cells which fold upon each other to form a tube. In order for the neural tube to close, the lips of the folding neural plate must be drawn together and then fused at several nucleation sites using a zippering mechanism similar to that seen in the final fusion of the epithelium in dorsal closure (reviewed in Colas and Schoenwolf, 2001). An actin network can be seen just below the apical surface of the neural plate cells and cytochalasin blocking experiments indicate that active actin polymerisation is required for the folding of the neural tube, at least in the cranial region (Morriss-Kay and Tuckett, 1985; Ybot-Gonzalez and Copp, 1999). Like dorsal closure, Rho GTPase activity is also required to close the neural tube, as the blocking of the Rho activator, Rho Kinase (ROCK) leads to a failure in this process as well as disruption of other morphogenetic movements in the mouse embryo (Wei et al., 2001). JNK1/JNK2 knockout mice also fail in neural tube closure, indicating that a JNK pathway is functioning here, just as in dorsal closure (Sabapathy et al., 1999).

Another midline fusion event in the vertebrate embryo is the closure of the secondary palatal shelves. Whilst many of the cleft palate phenotypes seen in knockout mice are likely to be a failure in the machinery that pushes the shelves together early in the process, it also appears that, just as in dorsal closure, actin protrusions are required for the final fusion of the two surfaces. The assembly of filopodia during palate fusion has been found to be dependent on TGFβ signalling, since TGFβ3 knockout mice fail to form filopodia as the palatial shelves come together, ultimately resulting in KO mice being born with a cleft palate (Taya et al., 1999).

The transient fusion of eyelids in the late gastrulation of many mammals is an event, which, superficially at least, bears startling resemblances to *Drosophila* dorsal closure. As the eyelids approach each other they extend filopodia allowing the edges to zip together from the nasal and lateral margins of the eye; electron microscopy shows that these protrusions interdigitate as the eyelids close, just as is seen in dorsal closure. These outward similarities also seem to be extended to the signalling pathways involved in the two processes as it appears that the JNK pathway is also crucial for eyelid closure because mice in which c-Jun is conditionally inactivated in keratinocytes, fail to complete eyelid close and are born with their eyes open (Zenz et al., 2003).

1.7.3 Wound healing

The closure of a hole caused by a wound in adult or embryonic epithelium is perhaps the most clinically relevant system to which clues gleaned from the study of dorsal closure can be applied. The mechanisms and signalling pathways used to close gaps in epithelial tissue during normal embryonic development appear to be largely reused when tissue is wounded either in the embryo or adult. The closure of wounds requires a number of co-ordinated cell migrations, all of which are dependent the actin cytoskeleton, much as has been described for dorsal closure.

Wound healing in adult mammalian tissue starts with the formation of a fibrin-rich clot and continues several hours later when keratinocytes at the cut edges begin to migrate to cover the hole. Just like leading edge cells in dorsal closure, keratinocytes in the front few rows of the migrating edge extend actin protrusions, which aid their migration and ultimately help seal the edges as they come into contact. Another crucial aspect of adult wound closure is the contraction of granulation tissue situated deep within the wound, which helps bring the cut edges together (reviewed in Martin, 1997; Werner and Grose, 2003). Some basic comparisons can be drawn between the role of granulation tissue in wound healing and the amnioserosa in dorsal closure, as both play active contraction roles which draw the epithelial edges towards each other. However, obvious differences do exist between these two tissues; granulation tissue is formed by the migration and proliferation of fibroblasts, whilst the amnioserosa is present from the start of dorsal closure and is an epithelial layer that is itself continuous with the migrating leading edge.

The signalling pathways used in morphogenetic events such as dorsal closure, are reused in wound healing, although the initial cues used to activate these cascades are probably different in the two scenarios. There is clear evidence from both adult and embryonic wounding models, that activation of the AP1 transcription complex is a vital early step in wound closure. Indeed, wounding adult flies leads to expression of the AP1 target, *puc*, around the wound site, and mild mutant alleles of *kay* show retarded healing (Ramet et al., 2002). Similarly, mice with targeted knockout of c-Jun in the epithelium show subtle wound healing defects, as well as the failure in eyelid fusion, as described in the previous section (Li et al., 2003a). However, unlike dorsal closure, activation of the AP1 complex in wound healing is not solely dependent on the JNK cascade, but instead it may be that mechanical damage to cells at the wound site triggers AP1 activation. Studies with *in vitro* scrape wounds have found that the influx

of Ca^{2+} into damaged front row cells after wounding leads to a wave of purine signalling, which in turn results in AP1 activity in cells just back from these damaged cells (Klepeis et al., 2001). Just as in dorsal closure expression of TGFβ is thought to be a downstream consequence of AP1 activation. In the case of wounding, TGFβ1 is expressed in the epithelium following AP1 activation and is subsequently released into the wound mesenchyme, and, in a paracrine fashion, triggers the contraction of this tissue (Martin et al., 1993).

In all adult wounds, tissue damage results in a robust inflammatory response in which neutrophils and macrophages, or their equivalent, chemotax to the wound site. Once at the wound these specialist white blood cells clear the damaged area and help fight infection. However, inflammation seems to be inextricably tied to the scarring and fibrosis seen when adult wounds heal, as wounds in embryos, where the inflammatory system is still developing, heal without a scar (reviewed in Redd et al., 2004). Moreover, PU.1 knockout mice, which lack neutrophils and macrophages show reduced fibrosis at wound sites (Martin et al., 2003). In both the wild type embryo or in PU.1 null neonatal mice, an important consequence of lacking a normal, adult, inflammatory response is a dramatic alteration in the profile of cytokines and growth factors normally released from the wound site during healing (Cooper et al., 2005; Martin et al., 2003; Whitby and Ferguson, 1991). A key factor, reduced in these cases, is TGFβ1, and it therefore appears that TGFβ1 could become an important therapeutic target to prevent the scarring process. Indeed, reducing the activity of TGFβ1 at wound sites in adult rats, by the addition of antibodies and via other strategies, leads to repair with reduced scarring (Shah et al., 1992; Shah et al., 1994; Shah et al., 1995).

Perhaps, the closest similarities between wound healing and dorsal closure come from comparisons of the actin machineries used to close epithelial holes in the two

scenarios. Embryonic wounds are of special clinical interest as they heal without leaving a scar, probably because of the lack of a mature inflammatory system (Martin et al., 2003). A striking aspect of embryonic wound healing is the assembly of an actin cable around the circumference of the wound, which, as in dorsal closure, associates with myosin to drive purse-string closure of the wound. Rho GTPase activity is essential for the formation of the actin cable and if cable assembly is inhibited by the addition of cytochalasin D or the Rho GTPase blocker, C3 transferase, wounds fail to re-epithelialise (Brock et al., 1996; McCluskey and Martin, 1995). In contrast to embryonic wound experiments, the majority of adult wounds that have been studied do not form strong actin cables, but rather closure appears to rely more heavily on the lamellipodial crawling of keratinocytes. However, it is certainly not the case that actin cable assembly is restricted to embryonic epithelium alone, as some adult wounds have been shown to assemble these structures, such as is seen when small wounds are made to the cornea of adult rabbits (Danjo and Gipson, 1998). Instead it appears that the choice between purse-string contraction and lamellipodial crawling may depend on the size and, perhaps, shape of the wound, with purse-string contraction being used to close small wounds in adult epithelium. Indeed, *in vitro* wounds made in the gut epithelial cell line, $Caco2^{BBE}$, close using different combinations of actin machinery, seemingly dependent on hole size, with small holes assembling a cable and closing via purse-string contraction, larger wounds closing by crawling and middle sized using a combination of these methods (Bement et al., 1993). This distinction is interesting when dorsal closure is considered as it too seems to utilise a combination of strategies to close a hole – purse-string contraction and epithelial zippering, which is presumably necessary to maintain the smooth epithelial surface and prevent the puckering which would surely result if purse-string contraction was used alone.

Live imaging of wound closure in *Drospohila* embryos has revealed further similarities in the roles of the actin cytoskeleton in wound healing and dorsal closure (Wood et al.,

2002). Small laser wounds can be made in the epithelium late in embryogenesis and their closure can be easily followed live using the expression of GFP-fusion proteins. Like dorsal closure, an actin cable assembles around the margin of the wound hole and associates with non-muscle myosin to form a contractile purse-string. At the same time, cells at the leading edge of the wound begin to extend actin protrusions, predominantly filopodia early in closure, with lamellipodia largely only being assembled once the opposing filopodia have first confronted one another. Just as in dorsal closure, the filopodia are seen reaching across the gap to interact with protrusions produced on the opposite side, and once contact is made they appear to help tug the wound closed.

The roles of the actin cable and filopodia in these wounds were further dissected by knocking out the function of Rho and Cdc42, respectively. In *Rho1* mutants, the embryo fails to assemble a cable around the wound hole, and consequently very little contraction of the wound edges occurred (Wood et al., 2002). However, filopodia do form at these wounds, and, in fact, are seen in larger quantities and are significantly longer than in wild type, suggesting that as in dorsal closure, the presence of the cable seems to restrain protrusion formation by the leading edge. Despite the lack of a cable, wounds in *Rho1* mutants do eventually close although they take almost twice as long as their wild type counterparts. After a long lag phase where very little closure takes place, the mutant wounds begin to close via interactions between filopodia in neighbouring cells. The actin protrusions form small foci around the circumference of the hole which zip together and ultimately seal the entire hole. However, if the actin cable is present, the role of the filopodia in the closure of these wounds seems to be limited to the final fusion event of healing. This is seen when dominant negative *Cdc42* is expressed in the epithelium around the wound, as whilst the cells around the wound edge fail to assemble actin protrusions in the absence of Cdc42 activity, these wounds close as quickly as their wild type equivalents, but cannot complete the final fusion to

seal the hole shut (Wood et al., 2002). This finding again reinforces the crucial role that filopodia appear to play in the fusion of two epithelial surfaces in a wide variety of events, including dorsal closure.

In my thesis I aim to define dorsal closure in greater detail using live imaging, and in particular will focus on the assembly and function of actin protrusions during this dynamic process. Firstly, I describe a detailed live analysis of wild type closure, which will provide a more comprehensive framework on which to compare mutant embryos. Secondly, I go on to investigate the role of the small GTPase, Rac, during closure and finally begin to explore a subset of unconventional myosins, which may prove to be important new players in actin protrusion function during dorsal closure

CHAPTER 2

Materials and Methods

2.1 FLY STOCKS AND GENETICS

Flies were cultured and crossed on yeast-cornmeal-molasses-malt extract medium at 25°C. The *Drosophila* lines used in this study are: *e22c-GAL4* (Brand and Perrimon, 1993); *UAS-GFP-actin, UAS-α-catenin-GFP* (Oda and Tsukita, 1999; Verkhusha et al., 1999); *en-GAL4-UAS-GFP-actin* (recombinant produced with stocks from Bloomington Stock Center and H.Oda); *UAS-Rac1^{N17}*, *UAS-Rac1^{V12}* (Luo et al., 1994); *Rac1^{J10} Rac2Δ mtlΔ /TM6B* and *Rac1^{J11} Rac2Δ mtlΔ* /TM6B (Hakeda-Suzuki et al., 2002); *UAS-hep^{CA}* (Adachi-Yamada et al., 1999); #11290: line carrying a P-element inserted 7kb upstream of *Myo10A* and #3612: *Δ2-3, Dr/TM3*, transposase line used to remobilise P-element (Bloomington Stock Center).

2.1.1 Generation of triple *Rac* germ line clones

Rac1^{J10} Rac2Δ mtlΔ germ line clones were generated using hsFLP with an ovo^{D1} insertion on the FRT80B chromosome (Hakeda-Suzuki et al., 2002). Heterozygous 2nd and 3rd instar larvae were heat-shocked at 37°C for 2hrs on consecutive days and the appropriate adult females were then crossed to *Rac1^{J10}Rac2ΔmtlΔ* males. For live imaging, *Rac1^{J10}Rac2ΔmtlΔ* and *Rac1^{J11}Rac2Δ mtlΔ* stocks were generated which carried *UAS-GFP-actin*, *UAS-α-catenin-GFP* or *e22c-GAL4* on the second chromosome. These were then crossed to produce zygotic triple *Rac* mutant embryos expressing GFP-actin or α-catenin-GFP.

2.1.2 Selection of triple *Rac* mutants

For live imaging, triple *Rac* mutants were selected by their dorsal closure phenotype which was clear under the confocal microscope and always observed in the appropriate Mendelian proportions, including when the *Rac* stocks were outcrossed. For *in situ* hybridisation, mutant embryos were selected using a GFP balancer (TM3, twi-*GAL4*, UAS-EGFP; from Bloomington Stock Center) prior to fixation. *Rac1^{J10} Rac2Δ*

mtlΔ stocks carrying UAS-GFP-actin were also employed to generate *Rac1*^{J10} *Rac2Δ mtlΔ* germ line clone embryos for live imaging using the scheme described above. Cuticle preparations (see Section 2.5) of these lays confirmed a similar range of phenotypes to those described previously (Hakeda-Suzuki et al., 2002), and as a result *Rac1*^{J10} *Rac2Δ mtl* germ line clone embryos to be used for imaging were selected by phenotype.

2.1.3 Rescue of triple *Rac* mutant phenotype with *UAS-hep*^{CA}

For rescue of the zygotic *Rac1*^{J11}*Rac2Δ mtlΔ* phenotype, *UAS-hep*^{CA} (Adachi-Yamada et al., 1999) on the second chromosome was crossed into a background of *Rac1*^{J11}*Rac2Δ mtlΔ*. Expression of *UAS-hep*^{CA} with the epithelial driver, *e22c-GAL4* produced severe early embryonic lethality (data not shown) that masked the *Rac1*^{J11}*Rac2Δ mtlΔ* phenotype, so rescue experiments were carried out using leaky expression of *UAS-hep*^{CA} in the absence of a driver. Embryonic lethality was compared for *Rac1*^{J11}*Rac2Δ mtlΔ* stocks in the presence or absence of *UAS-hep*^{CA}, and cuticle preparations of these dead embryos were assessed to determine the category of dorsal closure phenotype (puckered or wildtype-like fused seam).

2.1.4 Mobilisation of P-element to generate *Myo10A* mutant

Bloomington line #11290, EP1321 (hereafter referred to as *p(Myo10A)w*$^{+}$) carries an "EP" transposable element insertion containing the mini-white (w^{+mc}) gene, situated 7.8kb upstream of the 5' end of the *Myo10A* gene on the first chromosome (Figure 2.1). In an attempt to generate a *Myo10A* transcriptional null mutant by P-element excision, the transposable element was remobilised by crossing to the transposase stock #3612 (*Δ2-3,Dr/TM3*); for the crossing scheme see Figure 2.2. Females in which the P-element had excised, (*p(Myo10A)w**), were selected by light orange eye colour and individually crossed back to the FM7a balancer line. Revertant lines which gave

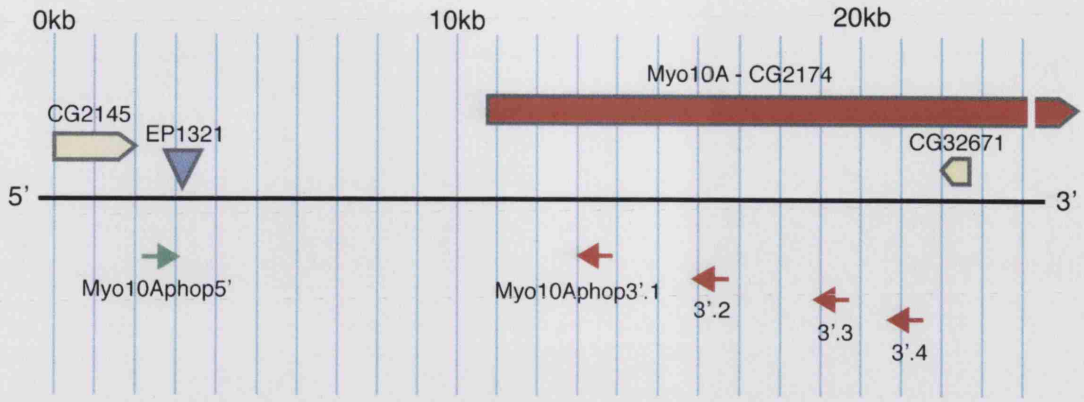

Figure 2.1 Location of an EP transposable element upstream of *Myo10A*

The *Myo10A* gene region is shown, with *Myo10A* in red (only the first ~13kb of *Myo10A* is shown, the full length of the gene is 25,598 bases). The transposable element, EP1321 (blue triangle), is inserted 7.8kb upstream of *Myo10A*. The two other genes closest to the P element are CG2145 and CG32671, the latter is located within the third intron of the *Myo10A* transcript. The approximate locations of PCR primers designed for screening potential P-element excisions of the 5' end of *Myo10A* are also shown (forward primer green arrow; reverse primers, red arrows).

Primer name			**Sequence**	
Myo10Aphop5'	fwd	5'	GACAACCCTGCAGTTGCACTCTTTCG	3'
Myo10Aphop3'.1	rev	5'	TGGACAGTCGCTTGACCACTTGTGGA	3'
Myo10Aphop3'.2	rev	5'	AACTGCACCAGAATCTCATCCCGCAAT	3'
Myo10Aphop3'.3	rev	5'	AGATGCAGATGGTGACTGCTGAT	3'
Myo10Aphop3'.4	rev	5'	TATCATACTGATCAGTAAAGTCAACCG	3'

Table 2.1 PCR primers for screening potential *Myo10A* excision mutants

Sequences of the oligonucleotides designed to screen for excision of the 5' end of the *Myo10A* transcript using PCR.

*p(Myo10A)w** males, and were therefore homozygous viable for the excision, were classed as precise excisions and discarded.

Of the approximately 150 remobilisation crosses which were set up, 6 imprecise excision lines were generated. To determine the extent of genomic excision, a PCR screening scheme was designed and is illustrated in Figure 2.2, with primer sequences shown in Table 2.1. In this scheme, only excisions which removed the required 5' region of the *Myo10A* gene would generate a PCR product. Single fly PCR preparations were carried with each of the 6 revertants and 4 primer pairs as described previously (Saiki et al., 1988). One *p(Myo10A)*/FM7a* revertant line, #76, gave a PCR product with primer Myo10Aphop3'.3. This fragment was cloned into the p*(Bluescript)* vector and sequenced. However, sequencing revealed that mis-priming had occurred as the cloned fragment was not from the *Myo10A* gene region. This could indicate that line #76 contains a very large excision which takes out a portion of genomic DNA that extends beyond the designed PCR primers.

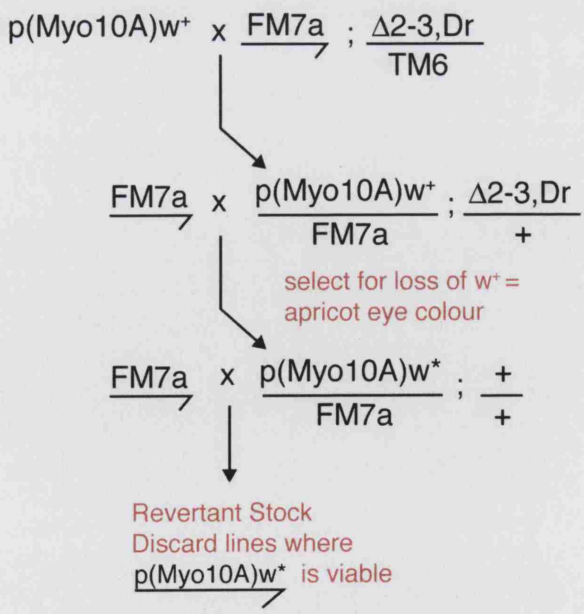

Figure 2.2 Crossing scheme for remobilisation of transposable element EP1321

The *p(M10A)w*$^{+}$ line was crossed with a transposase, *Δ2-3*, stock and the F1 generation was crossed back to the FM7a balancer. The F2 generation, which no longer carried the transposase, were screened for a loss of the P-element by scoring eye colour. Selected flies were crossed individually back to FM7a and maintained as revertant stocks. Lines in which *p(M10A)w** males were viable were classed as precise excisions and were discarded.

2.2 CLONING AND PROBE PRODUCTION

2.2.1 Cloning for *crinkled* and *Myo10A* dsRNA injection

A full length *crinkled* (*ck*) cDNA (LD14917) was obtained from the Berkeley *Drosophila* Genome Project (BDGP); for *Myo10A* a partial cDNA encoding the last (3') 4kb of *Myo10A* (LP03318) was obtained from BDGP. To generate *Myo10A* double stranded RNA (dsRNA) for injection, first a 360bp sequence from the 3' end of the *Myo10A* cDNA was amplified using PCR as either a 5'*Kpn*-3'*Eco*RI or 5'*Xba*I-3'*Eco*RI fragment. The two fragments were then cloned separately into the p(Bluescript) plasmid and these were used as templates for transcription reactions. Each template was linearised with *Kpn*-1 and single-stranded RNAs (ssRNA) were transcribed from the T7 promoter present in p(Bluescript) using the Megascript RNAi production system (Ambion). In this way two complementary single stranded *Myo10A* RNA fragments were transcribed and could then be annealed and purified as per the kit protocol to give *Myo10A* dsRNA. An identical scheme was used to generate a *ck* dsRNA fragment from a 420bp portion of the 3' end of the *ck* cDNA.

2.2.2 Cloning of Myo10A RNA interference snapback construct

A construct that would generate a double-stranded hairpin of Myo10A RNA (refered to here as an "RNAi snapback") when transcribed *in vivo* was designed as shown in Figure 2.3. To build the snapback construct the 5'*Xba*I-3'*Eco*RI cDNA fragment of Myo10A described in the previous section (2.2.1) was reutilised. The corresponding region of genomic DNA was amplified by PCR from genomic template DNA as a 5'*Kpn*I-3'*Eco*RI. This genomic Myo10A fragment was cloned into p(Bluescript) alongside, and in the opposite orientation to, the 5'*Xba*I-3'*Eco*RI cDNA fragment. The genomic fragment of Myo10A contains a single intron, whose post-transcriptional removal by splicing machinery is thought to aid the formation of dsRNA snapbacks. The snapback cassette was then subcloned into the UAS expression vector, pUASp,

(Rorth, 1998; Rorth et al., 1998) in preparation for embryonic injection (see Section 2.3.2)

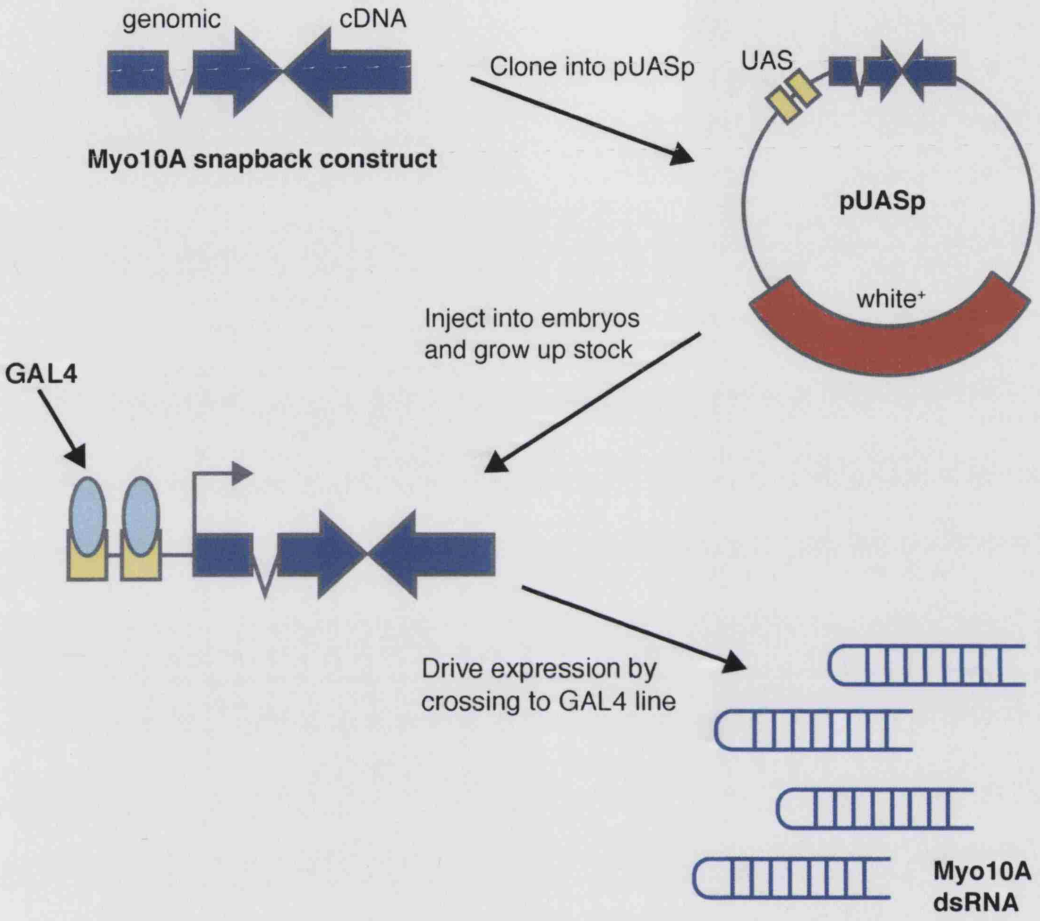

Figure 2.3 Schematic of *Myo10A* RNAi snapback design

An RNAi snapback cassette consisting of complementary fragments of the genomic and cDNA sequence of *Myo10A* was cloned into the UAS expression vector pUASp. This was then injected into embryos and snapback stocks were generated that could then be crossed to GAL4 driver lines, leading to tissue specific expression of *Myo10A* double stranded RNA.

2.2.3 Myo10A Antibody Production and Characterization

Three hydrophilic regions of Myo10A tail were chosen to generate antigen for polyclonal antibody production, it was ensured that the short (100bp) sequences selected (named 1608, 2083 and 2565, according to their start position in the Myo10A amino acid sequence), would recognise only Myo10A by running a BLAST sequence

search with each. The fragments were amplified from the Myo10A tail cDNA, LP03318, and cloned, in frame, into the GST vector, pGex3x. Balb/c BYJ Rb(8.12) 5BNR/J mice (Jackson Labs) were immunized with each GST-Myo10A protein and sera were collected. Antibody specificity was tested via Western blot using wildtype *Drosophila* whole cell extract (from 0-2hr embryos), which was a gift from T. Tsukiyama.

2.3 EMBRYO INJECTION

2.3.1 RNA interference (RNAi) in embryos

ck and *Myo10A* dsRNA were generated as described in Section 2.2.1. Preparation and injection was conducted as described previously (Kennerdell and Carthew, 1998). Isogenic w^{1118} embryos aged 15-45 mins, were hand dechorionated and injected at roughly 50% egg length with dsRNA (5 μM) or buffer control. Injected embryos were left to develop for 24hrs at 25°C, after which time lethality was counted and cuticle preparations of dead embryos were examined.

2.3.2 Germline transformation

The UAS-Myo10A-snapback vector (described in Section 2.2.2, 500 μg/ml) was injected along with the pTURBO helper plasmid (100 μg/ml) (Mullins et al., 1989) into isogenic w^{1118} flies as previously described (Spradling, 1986). Transgenic flies were scored by eye color and the insertions were mapped at the chromosome level and balanced using standard genetic methods.

2.4 LIVE IMAGING

Embryos expressing GFP-actin or GFP-α-catenin were dechorionated in bleach for 2 mins, rinsed in dH_2O and then mounted in Voltalef oil under a coverslip for live imaging using a Leica TCS SP confocal system. Images compiled from four or six confocal

optical sections (each averaged two times) were collected every minute. The time-lapse series were assembled and analysed using Image J software.

2.4.1 Quantification of amnioserosal contraction

For detailed quantification of wild type amnioserosal contraction, changes in amniserosa cell area were followed through the course of dorsal closure using expression of GFP-α-catenin. The amnioserosa was split into 5 regions or zones, a central region, 2 "canthi" ends and 2 intermediate areas (see Figure 3.2). Individual cells from each zone were followed live and their surface area measurements taken at 10 minute intervals (n=107 cells total). The manner in which each cell was lost from the surface, either extrusion from the amnioserosal layer or vanishing under the advancing leading edge, was also recorded.

To compare the relative movements of the amnioserosa and the leading edge in dorsal closure, pairs of cells from the lateral edges of the amnioserosa were selected and the distance between the cells were measured at 10min time points during closure. Five pairs of cells, distributed across the anterior-posterior axis of the amnioserosa, were followed through closure (see Figure 3.4). For each cell pair the changing distance between the adjacent epithelial leading edges was also recorded to allow for direct comparison between the rate of amnioserosa tissue contraction and the rate of epithelial advance in each region of the hole.

To compare amnioserosal contraction in *Rac1^{J11}Rac2Δ mtlΔ* and wild type embryos, single amnioserosa cells (n=10 for each embryo) from positions all across each amnioserosa, were followed through dorsal closure, again using expression of GFP-α-catenin. Embryos were matched by dorsal hole length at the start of the movies. The area of each cell was measured at 10 minute intervals until the cell was extruded from

the amnioserosal layer or disappeared under the advancing leading edge. These data were then accumulated (by aligning the final, pre-extrusion, measurements) and the mean cell area for each time-point was calculated for wild type and mutant and plotted on a scatter graph using Excel.

2.4.2 Quantification of protrusion area

For quantification of actin protrusion formation in wild type, *Rac1*^{V12}, *Rac1*^{N17} and *Myo10A* RNAi snapback expressing embryos, data was collected from movies of several embryos from each genotype (n=8, 6, 8 and 4 respectively), which were co-expressing GFP-actin. The maximum actin protrusion area formed by leading edge cells of a single engrailed stripe was measured at 10 minute timepoints. To ensure that the same stages of dorsal closure were compared, embryo collections were carefully timed so that embryos had developed for 17 to 19 hours at 18°C prior to imaging. Furthermore, the wild type, *Rac1*^{N17} and *Myo10A* RNAi snapback embryos were more precisely matched by counting the number of *engrailed* stripes which were closed at the start of the movie. Mean protrusion areas for each time point were calculated and plotted on scatter graphs using Excel software. As a control, the widths of *engrailed* segments in wild type and mutant embryos were measured (data not shown) and found not to vary significantly.

2.4.3 Measurement of filopodial extension and retraction rates

To follow the dynamics of wild type filopodial formation, embryos expressing GFP-actin in *engrailed* stripes were studied (n=8, dorsal closure staging in different embryos was determined as described above in Section 2.4.2). At 10 minute time-points the lengths of all filopodia present at the leading edge were measured and the mean calculated to give average filopodial length at each time-point. To measure filopodial extension and retraction rates, dorsal closure was split into 20 minute time periods within which

individual protrusion dynamics were followed by measuring filopodial length every minute from first extension to final retraction. Rates of extension and retraction were calculated for each filopodium and then combined to give mean rates for each 20 minute period (n=7 embryos, 88 filopodia). Extension and retraction rates were measured in a similar manner for dorsal closure filopodia in *Myo10A* RNAi snapback expressing embryos (n=2 embryos, 12 filopodia) and compared to wild type embryos filmed in identical conditions (n=2 embryos, 15 filopodia).

2.5 EMBRYONIC FIXED TISSUE ANALYSIS

For overall impression of morphological progression, embryos were viewed by scanning electron microscopy (SEM). For SEM, embryos were collected at dorsal closure stage (17-20hr after egg laying, aged at 18°C), dechorionated in 50% bleach for 5 min, and fixed overnight at 4°C in a 1:1 mix of heptane and fixative (4% paraformaldehyde, 2.5% glutaraldehyde and 1μg/ml phalloidin in PBS). After fixation, embryos were hand-devitellinized in PBS, postfixed in 1% osmium tetroxide in PBS and rinsed further in PBS. After dehydration in a graded ethanol series, specimens were critical point dried (or as an alternative to critical point drying: rinsed 3 times with Hexamethyl disilazane and left to air dry before being mounted) and sputter coated with gold and then imaged on a Jeol 5410 scanning electron microscope (Jacinto et al., 2002a).

To allow phenotypic assessment of larger numbers, embryonic cuticle preparations were carried out. For cuticle preps embryos were first dechorionated in 50% bleach rinsed in dH_2O and hand-devitellinized with forceps. Devitellinized embryos were then mounted in lacto-hoyers, under a glass coverslip, and incubated at 80°C for 2hr. For the highest quality cuticle preps, embryos were incubated at 80°C in dH_2O for 10sec prior to mounting in lacto-hoyers (Wieschaus and Nüsslein-Volhard, 1986).

2.5.1 *In situ* hybridisation

To assess *dpp* expression at the leading edge during dorsal closure, immunohistochemical whole mount *in situ* hybridisation was carried out using standard methods (Lehmann and Tautz, 1994) with digoxigenin-substituted RNA probes generated by transcription of the *dpp* cDNA. For *in situ* hybridisation, embryos were dechorionated in 50% bleach and fixed in a 1:1 mix of heptane and 4% paraformaldehyde (in PBS) for 35 min at room temperature and then rinsed several times with methanol. For pre-hybridisation, specimens were re-hydrated with a series of methanol:PBST (PBST: PBS + 0.1% Tween-20) dilutions and then post-fixed in 4% paraformaldehyde (in PBST) for 15 min at room temperature. Following five PBST washes, specimens were incubated in Proteinase K (20μg/ml in PBST, Roche) for 1.5 min at room temperature and subsequently washed twice with glycine (2mg/ml in PBST). After further PBST washes, specimens were fixed once more in 4% paraformaldehyde for 20 min at room temperature and then washed several times with PBST. Prior to probe hybridisation, specimens were prehybridised for 1hr at 60°C in HybA buffer (50% formamide, 5X SSC, 10μg/ml tRNA, 50μg/ml Heparin, 0.1% Tween-20; pH5) and then incubated with heat denatured probe in HybA buffer overnight at 60°C. The following day the probe was removed and specimens were washed 5 times for 45 min in HybB buffer (50% formamide, 5X SSC; pH5) at 60°C. Following a series of HybB:PBST and then PBST washes, specimens were blocked in 1% BSA in TBST (50 mM TrisHCl pH7.5, 10mM KCl, 150mM NaCl, 0.1%Tween-20) for 1hr at room temperature. Specimens were then incubated with anti-DIG-AP (1:2000, Jackson Labs) in 1% BSA in TBST for 1hr at room temperature and after further washes with TBST, signal was visualised using Substrate Kit II reagents (Vector Labs, Inc.) and stopped with several PBST rinses.

For *Myo10A* and *ck in situ* hybridisations, digoxigenin-substituted DNA probes were generated by amplification of the cDNA tail fragments described in Section 2.2.1 and whole mount *in situs* were carried out according to previously described methods (Tautz and Pfeifle, 1989). The protocol is similar to that described above for RNA probes except for the following: Proteinase K was used at 50μg/ml and specimens were incubated in this for 4 min at room temperature; hybridisations and subsequent Hyb washes were performed in HybC (50% formamide, 5X SSC, 10μg/ml tRNA, 50μg/ml Heparin, 0.1% Tween-20, 20μg/ml Salmon sperm DNA; pH not adjusted) at 48°C; and PbT (PBS + 0.2% BSA + 0.1% Triton X-100) was substituted for 1% BSA in TBST during blocking and anti-DIG incubations.

2.5.2 Antibody staining

For immunohistochemical studies, embryos were dechorionated in 50% bleach and fixed in 1:1 mix of heptane and 4% formaldehyde (in PBS) for 25 min at room temperature, subsequently devitellinized using methanol and then prepared and stained as described previously (Parkhurst et al., 1990). Primary antisera used were anti-Fas III (1:3, Developmental Hybridoma Bank), anti-phosphotyrosine (1:1000, Upstate Biotechnology Inc.) anti-Dfos (1:100, from D. Bohmann), anti-Myo10A (1:100, see Section 2.2.3). In all cases primary antisera were diluted in PAT (PBS + 0.2% BSA + 0.1% Triton X-100 + 0.02% Sodium azide) and specimens were incubated overnight at 4°C. Following several rinses with PbT (PBS + 0.2% BSA + 0.1% Triton X-100), Alexa 488 or 594-conjugated fluorescent secondary antibodies (Molecular Probes) were applied as dilutions (1:2000) in PbT and specimens were incubated for 1 hr at room temperature. After several PBST washes specimens were mounted in glycerol for confocal imaging.

To quantify Dfos staining, embryos were co-stained with the DNA marker, 4'-6-Diamidino-2-phenylindole (DAPI), to mark nuclei and anti-phosphotyrosine to outline cells. A Zeiss LSM 510 META NLO confocal was used to take Z-series (with 1μm intervals) of the triple stained embryos. Projected stacks were then analysed using Image J software as follows: individual cells of the leading edge in wild type and mutant embryos (n=10 for each) were selected and within each cell, mean pixel intensity along a fixed line was measured at 20 pixel intervals down the cell (from leading edge surface to ventral edge) in the DAPI and Dfos channels. Data from each channel was collated (cell measurements were aligned from the ventral edge) and mean pixel intensities were calculated for each position along the dorso-ventral length of the cells. I then normalized the pixel intensity values and cell length measurements to allow for clearer comparison between wild type and mutant.

2.6 CELL CULTURE

The *Drosophila* cell line, S2R+ (from S. Yanagawa), was used in this study. Cells were grown in Schnieder's medium (Invitrogen) supplemented with 10% heat-inactivated fetal bovine serum (FBS), 25mM glutamine, penicillin and streptomycin. Cells were grown at 25°C and passaged every 3-4 days.

2.6.1 Immunofluorescence in S2R+ cells

For immunofluorescence, cells were plated in 6-well culture dishes on coverslips coated with concanavalin A (Con A) coverslip. For coating, one coverslip was placed in each well, covered with a PBS solution containing 10μg/ml Con A, and incubated at room temperature for 30mins, after which time the Con A solution was removed and the wells were rinsed with PBS; the coated coverslips were used immediately. Cells were grown on the coated coverslips at 25°C for 18 hours and then coverslips were removed and the cells fixed in 4% formaldehyde in PBS for 15min. They were washed

3 times in PbT (PBS + 0.2% BSA + 0.1% Triton X-100) and then incubated in Myo10A 1° antibody (1:100 in PbT, see section 2.2.3 for generation of antisera) for 1hr at room temperature. They were again washed 3 times in PbT, and then incubated in Alexa 488 2° antibody (1:2000 in PbT, Molecular Probes) and Alexa 568-conjugated phalloidin (1:80, Molecular Probes) for 1hr at room temperature. Following the 2° incubation, they were washed 3 times in PbT and mounted on slides for visualization via confocal microscopy.

2.7 YEAST TWO-HYBRID SCREEN

2.7.1 Cloning Myo10A bait constructs

A 3.9kb fragment of the 3' end of Myo10A tail, encoding a region including the paired arrangement of MyTH4 domain and FERM domain, was amplified by PCR from the BDGP Myo10A cDNA (LP03318). This was cloned, in frame and with a functional termination site at the 3'end, into pBTM116 (TRP1), a LexA fusion yeast two-hybrid vector. This plasmid was then transformed into two yeast strains, AMR70 (*Matα his3Δ200 lys2-801am trp1-901 leu2-3, 112 URA3::(lexAop)8-lacZ*) and L40 (*Mata his3Δ200 trp1-901 leu2-3, 112 ade2 lys2-801am URA3::(lexAop)4-HIS3*) and grown on selective media lacking the amino acid tryptophan, which the pBTM116 vector encodes.

2.7.2 Performing the Yeast two-hybrid screen

The yeast two-hybrid screen was carried out using the Hollenberg system, as described previously (Alifragis et al., 1997; Hollenberg et al., 1995; Vojtek et al., 1993). Before the large scale screen with a cDNA library was attempted, controls were carried out in which the LexA-Myo10Atail fusion carrying yeast was mated to yeast carrying the empty pVP16 (LEU2) yeast two hybrid vector and tested for β-Galactosidase (β-Gal) activity. Yeast matings and β-Gal staining were carried out as described

previously (Ausubel, 1995). The control mating gave no β-Gal staining above background, and so the screen could proceed. LexA-Myo10Atail was screened against a *Drosophila* cDNA library in pVP16. Preparation of the cDNA library was as described previously (Poortinga et al., 1998). The library complexity was approximately $2.0x10^6$, with an average insert size of 1kb. Positive interactions were first selected by their ability to grow on media lacking histidine and then twice screened for β-Gal activity. From approximately one library complexity screened ($2.0x10^6$ colonies), 93 positive clones were identified. These were grown on selective media lacking lysine, which over a number of generations led to the loss of the LexA-Myo10Atail bait vector (verified by β-Gal staining). Once the bait had been lost, yeast mini preps of the pVP16-interactors were made, transformed into bacteria and sequenced by the Fred Hutchinson Center sequencing facility.

CHAPTER 3

Live analysis of dorsal closure

3.1 INTRODUCTION

3.1.1 Genetic studies of dorsal closure have revealed signal transduction pathways

The study of *Drosophila* dorsal closure began with the discovery of a number of "dorsal open" mutants in the large scale mutagenesis screens of the late 1980s (Nüsslein-Volhard, 1984; Wieschaus, 1984). These mutant embryos failed early in the closure process and displayed large holes on the dorsal side of their cuticles. Classical genetic studies of the dorsal open mutants revealed that many carried mutations in members of the JNK signalling cascade, as described earlier in Section 1.2.1. These discoveries led to an investigative focus on the signal transduction pathways underlying dorsal closure. This work resulted in great advances in our understanding of JNK signalling in dorsal closure and, more widely, the role of MAPK cascades in *in vivo* morphogenetic events (Noselli, 1998; Noselli and Agnes, 1999). Activation of the JNK pathway in the epithelial leading edge during dorsal closure is crucial for the continued dorso-ventral elongation of these cells and the transduction, via Dpp release, of an instructive signal to cells behind the leading edge telling them to also begin to elongate. It is clear that without activation of the JNK pathway and elongation of the cells of the epithelium, dorsal closure can not proceed far, failing before epithelial fusion has even begun (reviewed in Harden, 2002).

Along with the emphasis on the role of JNK signalling in dorsal closure, the actin cytoskeleton has also become a focus of attention in the study of this process. Analysis of actin structures in fixed embryos has revealed a striking accumulation of actin along the epithelial leading edge (Young et al., 1993). This actin organisation can be disrupted by the expression of mutant forms of members of the Rho family of GTPases, which are key regulators of the actin cytoskeleton. Similar to JNK mutants, the expression of dominant negative RhoA, Rac1 or Cdc42 throughout the embryo,

using a heat-shock promoter to drive expression, leads to a failure in dorsal closure and to cuticlar holes (see Section 1.4.3) (Harden et al., 1995; Harden et al., 1999).

The discovery of the JNK pathway and analysis of the actin cytoskeleton in fixed tissue have both shed a great deal of light on crucial aspects of dorsal closure. However, both of these approaches to the study of closure miss an important aspect of the process. Dorsal closure is, by definition, a dynamic process and with the huge advances in confocal imaging that have taken place over recent years, it has become highly amenable to live imaging. Over the last five years live studies of dorsal closure have exposed further complexities, and begun to unravel some of the forces involved in the process which were clearly missed in classic genetic and fixed tissue studies.

3.1.2 Leading edge actin protrusions are only revealed by live imaging

Fixed tissue analysis established three distinct phases of dorsal closure, described as initiation, spreading and suture (Noselli, 1998). Due to the discovery of the JNK cascade much of the focus had been on the first two stages with the emphasis resting on the co-ordinated cell shape changes seen in the leading edge. However, this work also described the ultimate fusion of epithelial sheets, as it was evident from analysis of fixed embryos that the two edges were "zipped" together from the two ends of the hole. What was not clear was how this fusion occurred and what cell machinery was needed. Answers came from live imaging, as a striking aspect of dorsal closure when viewed live is the extension of copious numbers of filopodia and lamellipodia by the epithelial leading edge. These fragile protrusions do not survive the fixation process well and are best visualised live with the expression of GFP fused to actin or an actin-binding protein such as moesin (Jacinto et al., 2000; Kiehart et al., 2000). The actin-rich protrusions can be seen extending across the amnioserosa from about halfway through closure. Once the two epithelial surfaces are close enough, which occurs first at the two ends of the eye-shaped hole, protrusions from the opposing epithelial edges

begin to interact with each other at these "zipping canthi" and subsequently interdigitate and zip the embryo shut (Jacinto et al., 2000).

The expression of mutant forms of Rho GTPases has proved a powerful method, when coupled with live imaging, to begin to understand the regulation and function of these dynamic actin structures. Expression of dominant negative *Cdc42*, the GTPase found to be responsible for filopodial assembly in tissue culture cells (Nobes and Hall, 1995), during dorsal closure eradicates filopodial formation by leading edge cells and results in midline fusion failures and to the misalignment of segments as the embryo closes. An analysis of the dorsal closure roles of the GTPase, Rac, which was shown to regulate lamellipodia formation in tissue culture studies (Ridley et al., 1992), is described in Chapter 4.

3.1.3 Live imaging demonstrates that dorsal closure is a multi-force process

Another aspect of dorsal closure for which live imaging is essential is the study of the relative contributions which the different tissues make as the hole closes. Elegant experiments where laser ablation is combined with live imaging have revealed that a number of different forces are required for closure (Kiehart 2000). For example, if a portion of the leading edge is carefully laser ablated, the cells at the edge of the ablation hole immediately spring back indicating that the leading edge is under tension. This result endorses the idea that the actin cable along the leading edge is a contractile structure that provides important tension during closure. Perhaps even more crucially, similar experiments in the amnioserosa also demonstrate this "spring back" effect, indicating that this tissue is also under tension, suggesting that it is providing a "pulling" force (Kiehart et al., 2000). This finding was important because up until this point it was not clear whether the amnioserosa was directly contributing to the closure process or instead was just a passive cell layer being pushed out of the way by the advancing epithelium. Certainly, the previous emphasis on the leading edge in dorsal closure

studies had meant that the amnioserosa was somewhat overlooked. This imbalance has been redressed by several recent studies, including one in which the amnioserosa was ablated by tissue specific expression of the toxin Ricin A, leading to failures in dorsal closure and the preceding germ-band retraction stage, demonstrating that this tissue is required for both of these morphogenetic events (Scuderi and Letsou, 2005).

Further live analysis of dorsal closure has allowed for mathematical models of the process to be built and these have begun to reveal the relative force contributions of the different tissues (Hutson et al., 2003). It appears that through most of closure the forces produced by the amnioserosa and the leading edge make similar contributions to bringing the epithelial surfaces together. Modelling can also take into account the contribution of the "zipping" force provided by the actin protrusions. It appears that whilst the contraction forces provided by the amnioserosa and leading edge actin cable are key for the first 2/3 of the process, zipping makes an important contribution to the final 1/3 of closure. Moreover, these studies indicate the plasticity and resilience of dorsal closure, where the contributing forces can compensate when one process is defective. For example, if the zipping "canthi" are persistently ablated with a laser the embryo can continue to close, with a slight delay, due to continued contraction of the amnioserosa and leading edge and the formation of new zipping canthi beyond the regions of ablation (Hutson et al., 2003).

3.1.4 What more can be learned from live imaging of wild type closure?

Whilst live imaging of dorsal closure has begun to give us a much more detailed picture of the process, there still remain many aspects of wild type closure which are uncertain and require further live analysis. An area in need of particular attention is the assembly and dynamics of the leading edge actin protrusions. For example, how does the extent of protrusion assembly vary during dorsal closure and is this related to rates of protrusion, extension, and retraction? Also, it has not been precisely determined when

the first protrusions extend and how this is related to the assembly of the actin cable in the leading edge. Away from protrusions, it is still unclear to what extent the epithelium physically moves over the amnioserosa during closure, and detailed live imaging can provide some answers to these issues. Finally, the current definitions of dorsal closure have relied on analysis of fixed embryos and, as described above, have split dorsal closure into 3 phases. Live imaging has revealed added complexity and it seems timely to characterise and quantify dynamic aspects of this process and indeed to define a new staging framework for wild type closure using live analysis, which can be used as a standard for comparison with mutant closure.

3.2 RESULTS

3.2.1 Dorsal closure begins with contraction of the amnioserosa and dorso-ventral elongation of the epithelial cells

To investigate the earliest cell movements and shape changes which underlie dorsal closure I carried out live imaging on embryos that had just reached the end of germ band retraction. In order to view cell shape changes I used embryos expressing *UAS-GFP-α-catenin*, a junctional component which outlines cells in the epithelium and amnioserosa, when driven by the GAL4 driver line *e22c-GAL4*. Live imaging shows that even prior to the completion of germ band retraction and, therefore, before the start of dorsal closure proper, cells of the amnioserosa begin to shrink (Figure 3.1A and B and Movie 1). At this stage the amnioserosa cells are more irregular in shape but, as they contract, their shapes resolve into the familiar pentagonal outline seen during the majority of dorsal closure (Figure 3.1A and B).

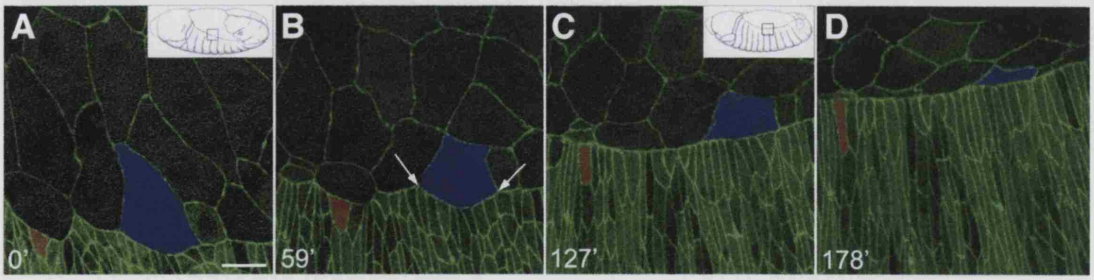

Figure 3.1 Cell shape changes in the amnioserosa and leading edge take place early in dorsal closure.

A series of confocal stills taken from a time lapse movie (Movie 1) of an embryo expressing GFP-α-catenin in the amnioserosa and epithelium. Schematic figures in the top right-hand corner of (A) and (C) indicate the approximate stage of the embryo and boxed regions indicate the imaged area. From just prior to the start of dorsal closure proper, the cells of the amnioserosa begin to contract (amnioserosa cell highlighted in blue). Simultaneously, leading edge epithelial cells begin to elongate in a dorso-ventral direction (cell highlighted in red). Early in closure the leading edge is scalloped in appearance, apparently held to the amnioserosa at cell-cell junctions (B, arrows), but as closure progresses the leading edge resolves to a taut, organised edge (C and D). Scale bar represents 10μm.

Concomitant with amnioserosal contraction, the cells of the leading edge begin to extend along their dorso-ventral axis, and as with contraction of the amnioserosa, the lengthening of these cells appears to initiate before dorsal closure has really begun (Figure 3.1A, B and C). As the leading edge cells elongate so do the more ventral cells behind them. There seems to be very little, if any, delay between the initiation of leading edge elongation and of cells positioned more ventrally (Movie 1). This virtually synchronous lengthening differs from that previously reported, where it was suggested that a wave of elongation passes back ventrally from the leading edge (Noselli, 1998).

Another clear change in leading edge morphology, which can be seen in movies of early dorsal closure, is the resolution of the leading edge from a scalloped, rather disorganised, edge seen in Figure 3.1A, to the straight, taut surface seen in Figure 3.1D. This transformation coincides with the assembly of the actin cable in leading edge cells, which is investigated in more detail in section 3.2.4. Together, the early contraction of the amnioserosa, elongation of the epithelial cells, and tightening of the leading edge, result in net movement of the epithelium towards the dorsal midline which sets up the embryo for the subsequent stages of dorsal closure (Figure 3.1 and Movie 1).

3.2.2 Amnioserosa cell contraction rates are similar across the tissue

The shrinkage of amnioserosa cells continues throughout dorsal closure, providing a major driving force for bringing the two epithelial edges together. To investigate whether the rate of amnioserosal cell contraction varies depending on the position of the cell in the tissue, I followed single amnioserosa cells through dorsal closure in an embryo expressing *GFP-α-catenin,* measuring cell area at 10 minute intervals until each cell was lost from the amnioserosa surface, either through extrusion or being overtaken by the advancing epithelial edge (see Movie 2). I divided the amnioserosa

into five sections: a central third, two canthi ends and two intermediate areas (see Figure 3.2A). When the contraction rates are compared between the three areas (canthi, intermediate and central zones, shown in Figure 3.2A) it appears that the rate of amnioserosa contraction does not vary significantly through the epithelial tissue (Figure 3.2B). However, the size of cells at the start of measurements did vary a great deal depending on their position in the amnioserosa, with cells in the centre of the tissue being about 1.5 times the size of those in the canthi regions (n=27). This suggests that cell contraction begins earlier in amnioserosal zones adjacent to the zippering canthi and perhaps this early start aids in bringing the epithelial surfaces closer in these regions first.

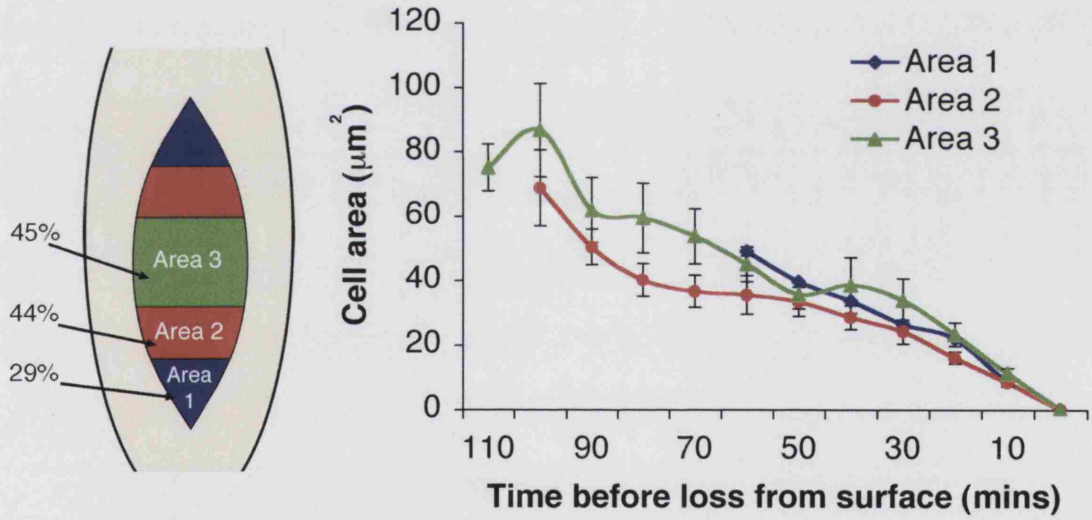

Figure 3.2 Amnioserosa cells contract at a similar rate wherever they are located in the sheet.

(A) Schematic diagram showing how the amnioserosa was divided into three regions in order for comparisons of cell contraction rates: Area 1 (canthi, highlighted in blue); Area 2 (intermediate, highlighted in red); Area 3 (central, highlighted in green); the figures shown indicate the percentage of amnioserosa cells extruded from each region. (B) Quantification of amnioserosa cell contraction in three regions of the amnioserosa sheet (plotted colours correspond to descriptions in (A) shows that cells contract at a similar rate wherever they are found in the amnioserosal sheet. Error bars represent the standard error of the mean.

3.2.3 Extruded amnioserosa cells contract at a faster rate than those which vanish under the advancing leading edge

Ultimately, all amnioserosal cells will end up below the epithelium where they degenerate, with the amnioserosa playing no further role in the development of the embryo. However as mentioned above, amnioserosal cells are lost from the exposed surface in one of two ways, either by being extruded from the amnioserosal cell layer or overtaken by the advancing leading edge. The most obvious cases of cell extrusion take place in the centre of the amnioserosal tissue, as is highlighted in Figure 3.3A. However, amnioserosal cells are also extruded closer to the leading edge and are lost only just before the leading edge advances over them (Figure 3.3A and Movie 2). In contrast, some amnioserosal cells are not extruded but instead are clearly seen to vanish under the advancing leading edge, although it must be pointed out that all cells lost from the surface in this manner also undergo contraction and are much reduced in size by the time they are covered over (Figure 3.3A). Overall, throughout the amnioserosa, I found that approximately 40% (n=107) of cells are extruded from the tissue layer during dorsal closure. This figure is higher than has been reported previously (Kiehart et al., 2000), possibly because other studies failed to class cells extruded close to the leading edge as extrusion. There is a slight variation in the proportion of amnioserosal cells being extruded or overtaken by the leading edge according to the location in the amnioserosa. In the "canthi" regions, only 29% (n=35) of amnioserosa cells are extruded, compared to 45% in the central zone (n=33), although the intermediate areas are similar with 44% (n=39).

The differences between proportions of extruded cells does not vary dramatically between different areas of the amnioserosa, so it seems unlikely that the position in the amnioserosa will be the major determinant of whether or not a cell will be extruded. However, if cell contraction rates are compared between extruded and non-extruded cells there is a definite difference, with cells which will be extruded contracting at a

faster rate then those which will be overtaken by the leading edge (Figure 3.3B). It therefore appears that the rate at which an amnioserosal cell contracts may help determine how it is removed from the exposed surface. It remains unclear whether control of amnioserosal contraction rate is random, or controlled in order to push a certain proportion of the amnioserosa towards extrusion.

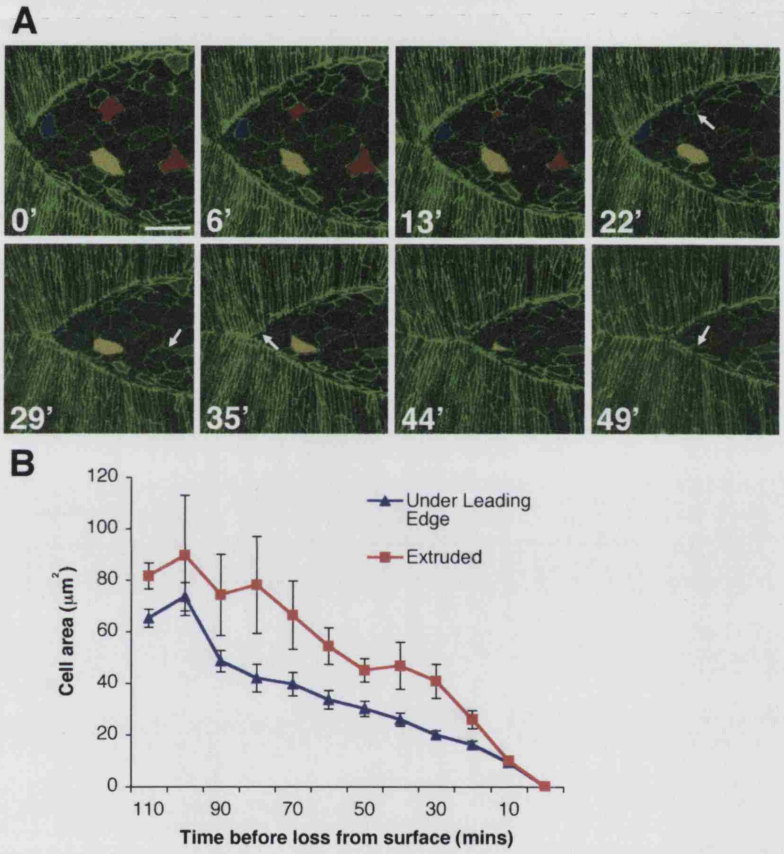

Figure 3.3 Extruded amnioserosa cells contract at a faster rate than those that will be lost under the advancing leading edge.

(**A**) A series of confocal stills taken from a timelapse movie (Movie 2) of a GFP-α-catenin expressing embryo that illustrate the contraction of amnioserosa cells, which leads to their ultimate exclusion from the surface of the embryo. A selection of amnioserosa cells were tracked throughout closure and are highlighted in different colours according to the manner of their loss from the cell layer: extrusion from centre of amnioserosa (red); extrusion close to leading edge (yellow); overtaken by leading edge (blue). Scale bar represents 20μm. (**B**) A comparison of amnioserosa cell contraction rates in cells which are extruded from the cell layer (red) compared to cells which are lost under the advancing leading edge (blue) indicated that extruded cells contract at a faster rate than those which are overtaken by the leading edge. Error bars represent standard error of the mean.

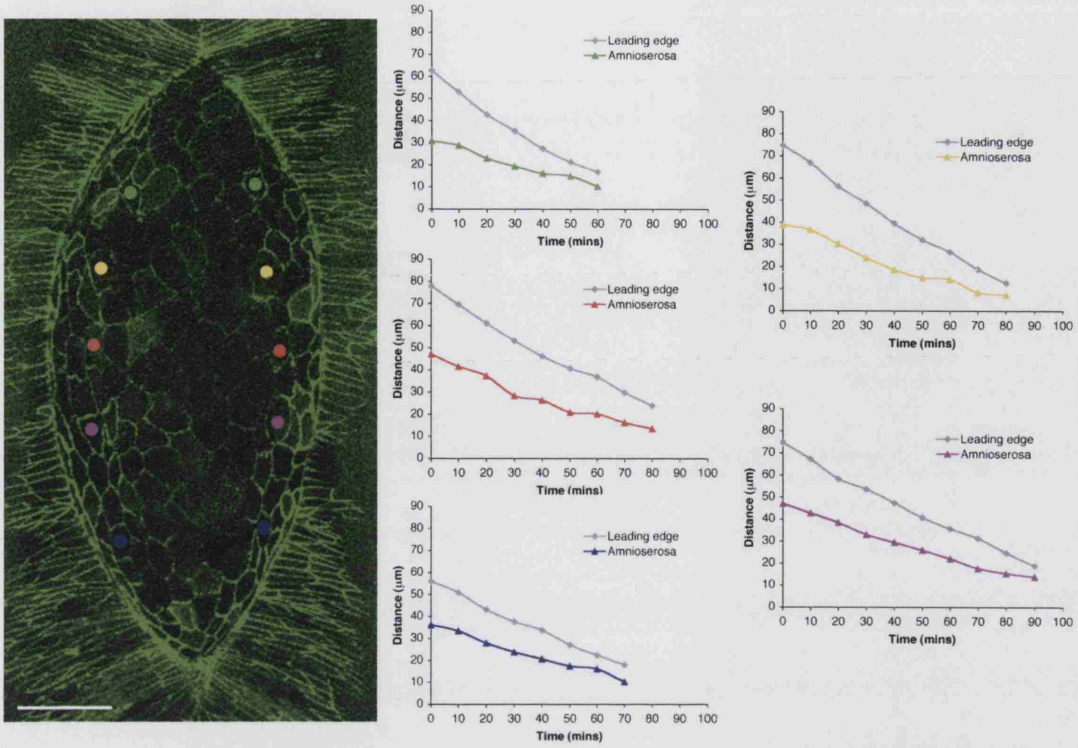

Figure 3.4 The leading edge advances faster than the amnioserosa contracts

Five pairs of cells in the amnioserosa (above left, marked with coloured dots) were followed through dorsal closure and the distance between each pair was measured at 10 min time points (coloured lines on graphs). At corresponding time points the distance between the two leading edges adjacent to each cell pair was also measured (grey lines on graphs). The average gradient of the leading edge plots was -0.67, whilst the average for the amnioserosa was -0.39, indicating that the leading edge advances approximately 1.75 times faster than the amnioserosa contracts. Scale bar represents 20μm

3.2.4 The leading edge advances at a faster rate than amnioserosa contraction

Over recent years, how extensively the leading edge moves over the amnioserosa during dorsal closure has become a somewhat controversial issue. Previous live analysis has suggested that the leading edge advances at approximately the same rate as contraction of individual, or clusters of, amnioserosa cells (Kiehart et al., 2000). This work suggests that there is very little net movement of the leading edge over the amnioserosa during dorsal closure and thus the movement of these two tissue sheets is inextricably linked. This certainly seems to agree with my live analysis of very early

dorsal closure where the epithelium advances dorsal-ward but does not appear to move over the amnioserosa (Movie 1). However, it falls down when considering the majority of the process because, as I presented in the previous section of this chapter, quantification suggests that about 60% of the amnioserosa cells vanish under the advancing leading edge (see also Movie 2).

A major problem with the published analysis of amnioserosa contraction versus epithelial advancement is that the rate of shrinkage of individual amnioserosa cells was compared to the speed at which the hole closes. The results obtained using this method will therefore vary a great deal depending on the amnioserosa cells which are followed and where they are positioned in the tissue. As I have presented above in Section 3.2.2, whilst the rates of contraction are similar between different regions of the amnioserosa sheet, individual cells at the anterior and posterior ends of the hole are more advanced in this contraction than those in the centre. To avoid these issues and compare more directly the relative movements of the amnioserosa and the leading edge, I developed a method of comparing contraction of the amnioserosa as a whole tissue, rather than just measuring individual cells. To do this I chose pairs of cells from the lateral edges of the amnioserosa and measured the distance between the cells during closure. Five pairs of cells, distributed across the anterior-posterior axis of the amnioserosa, were followed through closure (see Figure 3.4). For each cell pair the changing distance between the adjacent epithelial leading edges was also recorded for direct comparison. When the changes in these distances are compared graphically it is clear that the leading edges are progressing together faster than the amnioserosa cells (Figure 3.4). Indeed, on average, the leading edges move together at about 1.75 times the speed of the amnioserosa cells. This result definitely indicates that contraction of the amnioserosa, alone, does not account for all migration of the leading edge, and that there must be a significant amount of net movement of leading edge over amnioserosa during dorsal closure.

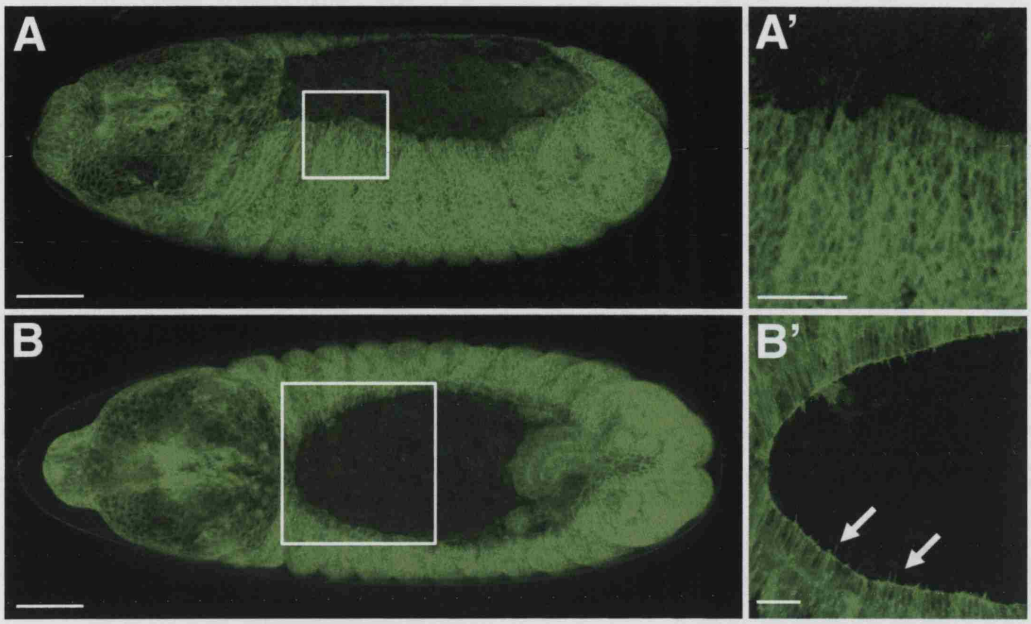

Figure 3.5 The leading edge becomes more organised and taut coincident with assembly of an actin cable and filopodial protrusions

Confocal stills of live wild type embryos expressing GFP-actin at low magnification (A and B) and zoomed in on the leading edge (A' and B', boxed regions). Just after germ band retraction (A) the leading edge is scalloped in appearance and shows no accumulation of actin. About 45 mins later (B) actin has begun to accumulate in the leading edge, resolving it into a straight taut edge (B'). As soon as actin starts to accumulate in the leading edge the first small filopodia are assembled by leading edge cells (arrows). Scale bars in (A) and (B) represent 50μm and in (A') and (B') represent 20μm.

3.2.5 Assembly of the actin cable coincides with the extension of the first actin protrusions by leading edge cells

To assess the actin dynamics of wild type dorsal closure I used embryos in which GFP-actin expression was driven either throughout the epithelium using the *e22c-GAL4* driver, or in segmental stripes using the *engrailed-GAL4* driver. In particular, I focused on various aspects of actin protrusion dynamics and how these vary during the closure process, as this has been mostly overlooked in other studies of dorsal closure. I first wanted to determine when and where along the leading edge actin protrusions are first

assembled. In the earliest stages of dorsal closure, when the germ band has just completed retraction, there is no apparent accumulation of actin in the leading edge cells (Figure 3.5A and A'). At this point the leading edge surface has a scalloped shape and appears somewhat disorganised compared to later in the closure process (Figure 3.5A'). Over the course of about 30-45 minutes (at room temperature) the hole begins to slowly reduce in size and actin starts to accumulate along the dorsal surface of the leading edge cells (Figure 3.5B and B'). Assembly of the cable appears uniform along the length of the leading edge. Presumably in these early stages, prior to the assembly of actin cable or protrusions, the contraction of the amnioserosa, as described in the previous sections, must provide a great deal of the force used to begin to close the hole.

As soon as actin begins to accumulate along the leading edge, the first actin protrusions are also extending from the leading edge cells (Figure 3.5B'). The protrusions are small filopodia, averaging 2.82±0.22μm in length, with no sign of the large lamellipodia that are seen later in the closure process. It seems unlikely that these tiny protrusions play much of a role so early in closure, as they are completely dwarfed by the huge expanse of exposed amnioserosa and they make only transient contacts with the amnioserosa. Even at the anterior and posterior ends of the hole, which are rounded and not yet matured into the pointed zippering "canthi" seen later in closure, the distance between the opposing epithelial edges is more than 10 times larger than the longest protrusion extended at this time (Figure 3.5B').

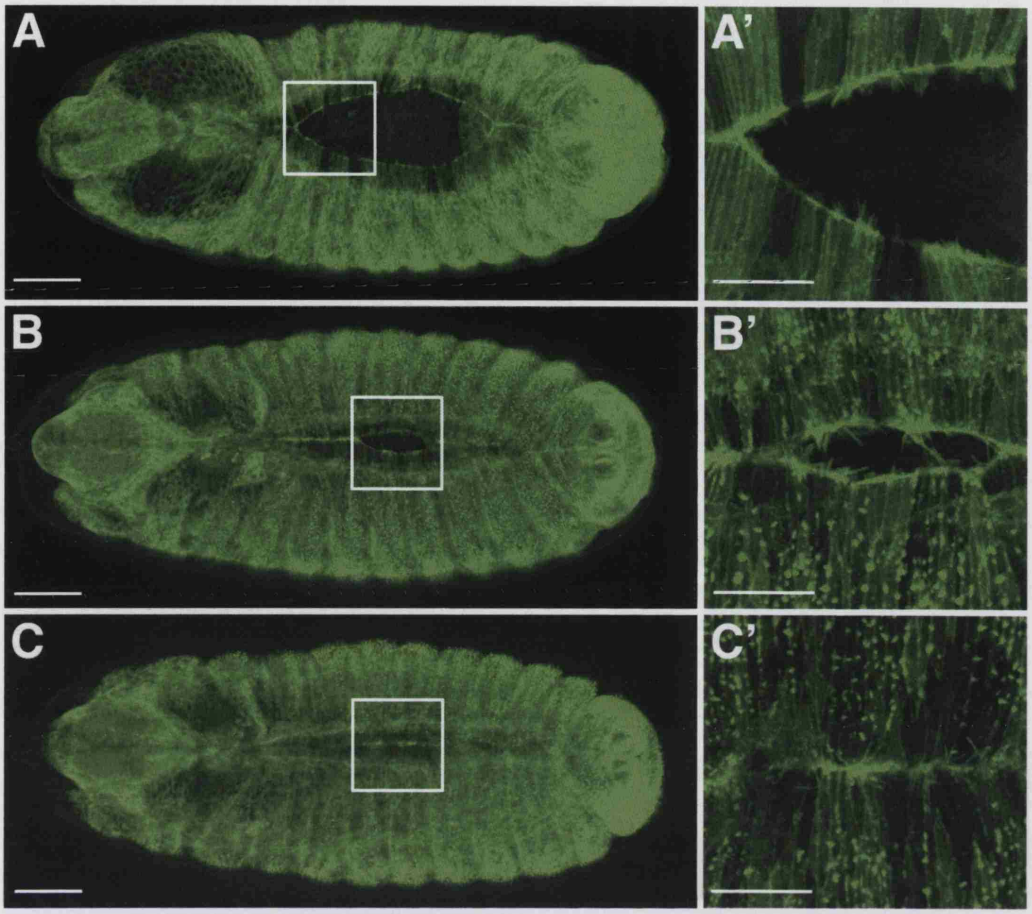

Figure 3.6 Dynamic actin structures dominate the leading edge in the second half of dorsal closure

Confocal stills of live GFP-actin expressing wild type dorsal closure stage embryos, imaged at low magnification (A, B and C) and zoomed in on leading edge (A', B' and C', boxed regions). Epithelial sweeping (A), is driven by the assembly and contraction of an actomyosin cable in the leading edge cells which brings the opposing edges closer in a process that takes about 1hr from the first accumulation of actin in the leading edge. During zippering (B) the epithelial fusion front spreads along the midline towards the centre. Filopodia from opposing epithelial surfaces interact and interdigitate (B') to bring the edges together. Closure finishes (C) as the final open edges are fused at the centre of the embryo. Approximately 90 mins elapsed between (A) and (C). Scale bars in (A), (B) and (C) represent 50μm and in (A'), (B') and (C') represent 20μm.

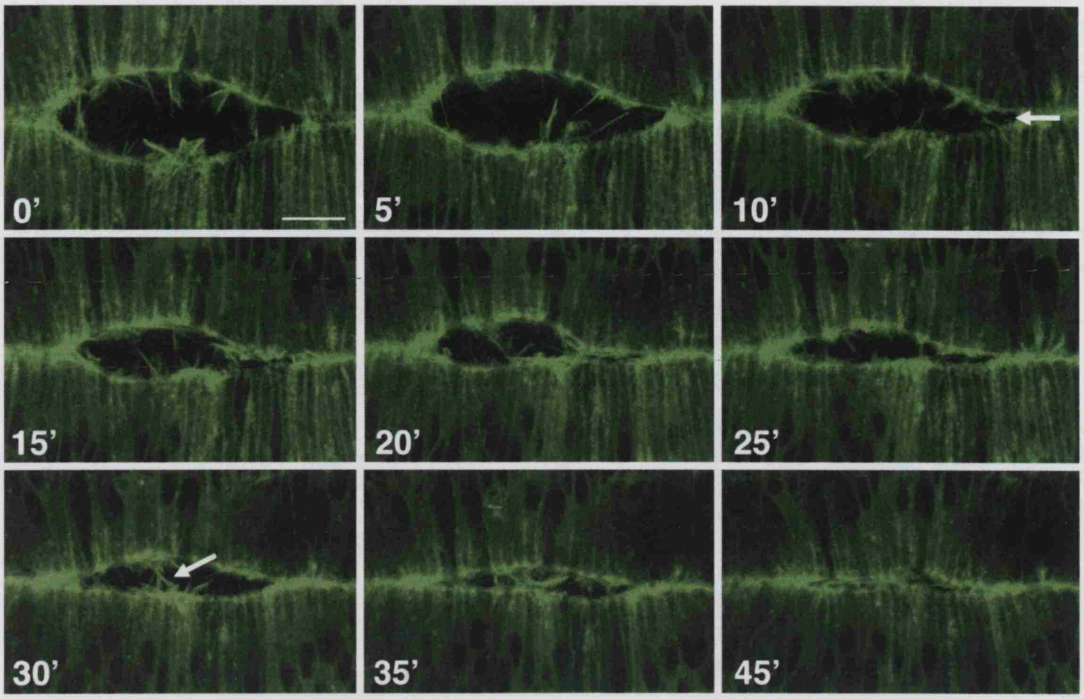

Figure 3.7 Filopodial interaction is limited to regions along the leading edge where the opposing epithelial surfaces are in close proximity

Confocal stills taken from a timelapse movie (Movie 3) illustrating the final zippering events (equivalent stage to embryo shown in 3.6B) in a wild type embryo with epithelial expression of GFP-actin. Throughout the majority of dorsal closure, filopodia can only interact and fuse the epithelial fronts at the two zipping canthi, found at the most anterior and posterior end of the hole (10', arrow). Filopodial interdigitation is limited to these regions until very final phase of dorsal closure when the opposing epithelial edges are very close (less than 10μm) along their length, at which point actin protrusions can interact away from the zipping canthi (30', arrow). Scale bar represent 10μm.

3.2.6 Zippering only begins once the epithelial surfaces are less than 10μm apart

The "Zippering" stage of dorsal closure can be defined as the point at which closure begins to occur by the interdigitation of actin protrusions at the anterior and posterior ends of the hole, "zipping" the epithelium shut from the ends towards the centre of the embryo. Up until the commencement of zippering, the epithelial hole has been reducing in size, through a combination of amnioserosa contraction and purse-string contraction of the actin cable, but very little epithelial fusion takes place during this early phase. Once zippering begins, epithelial fusion occurs rapidly and dorsal closure

is complete within about 90 minutes (Figure 3.6A, B and C). However, I found that zippering only begins once the epithelial surfaces are within about 10μm of each other. Throughout almost the entirety of dorsal closure this proximity only occurs at the ends of the hole, meaning that these serve as zippering fronts or canthi, from which zippering and, therefore epithelial fusion, radiates towards the centre of the embryo. Furthermore, just prior to the start of zippering, the canthi lose their rounded shape and become more pointed in appearance (compare Figure 3.5B, B' and Figure 3.5A, A'), helping to bring the opposing epithelial edges in closer proximity at the zipper fronts.

By the zippering stage the average length of actin protrusions assembled at the leading edge is much increased and they can be clearly seen reaching across the amnioserosa and interacting with protrusions on the opposing epithelium (Figure 3.7, 10', and Movie 3). Quantification of actin protrusion length during the zippering stage of dorsal closure indicates that they reach an average length of 4.48±0.22μm, illustrating why the epithelial surfaces must be within 10μm of each other in order for zippering to take place. In wild type dorsal closure this close proximity only occurs at the zippering canthi, although sometimes at the very end of closure the opposing epithelial surfaces come within 10μm away from the canthi and actin protrusions interact and draw the epithelium shut in the centre of the embryo (Figure 3.7, 30'). A further aid to zippering towards the end of dorsal closure is the fact that the actin protrusions assembled by the leading edge increase in length and area, with occasional filopodia reaching lengths in excess 10μm. The changing dynamics of leading edge actin protrusions during the later stages of dorsal closure is discussed in the following sections.

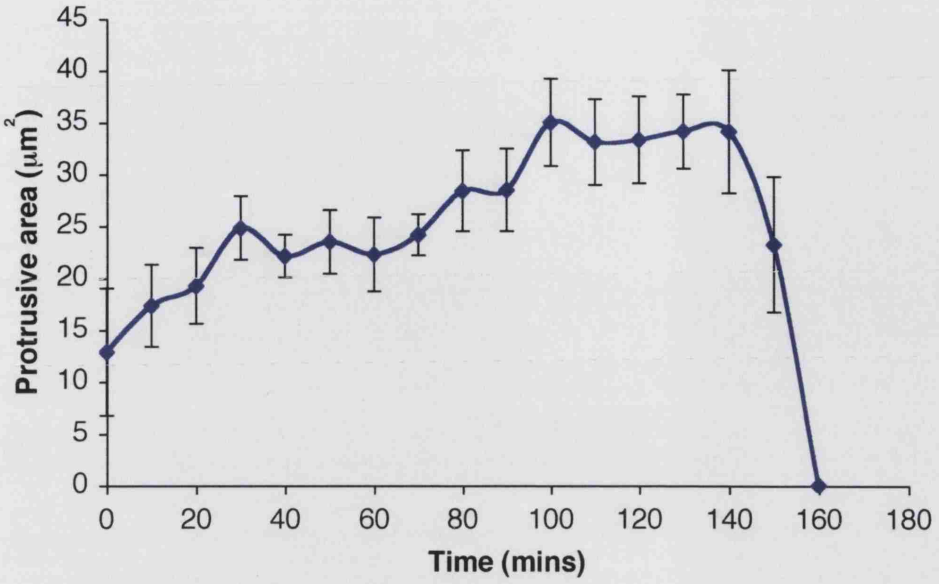

Figure 3.8 Actin protrusion area increases gradually during the course of dorsal closure

The area of protrusions formed by *engrailed* cells of wild type GFP-actin expressing embryos was measured at 10 min time points during dorsal closure. Protrusion area is plotted against time, with 160 min being the point at which epithelial fusion was complete. Error bars represent the standard error of the mean.

3.2.7 The area of actin protrusions assembled by the leading edge increases gradually and then plateaus prior to completion of closure

As well as an increase in length of filopodia as dorsal closure proceeds, leading edge cells also begin to assemble a broader range of filopodia and lamellae. To quantify these changes in actin protrusions during closure I measured the area of actin protrusions assembled by the leading edge from when they first appeared, through to zippering and the completion of dorsal closure (n=8 embryos, see Movie 4 for an example of time-lapse used for quantification). These data show that the size of actin protrusions assembled by the leading edge varies during the closure process (Figure 3.8). When they first appear, the protrusions are small with an average area of 12.86±6.14μm^2. Over the course of the next 100 minutes, the protrusions steadily increase in area, and it is during this rise in protrusion size that zippering begins (at about 60mins in Figure 3.8). Once protrusion area reaches around 34μm^2, the size

increase seems to plateau and no further significant rise is seen. Finally, in the last 20 minutes of closure, as the remaining central regions of the embryo are zipped closed, actin protrusion area decreases until the epithelium is completely fused, at which point the extension of protrusions ceases (Figure 3.8).

Similar to the increase seen in protrusion area, the average length of filopodia assembled by the leading edge also increases during the course of dorsal closure (Figure 3.9). As dorsal closure progresses the leading edge extends longer filopodia, reaching a maximum length as the final fusion events are taking place.

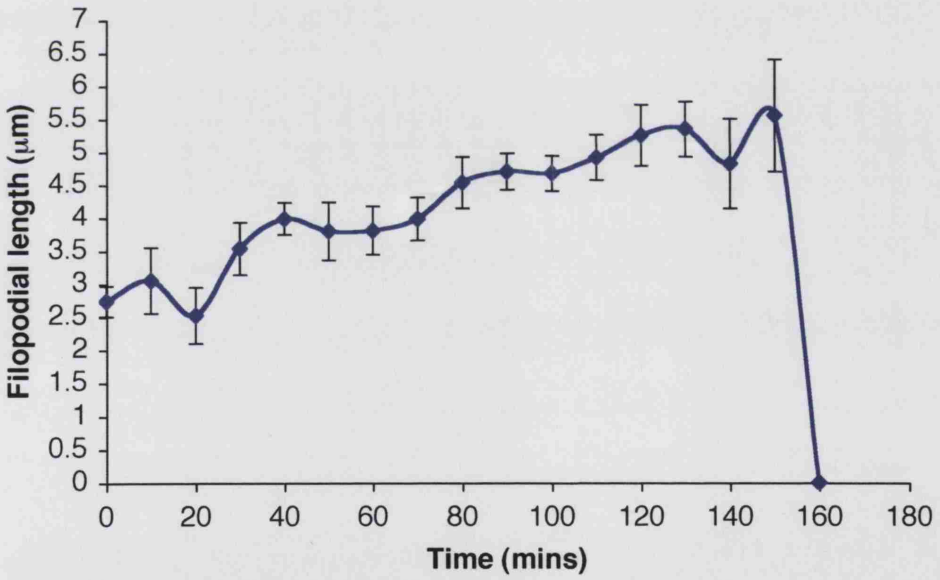

Figure 3.9 Filopodial length shows a steady increase during closure

Quantification of mean filopodial length during dorsal closure in embryos expressing GFP-actin in *engrailed* stripes indicates that filopodial length increases gradually during the process. Measurements were taken at 10 min time points, closure was complete at 160 min. Error bars represent the standard error of the mean.

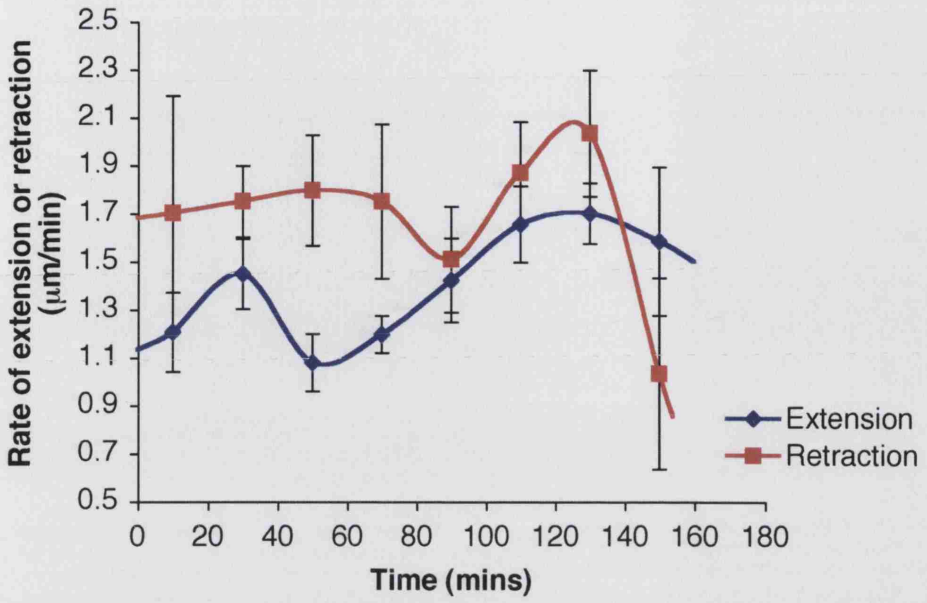

Figure 3.10 Rates of actin protrusion extension and retraction increase slightly during dorsal closure

The mean rates at which leading edge actin protrusions extend and retract was measured in 20 min time windows in embryos expressing GFP-actin in *engrailed* stripes. Protrusion retraction (red squares) is consistently faster than extension (blue diamonds) throughout most of dorsal closure. Just before closure completes (160 min), the retraction rates drop dramatically indicating a more general trend whereby protrusion retraction is suppressed when opposing filopodia interact. Error bars represent the standard error of the mean.

3.2.8 The rates of actin protrusion extension and retraction increase during dorsal closure but retraction is suppressed when two opposing protrusions meet

To assess how the actin dynamics of the protrusions varied during dorsal closure, I followed individual protrusions live from when they first arise prior to zippering to the completion of closure, measuring the rates at which they extend and retract. Over the entire period the mean extension rate was 1.44±0.06μm/min, whilst the mean rate of filopodial retraction 1.71±0.10μm/min. Throughout the majority of dorsal closure the rate of retraction is slightly faster than the rate of extension of protrusions (Figure 3.10). The extension rate does increase gradually as closure proceeds, although interestingly, there is a slight dip at the approximate point where zippering starts (around 60mins on Figure 3.10). To a lesser extent, the retraction rates also appear to

increase during dorsal closure, although there is a dramatic drop in the final 30 minutes of closure.

The striking reduction in retraction rates in the final stages of dorsal closure, illustrates a crucial aspect in the control of actin dynamics during epithelial fusion. During zippering, whenever protrusions from the opposing epithelium contact each other, retraction appears to be suppressed and the protrusion persists, occasionally developing into a lamellae, which may help knit the two edges together. This happens continually at the zipper fronts, but is largely masked in the majority of the measurements displayed in Figure 3.10, as retraction rates were measured throughout the leading edge. It is only in the final few minutes, when interactions are occurring between protrusions along the entire length of the remaining leading edge, that it is possible to see the suppression of retraction which allows the filopodia and lamellipodia to persist and knit the two surfaces together.

3.3 DISCUSSION

3.3.1 Defining the stages of dorsal closure

The detailed analysis of dorsal closure using live imaging techniques, which I present in this chapter, suggests the need to redefine the stages of dorsal closure that have been described previously (Noselli, 1998). In particular, earlier descriptions of this closure process, which were based on work with fixed embryos, overlooked the important role that actin protrusions play in the later stages of closure, since these structures are mostly lost during fixation. With the new information from these studies I suggest that dorsal closure can best be split into four distinct phases, which I have named, Initiation, Epithelial sweeping, Zippering and Termination. Below I detail the important events contained within these stages, focussing, in particular, on the dynamic changes that characterise each phase.

i) Initiation – starts ~8:30 hours after egg laying (AEL)

Dorsal closure is usually considered to begin only once the germ-band has reached its final position at the posterior of the embryo. However, the live imaging presented in this chapter indicates that initiation of some of the crucial movements may take place earlier than this, whilst the germ band is still retracting. It is clear that almost as soon as the amnioserosa is exposed, which occurs first at the anterior end of the hole, amnioserosa cells are already contracting (Figure 3.2A and B, Movie 1). The cells of the epithelium also begin to elongate slightly along their dorso-ventral axis, although this lengthening is not as dramatic as is seen slightly later in the process and may, at this early stage, just be a result of passive stretching by the contracting amnioserosa.

The signals that initiate dorsal closure are poorly understood, as these early events have been considerably less well studied than later stages. As a result there are no genetic clues as to what the primary initiating cues are for dorsal closure. One possible

speculation is that mechanical forces, and in particular, changes in tension in leading edge and amnioserosa cells, act as an initiator in dorsal closure. As the germ band retracts the embryo is stretched in an anterior-posterior direction that would result in increased tension in the leading edge and amnioserosa. Previous studies have shown that once dorsal closure begins there is considerable tension in both the amnioserosa and leading edge epithelium and that these forces contribute to closure (Kiehart et al., 2000) Furthermore, work in the early fly embryo has shown that changes in force can impact gene expression, as it was discovered that the application of a depressive force on embryos could drive expression of the dorso-ventral polarity gene, *twist* (Farge, 2003). Whilst these points provide only circumstantial evidence for mechanical force being an instigator for dorsal closure, it is also interesting to consider tissue culture studies where the effects of mechanical stretching forces on regulation of the actin cytoskeleton has been explored. For example, work in fibroblasts found that the application of mechanical force to small focal complexes led to the maturation of these adhesions into focal contacts, a process that requires recruitment of actin stress fibres to the complexes and acts through a Rho dependent pathway (Riveline et al., 2001). The concept that externally applied force can lead to activation of Rho and reorganisation of the actin cytoskeleton suggests that changes in tension in the developing embryo could lead to initiation of dorsal closure, but discovering whether this is indeed the case, or if there is some other initiator, remains a major experimental challenge.

What appears certain is that these initiation cues must somehow trigger the changes in JNK signalling which are seen in the two main cell types at the commencement of dorsal closure. Coincident with the earliest forward movement, JNK activity is upregulated in the leading edge cells and downregulated in the cells of the amnioserosa (Reed et al., 2001; Stronach and Perrimon, 2002). As described in section 1.2.1, activation of the JNK cascade in the epithelial leading edge is thought to

be involved in the elongation of the epithelium. In keeping with the idea presented here that the cell shape changes, including epithelial elongation, involved in dorsal closure initiate earlier than previously suggested, is the observation that leading edge levels of *dpp* expression, a downstream target of JNK signaling, peak very early in the closure process and are high while the germ band is still retracting (my own observations and (Stronach and Perrimon, 2002). *Dpp* levels in the leading edge dwindle later in closure and, by the zippering stage, have become very weak.

During the initiation stage of dorsal closure the epithelial cells of the leading edge possess none of the actin-based features seen in later phases and form a somewhat disorganised, scalloped edge. With no actomyosin cable the cells of the leading edge presumably have very little internal tension and the scalloped appearance of the edge may be caused by these malleable cells being tugged by the amnioserosa cells at restricted points of adhesion (Fig 3.1B). At this earliest phase the epithelial cells are advancing dorsally, although at a somewhat slower rate than that seen later. There seems to be no apparent movement of epithelia over the amnioserosa, suggesting that this phase of closure is largely a consequence of amnioserosa cell contraction. Indeed, it is clearly the case that these cells reduce the size of their apical surface substantially during this early phase (Figs 3.1A and B).

ii) Epithelial Sweeping – Stage 13, starts ~10 hours AEL

The "Epithelial Sweeping" phase of dorsal closure is characterised by changes in leading edge cell shape and actin organisation. During this stage these cells begin to polarise as filamentous actin accumulates at their apical edge to form a thick actin cable (Figure 3.5B). The assembly of this cable coincides with, and may be responsible for, the transformation of the lead edge from floppy and scalloped into a smooth, neat row of cells (3.5A and B). Simultaneously, the leading edge cells elongate in a dorso-

ventral direction across the amnioserosa such that now a net movement of epithelium over amnioserosa is seen (Figure 3.4 and Movie 2).

Throughout this stage of dorsal closure, the epithelial hole reduces in size, due presumably to a combination of epithelial cell elongation, continued amnioserosa cell contraction, and contraction of the actin cable. Certainly, it is clear from the observations described here that contraction of the amnioserosa continues through to the end of closure, with 39% of amnioserosal cells being extruded from the surface of the monolayer, whilst the remainder are overtaken by the advancing epithelial leading edge. Previous laser ablation studies during dorsal closure have shown that at this stage, both the amnioserosa and epithelium are under tension, as laser wounds in either cell layer caused gaping around the wound (Kiehart et al., 2000). These experiments indicate that both tissues are actively contracting, arguing against a situation where either tissue is being passively pushed or pulled by the other.

Another event that occurs during epithelial sweeping is the first emergence of actin protrusions from the leading edge. Filopodia, and to a much lesser extent lamellipodia, begin to be assembled by the leading edge as soon as actin starts to accumulate at the edge. However, the protrusions at this stage are very small and it is uncertain what role they may fulfil as the opposing epithelial sides are still too far apart, even at the most anterior and posterior ends of the hole, for filopodia from opposite sides to reach one another and zip together as seen in the next phase of dorsal closure. One possibility is that at this early point in closure, the filopodia may play some sensory role since they do make contact with the amnioserosa sheet ahead of them. Potentially, signalling between the epithelium and amnioserosa could be mediated through these initial filopodial contacts, a role analogous to that played by cytonemes in imaginal discs (see Section 1.6.4) (Ramirez-Weber and Kornberg, 1999).

iii) Zippering – Stage 14, starts ~11 hours AEL

The "Zippering" phase of dorsal closure begins once opposing leading edges at the most anterior and posterior ends of the hole are close enough for filopodia to reach across and touch the opposite epithelial edge. This appears to happen only once the two edges are less than 10μm apart. By the start of this phase, closure of the hole by mechanisms other than zippering has already brought the dorsal epithelium of the first (most anterior) and last (most posterior) segments together. For the remaining segments, the filopodia produced by the leading edge cells appear crucial for correct closure. They act to tug and tightly adhere the opposing epithelial surfaces together, and also appear key for the correct matching of the embryonic segments as the hole closes along the midline seam (Jacinto et al., 2000) (Movie 3). However, in addition to filopodia, it is highly likely that both contraction of the actin cable and continued amnioserosa cell contraction still play roles, albeit lesser ones than seen in the Initiation and Epithelial Sweeping phases, in bringing the sides together.

An important element in the control of filopodial function during zippering appears likely to be the regulation of the dynamic assembly and disassembly of actin protrusions by the leading edge. Quantification shows that the area and length of protrusions formed by the leading edge increases during the course of closure, rising to a peak in the last 60 minutes of the process, when zippering is taking place (Figures 3.8 and 3.9). Furthermore, rates of protrusion extension and retraction both steadily increase during closure as zippering proceeds. Significantly, actin retraction rates appear to be suppressed once the protrusions manage to touch the opposite edge or opposing filopodia, allowing a prolonged interaction between protrusions and ultimately the formation of mature adhesions between the abutting epithelial cells.

A further level of complexity to the control of actin dynamics at the leading edge is added by the requirement to correctly match the segments of the embryo as the dorsal hole closes. Again, controlling the persistence of the actin protrusions may be important for correct segmental matching. During dorsal closure, filopodia can often be seen reaching out and interacting with leading edge cells in an incorrect segment, but when this occurs the filopodium retracts whereas in contrast an interaction with the appropriate segmental partner leads to suppression of retraction and a prolonged interaction resulting in epithelial fusion (Jacinto et al., 2000). The role of actin protrusions in segmental matching and how this function might be controlled is explored in greater detail in Chapters 4 and 5.

iv) Termination – Stage 15, ends ~13hours AEL

As is the case for the other phases of dorsal closure, the final stage of this process exhibits a temporal progression, spreading like a wave within the seam behind the two advancing zipper fronts. A crucial aspect of termination is that once leading edge cells from opposing sides have made contact they must stop moving and form a tight seam along the midline. In keeping with this, live imaging clearly shows that fusion of the two epithelial edges is quickly followed by the quelling of actin protrusion assembly (see Movie 3 and Figure 3.8).

There must, therefore, be some form of "stop" signal to prevent the cells from overshooting. This signal can be considered as an example of contact inhibition, which provides another exciting avenue to pursue using the genetically tractable model of dorsal closure. It seems likely that regulation of JNK signalling may play a role in this termination phase just as for initiation of dorsal closure. Indeed, previous studies have shown that if the normal down regulation of JNK signalling is prevented in the amnioserosa dorsal closure fails to complete (Reed et al., 2001). It is speculated that,

in this case, the amnioserosa emits precocious "stop" signals to the adjacent epithelial cells which causes closure to cease, suggesting that in wild type closure the leading edge cells stop moving once they come into contact with cells expressing similar levels of JNK activity, i.e. the opposing leading edge. Ideas surrounding contact inhibition and the termination of dorsal closure are further explored in Chapter 4.

In addition to stopping, the abutting epithelial cells must also convert the transient adhesions formed between filopodia into tight, permanent, adhesive junctions. As described above, the initial interaction between opposing protrusions is probably assisted by a suppression of filopodial retraction. Once these temporary contacts are made mature adherens junctions can begin to form, in a similar manner to that seen in *C.elegans* ventral enclosure and in keratinocyte tissue culture models (Jacinto et al., 2000; Raich et al., 1999; Vasioukhin et al., 2000).

In conclusion, the dynamic analysis of dorsal closure described in this chapter demonstrates the great strengths of live imaging for the study of tissue migrations and morphogenesis. Importantly, this study of wild type dorsal closure also provides a framework from which to compare the same process in mutant embryos. In particular, live imaging can reveal crucial intricacies in mutant phenotypes that would go unnoticed if analysed in fixed tissue.

CHAPTER 4

Rac plays multiple, dynamic roles in dorsal closure

4.1 INTRODUCTION

4.1.1 Rac induces membrane ruffling and the formation of lamellipodia

As described in Chapters 1 and 3, the Rho family of small GTPases are key regulators of the actin cytoskeleton and their study in dorsal closure is crucial to understanding the different roles played by actin structures *in vivo*. In dorsal closure, Rho1 appears to be the GTPase responsible for organization of actin into a leading edge actin cable, mirroring findings in cell culture where Rho is required for the formation of cable-like stress fibres. In a similar way the role of Cdc42 in the organization of the actin cytoskeleton during dorsal closure correlates with tissue culture findings, where in both cases Cdc42 is involved in the formation of filopodia.

The third Rho family small GTPase, Rac, was shown to direct the assembly of the actin meshworks that form dynamic lamellipodia and membrane ruffles. Tissue culture studies revealed that growth factor mediated membrane ruffling could be abolished by transfection with a dominant negative form of Rac, whilst, conversely, expression of constitutively activated Rac produced ruffling in the absence of growth factor stimulation (Ridley et al., 1992).

4.1.2 Downstream effectors of Rac – clues from tissue culture

Activated Rac has been shown to work on a number of downstream effectors to generate lamellipodia in cultured cells (reviewed in Burridge and Wennerberg, 2004). Crucially, Rac activates the WAVE/Scar protein, through an indirect mechanism, and activated WAVE/Scar then goes on to stimulate the Arp2/3 complex to nucleate actin at branch-points along filaments, ultimately generating a meshwork of actin (Machesky and Insall, 1998; Miki et al., 1998). It has been shown that IRSp53 can provide a link between activated Rac and WAVE/Scar (Miki et al., 2000) but also WAVE has been found to be present in cells as a inactive complex with two Rac binding proteins,

Nap125 and PIR121, and the removal of these by Rac may provide an alternative route for Rac activation of WAVE (Eden et al., 2002) (see Figure 4.1).

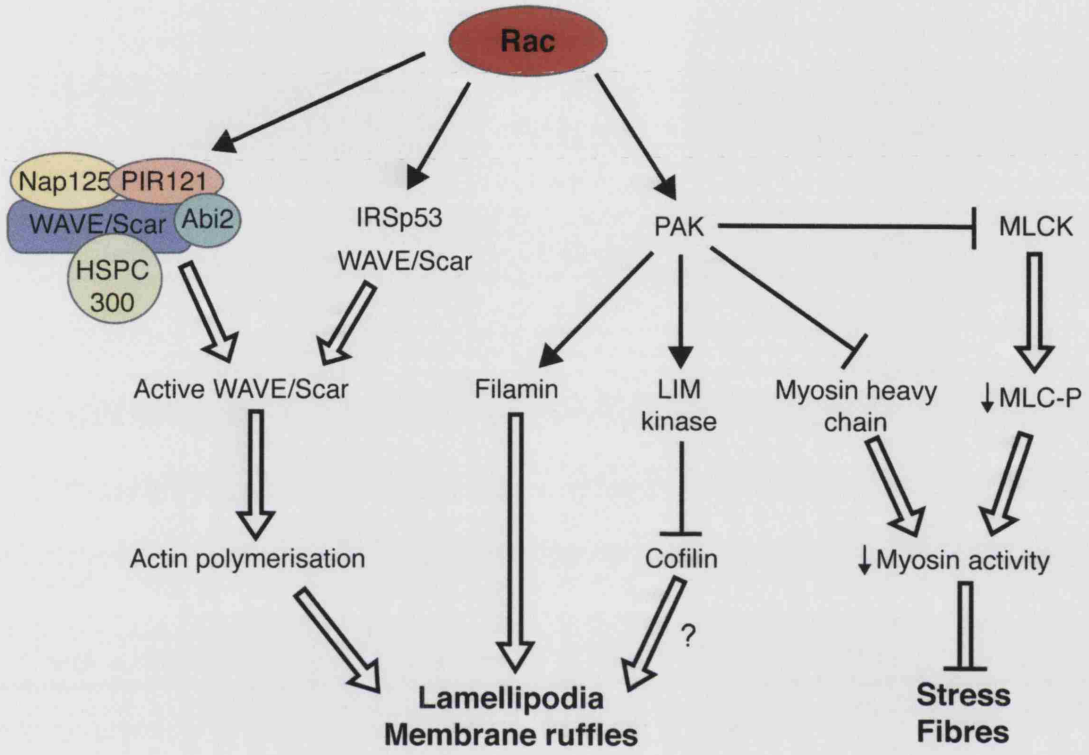

Figure 4.1 Signalling from Rac to the cytoskeleton: clues from tissue culture
Work in cultured cells has built up a network of pathways which lead from Rac activation to the formation of lamellipodia and the suppression of stress fibres. Direct interactions are displayed by solid arrows and inhibitory signals by bars. Double-lined arrows and bars indicate the net result of the signalling pathway (adapted from Burridge and Wennerberg, 2004).

Other signalling pathways that also mediate Rac regulation of actin structure, include PAK, a serine/threonine protein kinase, whose downstream effects include the organization of lamellipodial protrusions (Figure 4.1) (Sells et al., 1997). PAK appears to have a number of potential binding partners including LIM kinase (Edwards et al., 1999) and the actin binding protein, Filamin, which may promote lamellipodial formation (Vadlamudi et al., 2002). In addition, PAK can also inhibit myosin and myosin light chain kinase (MLCK), resulting in reduced stress fibre assembly (Sanders et al., 1999). Rac can also activate MAPK pathways, including the JNK cascade, which leads

to the phosphorylation and activation of various transcription factors that are involved in a wide range of vital cellular processes such as cell cycle progression and differentiation (Coso et al., 1995; Minden et al., 1995).

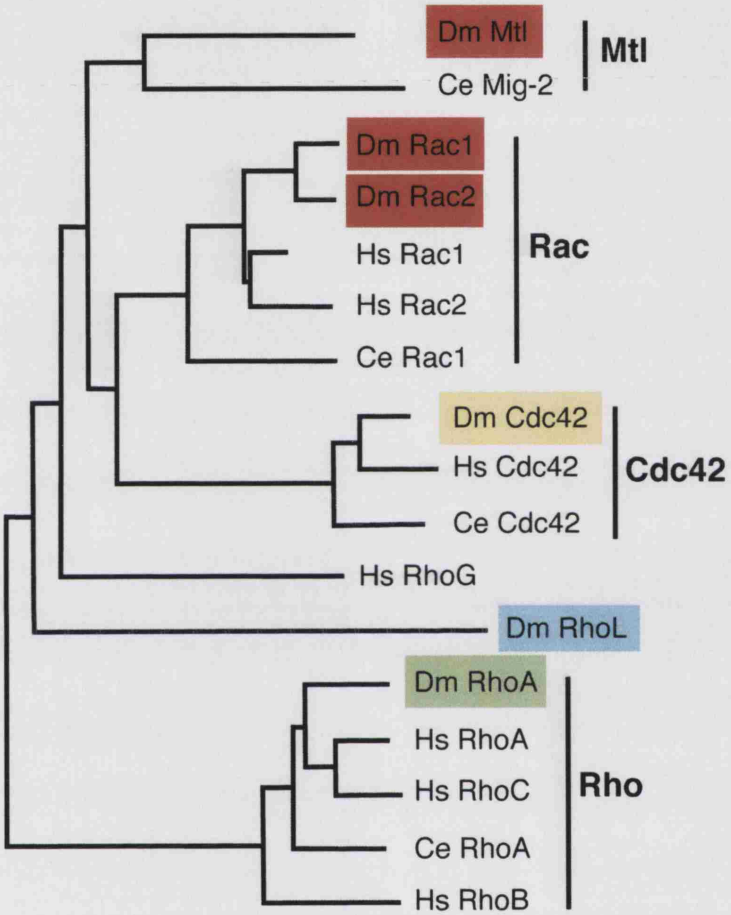

Figure 4.2 *Drosophila* have three *Rac*-like genes

A phylogenetic tree of *Drosophila* (Dm), *C. elegans* (Ce) and selected human (Hs) Rho family GTPases. The *Drosophila* genome encodes three Rac-like genes, *Rac1* and *Rac2*, which share homology with human Racs and *mtl*, which although it belongs to a distinct subclass of Rho GTPases, is thought to behave functionally as a Rac (adapted from Newsome et al., 2000).

4.1.3 *Drosophila* have three *Rac*-like genes

The *Drosophila* genome contains three *Rac*-like genes: *Rac1, Rac2* and *Mtl*. *Rac1* and *Rac2* are two highly similar *Rac* genes which are most homologous with mammalian *Rac1* (Figure 4.2). The *Mtl* gene encodes for a related GTPase that is structurally

similar to both Rac and Cdc42 GTPases (Newsome et al., 2000). However, at the functional level it appears that *Mtl* behaves more like Rac than Cdc42 and so tends to be grouped with the *Drosophila Rac* genes (Hakeda-Suzuki et al., 2002; Ng et al., 2002). All three *Rac* genes are ubiquitously expressed during *Drosophila* development (Harden et al., 1995; Hariharan et al., 1995; Luo et al., 1994; Newsome et al., 2000).

4.1.4 Rac is required for dorsal closure and organizes leading edge actin

To date much of our understanding of Rac function during dorsal closure has come from experiments where constitutively active or dominant negative forms of *Drosophila Rac1* transgenes are ectopically expressed in the embryo. Expression of dominant negative *Rac1* ($Rac1^{N17}$) from a heat shock promoter during embryogenesis leads to a failure in dorsal closure, as revealed by the presence of dorsal holes or scabs in the cuticles of affected embryos. A minority of $Rac1^{N17}$ expressing embryos fail in the earlier morphogenetic event of germ-band retraction (Harden et al., 1995). When assessed as fixed preparations, the $Rac1^{N17}$ embryos display a drastic reduction in actin and myosin accumulation at the epithelial leading edge during dorsal closure, suggesting that Rac plays a key role in organizing the actin cytoskeleton in these cells. Furthermore, some cells along the leading edge of these embryos lose their dorso-ventral elongation and are polygonal rather than rectangular in shape, the implications of which are discussed in the following Section, 4.1.5. A further study, utilising constitutively active and dominant negative *Rac1*, has also indicated a requirement for Rac in the amnioserosa, since specific expression of either transgene in this tissue leads to dorsal open phenotypes (Harden et al., 2002). Strikingly, amnioserosal expression of $Rac1^{V12}$ resulted in over-contraction of the amnioserosa, causing the embryos to become bowed as the head and tail ends are pulled towards each other. Correlating with this excessive constriction, amnioserosa cells in these embryos display higher than normal levels of F-actin and myosin accumulation. Conversely,

expression of *Rac1*^{N17} in the amnioserosa led to reduced levels of F-actin in this tissue and a failure of amnioserosal cell contraction (Harden et al., 2002).

More recently, Rac function in dorsal closure has been briefly assessed in mutants which are null for all three *Drosophila* Rac genes. Embryos that lack both zygotic and maternal contributions of *Rac1, Rac2* and *Mtl*, fail to complete dorsal closure and show large dorsal and anterior holes in their cuticles (Hakeda-Suzuki et al., 2002). Work on fixed tissue found that triple mutant embryos display very little actin accumulation along their epithelial leading edge. However, in contrast to the findings with amnioserosal expression of *Rac1*^{N17} and *Rac1*^{V12} (see above), the amnioserosa, when viewed fixed, appears unaffected in the triple *Rac* mutants. Embryos mutant for any one of the three *Rac* genes complete dorsal closure, as do *Rac2 Mtl* double mutants. However, weak dorsal closure defects are seen in *Rac1Rac2* and *Rac1Mtl* double mutants. Together these results indicate that any one of the three *Drosophila* Racs can be largely sufficient for dorsal closure to complete, although *Rac1* appears to make the greatest contribution to the process.

4.1.5 Evidence that Rac activates the JNK cascade during dorsal closure

As described in section 4.1.4, expression of *Rac1*^{N17} during dorsal closure leads to a failure in the usual dorso-ventral elongation of epithelial cells, as well as loss of the leading edge cytoskeleton. These phenotypes are similar to those in embryos mutant for elements of the JNK cascade, suggesting that Rac may function in this pathway. Furthermore, it has been found that expression of constitutively active Jun can partially rescue the *Rac1*^{N17} induced dorsal closure defects, tentatively positioning the JNK pathway downstream of Rac activity (Hou et al., 1997). In the converse experiment, expression of *Rac1*^{V12} drives ectopic expression of *dpp* (see section 1.2.1 for JNK pathway details), indicating that Rac may act as an upstream regulator of the JNK

cascade (Glise and Noselli, 1997). However, the link between Rac and the JNK pathway has yet to be verified in the *Rac* triple mutant embryos.

4.1.6 Other likely Rac interactors during dorsal closure

It remains unclear how Rac might activate the JNK pathway during dorsal closure. One possibility is the Rac effector, PAK, which localises to the epithelial leading edge during dorsal closure in a Rac dependent manner (Harden et al., 1996). Zygotic *PAK* loss-of-function mutants survive embryogenesis (Hing et al., 1999), but when the maternal contribution of *PAK* is eradicated embryos fail in dorsal closure and have a buckled leading edge. However, it appears that PAK does not feed into the JNK pathway as the mutant embryos show no loss of JNK activity along the leading edge (Conder et al., 2004). Another potential downstream target of Rac in dorsal closure is Pkn, a member of the PKN-family of PKC-related kinases, which has been found to bind specifically to activated *Rac1*. But, like PAK, Pkn appears to act independently of the JNK pathway to regulate the actin cytoskeleton because, although Pkn mutants exhibit dorsal closure failures, the JNK pathway remains undisrupted in these embryos (Lu and Settleman, 1999). A further possibility is that Rac activates the JNK pathway through a direct interaction with the JNKKK, Slipper (Slpr), as it possesses a putative Cdc42/Rac interacting domain (Burbelo et al., 1995), but this has yet to be investigated.

A likely activator of Rac during *Drosophila* embryogenesis appears to be Myoblast city (Mbc). Mbc is highly homologous to DOCK180, a mammalian activator of Rac. Embryos mutant for *mbc* have dorsal closure defects and show abnormalities in their leading edge actin cytoskeleton and reductions in expression of dpp, phenotypes similar to those of embryos expressing $Rac1^{N17}$ (Nolan et al., 1998). Tissue culture evidence suggests that DOCK180 may be a mediator of integrin signaling, and although this has not been investigated in dorsal closure, the integrin mutants

myospheroid (*mys*) and *scab* (*scb*) do exhibit defects in dorsal closure (Brown, 1994; Brown et al., 2000; Stark et al., 1997).

4.1.7 Rac function in dorsal closure has not been assessed dynamically

Thus far all investigation of Rac GTPase function in dorsal closure have been carried out in fixed embryos. As discussed in Chapter 3, dorsal closure is a highly dynamic process and much can be learned from studying it using live microscopy approaches. In particular, live imaging allows one to follow the assembly of leading edge filopodia and lamellae, which are largely lost during the fixation process. As work in tissue culture indicates that Rac is the key GTPase for the assembly of lamellipodia it is particularly pertinent that its function in dorsal closure is assessed live.

4.2 RESULTS

4.2.1 Expression of constitutively active *Rac1* (*Rac1^{V12}*) induces the assembly of overly large lamellipodia by leading edge cells

I began my dynamic studies of Rac function in dorsal closure by expressing a constitutively active form of *Rac1* (*UAS-Rac1^{V12}*) in the embryonic epithelium. When *Rac1^{V12}* is expressed throughout the epithelium, using the *e22c-GAL4* driver, embryos die prior to dorsal closure. To circumvent this I expressed *Rac1^{V12}* in segmental stripes of the epithelium using the *engrailed* driver, which allows the embryo to survive through to dorsal closure due to the presence of non-expressing wild type epithelial cells. Another advantage of using the *engrailed* driver is that one can view wild type and mutant transgene expressing cells side by side, allowing for direct comparison between the two neighbouring cell populations. To visualise actin remodelling in real time I co-expressed GFP-actin along with *Rac1^{V12}*. I find that expression of *Rac1^{V12}* leads to a vast over-production of actin protrusions by leading edge cells. (compare Figures 4.3A and 4.4A and Movies 4 and 5). In addition, *Rac1^{V12}* expressing cells fail to assemble a normal actin cable and the leading edge of these embryos is highly disorganized.

To assess the extent of over assembly of lamellipodia when constitutively active *Rac1* is expressed I quantified the maximum protrusive area in wild type versus *Rac1^{V12}* embryos (Figure 4.6). I find that *Rac1^{V12}* expressing cells show an approximate 4-fold increase in the area of protrusions formed along the leading edge; for example at 100mins into closure the average maximum protrusive area assembled by wild type cells is 35.0±4.2μm^2 compared to 136.7±17.5μm^2 in *Rac1^{V12}* cells.

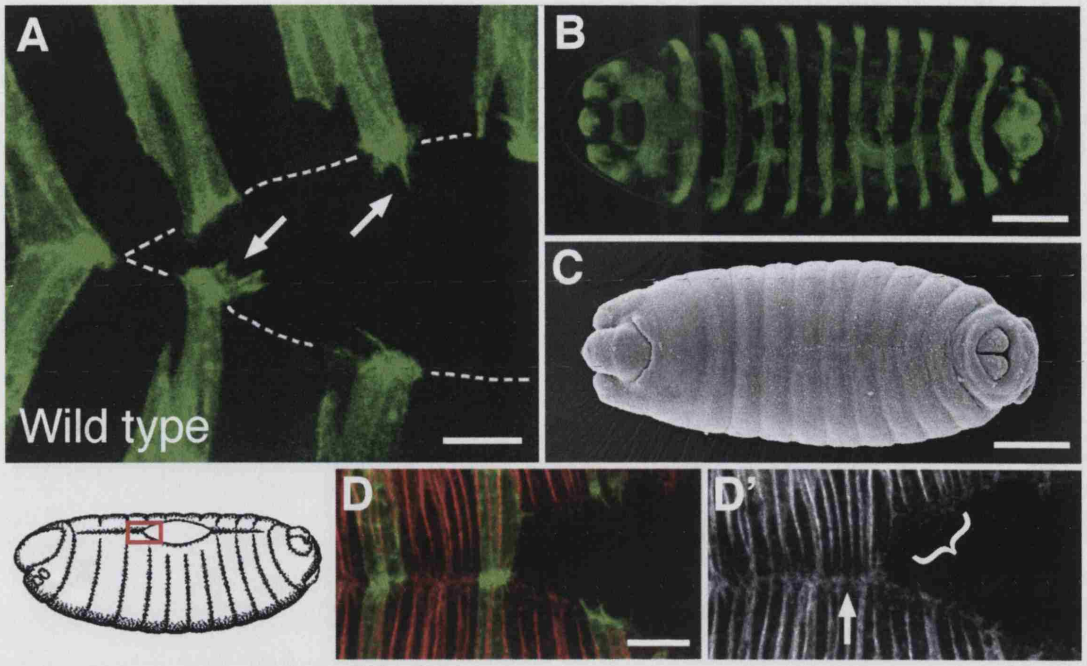

Figure 4.3 Wild type dorsal closure in embryos expressing GFP-actin in *engrailed* segmental stripes

(A) High magnification still from a confocal movie of a wild type embryo expressing GFP-actin in *engrailed* cells. Filopodia and occasional lamellae can be seen extending from the leading edge cells. At the completion of dorsal closure, wild type embryos display segmental alignment along the fused midline seam (B), which is also shown by scanning electron microscopy (SEM) in (C). (D), and (D'), dorsal closure stage embryos stained with anti-Fasicilin III antibodies (red in D and single channel in D') and also expressing GFP-actin (green in D). Boxed zone on the embryo schematic indicates the region magnified in D and D'. In wild type leading edge cells, Fas III is localised cortically but excluded from the dorsalmost side (D', bracketed region), until the epithelial surfaces meet at the midline (D', arrow). Scale bars in (A) and (D) represent 10μm and in (B) and (C) represent 100μm.

4.2.2 *Rac1*^{V12} cells have a migrational advantage over their wild type neighbours and take over the leading edge but subsequently epithelial sweeping halts precociously

A further consequence of expression of *Rac1*^{V12} is that the mutant cells appear to have a migrational advantage over their wild type neighbours and move past them at the leading edge. As a result of this, the *Rac1*^{V12} cells in adjacent *engrailed* stripes fuse with one another (Figure 4.4A) so that later in dorsal closure virtually the entire leading

edge is composed of *Rac1*^{V12} cells (Figure 4.4B). At this point, dorsal closure stalls and the embryo fails to close its epithelium further (Figure 4.4C).

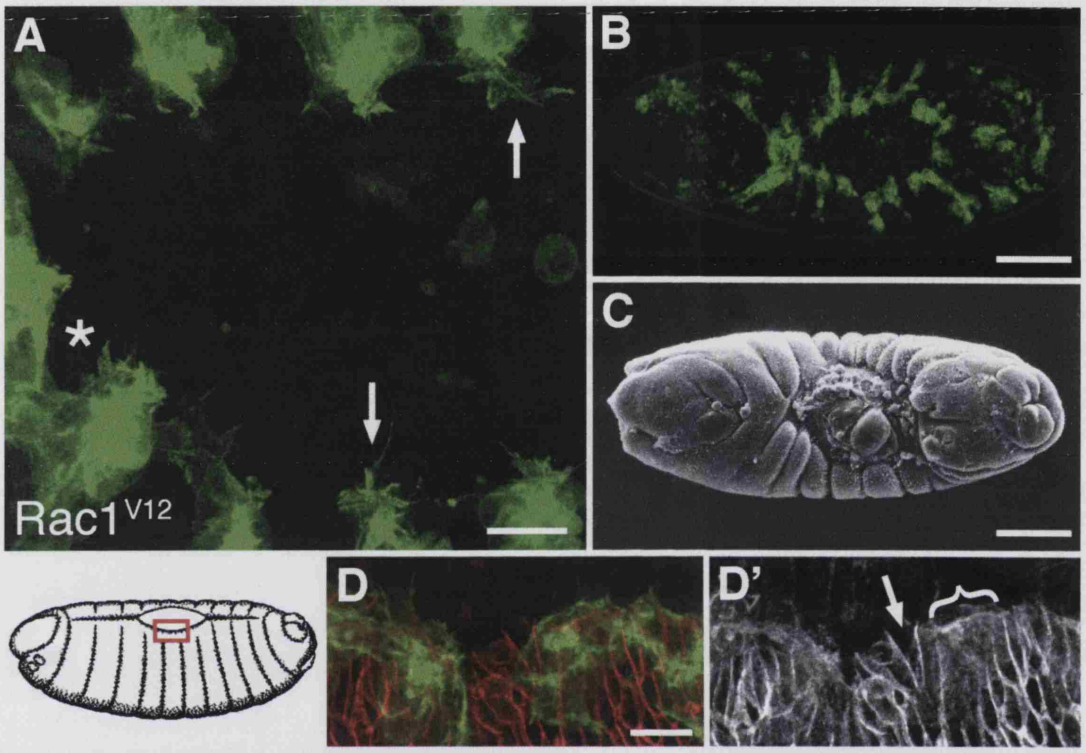

Figure 4.4 Leading edge cells expressing constitutively active *Rac1* (*Rac1*^{V12}) assemble excessively large lamellipodia

Rac1^{V12} was co-expressed with GFP-actin in *engrailed* stripes. (A): High magnification still from a confocal movie. The *Rac1*^{V12} expressing cells produce overly large lamellipodia (arrows) and bypass wild type neighbours to interact with cells in adjacent engrailed stripes (asterisk). (B): A low magnification confocal still of a *Rac1*^{V12} expressing embryo later in closure when virtually the whole leading edge is composed of the *Rac1*^{V12} expressing cells, causing a premature termination in dorsal closure and leading to a dorsal large hole, shown clearly by SEM in (C). (D) and (D') Dorsal closure stage *Rac1*^{V12} expressing embryo stained with anti-Fasicilin III antibodies (red in D, single channel in D') and also expressing GFP-actin (green in D). Boxed zone on the embryo schematic indicates the region magnified in D and D'. *Rac1*^{V12} expressing leading edge cells (co-expressing GFP-actin) prematurely localise Fas III to their dorsal edge (D', bracketed region) whilst some wild type cells (identified by absence of GFP-actin in D) in these embryos maintain the correct localisation (D', arrow). Scale bars in (A) and (D) represent 10μm and in (B) and (C) represent 100μm.

4.2.3 *Rac1*^{V12} cells localize Fasciclin III to the leading edge surface before epithelial edges have met

Previous studies have shown a similar migrational advantage when epithelial stripes expressing dominant negative *Rho1* lose their "restraining" leading edge cable. However, in the case of *Rho*, the transgene-expressing cells continued to advance and close the hole (Jacinto et al., 2002a). An explanation for the inability to advance once constituently active *Rac1* cells have taken over the leading edge may be that these cells read some form of inhibitory cue when they contact their adjacent neighbours, a cue which they would normally only be exposed to on reaching the opposing epithelial edge. Upon "reading" this cue the *Rac1*^{V12} cells respond by slowing their migration, resulting in the bunching I see along the leading edge. (Figure 1F).

In wild type embryos, Fasciclin III (Fas III), a component of septate junctions, is excluded from the dorsalmost side of the epithelial leading edge cells (Figure 1D') until the opposing surfaces touch and fuse, at which point Fas III accumulates along this edge (Figure 1D'). However, in *Rac1*^{V12} expressing cells I find that Fas III is prematurely localised to the dorsal side of the leading edge cells before the opposing epithelial surfaces have made contact (Figure 1D'). This premature dorsal accumulation of Fas III indicates that *Rac1*^{V12} expressing cells may have already adopted the state of cells that have completed migration. I therefore speculate that a contributing factor in the precocious halting of epithelial movement observed in these embryos is that, once the *Rac1*^{V12} cells have advanced to take over the leading edge, the embryo is left with a majority of cells along the edge which incorrectly "sense" that they have met their contralateral neighbours and are thus "contact-inhibited" from further migration.

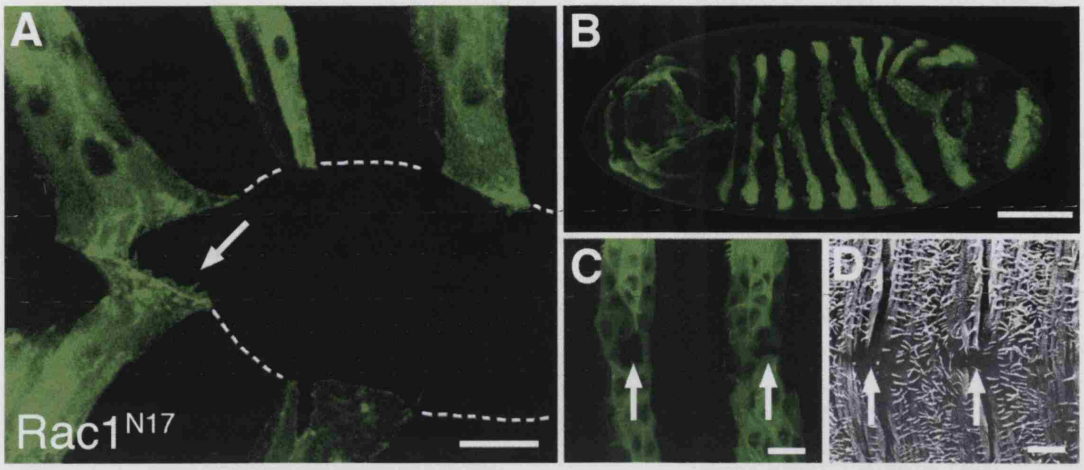

Figure 4.5 Expression of dominant negative *Rac1* (*Rac1^{N17}*) eradicates actin protrusion assembly

Rac1^{N17} was co-expressed with GFP-actin in *engrailed* cells. (A) High magnification confocal still of dorsal closure stage embryo, *Rac1^{N17}* expressing leading edge cells assemble only the most rudimentary actin protrusions (arrow) and also show a lack of actin cable formation. These embryos do close, due to the contribution of wild type epithelial cells, but at low magnification (B) it is clear that the normal segmental alignment has not been maintained. In addition, *Rac1^{N17}* expressing cells fail to fuse properly leaving small holes at the midline as revealed both by higher magnification confocal microscopy (C, arrows) and SEM (D, arrows). Scale bars in (A), (C) and (D) represent 10μm and in (B) represent 100μm.

4.2.4 Expression of dominant negative *Rac1* (*Rac1^{N17}*) causes a failure in the assembly of actin protrusions and actin cable by leading edge cells

I next investigated the consequence of expressing dominant negative *Rac1* (UAS-*Rac1^{N17}*) in the epithelium, again using the *engrailed* driver. I found that *Rac1^{N17}* inhibits actin protrusion assembly, with expressing cells producing only the most cursory projections throughout dorsal closure (Figures 4.5A and Movie 6). Actin cable assembly is also reduced in some *Rac1^{N17}* cells (Figure 4.5A).

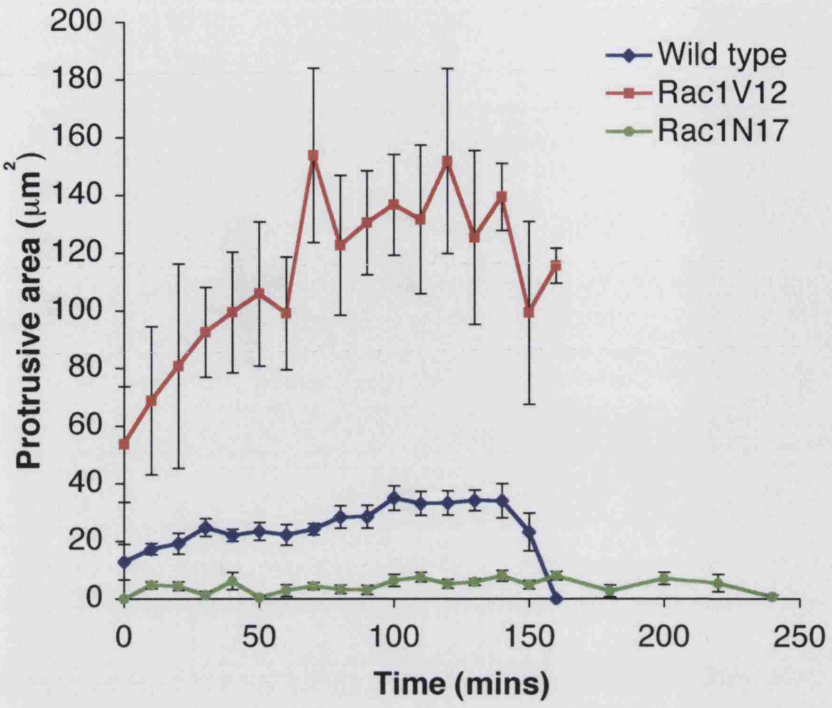

Figure 4.6 Quantification of actin protrusion area reveals a large increase in size when *Rac1*^{V12} is expressed, and a decrease with expression of *Rac1*^{N17}

Quantification of actin protrusions formed in wild type (blue diamonds) compared to *Rac1*^{V12} (red squares) and *Rac1*^{N17} (green circles) expressing embryos. The mean protrusion area for each time-point is displayed here, with error bars representing standard error of the mean. Wild type embryos were closed by 160mins and no longer making protrusions, but as *Rac1*^{N17} expressing embryos did not close until 240mins, later time-points are displayed for these embryos.

4.2.5 *Rac1*^{N17} cells fail to fuse at the midline and exhibit segmental mismatch

Embryos expressing *Rac1*^{N17} in *engrailed* stripes are able to complete dorsal closure due to the contribution of the wild type cells but the *Rac1*^{N17} cells fail to fuse correctly at the midline, leaving small gaps in the epithelial seam, a phenotype seen in 89% (n=75) of these embryos (Figure 4.5B, C and D). A further consequence of *Rac1*^{N17} expression is that embryos show segmental mismatching along the midline; 69% (n=75) of the embryos I assessed displayed segmental mismatch, with the majority of these (81%) showing mismatch of more than one pair of segments (Figure 4.5B). In both these regards my dominant negative *Rac1* data is reminiscent of previous studies in which Cdc42 activity was blocked by expression of dominant negative *Cdc42* (Jacinto et al.,

2000), suggesting that *Cdc42* and *Rac1* exhibit overlapping, yet non-redundant, functions in dorsal closure.

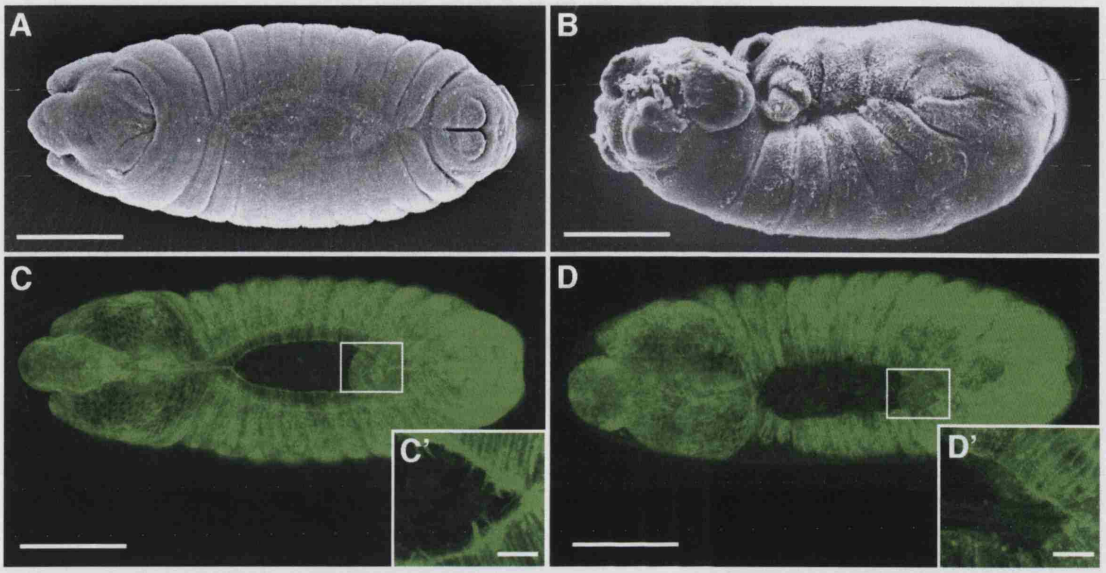

Figure 4.7 Triple *Rac*^{J10} mutant germ line clone embryos show failure in germband retraction, head involution and dorsal closure.

(A) and (B) are SEMs of a wild type dorsal closure stage embryo (A) and an equivalent stage *Rac1*^{J10} *Rac2Δ MtlΔ* germ line clone embryo (B) which shows a failure to complete germ band retraction and head involution. (C) and (D) are confocal images of live dorsal closure stage embryos expressing *UAS-GFP-actin* driven by the epithelial driver *e22c-GAL4*, with wild type embryo (C) revealing both actin cable and protrusions along the leading edge (boxed region at higher magnification in C'), while the *Rac1*^{J10} *Rac2Δ MtlΔ* germ line clone embryo (D and D'), shows an absence of actin cable and protrusions at the leading edge.

Scale bars in (A), (B), (C) and (D) represent 100μm and in (C') and (D') represent 10μm.

4.2.6 Triple *Rac* germ line clone embryos fail in germband retraction, head involution and early dorsal closure

An alternative explanation for the similarities between expression of dominant negative *Cdc42* and *Rac1* is that these transgenes are somewhat non-specific in their actions. Recent identification of triple *Rac* mutants allowed me to address this possibility by directly testing *Rac* function during dorsal closure in embryos lacking functional copies of all three *Drosophila Rac* genes (Hakeda-Suzuki et al., 2002; Ng et al., 2002). In the

triple *Rac* mutant, the *Rac2* and *Mtl* genes are excised whilst *Rac1* carries one of two point mutations: a hypomorphic allele called *J10* or a complete loss-of-function allele, *J11*. As previously reported (Hakeda-Suzuki et al., 2002), I find that germ line clones of the $Rac1^{J11}$, *Rac2Δ, MtlΔ* triple mutant (hereafter referred to as Rac^{J11}) fail to produce embryos; the hypomorphic triple *Rac* mutant, $Rac1^{J10}$, *Rac2Δ, MtlΔ* (hereafter referred to as Rac^{J10}) does produce germ line clone embryos but the majority of these, (89% by cuticle preparation analysis, n=54) fail in head involution and/or germband retraction, as well as dorsal closure (Figure 4.7B). The Rac^{J10} germ line clone embryos with the least severe phenotypes that exhibit only dorsal holes (11%, n=54) all fail at the very earliest stages of closure (Figure 4.7D).

4.2.7 The leading edge of triple Rac germ line clone embryos fails to assemble actin cable and protrusions

To assess the actin cytoskeleton dynamically in Rac^{J10} germ line clone embryos I expressed GFP-actin throughout their epithelium using the *e22c-GAL4* driver. I find that these embryos have very little actin accumulation, with little or no cable at the epithelial edge (Figure 4.7D, compare to 4.7C). Furthermore, timelapse analysis of the leading edge of Rac^{J10} germ line clone embryos shows virtually no protrusive activity (Figure 4.7D').

4.2.8 Zygotic triple *Rac* mutants complete dorsal closure but show puckering along the dorsal midline

As the triple *Rac* mutant germ line clones fail at the very start of dorsal closure, or earlier in embryogenesis, I chose to study in detail the phenotypes seen in zygotic triple *Rac* mutants. With the maternal contribution of Rac proteins intact in these embryos, they survive beyond early dorsal closure allowing me to assess the function of Rac in the later zippering stages. Rac^{J11} homozygotes show 100% embryonic

lethality and although cuticles of these embryos do not have dorsal holes, 82% (n=112) display puckering along the dorsal side indicating that dorsal closure in these mutants succeeds in sealing the hole but does so in an abnormal fashion (Figure 4.8A).

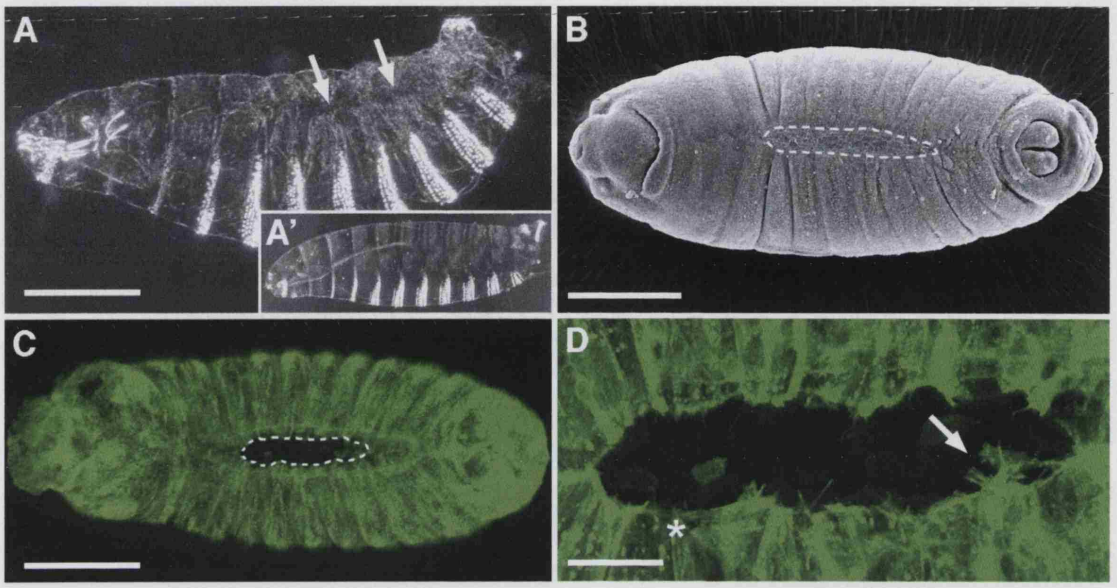

Figure 4.8 The zygotic triple *Rac* mutant exhibits a "letterbox-shaped" hole during dorsal closure and puckering along the dorsal side once closure is complete

(A): Cuticle preparation of *Rac1*^{J11} *Rac2Δ mtlΔ* homozygote (lateral view) showing puckering along the dorsal midline (arrows), indicating aberrant dorsal closure, compared to wild type cuticle (A'). (B): SEM and (C): still from a GFP-actin (expressed by epithelial driver, *e22c-GAL4*) movie of dorsal closure stage *Rac1*^{J11} *Rac2Δ mtlΔ* embryos, both illustrating the long, slit shaped dorsal hole found in these mutants. At higher magnification (D) the leading edge of the *Rac1*^{J11} *Rac2Δ mtlΔ* mutants is clearly disorganised with some cells of the leading edge assembling actin cable and actin protrusions (arrow), while in other stretches (asterisk) these structures are absent.

Scale bars in (A), (B) and (C) represent 100μm and in (D) represents 20μm.

4.2.9 During the later stages of dorsal closure zygotic triple *Rac* mutants exhibit a long, thin, "letterbox-shaped" hole

In wild type embryos the epithelial hole at dorsal closure takes on an oval, eye-like shape early in the process that progressively decreases in size as the epithelial fronts zipper together (Figure 4.7A and 4.11A). In contrast, SEMs of triple *Rac* mutant

embryos show that these embryos have an unusual, long slit-like hole during the later stages of dorsal closure (Figure 4.8B).

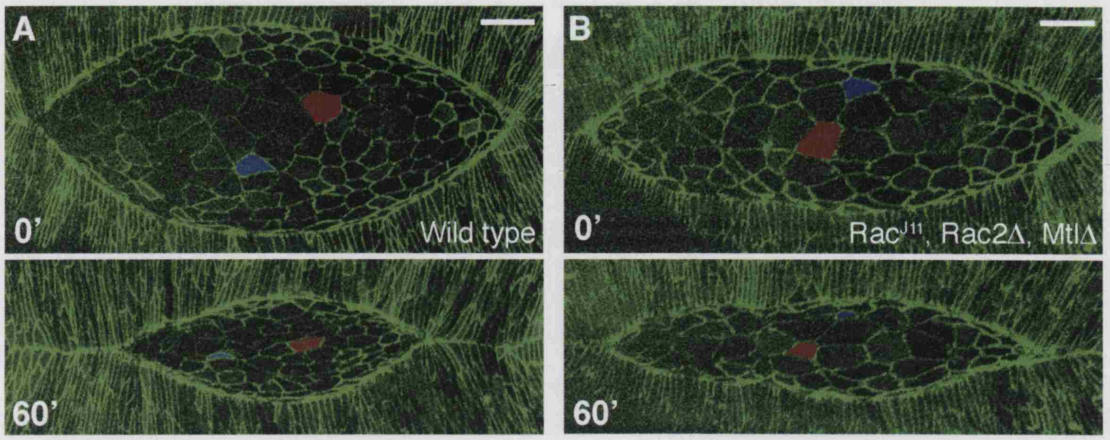

Figure 4.9 Amnioserosal cells contract in zygotic triple *Rac* mutant embryos
(A) and (B) Stills from timelapse confocal movies (Movies 2 and 7) of wild type and *Rac1^{J11} Rac2Δ mtlΔ* mutant embryos respectively, expressing *UAS-α-catenin-GFP* (driven by *e22c-GAL4*) in the epithelium and amnioserosa. 60mins later, for both wild type and mutant embryos, there is evidence of amnioserosal contraction (individual cells are highlighted in red and blue). Scale bars represent 20μm.

4.2.10 The amnioserosa contracts normally in zygotic triple *Rac* mutants

An explanation for why triple *Rac* mutants exhibit a long, thin hole during dorsal closure may be that the amnioserosa continues contracting as normal, but that epithelial zippering is impaired. To test this hypothesis I expressed *UAS-α-catenin-GFP* in triple *Rac* mutants using the *e22c-GAL4* epithelial driver. α-catenin is a component of adherens junctions and this GFP-fusion outlines all cells in the epithelium and amnioserosa when driven by *e22c-GAL4*. Live imaging indicates that amnioserosa cells in the *Rac^{J11}* mutants are able to contract in a similar manner to wild type (Figure 4.9A and B, Movies 2 and 7).

To investigate this further I compared amnioserosa cell contraction in mutant and wild type embryos by measuring the reduction in cell area during dorsal closure. I found that

at the time I began my measurements (when wild type and mutant holes were around 180μm in length) the mutant cells were significantly larger than wild type (Figure 4.10), suggesting a delay in early amnioserosal contraction. However, as dorsal closure proceeds these cells shrink in size and do so at a similar rate to wild type (Figure 4.10). Ultimately, all cells measured in both the wild type and *Rac*^{J11} amnioserosa contracted to 0μm^2 and were either extruded from the centre of the amnioserosal sheet (approximately half of cells followed in both wild type and *Rac*^{J11} mutant), or disappeared under the advancing epithelial edge.

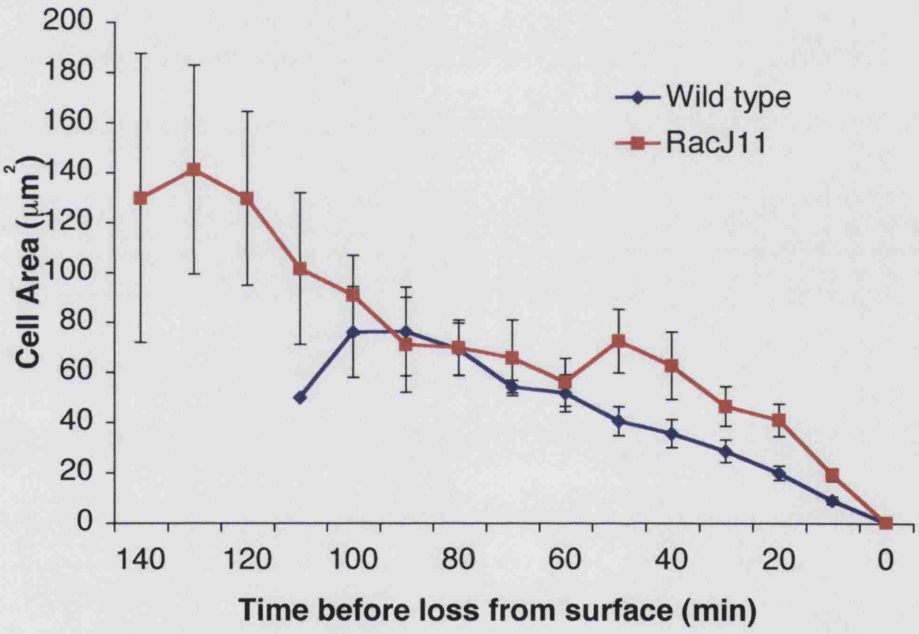

Figure 4.10 The contraction of amnioserosal cells in zygotic triple *Rac* mutants is initially delayed but then proceeds at a wild type rate

Quantification of amnioserosal cell contraction in wild type (blue diamonds) compared to *Rac1*^{J11} *Rac2Δ mtlΔ* mutant (red squares) shows that amnioserosa cells in the mutant are larger early in dorsal closure but are ultimately able to contract, at a similar rate to wild type. Data was collected from Movies 2 and 7, 10 cells from each embryo were followed and measured at 10min time-points until extruded or covered by the leading edge. Mean areas for each time-point are displayed here, with error bars representing standard error of the mean.

These data suggest that the three Rac proteins may not be essential for contraction of amnioserosa cells during the later stages of dorsal closure, although loss of Rac does delay the start of contraction. My data contrast with previously reported experiments in which dominant negative *Rac1* expressed in the amnioserosa leads to failure of dorsal closure (Harden et al., 2002).This disparity may in part be due to maternal levels of Rac in the triple *Rac* mutant being maintained longer or required at lower levels in the cells of the amnioserosa compared to the epithelium, or alternatively may indicate that the *Rac1* dominant negative transgene has non-specific affects in the amnioserosa that may block its contraction.

4.2.11 The mutant leading edge shows discrete stretches where actin cable and protrusions fail to assemble

In order to dynamically investigate epithelial zippering and the organisation of the actin cytoskeleton in the triple *Rac* mutant I expressed *UAS-GFP-actin* throughout the epithelium using the *e22c-GAL4* driver. At low magnification the long, thin hole identified using SEM can clearly be seen in these embryos by confocal imaging also (Figure 4.8C). Live imaging at high magnification reveals a number of abnormalities in the organisation of the actin cytoskeleton in leading edge cells of triple *Rac* mutants. The actin cable is incomplete in discrete regions along the leading edge of Rac^{J11} mutants and in these regions the edge is highly disorganised and no longer taut (Figure 4.8D). The leading edge of the hypomorphic, Rac^{J10} mutant appears less disordered but also shows areas where cable is absent (Figure 4.11B).

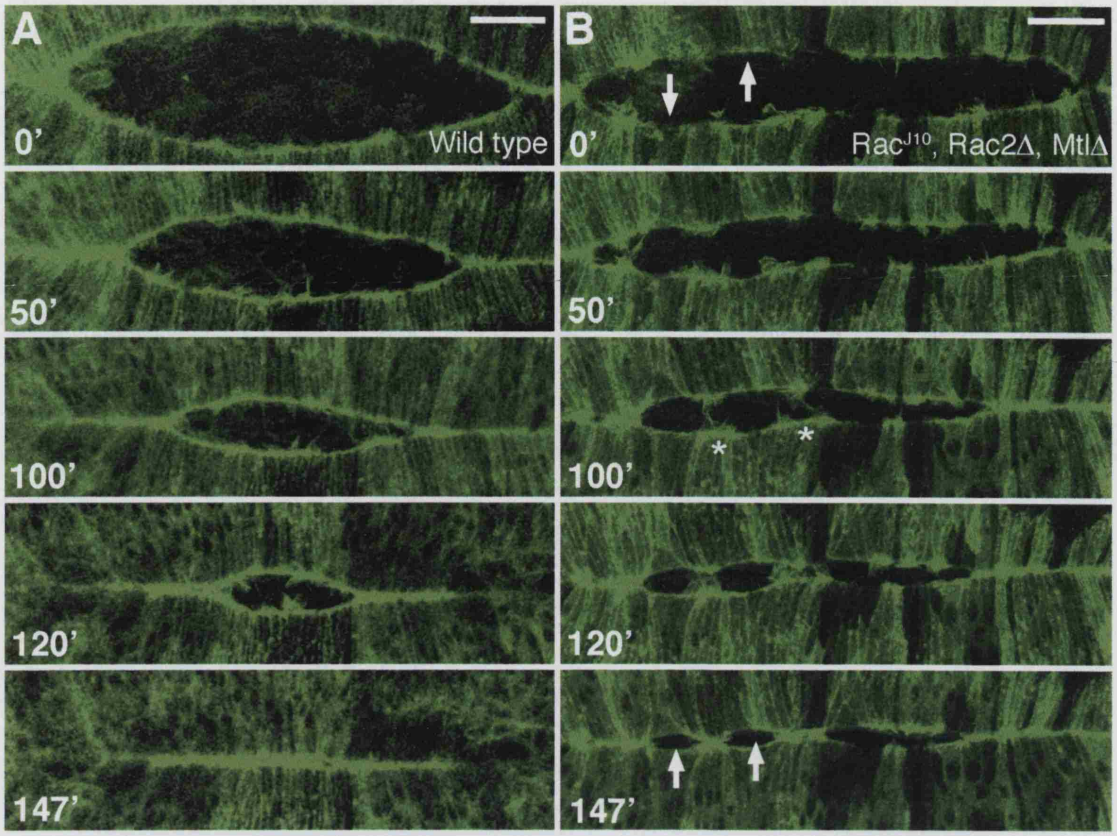

Figure 4.11 Zygotic triple *Rac* mutant closes through continued amnioserosal contraction and the formation of new zipper fronts.

(A) and (B): A series of stills taken from timelapse confocal movies of wild type (A), and *Rac1^{J10} Rac2Δ mtlΔ* mutant (B) embryos expressing *UAS-GFP-actin* in the epithelium (driven by *e22c-GAL4*). The mutant embryo displays a slit-shaped hole compared to the eye-shaped wild type hole, and the mutant has stretches of leading edge that consistently fail to assemble both actin cable and protrusions (arrows). The dorsal hole in the *Rac1^{J10} Rac2Δ mtlΔ* embryo eventually closes by skipping of the actin deficient stretches and formation of new zippering fronts (B, asterisk) beyond the areas that lack actin protrusions. Scale bars in (A) and (B) represent 20μm.

4.2.12 Triple *Rac* mutants close via continued amnioserosal contraction and the formations of new zipper fronts

Live imaging of both triple *Rac* mutants reveals that regions lacking cable also consistently fail to assemble protrusions and, where this happens, the zipper halts. However, the mutants do manage to close their epithelial hole by skipping the actin deficient regions and forming new zipper fronts beyond these "protrusionless" stretches

(Figure 4.11A and B and Movie 8). That these embryos are able to complete dorsal closure, despite stretches of leading edge that cannot assemble protrusions or cable, reflects how the remaining forces of dorsal closure are able to compensate for an assault on the zipper machinery.

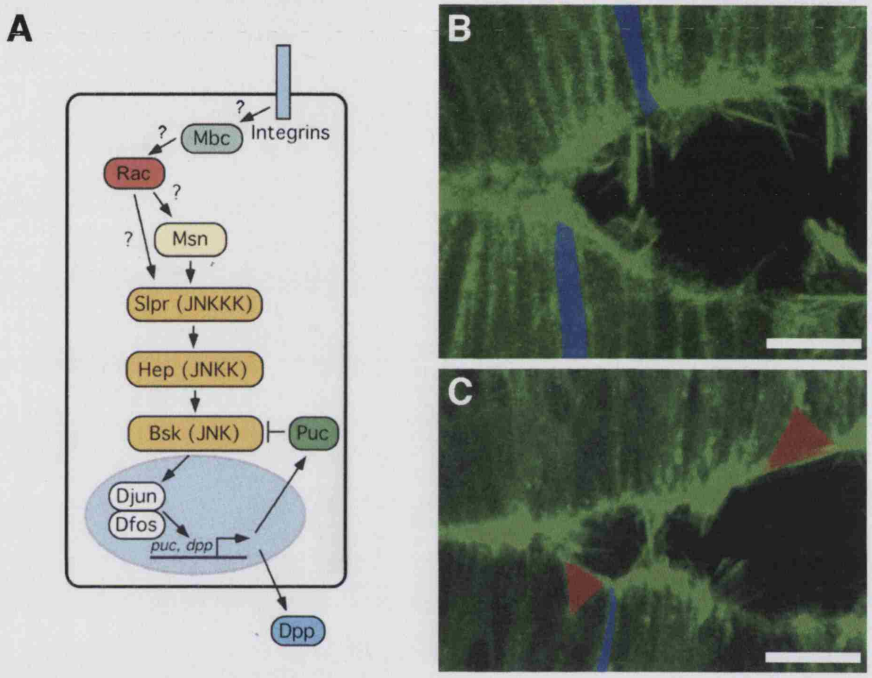

Figure 4.12 The leading edge of zygotic *Rac* mutants possesses cells that are polygonal in shape

(A): Diagram of JNK cascade within an individual leading edge cell showing the putative upstream location for Rac in this pathway. (B) and (C) are high magnification confocal images of GFP-actin in the leading edge (driven by *e22c-GAL4*). Leading edge cells in wild type embryos (B) are dorso-ventrally elongated (e.g. cells highlighted in blue); whereas many cells along the leading edge of the $Rac1^{J11}$ *Rac2Δ mtlΔ* mutants (C) are polygonal in shape (e.g. cells highlighted in red). Scale bars represent 10μm.

4.2.13 JNK pathway activity is reduced in triple *Rac* mutants

Cells along the leading edge usually display a characteristic dorso-ventrally elongated, thin rectangular shape in wild type embryos (Figure 4.12B). However, I found that many leading edge cells in triple *Rac* mutants are polygonal in shape and therefore lack any apparent dorso-ventral polarity (Figure 4.12C). As described in Section 1.2.1,

this phenotype is also seen in mutants of members of the JNK pathway, a MAPK cascade activated at the start of dorsal closure which is essential for the closure process and whose major action appears to be to bring about dorso-ventral elongation of the epithelial cells (Glise et al., 1995; Kaltschmidt et al., 2002; Riesgo-Escovar and Hafen, 1997b; Sluss et al., 1996; Stronach and Perrimon, 2002). Previous work using dominant negative *Rac1* transgenes has suggested that Rac proteins may act upstream in the JNK cascade during dorsal closure (Glise et al., 1995; Hou et al., 1997) (Figure 4.12A). The triple *Rac* mutant provided an ideal opportunity to test this possibility further.

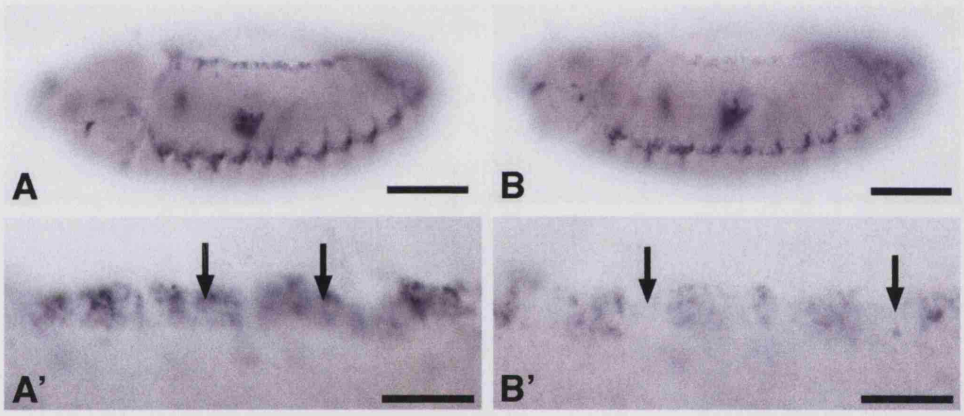

Figure 4.13 Leading edge expression of *dpp* is reduced in zygotic triple *Rac* mutant

(A) and (B): Whole mount *in situ* hybridisation to *dpp*. In wild type embryos (A), and at higher magnification in (A'), *dpp* is expressed along the epithelial leading edge, (arrows) as a consequence of JNK pathway activation, whereas in $Rac1^{J11}$ *Rac2Δ mtlΔ* mutants (B) and (B') this expression is significantly reduced in a reiterated pattern along the leading edge (arrows). Scale bars represent 100μm.

To obtain a read out of JNK pathway activity in the triple *Rac* mutants I analysed the expression of *decapentaplegic* (*dpp*) and the localisation of Dfos protein in Rac^{J11} mutants. I found that leading edge expression of *dpp* is considerably reduced in the triple *Rac* mutants compared to wild type (Figure 4.13A and B). Intriguingly, loss of *dpp* expression along the leading edge of Rac^{J11} mutants shows a reiterated pattern

similar to the on-off loss of actin cable and protrusion that I also see in these mutants (Figure 4.13B'). Analysis of Dfos antibody staining shows that in wild type leading edge cells during dorsal closure Dfos is found primarily in the nucleus, where its staining pattern colocalises with the DNA marker DAPI (Figure 4.14A and C). In contrast, Dfos protein in Rac^{J11} mutants fails to translocate to the nucleus in leading edge cells, resulting in a more diffuse localisation pattern (Figure 4.14B), which no longer aligns with DAPI staining (Figure 4.14D).

4.2.14 Expression of constitutively active *hemipterous* (JNKK) partially rescues the Rac^{J11} mutant phenotype

To investigate the link between Rac and the JNK pathway further I attempted to rescue the Rac^{J11} dorsal closure phenotype using a constitutively active form of JNKK, *hemipterous* (*UAS-hep*^{CA}). Expression of *UAS-hep*^{CA} in the epithelium using *e22c-GAL4* led to early (pre-dorsal closure) lethality making this unfeasible for a rescue experiment. However, I found that leaky expression of *UAS-hep*^{CA} without a GAL4 driver was sufficient to give a significant ($p<0.05$) rescue of Rac^{J11} homozygote lethality, such that whilst a heterozygote Rac^{J11} stock gives the expected Mendelian lethality of 26.7% (n=487), crossing in one copy of *UAS-hep*^{CA} reduces lethality to 20.8% (n=375). Furthermore, when the cuticles of dead embryos produced by these crosses are assessed I saw a clear shift from the Rac^{J11} dorsal puckering phenotype (shown in Figure 3A) to cuticles with a wild type, unwrinkled dorsal surface when *hep*^{CA} was also present. 82% of dead cuticles from a balanced heterozygote Rac^{J11} stock have a mutant phenotype, while just 18% appeared to have a wild type dorsal seam (n=92); addition of *UAS-hep*^{CA} nearly doubles the proportion of the wild type phenotype to 32% (n=76). Together, these results indicate that the Rac proteins do indeed act upstream in the JNK cascade during dorsal closure, providing a further explanation for the complexity of phenotype that I see in the triple *Rac* mutants.

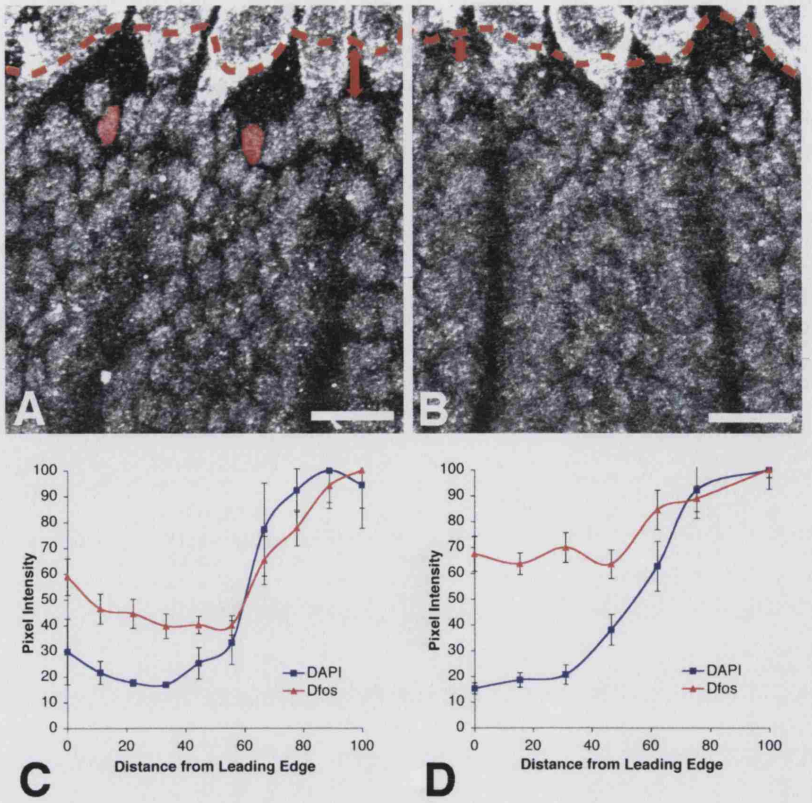

Figure 4.14 Dfos is not efficiently translocated to the nucleus in the zygotic triple *Rac* mutant leading edge

(A) and (B) High magnification lateral views of dorsal closure stage embryos (the position of the leading edge, established by co-staining with anti-Phosphotyrosine, is marked with a red dotted line) stained with anti-Dfos antisera. In wild type leading edge epithelium (A), Dfos is localised to the nucleus (examples of nuclear staining highlighted in red); whereas equivalent staining in the *Rac1*^{J11} *Rac2Δ mtlΔ* mutant embryo (B) is markedly more diffuse and extends closer to the leading edge of front row cells, away from the nucleus, (red arrows indicate distance from leading edge to Dfos staining in wild type and mutant). (C) and (D) Quantification of Dfos (red triangles) and DAPI (blue squares) staining in wild type (C) and *Rac1*^{J11} *Rac2Δ mtlΔ* (D) epithelial leading edge cells. In wild type cells the intensity of Dfos staining follows closely that of DAPI, whilst in *Rac*^{J11} mutant cells Dfos staining does not align well with DAPI, i.e. is no longer largely localised to the nucleus. To allow for easy comparison between wild type and mutant data all measurements were normalised on a scale of 0 to 100; error bars indicate standard error of the mean. Scale bars represent 10μm.

4.3 DISCUSSION

In this chapter I show that the three *Drosophila* Rac small GTPases play multiple roles during the epithelial migration and fusion events of dorsal closure. My work with constitutively active and dominant negative *Rac1* transgenes reveals a crucial role for Rac in both the production of filopodia and lamellipodia by leading edge cells and in the assembly of actin cable by these cells. Loss-of-function studies show that the three *Rac* genes are essential to proceed through dorsal closure since embryos lacking both maternal and zygotic contributions of Rac proteins fail early in the process.

4.3.1 Rac plays central role in dorsal closure, controlling cell shape changes and actin cytoskeleton organisation in the leading edge

In those embryos lacking only zygotic copies of the three *Racs* I see perturbations of the leading edge actin cytoskeleton and also a failure in the normal dorso-ventral elongation of these cells. It would therefore appear that Rac plays a central role in dorsal closure, functioning both to direct changes in cell shape and to organise the actin cytoskeleton of the leading edge. Rac may fulfil these functions by acting on a number of downstream targets. My data indicate that Rac acts upstream in the JNK pathway to control cell shape. However, as described in Section 4.1.6, the means by which Rac can activate the JNK cascade in dorsal closure remains uncertain. One possible link is the serine/threonine kinase PAK, which displays Rac dependent enrichment at the leading edge (Harden et al., 1996) and in mammalian cells has been found to trigger JNK activation through Rac and Cdc42 (reviewed in Van Aelst and D'Souza-Schorey, 1997). Alternatively, Rac may activate the JNK pathway more directly by interacting with the JNKKK, Slpr (reviewed in Harden, 2002).

However, Rac is unlikely to fulfil all its dorsal closure functions through activation of the JNK pathway alone. Other key downstream targets of Rac in dorsal closure may include Pkn, a member of the PKN family of PKC-related kinases known to influence

both cell morphology and actin organisation in dorsal closure (Lu and Settleman, 1999), and also members of the Wiskott-Aldrich protein (WASP) family which provide a direct link to the actin cytoskeleton (reviewed in (Takenawa and Miki, 2001).

4.3.2 Triple *Rac* mutants show reiterated loss of the actin cytoskeleton along the leading edge

An intriguing observation seen with live analysis of the zygotic triple *Rac* mutants is the inconsistent organisation of actin along the leading edge, with some leading edge cells assembling actin cable and protrusions while neighbouring regions do not. One possible explanation for this on-off pattern of actin assemblies is that the maternally contributed Rac proteins are retained to varying degrees or required at different threshold levels along the leading edge, an idea that is, perhaps, endorsed by the reiterated loss of *dpp* expression which I see in the zygotic triple *Rac* mutant. In previous studies where dominant negative *Rho1*, *Rac1* or *Cdc42* were expressed under the control of a heat shock promoter, a similar on-off effect on levels of leading edge actin and myosin was reported, with cells at segment boundaries showing reduced levels while other stretches of the leading edge appeared normal (Harden et al., 1999). My data support the view that small GTPase activity may vary in intensity along the leading edge and that these variations are reflected in assembly of dynamic actomyosin machineries along the edge.

4.3.3 Multiple tissue forces contribute to dorsal closure

Strikingly, even with the perturbations to cell shape and actin machinery found in the leading edge epithelial cells of zygotic triple Rac embryos, I still see a continued drawing closed of the hole through lateral amnioserosal contraction. My data highlight how the multiple forces driving dorsal closure can compensate when one of the contributing tissues is disabled. This compensation and the formation of new zippering fronts in triple *Rac* mutants can also be considered as a genetic mirror of recent laser

ablation studies of dorsal closure whereby the zippering canthi were persistently destroyed and yet dorsal closure proceeded because of continued amnioserosal contraction and the formation of new zipper fronts beyond the ablation zones (Hutson et al., 2003). Together these observations highlight the robustness of morphogenetic episodes such as dorsal closure where drastic alterations in actin assemblies that disable the standard epithelial migration machinery can be almost entirely compensated for by other contributing tissue contractions.

4.3.4 Investigating Rac function reveals that actin protrusions play three key roles during dorsal closure

The phenotypes I observe after expression of dominant negative *Rac1* in *engrailed* segmental stripes are very similar to previous findings with dominant negative *Cdc42*, which I described in Section 1.4.2 (Jacinto et al., 2000). In both cases the transgene expressing cells do not assemble actin protrusions at the leading edge during dorsal closure, and as a result these cells fail to fuse at the midline. Furthermore, in both cases there is clear mismatching of opposing segments along the midline seam, suggesting that the actin protrusions play at least two crucial roles during dorsal closure – a sensing function enabling the cells to find their correct segmental partner on the opposing epithelial edge, and a zippering role in which interdigitation of the protrusions aids fusion of the two sheets. In addition, my findings with constitutively active *Rac1*, where expressing cells produce overly large lamellipodia and precociously halt after premature localisation of Fas III to the leading edge surface, suggest a third function for the actin protrusions – to "read" contact inhibition cues so that leading edge cells can sense when they have reached the opposing edge. The identity of the receptors that enable these sensory functions for filopodia remain unknown, and it is certainly possible that all three roles may be performed by the same or similar molecules; likely candidates for such players include members of the cadherin super-

family of cell-cell adhesion molecules, and axon guidance molecules such as the EphR/ephrins and plexin/slit families.

CHAPTER 5

A Role For Unconventional Myosins In Dorsal Closure?

5.1 INTRODUCTION

5.1.1 Searching for new candidates involved in actin protrusion assembly and function during dorsal closure

As described in Chapters 3 and 4, my analysis of dorsal closure and the functions of the Rho family of GTPases suggests that actin protrusions play three major roles during the closure process: segmental matching, "contact inhibition" to prevent over-running once leading edge epithelial fronts have met and, finally, fusion of the two epithelial sheets. However, it remains unclear at the molecular level how the protrusions are able to perform these three functions and how this is linked to their assembly at the leading edge. One route towards addressing these issues is to consider the "business end" of the filopodia, the barbed end tip, and to establish what key molecules localize here during dorsal closure. Once filopodial tip candidates have been established, their function(s) during dorsal closure can be investigated and may provide more clues as to how these protrusions perform the roles described above.

Clues as to which proteins might localize to the filopodia formed in dorsal closure can be taken from studies of filopodia in other systems, including tissue culture. One family of filopodial tip candidates of significant interest are a group of unconventional myosins. The especially interesting property of these myosins, which warranted further investigation in dorsal closure is that, not only are they found at filopodial tips in several other systems (Berg and Cheney, 2002; Tuxworth et al., 2001), but that they have also been shown to carry various cargoes up to the tip (Tokuo and Ikebe, 2004; Zhang et al., 2004). Therefore, if a "filopodial" myosin that plays a role during dorsal closure could be found, analysis of its potential cargo might reveal key molecular players in one or more of the functions of filopodia in this process.

5.1.2 Myosins are molecular motors that perform a wide variety of cellular functions

The myosin superfamily is a very large group of actin based motor proteins which play key roles in a number of cellular processes, including cell motility, cytokinesis, phagocytosis, membrane trafficking and signal transduction (reviewed in Berg et al., 2001). A fundamental property of myosins is the ability to use hydrolysis of ATP to drive movement of the myosin along actin filaments. More recently, a number of intriguing additional properties have been attributed to myosins, for example there is evidence that some myosins may actually contribute to actin polymerization itself (Evangelista et al., 2000; Lechler et al., 2000; Lee et al., 2000).

Myosins are defined by the presence of a heavy chain containing a conserved catalytic head domain. The head domain is required for binding to F-actin and production of force via ATP hydrolysis. In most myosins the head domain is followed by a regulatory "neck" region containing IQ motifs which provide binding sites for calmodulin or calmodulin-like light chains. Beyond the neck region is a highly divergent tail domain which is thought to endow the class specific properties displayed by myosins (Oliver et al., 1999). Myosins are broadly split into two groups - conventional and unconventional. The conventional, or Class II, myosins are defined by the fact that they form bipolar filaments, and whilst they make up only a small proportion of total myosin genes they have been the most extensively studied due to their role in muscle contraction. All other myosins are described as unconventional, although this is a huge and diverse category comprising of many discrete classes. In humans around two-thirds of known myosin genes are unconventional whilst in *Drosophila* 11 out of 13 encoded myosins fall into this category (Berg et al., 2001; Tzolovsky et al., 2002). A particularly interesting attribute which some of the unconventional myosins share, which muscle myosins do not possess, is an ability to bind or localize to cell membranes.

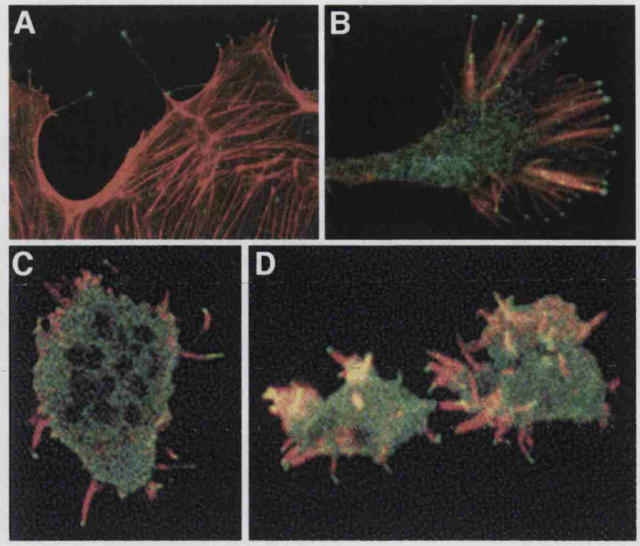

Figure 5.1 Myosins VII and X localize to the tips of filopodia

Localisation pattern of Myosin X (MyoX, A and B) and Myosin VII (MVII, C and D) in mammalian and *Dictyostelium* cells respectively. (A) Endogenous MyoX (green) is found at filopodial tips in cow pulmonary artery endothelial cells. (B) Similar staining is seen with exogenous MyoX (green) in a mouse neuronal cell line. Actin (red) is visualized using rhodamine-phalloidin (Berg and Cheney, 2002). (C) and (D) GFP-MVII (green) in live dictyostelium cells also localizes to the tips of filopodia, actin is shown in red (Tuxworth et al., 2001).

5.1.3 A subset of unconventional myosins localize to filopodial tips

Members of two classes of myosins have been found to localize to the tips of filopodia and the edges of lamellipodia. Work in mammalian cell lines showed that Myosin X (MyoX) localizes to the tips of extending filopodia and remains at the tips during filopodial extension and retraction (Figure 5.1A). Using GFP fusion constructs of various portions of MyoX it was shown that full-length MyoX undergoes intrafilopodial motility, in both forward (towards the filopodial tip) and rearward (towards the cell body) directions (Berg and Cheney, 2002). The head domain of MyoX is necessary and sufficient for its localization to the filopodial tip. Interestingly, expression of MyoX also dramatically increases the length and number of filopodia in a variety of mammalian cells, although this effect requires intact, full length MyoX (Berg and Cheney, 2002).

The slime mold, *Dictyostelium*, has no Class X myosins, but, a closely related Class VII myosin (MVII) appears to act in a similar manner to mammalian MyoX and localizes to the tips of filopodia produced by *Dictyostelium* amoeboid cells (Figure 5.1C and D). Like MyoX in mammalian cells, MVII appears to be involved in the extension of filopodial protrusions, as whilst starved wild type cells produce large filopods, MVII null cells under the same conditions do not (Tuxworth et al., 2001).

5.1.4 "Filopodial" myosins contain FERM domains

The "filopodial" myosins, VII and X, contain two highly conserved domains in their tails, the Myosin Tail Homology 4 (MyTH4) and FERM (band 4.1, Ezrin, Radixin, Moesin) domains, which may mediate their localization pattern and be crucial for their *in vivo* functions. Very little is known about the function of MyTH4 domains, but they are found in several motor proteins, including class 4, 7, 10, 12, and 15 myosins (Oliver et al., 1999) and also in a plant microtubule motor protein, kinesin-like calmodulin binding protein (KLCBP) (Reddy et al., 1996; Song et al., 1997). The first clue as to the function of these domains came from work with KLCBP in *Arabidopsis* where the MyTH4 domain appears to mediate microtubule binding (Narasimhulu and Reddy, 1998). Recently, the MyTH4 domain of MyoX has also been found to be able to bind to microtubules (Weber et al., 2004).

FERM domains are found in a diverse group of proteins including filopodin, merlin, talin, ezrin, radixin, moesin, some tyrosine phosphatases, as well as myosins of classes 7, 10 and 15. Perhaps the most well studied of this large superfamily are the ERM (ezrin, radixin, moesin) proteins, which are thought to act as membrane-cytoskeleton linkers (reviewed in Mangeat et al., 1999). Mirroring the localization pattern of myosins VII and X, ERM proteins also concentrate to specialized actin/plasma membrane extensions, such as filopodia, microvilli and membrane ruffles. The FERM domains of ERM proteins are thought to mediate membrane attachment,

either by directly binding to phospholipids or indirectly through interactions with membrane proteins, such as CD44 and intercellular adhesion molecules (ICAMs). It therefore seems likely that the FERM domains of "filopodial" myosins will be crucial for their localization and action.

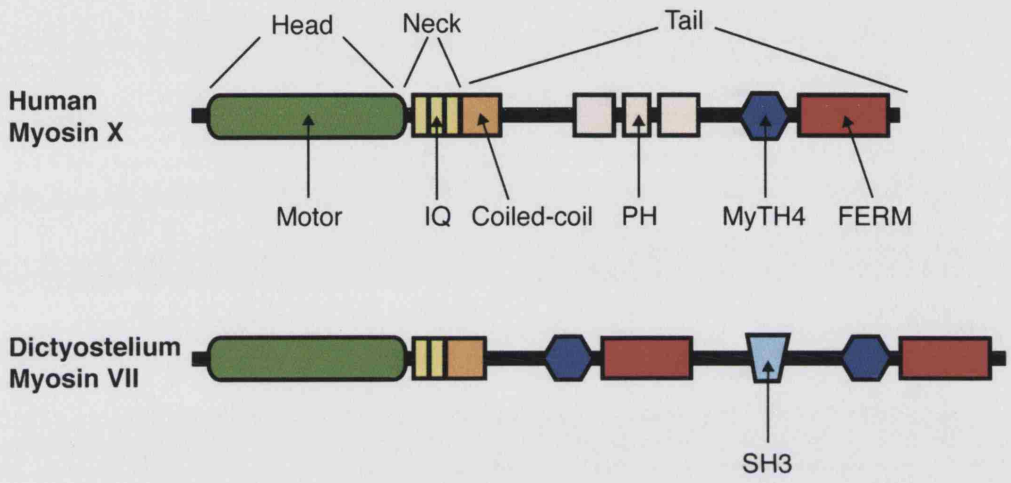

Figure 5.2 Schematic of "filopodial" myosins

The major protein domains found in the "filopodial" myosins, myosin X and myosin VII are displayed. Collated with information from CDART, the Conserved Domain Architecture Retrieval Tool (Marchler-Bauer and Bryant, 2004).

It is interesting to note that in MyoX and MVII the MyTH4 and FERM domains are arranged in tandem, with MyoX possessing one tandem set and MVII having a second pairing closer to the head domain (Figure 5.2). Some, although not all, class 15 myosins also carry a single tandem set of these domains. The conservation of this domain arrangement across three classes of myosins and in different animal species suggests that it may have important implications for the actions of these myosins. This appears to be the case with the microtubule binding activity of MyoX, as whilst the

MyTH4 domain alone can bind purified microtubules, the association is stronger when the FERM-MyTH4 cassette is used (Weber et al., 2004).

5.1.5 Unraveling the molecular actions of the "filopodial" myosins – roles in adhesion and phagocytosis

As discussed in Section 5.1.2, MyoX in mammalian cells and MVII in *Dictyostelium* can direct, and may be necessary for, filopodial extension. Recent work has begun to elucidate some clues as to the molecular basis of this action. In a yeast two-hybrid screen using the human integrin β_5 cytoplasmic domain as bait, MyoX was found to interact strongly (Zhang et al., 2004). Immunoprecipitation experiments endorsed this result and indicated interactions between MyoX and β_1 and β_3 integrins also. The binding of MyoX to integrin appears to be mediated through its FERM domain and an NPXY signaling motif in the integrins. As would be expected from the interaction results, integrins colocalise with MyoX at the filopodial tips of a variety of mammalian cell lines. Overexpression of GFP-MyoX causes both an increase in filopodial length and of integrin staining at the tips. In contrast, mutant forms of GFP-MyoX, where putative binding sites for integrin in the FERM domain had been removed, fail to colocalise with integrin and no longer triggered filopodial growth. Mirroring these results, cells that expressed a mutant form of β_1 integrin which lacked MyoX binding capacity no longer responded to transfection with GFP-MyoX and did not produce long filopodia (Zhang et al., 2004).

The interaction between MyoX and integrins and the requirement for MyoX to localize integrin at filopodial tips suggests that this myosin has an important function in organizing at least this aspect of adhesion complexes at filopodial tips. This correlates well with findings in *Dictyostelium* where the filopodial myosin, MVII, seems to play a crucial role in adhesion. As described earlier, MVII null *Dictyostelium* cells fail to

assemble wild type protrusions but, in addition, they also display problems with cell-cell and particle adhesion, as required for phagocytic engulfment. It appears that whilst MVII null *Dictyostelium* cells can extend a phagocytic cup prior to engulfment of particles they fail to properly bind the particle, suggestive of a problem with adhesion. Furthermore, MVII is also crucial for cell-cell adhesion and substrate adhesion in *Dictyostelium* cells, as the null cells fail to form aggregates when in suspension and show a reduced area of contact with their substrate when migrating (Tuxworth et al., 2001).

Mammalian MyoX, like *Dictyostelium* MVII, also appears to play a role in phagocytosis and has been found to localize to the phagocytic cups extended by macrophages (Cox et al., 2002). Knocking out MyoX function, either through expression of a truncated version of the myosin containing just the tail, or by introduction of neutralizing antibodies raised against MyoX, drastically reduced phagocytosis by reducing pseudopod extension. Interestingly, a link has been shown between MyoX and PI3K in phagocytosis, as the recruitment of MyoX to the phagocytic cup could be inhibited by incubation with wortmannin, a potent inhibitor of PI3Ks. It has been speculated that MyoX may bind PIP_3, a lipid product of PI3K, and could help to couple movement of the actin cytoskeleton with the outward expansion of the plasma membrane during pseudopod extension (Cox et al., 2002).

5.1.6 Myosin X may play a direct role in filopodial extension through Mena/VASP

A more direct role for MyoX in filopodial extension may have been revealed by the finding that this myosin can also bind to the actin binding proteins Mena/VASP (Tokuo and Ikebe, 2004). It is thought that Ena/VASP functions in actin dynamics by antagonising the capability of capping proteins to inhibit further elongation of actin filaments at their barbed ends. It therefore seems likely that the localisation of Ena/VASP to particular regions of the plasma membrane will play an important role in

the spatial regulation of actin protrusion assembly (Bear et al., 2002). Co-immunoprecipitation experiments have found that MyoX can bind to Mena/VASP *in vitro*, and indeed live analysis with fluorescent fusions of MyoX and Mena/VASP found that they colocalise and travel to filopodial tips in cultured cells. A further intriguing finding is that there was found to be a correlation between the concentration of MyoX and Mena/VASP at filopodia tips and the lengths of the filopodia themselves, with longer filopodia containing larger amounts of both proteins (Tokuo and Ikebe, 2004). However, no functional analysis of the interaction between MyoX and Mena/VASP has so far been carried out, so further evidence is required to be certain that this interaction is directly affecting filopodial activity.

5.1.7 "Filopodial" myosins in deafness and vestibular dysfunction

Two FERM domain containing myosins, VIIa and XVa, have been linked for some time with deafness and vestibular dysfunction in both mice and humans. Mutations in human Myosin VIIa are responsible for a disease called Usher syndrome type 1b, the most common cause of combined deafness and blindness in the industrialized world (Eudy and Sumegi, 1999); whilst mutations in Myosin XVa cause *DFNB3*, another form of congenital profound deafness (Liang et al., 1999). Similar deafness and vestibular defects are seen in the *shaker-1* mouse mutant and in zebrafish *mariner* mutants, both of which carry mutations in Myosin VIIa, and also in *shaker-2* mice where Myosin XV is mutant. Work in these model systems has begun to elucidate how crucial structures in the inner ear are affected by loss of these two myosins (reviewed in Maniak, 2001).

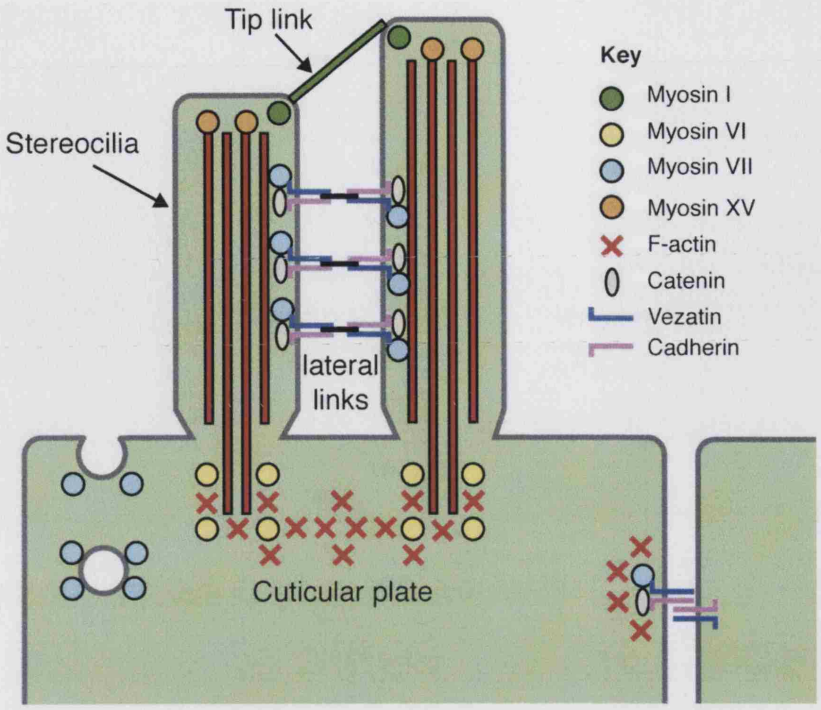

Figure 5.3 Unconventional myosins localise to specific regions of stereocilia

The apical portion of a hair cell with two stereocilia is shown. Four unconventional myosins show specific localisation within the hair cell: Myosin I is found at the tip where it is closely associated with the tip link, which connects the stereocilia; Myosin VI is localised in the cuticular plate where it appears to help anchor the bundles of actin (red bars) which run down the stereocilia; Myosin VII is found in the pericuticular necklace (left), where it is thought to mediate endocytosis and also at the lateral links between stereocilia, where it associates with vezatin; Myosin XV localises to the stereocilia tip complex and appears to be involved in regulating the length of stereocilia Adapted from (Maniak, 2001) with additional Myosin XV information from (Rzadzinska et al., 2004).

Our sense of hearing and balance depends on specialised sensory hair cells found within the inner ear. The hair cells consist of bundles of mechanosensitive, finger-like, microvilli protrusions called stereocilia which project into the fluid filled cavity of the inner ear. Stereocilia length, bundle shape and mechanical properties are all crucial to the sensitivity of the hair cells. The core of each stereocillium consists of an array of several hundred parallel, uniformly polarized, cross-linked actin filaments, arranged with their barbed ends pointing out towards the tip of the stereocilium (Figure 5.3), an arrangement similar to that found in filopodia (Rzadzinska et al., 2004).

Myosin VIIa is expressed in both vestibular and auditory hair cells where it is found in two interesting locations: along the length of the stereocilia beside lateral linkers that hold the stereocilia together and in the pericuticular necklace, a vesicle-rich region close to the apical surface of the hair cell (Figure 5.3) (Hasson, 1999; Hasson et al., 1995). EM analysis of the haircells in both *shaker-1* and *mariner* mutants reveals splayed and disorganized bundles of stereocilia, it seems that myosin VIIa is required to maintain the organization of the bundle and contributes to adhesion between adjacent stereocilia (Ernest et al., 2000; Self et al., 1998). The link between myosin VIIa and stereocilia adhesion was strengthened when a yeast two-hybrid screen using the tail of this myosin pulled out vezatin, a transmembrane protein that is localized to the lateral links between sterocilia and is found associated with cell-cell adherens junctions in hair cells as well as in other epithelial tissue (Kussel-Andermann et al., 2000). The requirement for myosin VIIa for stereocilia linking/adhesion in the inner ear obviously correlates nicely with the findings in *Dictyostelium* where myosin VII plays roles in cell-cell and cell-substrate adhesion (described in the section 5.1.5) (Tuxworth et al., 2001).

The hair cells in *shaker-2* mice, where myosin XVa is mutated, also show structural abnormalities but in this case the stereocilia are much shorter than wild type and abnormal actin filaments are found basally in the hair cells also (Anderson et al., 2000). Myosin XVa is found in puncta along the length of wildtype stereocilia and localizes strongly to the stereocilia tip where it is a component of the electron-dense tip complex (Figure 5.3) (Rzadzinska et al., 2004). Intriguingly, the amount of Myosin XVa at the tip correlates to the length of the stereocilia, with long stereocilia showing the highest levels, a similar finding to high concentrations of MyoX and Mena/VASP in long filopodia (Tokuo and Ikebe, 2004). Indeed, outgrowth of stereocilia appears to occur in a similar manner to the extension of filopodia, with actin monomers being added to the barbed end of growing actin filaments, situated at the tip of the stereocilia, and

dissociating at the pointed end of the filaments. The concentration of Myosin XVa at the tips of stereocilia, particularly those greatest in length, along with the shortened stereocilia phenotype seen in *shaker-2* mice suggests that this myosin is involved in stereocilium elongation, with the possibility that it is acting with other components of the tip complex to regulate actin polymerization (Rzadzinska et al., 2004).

5.1.8 There are three myosins in *Drosophila* which share most homology with the "filopodial" myosins

Drosophila possess three myosins which appear most closely related to the "filopodial", FERM domain containing myosins. These are two Class VII myosins, *crinkled* (*ck*) and *Myo28B1*, and one Class XV, *Myo10A*. To date no Class X myosins have been found in the *Drosophila* genome, and it seems likely that *Drosophila* do not possess a myosin of this class. The close relationship between these *Drosophila* myosins and the "filopodial" myosins in other systems can be see in phylogenetic trees constructed through alignment and comparison of myosin head domains (Figure 5.4) (Berg et al., 2001). Crucially, these *Drosophila* myosins also share the key tail domains seen in the "filopodial" myosins, as all three possess MyTH4 and FERM domains (Figure 5.5). Ck and Myo28B1 both contain two tandem pairs of FERM and MyTH4 domains as are found in Class VII myosins in other systems. Using the NCBI Conserved Domain Architecture Retrieval Tool (CDART, (Marchler-Bauer and Bryant, 2004), I identified a pair of these domains at the C-terminal end of the Myo10A tail along with a single MyTH4 domain situated close to the head of the myosin. In previous reports Myo10A is presented with just the N-terminal MyTH4 domain and no MyTH4 associated with the FERM domain. Given the apparent crucial roles of these domains and their highly conserved paired arrangement in Class VII, X and some XV myosins this difference could be significant.

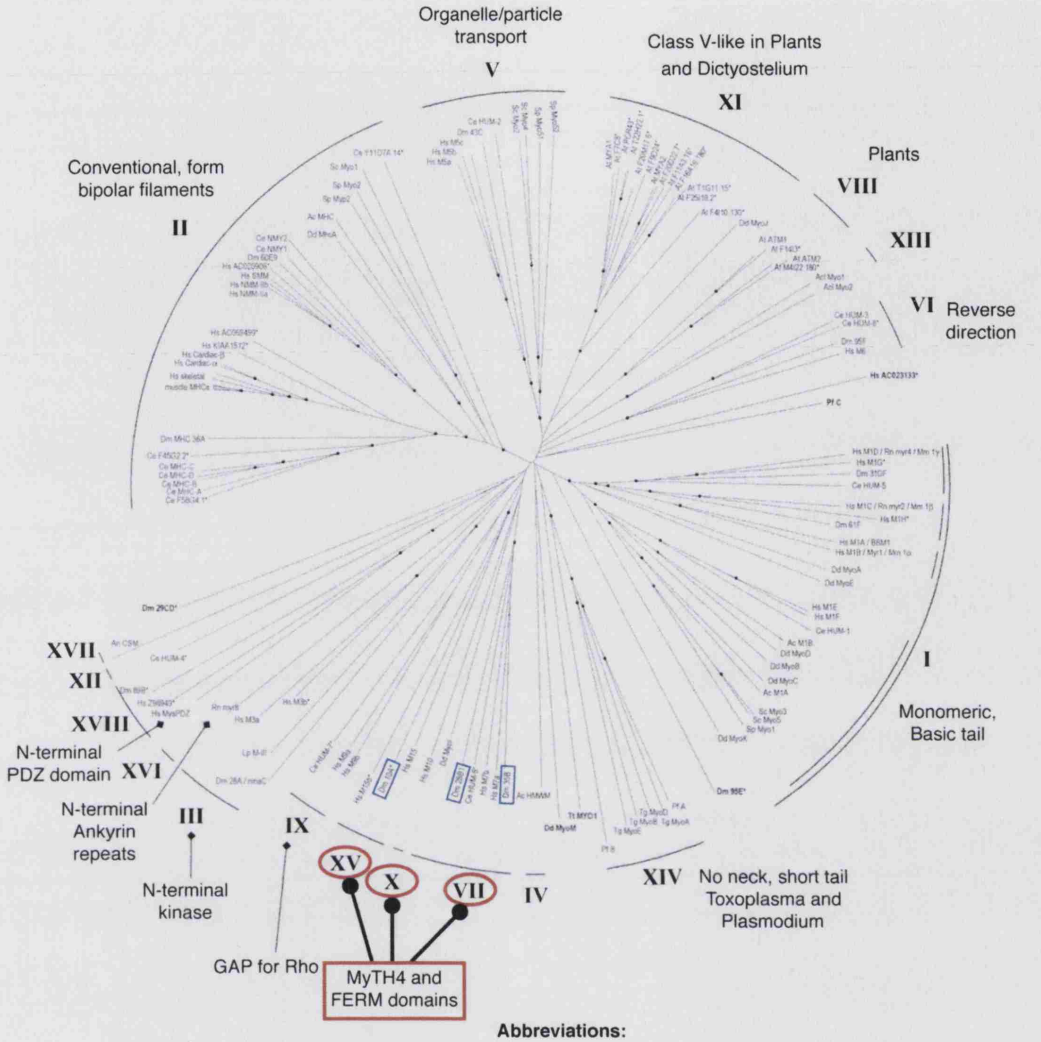

Figure 5.4 Phylogenetic wheel of the myosin superfamily

An unrooted phylogenetic tree, constructed using myosin head domain protein sequences. The subset of closely related myosins that contain MyTH4 and FERM domains within their tails are highlighted in red, with the three *Drosophila* myosins within this group outlined in blue: Dm 10A Myosin 10A), Dm 28B1 (Myosin 28B1), and Dm 35B (Crinkled). Adapted from (Berg et al., 2001).

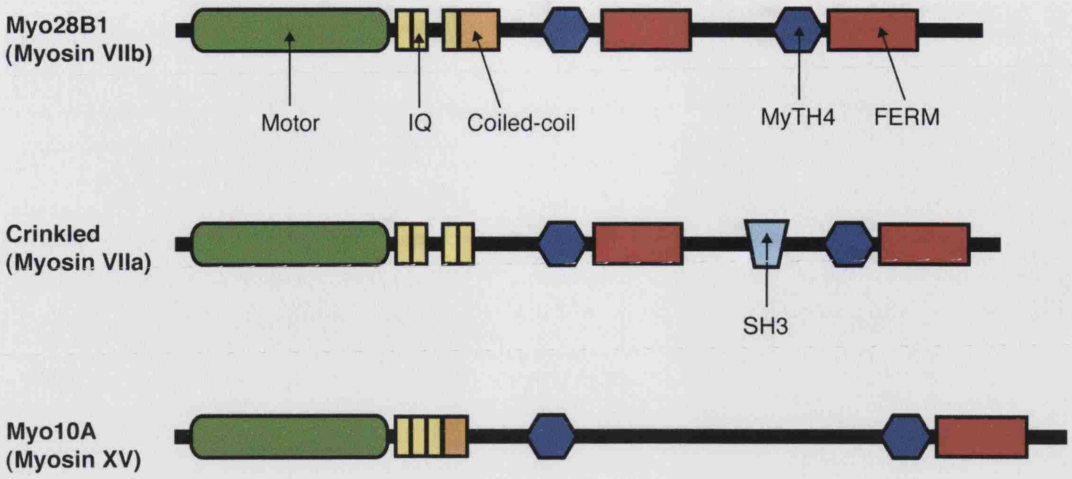

Figure 5.5 *Drosophila* has three FERM domain containing myosins

Schematic diagram showing the major protein domains found in the three FERM containing myosins encoded by the *Drosophila* genome. Collated with information from CDART, the Conserved Domain Architecture Retrieval Tool (Marchler-Bauer and Bryant, 2004).

Very little is known about the functions of either *Myo28B1* or *Myo10A* as no mutant has been described for either. *Ck* is by far the best studied of these three myosins, as a number of *ck* mutants have been described in the literature and a P-element insertion line is publicly available from the Bloomington Stock Center. All severe *ck* mutants described to date are semi-lethal with the majority of mutants dying as embryos or larvae, however all alleles yield some individuals which survive to adulthood (Kiehart et al., 2004). The adult escapers exhibit defects in their aristae (terminal segment of the antenna), bristles and wing hairs, with all three structures tending to be shorter and more branched compared to wild type (Kiehart et al., 2004). Aristae, bristles and hairs in *Drosophila* are all actin based structures and so these phenotypes are indicative of structural problems with the actin cytoskeleton. No morphological defects have yet been reported for the lethal phenotypes and as such there is no evidence so far of a role for Ck in dorsal closure. No live imaging of *ck* mutants has been performed to date

and it may be that this could reveal more subtle defects in actin regulation in morphogenetic processes such as dorsal closure.

The Berkeley *Drosophila* Genome Project is in the process of building a public "Gene Collection" of *Drosophila* cDNA clones. The collection contains a full length cDNA for *ck,* while, currently, only partial cDNA clones are available for *Myo10A* and *Myo28B1.* The cDNA of *Myo10A* consists of the tail domain, however the only available cDNA for *Myo28B1* encodes just the motor head domain, which is highly conserved among myosins reducing its usefulness for making gene specific *in situ* probes or RNAi constructs. For these reasons I chose to focus my experiments here on *ck* and *Myo10A.*

5.2 RESULTS

5.2.1 *In situ* hybridization reveals expression of the unconventional myosins *crinkled* and *Myo10A* in dorsal closure stage embryos

As a first step to investigate whether the selected unconventional myosins, *crinkled* (*ck*) and *Myo10A* might play a role in dorsal closure, it was necessary to determine if these genes were expressed in the appropriate tissues in dorsal closure stage embryos. To this end I prepared cDNA *in situ* probes using small regions of the 3' end of each gene, which were highly specific to each transcript. *In situ* hybridization using these probes showed that both *ck* and *Myo10A* are indeed expressed in a number of tissues in dorsal closure stage embryos (Figure 5.6).

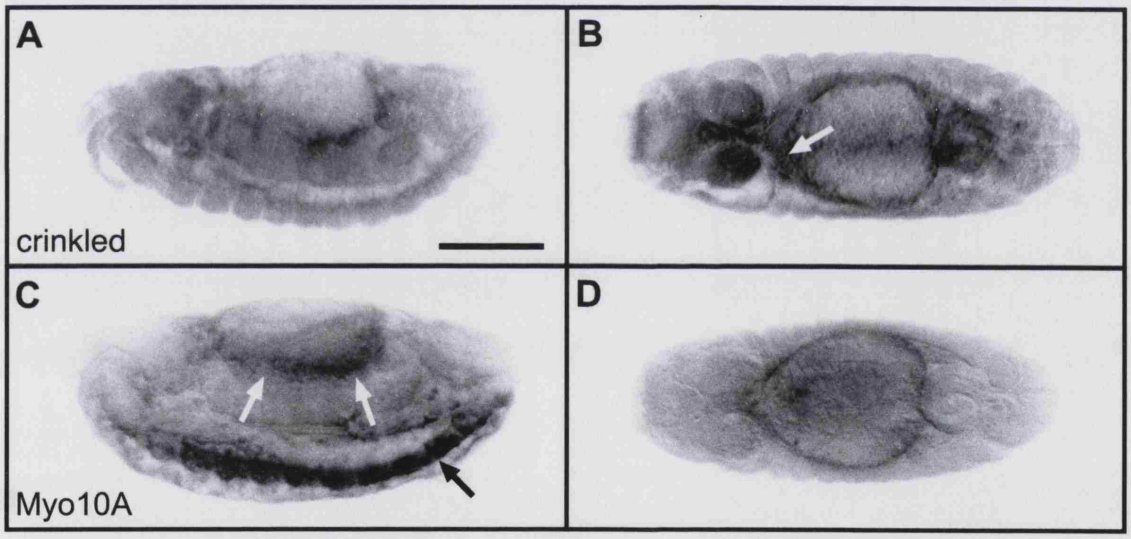

Figure 5.6 *Crinkled* and *Myo10A* are expressed in the epithelium in dorsal closure stage embryos

The expression patterns of *ck* (A and B) and *Myo10A* (C and D) in wild type embryos undergoing dorsal closure are revealed by *in situ* hybridization. *Ck* is expressed in the epithelium in dorsal closure stage embryos (A) and is also expressed in the mesoderm (B, arrow) and spiracles. High levels of *Myo10a* expression is seen in the epithelial leading edge (C, white arrows), and also in the developing nervous system (C, black arrow) and mesoderm (D). Scale bar represents 100μm.

Crucially, both myosins show expression in the epithelium, and *Myo10A* appears greatly enriched at the epithelial leading edge (Figure 5.6C and D). *ck* expression may also be increased in the leading edge but this staining is somewhat obscured by very high expression in the underlying mesoderm and gut tissue (Figure 5.6A and B). Interestingly, *Myo10A* is also highly expressed in the developing nervous system (Figure 5.6C).

	Buffer injected	***Crinkled* RNAi**	***Myo10A* RNAi**
Lethality	14% (n=43)	63% (n=38)	78% (n=46)
Cuticle phenotype: (as % of dead embryos)			
1. Wild type	48%	21%	22%
2. Wrinkled dorsal surface	0%	58%	17%
3. Puckered dorsal surface	0%	13%	23%
4. Germ band retraction defect	0%	0%	10%
5. Other	52%	8%	28%

Table 5.1 Injection of *crinkled* and *Myo10A* dsRNA leads to high embryonic lethality and dorsal cuticle defects

The injection of *crinkled* or *Myo10A* dsRNA leads to much higher embryonic lethality than buffer injected controls. Cuticle preparations were made of dead embryos and scored for the phenotypes shown above left, the phenotypes are displayed as percentages of the dead embryos counted.

5.2.2 Injection of *ck* and *Myo10A* dsRNA into presyncytial embryos leads to late embryonic lethality.

In order to begin to assess functionally whether Ck or Myo10A may play a role in dorsal closure, I performed RNAi knockdown experiments using injection of double-stranded RNA (dsRNA), which has been shown previously to elicit a knockdown in expression of targeted genes (Kennerdell and Carthew, 1998). I generated *ck* and *Myo10A* dsRNA from the same 3' templates used to make probes for the *in situ* hybridations described in the previous section. The dsRNA was injected into pre-

syncytial embryos, the embryos were left to develop, and the resulting lethality rates were counted. Injection of *Myo10A* and *ck* dsRNA resulted in high lethality rates when compared to buffer injected controls (Table 5.1). Cuticle preparations were used to assess the phenotypes of affected embryos and showed that in both cases embryos died late in embryogenesis (Figure 5.7).

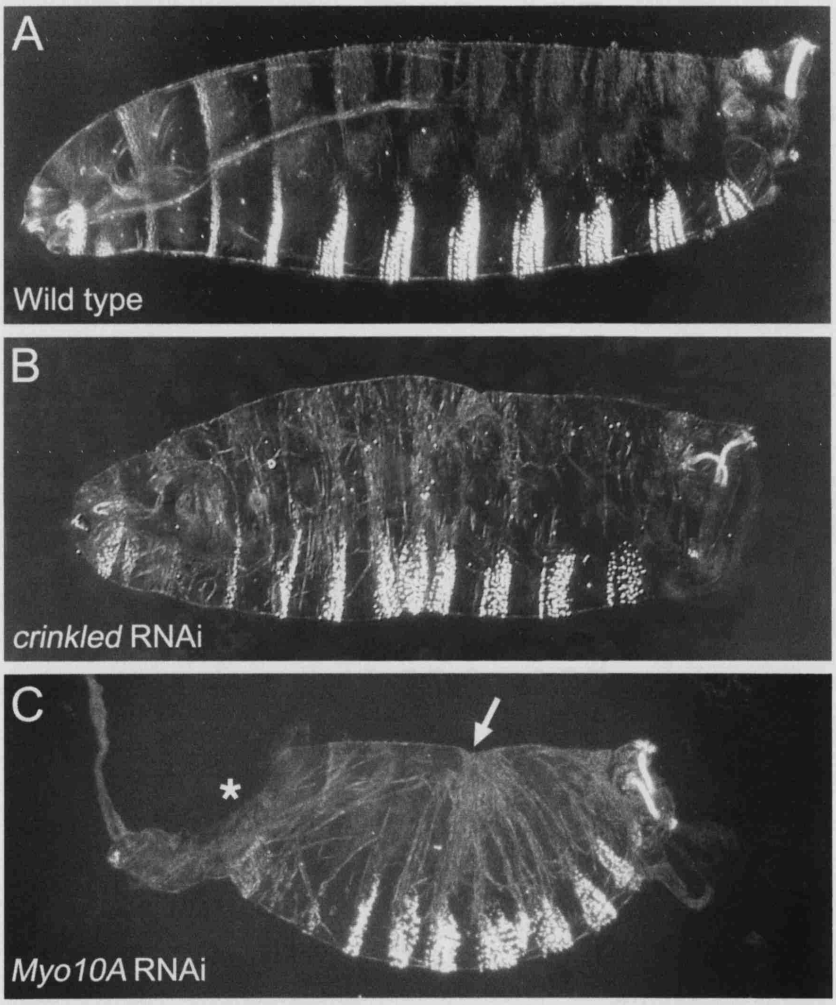

Figure 5.7 Injection of *crinkled* and *Myo10A* dsRNA leads to head defects and dorsal wrinkling

Cuticle preparations of buffer (A), *ck* dsRNA (B) and *Myo10A* dsRNA (C) injected embryos. *Ck* dsRNA injected embryos (B) show slight head and mouth-part defects, disorganized denticles and wrinkling of the cuticle along the dorsal side. Injection of *Myo10A* dsRNA (C) leads to severe head defects (asterisk) and puckering along the dorsal surface (arrow), indicating that dorsal closure is abnormal in these embryos.

All *ck* dsRNA injected embryos develop to a point beyond dorsal closure and show mild head and mouth part defects as well as slight wrinkling of the dorsal side of the cuticle, which could be indicative of subtle defects in dorsal closure process (Figure 5.7B and Table 5.1). Injection of *Myo10A* dsRNA, on the other hand, produced more severe defects with some embryos failing as early in development as germ band retraction (Table 5.1). Head defects were also seen in these embryos, and in many cases virtually the entire head was missing (Figure 5.7C). However, perhaps most interestingly for this study, injection of *Myo10A* dsRNA led to many embryos displaying puckering along the dorsal side of the cuticle (Figure 5.7C), similar to that seen in zygotic triple *Rac* mutants (See Section 4.2.8), suggesting that although dorsal closure does complete in these embryos it is not proceeding normally.

Whilst Ck does show some promise for a role in dorsal closure with expression at the appropriate time and location and some interesting RNAi phenotypes, Myo10A appeared an even more exciting candidate, with more dramatic expression in the leading edge during the dorsal closure period and a dorsal puckering RNAi phenotype. I therefore decided to focus my attention more fully on investigating a role for Myo10A in dorsal closure.

5.2.3 Generation of polyclonal antibodies to Myo10A

As a tool to further investigate Myo10A I raised polyclonal antibodies to the tail region of Myo10A. I chose three highly specific, hydrophilic, stretches of the Myo10A tail, which were used to immunize mice as glutathione S transferase (GST) fusion proteins (Figure 5.8A). Western blot analysis was used to assess the specificity of each antiserum. All three antisera recognized a band of the correct molecular weight for Myo10A (290kD) in whole cell extract (Data shown for just one antiserum in Figure 5.8B).

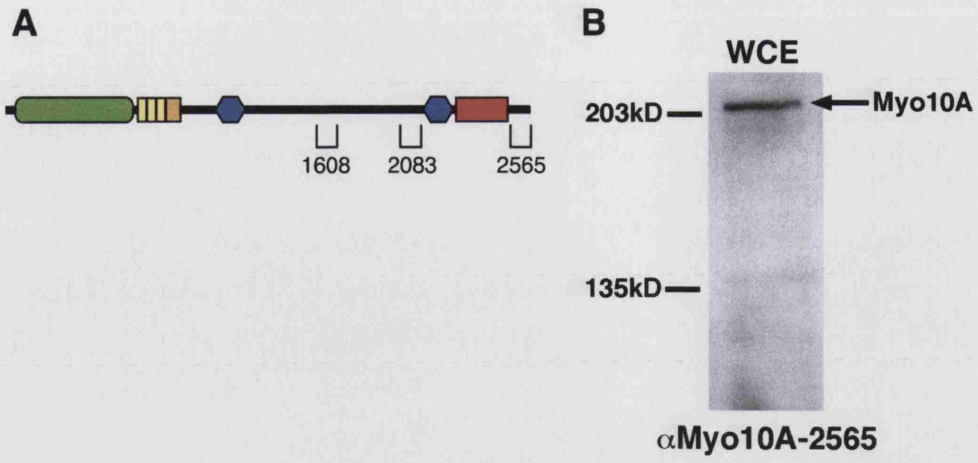

Figure 5.8 Generating polyclonal antibodies to Myo10A

(A) Schematic diagram of Myo10A domain structure indicating regions to which antisera were raised (labelled 1608, 2083 and 2565, according to position in amino acid sequence of Myo10A). (B) Western blot of embryonic whole cell extract (WCE), blotted with αMyo10A-2565 antiserum.

5.2.4 Myo10A is localized at the tips of filopodia in *Drosophila* S2R+ cells

As related FERM domain containing myosins have been found to localize to filopodial tips (see section 5.1.3) in other systems, I wanted to assess if this was the case with Myo10A in *Drosophila.* I began to address this question by staining cultured *Drosophila* S2R+ cells using the Myo10A antibodies described in the previous section. I chose to concentrate on cells as opposed to dorsal closure stage embryos because the actin protrusions assembled by these cells are more robust and survive the fixation protocols necessary for immunostaining better than the actin protrusions formed by the leading edge.

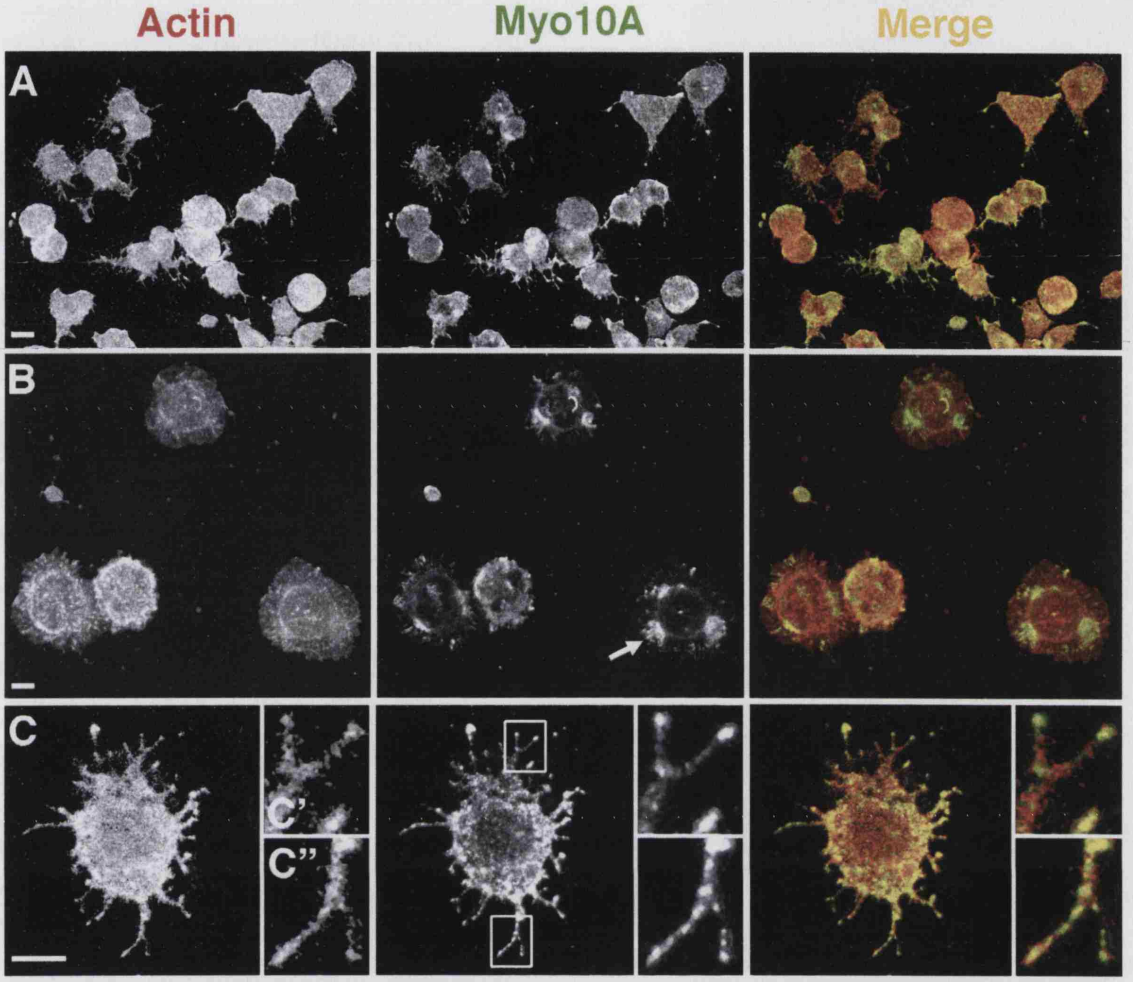

Figure 5.9 Myo10A localizes to the filopodial tips of *Drosophila* S2R+ cells

S2R+ cells grown on concanavalin A assemble filopodia (A and C) and large lamellipodia (B). Cells were costained with α-Myo10A antisera (green) and phalloidin to visualise actin (red). In lamellipodia, Myo10A localises to sectors (B, arrow), which correspond to areas of increased actin accumulation. Myo10A localizes to the tips of filopodia (A, C and C') and is also found in "beads" along filopodial extensions (C"). Scale bars in (A) and (B) represent 20μm and in (C) represents 10μm.

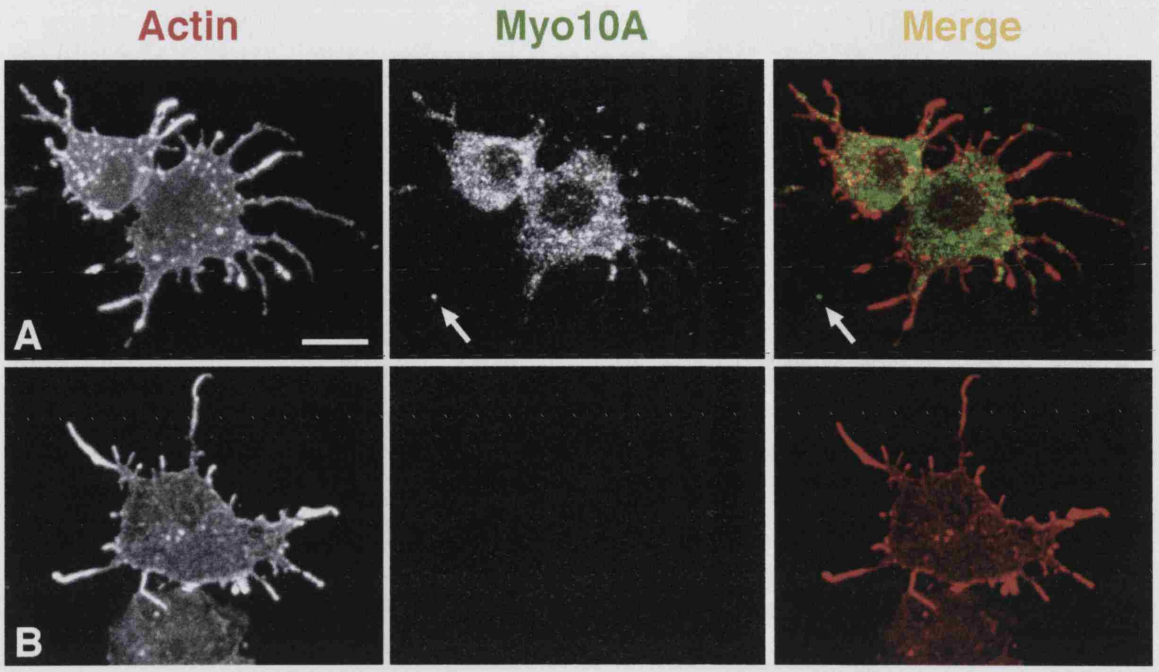

Figure 5.10 Myo10A pre-immune sera show no filopodial staining pattern

S2R+ cells grown on concanavalin A were stained with αMyo10A antiserum (A, green) and the appropriate pre-immune serum (B), confocal settings were identical for each. Pre-immune sera give no discernable cell staining pattern (B) and also lack the specks of staining seen on the substrate with αMyo10A antiserum (A, arrows). Scale bar represents 10μm.

The S2R+ cells assembled particularly large protrusions when plated on coverslips coated with the lectin concanavalin A (con A), with some cells extending large filopodia and others spreading and forming lamellae around their entire circumference (Figure 5.9A and B). Cells were co-stained with fluorescently conjugated phalloidin to reveal F-actin and with Myo10A antisera (Figure 5.9A, B, C and D). Control cells were also stained with the corresponding pre-immune sera (Figure 5.10B). Staining of S2R+ cells revealed that Myo10A does indeed localize in filopodia and also in zones within lamellipodia (Figure 5.9B and C). Interestingly, these lamellipodial regions of Myo10A seem to correspond to areas where F-actin accumulation is slightly higher. The localization of Myo10A in filopodia varies between protrusions, with some seen at the filopodial tips (Figure 5.9C') and other staining seen as "beads" along the length of the filopodia, possibly in transit to or from the tip (Figure 5.9C''). Neither the filopodial or

lamellipodial staining is seen when pre-immune sera is used indicating that this staining is real (Figure 5.10B). Another interesting difference between the staining seen with Myo10A antibody and the pre-immune serum is the presence of small specks of staining found on the substrate close to cells but not within any protrusion (Figure 5.10A). These specks are not seen with the pre-immune serum and might represent small regions of plasma membrane with Myo10A attached, which have been left stuck to the substrate when a protrusion has retracted.

5.2.5 A transposable P-element is located upstream of the *Myo10A* gene and can be mobilized to generate an excision mutation

The *Myo10A* gene covers a large region of about 25kb and, unusually for a *Drosophila* gene, contains three nested genes within its large third intron. This adds some obvious complications to generating a null mutant and currently there are no publicly available mutants of *Myo10A*. However, there is a transposable P-element situated approximately 7.8kb upstream of the 5' end of the *Myo10A* gene. I re-mobilized the P-element with the aim of generating imprecise excisions which remove portions of the 5' end of *Myo10A*; an ideal excision being one that would take out about 17kb of genomic DNA, removing exons 1 and 2 entirely and a large portion of the third exon, but would leave the nested genes intact.

Once the P-element had been remobilized by crossing the P-element carrying line to a transposase expressing line, revertants were selected by eye colour. As *Myo10A* is found on the X chromosome any revertant lines in which males could carry the reverted chromosome (and were, therefore homozygous for the excision) were assessed as being precise excisions in which the P-element did not carry any genomic DNA when remobilised and were discarded. A first screen produced six lines carrying imprecise excisions which were homozygote lethal, and could therefore be carried only by females.

To test the extent of the excision in each revertant line I designed a PCR scheme with a 5' primer just upstream of the P-element and a set of 3' primers at 3kb intervals into the *Myo10A* gene. A PCR product would only be obtained if an excision had removed a portion of the *Myo10A* gene. Of the six revertants only one, line #76, gave a PCR product. This was cloned and sequenced, however, disappointingly the sequence did not correspond to the Myo10A gene region, but instead to an unrelated region on chromosome 2. This suggests that mis-priming was occurring, although as this PCR product was not seen with any of the other revertant lines, it may have been that the balance was pushed towards this mis-priming event because the correct 3' primer site had been excised. It is possible, therefore, that line #76 carries a large excision which extends beyond the set of 3' primers I designed. Unfortunately, line #76 proved to be an extremely sickly stock and it was impossible to pursue this hypothesis further, although, intriguingly, the larvae of this line were observed to move aberrantly, with some holding their tails up, as has been reported for some kinesin (microtubule motor proteins) mutants (Hurd and Saxton, 1996; Saxton et al., 1991).

5.2.6 Expression of a *Myo10A* RNAi snapback leads to knockdown of Myo10A protein levels.

As a *Myo10A* mutant has yet to be generated, a different approach to stably knockdown levels of this myosin in embryos was required. To this end, a *Myo10A* RNAi snapback construct was cloned under the control of inducible UAS enhancer elements. The construct consisted of a small cDNA fragment of *Myo10A* (the same fragment as used in the *Myo10A* dsRNA injection experiments described in Section 5.2.2) cloned back-to-back with the identical genomic region of *Myo10A*. A dsRNA snapback is generated when these complementary sequences are transcribed. An intron was included in the genomic fragment as the post-transcriptional removal of this by splicing factors is thought to aid dsRNA hairpin formation (Kalidas and Smith, 2002). The

snapback construct was cloned into the pUASp expression vector and transformant lines were generated and identified by eye colour. Expression of the RNAi snapback, and consequent knockdown of *Myo10A* gene expression, could be driven in specific tissues of the embryo by crossing these transformant lines to particular GAL4 driver lines.

To check that *Myo10A* gene expression was indeed reduced by expression of the RNAi snapback, embryos were stained with the Myo10A antibodies described in Sections 5.2.3 and 5.2.4. Expression of the snapback was driven using the *engrailed* driver, along with GFP-actin, in the embryonic epithelium. At dorsal closure, embryos carrying just one copy of the snapback construct show a reduction in levels of Myo10A in engrailed segments of the epithelium compared to wild type embryos where just GFP-actin is expressed (Figure 5.11A and B). The reduction is not complete but this may be due to background staining that I see with the Myo10A antibodies in embryos and it may also be possible to increase knockdown by recombining the snapback lines to produce flies which carry multiple copies of the snapback construct.

5.2.7 Knockdown of *Myo10A* by RNAi snapback expression leads to segmental mismatching during dorsal closure

Embryos expressing the *Myo10A* RNAi snapback, along with GFP-actin, in *engrailed* stripes complete dorsal closure but 33% (n=30) show segmental mismatch at the midline, when assessed at the end of the process. To learn more about the effects of snapback expression during dorsal closure I followed the process live using time-lapse confocal imaging. Superficially, most of dorsal closure in these embryos looks close to normal, however, towards the end of dorsal closure the zippering leading edge cells begin to fuse to incorrect partners on the opposing edge, resulting in segmental mismatches which are thus concentrated towards the centre of the embryo (Figure 5.12D).

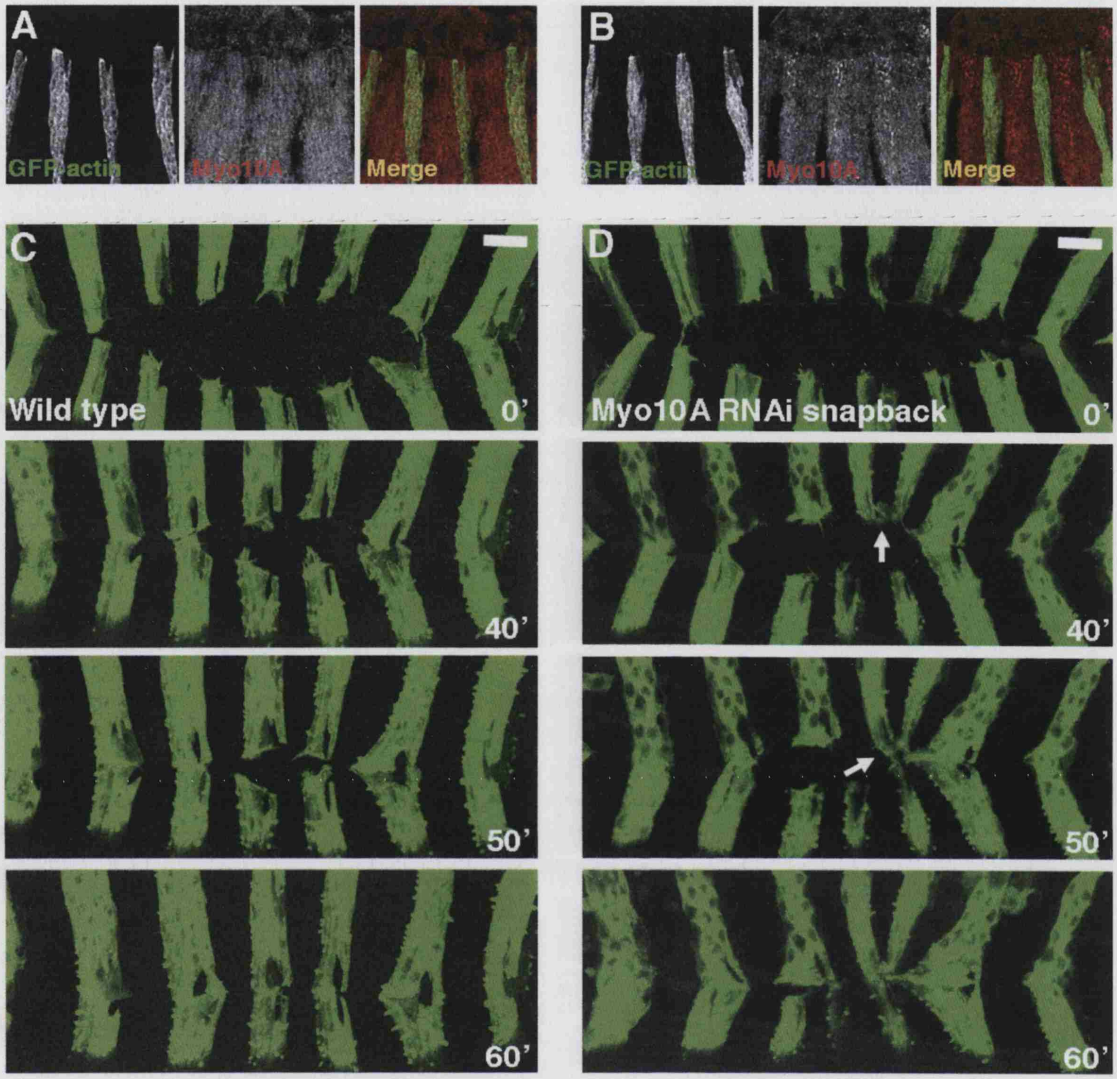

Figure 5.11 Expression of a *Myo10A* snapback RNAi in *engrailed* cells reduces levels of Myo10A in these cells and leads to segment mismatching during dorsal closure

The *Myo10A* RNAi snapback construct was co-expressed with GFP-actin using the *engrailed* driver (B and D). When embryos are stained with anti-Myo10A antisera (A and B) it is possible to see a variation in levels of Myo10A in the epithelium where the Myo10A RNAi snapback is expressed in *engrailed* cells (B), indicating a reduction in Myo10A levels in these cells. Comparison of movies of dorsal closure in wild type (C) and Myo10A snapback expressing embryos (D, Movie 9) show that closure proceeds normally in the snapback expressing embryos until the final fusion events when segmental mismatching occurs (D, arrows). Scale bars represent 10μm.

5.2.8 *Myo10A* RNAi snapback expressing cells assemble excessively long filopodia which retract faster than wild type

In order to determine if the assembly or dynamics of the actin protrusions formed by the snapback expressing cells during dorsal closure were different to wild type, I used timelapse movies of embryos where the Myo10A snapback was coexpressed with GFP-actin (n=4) to quantify actin protrusion areas, lengths and the rates of protrusion extension and retraction. Unlike expression of constitutively active and dominant negative *Rac1*, expression of the Myo10A RNAi snapback does not appear to have a significant impact on the maximum area of actin protrusions assembled by the leading edge during much of dorsal closure (Figure 5.12A). However, the process of closure is delayed by about 40mins compared to wild type, and in the extended period just prior to complete fusion, the snapback expressing leading edge produces protrusions of a slightly larger area (Figure 5.12A).

To further dissect the actin dynamics in the snapback leading edge I followed the extension and retraction rates of filopodia assembled by the snapback expressing cells. The rate of filopodial extension by snapback expressing cells was 1.60±0.26μm/min (n=12 filopodia), a rate similar to that seen in wild type embryos, 1.33±0.15μm/min (n=15 filopodia). However the rate of filopodial retraction was almost twice as fast in snapback expressing cells, (2.18±0.29μm/min) compared to wild type leading edge cells (1.27±0.21μm/min). A further difference seen in the actin protrusions formed by Myo10A snapback expressing cells is that the filopodia seem reach a greater length and persist at this length before retracting rapidly, such that the average maximum length of filopodia produced by snapback expressing cells are 10.46±1.35μm (see Figure 5.12B and Movie 10) compared to an average of 5.56±0.74μm in wild type embryos.

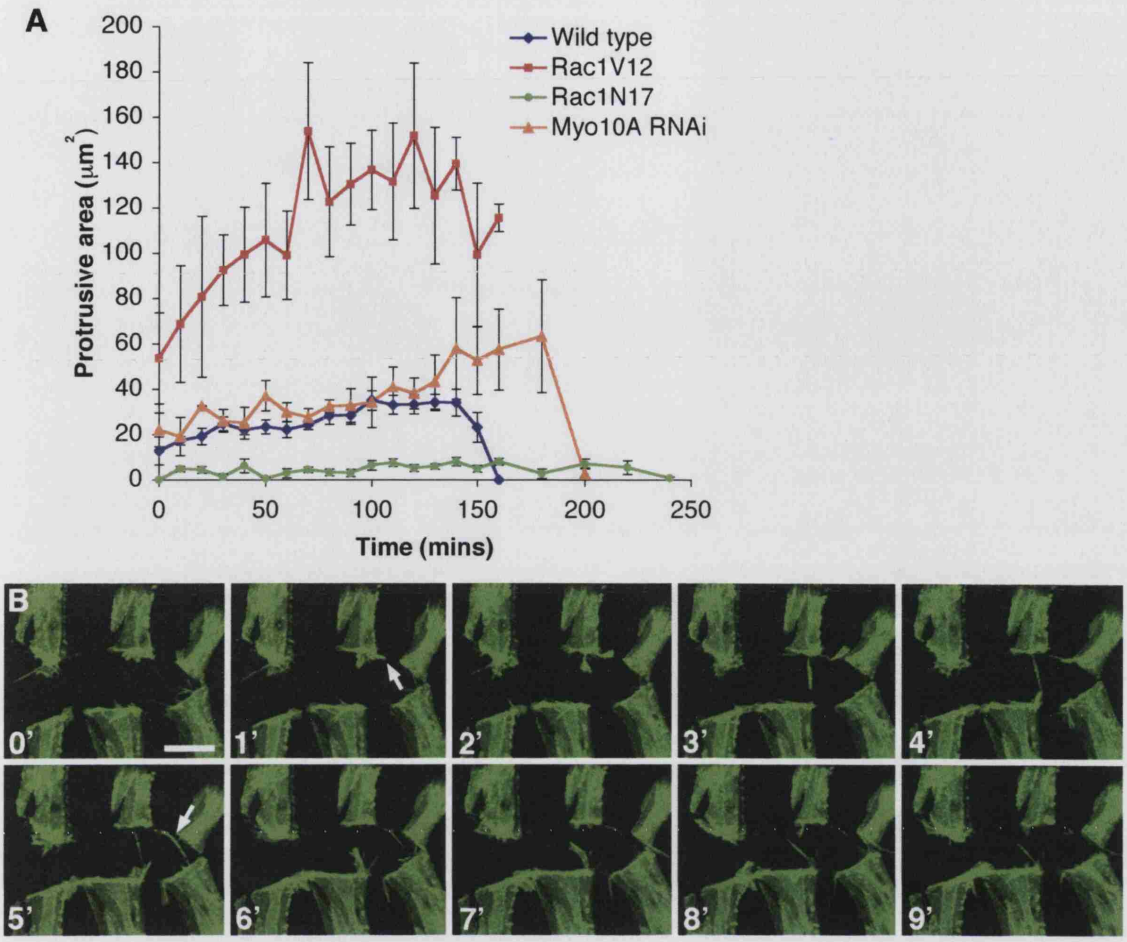

Figure 5.12 Expression of the *Myo10A* RNAi snapback leads to the formation of exceptionally long filopodia

(A) Quantification of the area of actin protrusions assembled by leading edge cells expressing the *Myo10A* RNAi snapback (orange triangles) indicates very little variation from wild type cells (blue squares). However quantification of filopodial length indicates that the snapback expressing cells assemble abnormally long filopodia and (B, Movie 10) displays a 10min section from a movie of an embryo in which the *Myo10A* RNAi snapback is expressed in *engrailed* stripes, where excessively long filopodia (arrow) are seen extending from the snapback expressing cells. Scale bar represents 10μm.

5.2.9 A yeast two-hybrid screen to find Myo10A interactors and putative cargos

The segmental mismatching and increased filopodial length seen with expression of the Myo10A RNAi snapback, coupled with the localization of Myo10A protein to filopodial tips in S2R+ cells indicates that this myosin may be playing a fundamental role in both filopodial assembly and their function during dorsal closure. However, the

mode of Myo10A function remains entirely unclear. Given the cargo carrying capacity of this myosin, and the results of work on filopodial myosins in other systems (see Sections 5.1.5 and 6), it seems likely that Myo10A may be operating as a motor trafficking and anchoring crucial cargos to the filopodial tips. An obvious next step in understanding how Myo10A functions in dorsal closure was to search for possible cargos of this myosin.

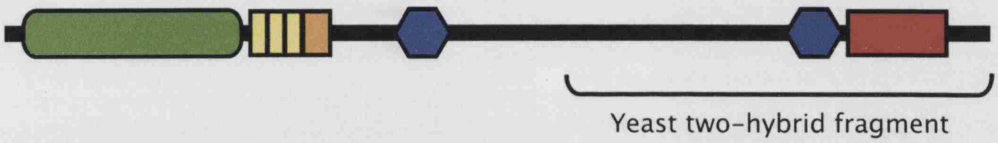

Figure 5.13 The MyTH4-FERM domain cassette of Myo10A was included as bait in a yeast two-hybrid screen

A schematic figure indicating the tail region used as bait for the yeast two-hybrid screen, crucially it contains the MyTH4 and FERM domain pairing.

In order to begin to address the cargo question, I decided to carry out a yeast two-hybrid screen with a 1300aa section of the tail of Myo10A. The Myo10A fragment used in the screen is highlighted in Figure 5.13 and includes the FERM domain and C-terminal MyTH4 domain. The Myo10A bait was screened against a *Drosophila* cDNA library and positives were selected first for an ability to grow on histidine deficient media and then re-selected using a β-Galactosidase assay. Histidine selection gave 823 positive colonies, but re-screening with β-Galactosidase reduced this number to 193 putative interactors. Of these, the bait was lost successfully from 35 and these were then sequenced. The sequences were used to search the *Drosophila* genome sequence using a BLAST nucleotide search and 24 were matched to known genes (shown in Table 5.2). Perhaps the most exciting potential cargo, with regard to filopodial function, identified in the screen is E-cadherin, although the link between Myo10A and microtubules indicated by α-tubulin, Eb1 and katanin-60 is also highly

intriguing, these and other aspects of Myo10A function are discussed in the following section.

Clone No.	Flybase No.	Gene	Function
3	CG2512	α-tubulin	Component of microtubule
86	CG3265	EB1	Microtubule binding/at tips of microtubules
30	CG10229	katanin-60	Microtubule binding
9	CG3722	shg	E-cadherin, adherens junctions
1	CG9423	Kap-α3	Protein nuclear import
49	CG13777	milt	Axon transport of mitochondria
42, 88	CG32810		Ion channel activity/transporter, BTB/POZ domain
4	CG5422	Rox8	RNA binding, involved in mRNA splicing
11	CG5263	smaug	RNA binding, involved in translational repression
8	CG3661	RpL23	Ribosomal protein
91	CG9354	RpL34b	Ribosomal protein
55	CG8146	Socs16D	Suppressor of cytokine signalling
22	CG11987	tango	HLH transcription factor
48	CG4303	Bap60	Subunit of Brahma complex
31	CG7555	Nedd4	Ubiquitination, WW domain
76	CG10110	cpsf	Cleavage and polyA specificity factor
32, 40	CG17033		RING finger, phosphoglycerate mutase like
13, 73	CG1078		Unknown function
18	CG5613		Unknown function
61, 62	CG2765		Unknown function

Table 5.2 Preliminary results from Myo10A yeast two-hybrid screen

Details of the first 24 putative Myo10A interactors pulled out of the yeast two-hybrid screen, in which the bait was a portion of the tail of Myo10A containing the MyTH4-FERM domain pair.

5.3 DISCUSSION

In this chapter I have shown that the unconventional myosins *Ck* and *Myo10A* are expressed in the epithelium during dorsal closure and that RNAi, using injection of dsRNA, leads to defects along the dorsal side of the embryo. Furthermore, Myo10A, which shows strong expression in the leading edge during closure, was found to localize to filopodial tips in cultured *Drosophila* cells. Expression of a *Myo10A* RNAi snapback construct in the epithelium during closure appeared to induce the formation of longer filopodia and resulted in a failure to correctly match segments as the epithelium closed. Finally, I present evidence from a yeast two-hybrid screen that Myo10A can interact with a variety of potential cargoes, including E-cadherin.

5.3.1 Expression of Myo10A dsRNA alters filopodial dynamics

One of the more intriguing results presented in this chapter is the effect of the Myo10A RNAi knockdown on filopodial dynamics at the leading edge. Cells expressing the snapback appear to assemble filopodia which extend up to twice as long as in wild type leading edge cells. These filopodia extend at a similar rate to wild type but appear to retract at almost twice the normal rate. Reducing Myo10A levels appears to enable leading edge filopodia to continue to extend for longer periods than in wild type, ultimately reaching further before rapidly collapsing. This effect on filopodial dynamics could offer a possible explanation for the segmental mismatch phenotype also seen when the Myo10A RNAi snapback is expressed in *engrailed* stripes. Perhaps the increased length and persistence of the snapback filopodia allow them to interact more easily with cells in segments further away than normal.

The filopodia extension phenotype I see with the Myo10A RNAi snapback clashes somewhat with what has been reported previously for FERM domain myosins. As described in Section 5.1.3, overexpression, rather than knockdown, of MyoX in mammalian cell lines leads to an increase in filopodial length and similarly in

Dictyostelium amoebae loss of MVII causes a failure to extend filopods (Berg and Cheney, 2002; Tuxworth et al., 2001). Mine is the first report of a class XV myosin localising to filopodial tips, although Myosin XVa has been shown to localize to tips of the closely related actin structures, stereocilia, in mouse hair cells where it appears to be involved regulating their length (Rzadzinska et al., 2004). Careful quantification of my Myo10A RNAi snapback specimens suggests that during dorsal closure Myo10A, like the myosins described above, plays some role in the regulation of filopodial extension, although its effect appears to oppose that found for the other FERM domain containing myosins. This difference may stem either from the cargoes Myo10A might be carrying to the tip or may reflect some intrinsic property of dorsal closure. One possible speculation is that Myo10A is required for the transport of a sensing or adhesion molecule to the tip that enables the filopodium to recognize contact inhibition cues and retract. Without the appropriate delivery of these molecules, the filopodium is not able to properly sense its environment and as a result continues to extend.

5.3.2 Is Myo10A functioning with E-cadherin in dorsal closure?

My yeast two-hybrid screen, described in section 5.2.9, revealed E-cadherin as to be an interactor with Myo10A, and thus a potential cargo. E-cadherin is a core component of adherens junctions, and its extracellular domain is required to facilitate homotypic, adhesive interactions with E-cadherin molecules expressed on the surface of other cells. Adherens junctions are required for cell-cell adhesion in both the initial fusion of epithelial cells and for the maintenance of epithelial integrity (Vasioukhin and Fuchs, 2001). As cultured keratinocytes fuse to form epithelial sheets they extend filopodia which carry clusters of adheren junction proteins at their tips allowing adjacent keratinocytes to zip together by interdigitation of these "sticky" filopodia (Vasioukhin et al., 2000). In a similar way, the filopodia assembled by leading edge cells during dorsal closure have been shown to prime future adherens junctions (Jacinto et al., 2000). An interaction between Myo10A and E-cadherin suggests that Myo10A might play a role in

delivering E-cadherin to the filopodial tip in order to prime them for epithelial fusion events.

Previous studies have demonstrated a link between mouse and human myosin VIIa and E-cadherin, although this is an indirect interaction working through the transmembrane protein vezatin. It seems that in this case, the anchoring of myosin VIIa to cadherins via vezatin creates a tension force between adherens junctions and the actin cytoskeleton which strengthens cell-cell adhesion (Kussel-Andermann et al., 2000). Furthermore, in hair cell stereocilia vezatin colocalises with myosin VIIa at the sites where tip linkers hold individual stereocilia together, which may account for the splayed stereocilia seen in *myosin VIIa/shaker-1* mutant hair cells (Kussel-Andermann et al., 2000). Interestingly, mutations in cadherin 23 (CDH23) have recently been found to be responsible for another form of hereditary deafness, Usher syndrome type 1D. CDH23, like vezatin and myosin VIIa, is also found at stereocillia linker regions and may act to connect stereociliary tips, as in *waltzer* mice, where *cdh23* is mutant, also exhibit splayed stereocillia (Siemens et al., 2004).

5.3.3 Microtubule related proteins and Myo10A

Another interesting group of Myo10A interactors revealed by the yeast two-hybrid screen were α-tubulin and the microtubule associated proteins, EB1 and katanin-60. The role of microtubules in dorsal closure has not been thoroughly investigated and to date it is not known what, if any, aspects of this morphogenetic process they may contribute to. However, the finding that the Myo10A tail section used in this screen can bind to α-tubulin is intriguing because it could indicate that the putative microtubule binding MyTH4 domain, located in this fragment, which was not shown in previous reports of Myo10A domain structure, is indeed present and functioning. The mammalian myosin, MyoX, has recently been found to bind microtubules and is

required for assembly of the meiotic spindle. The MyTH4-FERM domain cassette of MyoX is sufficient for the interaction with microtubules, although interestingly, the MyTH4 domain alone is capable of binding microtubules to a lesser degree, whilst the FERM domain alone cannot (Weber et al., 2004). This evidence seems to reinforce the idea that it probably is the MyTH4-FERM domain cassette in Myo10A which is associating with microtubules, although clearly, further analysis will be necessary to verify that the interaction between Myo10A and α-tubulin is direct and facilitated by this cassette.

The microtubule binding protein EB1 is another interesting potential binding partner for Myo10A, as recent work in *Drosophila* S2 cells could indicate a role for this protein in morphogenetic movements like dorsal closure. EB1 binds to the plus ends of microtubules and plays an important role in regulating microtubule dynamics and in the assembly and dynamics of the mitotic spindle (Rogers et al., 2002). However, EB1 has also been found to bind to *Drosophila* RhoGEF2 allowing this Rho1 activator to travel on the plus ends of growing microtubules to the reach the cell cortex (Rogers et al., 2004). It is thought that selective dissociation of RhoGEF2 from the microtubules allows it to be targeted to regions of cortical actin and thus to facilitate localized activation of Rho1 at sites where specialized actin structures, such as acto-myosin cables, need to be assembled.

5.3.4 Other possible cellular roles for Myo10A

The majority of the Myo10A interactors so far identified by my yeast two-hybrid screen do not initially appear to have likely roles in filopodia function or dorsal closure, suggesting that this myosin may be involved in numerous other processes, possibly trafficking a large number of cargoes to various locations within the cell. A theme that runs through many of these interactors, and which ties in well with Myo10A's function

as a molecular motor, is cellular transport. For example one interactor, Milton, is known to be required for transport of mitochondria along neuronal axons (Stowers et al., 2002). Two interactors are ribosomal proteins, and perhaps Myo10A is transporting these as either subunits or whole ribosomes. Furthermore, a protein involved in the nuclear import of proteins, Kap-α3, was also pulled out of the screen. On a slightly different note, three proteins identified as interactors in this screen, Rox8, Smaug and Cpsf, possess RNA binding capacities, and one possibility is that Myo10A is involved in localizing these to specific regions of the cell or even the oocyte in order to regulate their action. Perhaps the most surprising interactors to come out of the screen so far are the transcription factors, Tango and Bap60, which one might expect to find in the nucleus. Naturally, all of the interactors revealed by my yeast two-hybrid screen will need further analysis to confirm whether that they interact directly with Myo10A.

5.3.5 Future directions for Myo10A investigation

The work presented in this chapter suggests that Myo10A is playing an important role in the assembly and function of filopodia during dorsal closure. To further investigate and validate these findings it would be extremely useful to be able to follow the localization of Myo10A live in the filopodia of both cultured cells and epithelial leading edge cells during dorsal closure. For this a GFP or RFP-Myo10A fusion construct would need to be cloned for expression in cells and embryos. Live imaging could prove particularly useful in the embryo, where actin protrusions are lost during fixation and where the current Myo10A antibody staining appears to have a high background. The use of fluorescent proteins other than GFP, such as RFP, would allow live colocalisation studies to be carried out with more established GFP lines such as GFP-actin or GFP-αcatenin.

Clearly, the Myo10A yeast two-hybrid screen is beginning to pull out some intriguing potential binding partners for this myosin. These interactions will need to be verified using alternative methods, such as co-immunoprecipitation, to ensure that they are real and direct. Further investigation of cargo could be performed genetically in the fly, for example looking for dominant interactions between cargo mutants and *Myo10A*. This latter approach would require the generation of a *Myo10A* null mutant, which may prove easier than described in this thesis as two new P-element stocks with insertions within the Myo10A gene region have recently been released. Live imaging could also be used in cells or embryos to investigate whether potential filopodial cargoes are still delivered to filopodial tips when Myo10A is knocked down or mutant, so indicating whether Myo10A is the obligatory motor for delivery of these molecules to the tips of filopodia. However, what already appears clear from the yeast two-hybrid data, is that Myo10A has a sizable range of putative cargoes, which can carry out many different functions in the cell and the developing embryo. This in turn leads to a number of further questions which will require additional study in the future, a major one being what controls the choice of cargo for myosins like Myo10A?

CHAPTER 6

General Discussion and Future Directions

6.1 WHAT CAN LIVE ANYALYSIS TEACH US?

A major focus throughout this study has been the use of live imaging to learn more about the dynamic tissue movements involved in embryonic morphogenesis. Live imaging is particularly pertinent in dorsal closure, as the fragile and very dynamic actin protrusions extended by the leading edge epithelial cells can only be viewed live and also because the process involves the co-ordinated migration of two tissues, whose relative contributions to closure can only be dissected by careful dynamic analysis.

6.1.1 Live imaging allows a more detailed dissection of morphogenesis

In Chapter 3, I describe a comprehensive live analysis of wild type dorsal closure. Primarily this study has provided a valuable dynamic staging framework with which to compare mutant closure. However, this analysis also highlights some interesting new avenues for investigation in dorsal closure. The first of these concerns precisely how actin protrusion dynamics are regulated by the leading edge cells, as I see a modulation of protrusion assembly during the temporal course of wild type closure, with lamellipodia getting larger and filopodia increasing in length as the process progresses. Another intriguing aspect of protrusion dynamics is the response when opposing filopodia touch, as I seem to see a suppression of the usual retraction dynamics when this occurs. Whilst it is clear that the Rho family of small GTPases play a key role in the initial assembly of the actin cytoskeleton during dorsal closure, they seem to have a rather "all or nothing" effect, with, for example, expression of dominant negative *Cdc42* (Jacinto et al., 2000) or *Rac1* (Chapter 4) leading to a virtual eradication of actin protrusion formation. It therefore seems likely that there is a higher level of regulation of actin protrusion assembly during epithelial migration, which can "fine tune" filopodial dynamics. Prime candidates for this kind of control can come from tissue culture models of protrusion assembly and will include regulators such as Capping protein, IRSp53, Cofilin and Ena. Indeed, it certainly appears that Ena plays a role in the fine

control of filopodial assembly by the leading edge, as the expression of an Ena construct which preferentially localises to the plasma membrane leads to the formation of excessively long filopodia (Mark Peifer, personal communication). Another possible route to investigate this question will be to look at how the localisation of factors such as Ena and Capping protein is controlled during dorsal closure, and cargo-carrying myosins such as Myo10A may provide a means to do this, an area which is discussed below in Section 6.4.

A second field in dorsal closure, which has yet to be addressed, is how the process initiates. It is clear from live imaging that the initial cell shape changes which underlie dorsal closure begin earlier than had previously been described, with the amnioserosa cells starting to contract whilst the germ-band is still completing its retraction. The timing of dorsal closure initiation as assessed live could fit with two possible kick-start activation cues: either local changes in mechanical force or systemic ecdysone signalling. The effects of tension during development is an area that is only just beginning to be explored, presumably because it is very difficult to measure effectively *in vivo.* However, there is a precedent for mechanical force affecting gene expression in *Drosophila* embryos, as an innovative study found that expression of the dorso-ventral polarity gene, *twist*, could be mechanically induced by applying pressure to the early embryo (Farge, 2003). There is good evidence that mechanical "stretching" signals may play an inductive role later in development to trigger *twist* expression in the cells of the stomodeal primordium. These cells are deformed naturally as the germ-band extends and in mutant embryos where germ-band extension fails, *twist* is no longer expressed in the stomodeal primordium, but expression can be restored by the application of a comparable mechanical compression (Farge, 2003). The molecular mechanisms underlying tension sensing *in vivo* remain largely unknown, although a recent study has uncovered a means by which *Drosophila* border cells can sense stretching forces as they migrate during oogenesis (Somogyi and Rorth, 2004). As

these cells begin to migrate, a transcriptional cofactor called MAL-D translocates from the cytoplasm into the nucleus. The activity of MAL-D is required in migrating border cells to strengthen the actin cytoskeleton, as cells which lack its activity break apart as they initiate migration. In mutant border cells that cannot migrate, MAL-D remains in the cytoplasm, but it does accumulate in the nucleus if the mutant cells are pulled by wild type migratory cells, suggesting that the translocation of MAL-D is a response to cell stretching (Somogyi and Rorth, 2004). When considering dorsal closure, it is easy to imagine that changes in tension across the amnioserosa and/or the epithelium may play crucial roles in starting the process, with dorsal closure beginning just as the germ-band is pulling back, an event that must instigate huge changes in tension in these two tissues. This is certainly an exciting area for future research in dorsal closure, and more widely in morphogenesis, and one for which live imaging will surely be an important tool.

As mentioned above, a second possible kick-start cue could come from ecdysone signalling. Ecdysone is a steroid hormone best known for its regulation of *Drosophila* metamorphosis. However, recent evidence has begun to suggest that ecdysone may also play a role in the morphogenetic events which characterise late embryogenesis, including dorsal closure. Intriguingly, there is a surge of ecdysone release in the embryo that peaks towards the end of germ band retraction (Richards, 1981), which is obviously well timed for the earliest signs of the initiation of dorsal closure. Further investigation indicates that at the end of germ-band retraction, the amnioserosa itself contains a high concentration of active ecdysteroids, as a range of ecdysone-dependant reporter constructs come on strongly in the amnioserosa at this time (Kozlova and Thummel, 2003). In keeping with a role for ecdysone in dorsal closure, embryos mutant for components of the ecdysone synthesis pathway show failures in dorsal closure, as well as germ-band retraction (Chavez et al., 2000). So far, all investigations of these mutants have been carried out in fixed tissue; it would therefore

be very interesting to explore the dorsal closure phenotypes in more detail using live imaging.

6.1.2 Dorsal closure is a resilient multi-force process

Historically, much of the emphasis in the study of dorsal closure has been on mutants that fail entirely in the process and give large cuticlar holes. However, with the advent of good live imaging it is now possible to study more subtle perturbations in the closure process. This manner of analysis tends to highlight how resilient dorsal closure is, as many seemingly severe problems are overcome and the embryo manages to close its hole, albeit often imperfectly. The results I present in Chapter 4, in my investigation of Rac function during dorsal closure, illustrate this concept well. In the zygotic triple *Rac* mutant, although the epithelial leading edge is considerably disabled by the loss of Rac, with areas along it lacking actin cable and protrusions, the embryo still manages to close the hole through continued amnioserosal contraction and by skipping the affected leading edge regions. In a similar way, the expression of dominant negative *Rac1* in *engrailed* stripes, whilst preventing these cells from assembling the usual actin structures, does not stop dorsal closure as the remaining wild type cells can compensate and the hole is still closed. In both cases closure is imperfect and the embryos do not survive to become larvae, but the fact that these holes can close at all illustrates the plasticity of dorsal closure. The resilience and multi-force nature of dorsal closure is also demonstrated when wild type embryos are subjected to similar perturbations through laser ablations of the leading edge, where, for example, continued ablation of the zipping canthi only results in a slight delay in closure (Hutson et al., 2003). It seems likely that maintaining this sort of flexibility will be important much more generally in embryonic development, in order for embryos to tolerate environmental assaults and, ultimately to allow for adaptive tweaks during the course of evolution.

6.2 REGULATION OF ACTIN PROTRUSION FORMATION IN DORSAL CLOSURE

In Chapter 4, I explored the functions of the small GTPase Rac during dorsal closure. Here I will focus on how my findings relate to the assembly of filopodia and lamellipodia by the leading edge and what clues this work, combined with previous studies, gives for a model of actin protrusion formation by the leading edge during closure.

6.2.1 The role of Rac in protrusion assembly during closure

So, how far can we extrapolate the, now classic, fibroblast findings that Rac controls the assembly of lamellipodia, to the *in vivo* system of dorsal closure? Well, certainly my findings with expression of constitutively active *Rac1* where excessively large lamellipodia are formed by the affected leading edge cells, seem to recapitulate the tissue culture findings very closely. However, the picture is complicated slightly when considering expression of dominant negative *Rac1* ($Rac1^{N17}$) and the loss-of-function mutants. When $Rac1^{N17}$ is expressed in *engrailed* stripes, not only do these cells fail to assemble lamellipodia, but they form hardly any actin protrusions at all and actin cable assembly is also reduced in many of the expressing cells. Similarly, in *Rac* loss-of-function mutants, all actin assembly is affected, whether it is along the entire edge as in the germ line clone embryos, or in patches along the edge as is seen in the zygotic triple *Rac* mutant. It therefore seems that the three *Drosophila* Rac GTPases are involved not just in the assembly of lamellipodia, but filopodia and, to a slightly lesser extent, actin cable too. One possibility is that each of the three *Drosophila* Racs, Rac1, Rac2 and Mtl, may play slightly different roles in actin organisation at the leading edge, which could be discerned by live imaging, and this would be a useful avenue to pursue with single and double mutants of the three.

However, it is the case that expression of dominant negative *Cdc42* during dorsal closure also leads to a loss of both lamellipodia and filopodia, although not cable, assembly at the leading edge (Jacinto et al., 2000). Whilst it is possible that the

similarities between protrusion phenotypes with expression of dominant negative *Cdc42* and *Rac1* could reflect non-specificity of the dominant negative GTPase constructs, this seems unlikely because of the other differences in the phenotypes between the two, such as the loss of actin cable with $Rac1^{N17}$ but not with dominant negative *Cdc42*. Therefore, the loss of filopodia and lamellipodia together in all these cases could indicate that the regulation of the formation of these structures are linked, an idea which is discussed in the next section.

6.2.2 Evidence of a cascade model for protrusion formation during closure?

In the "classic" view of actin protrusion formation, the decision between whether filopodia or lamellipodia are formed is made at the level of the GTPase, with activation of Rac leading to the assembly of lamellipodia via Scar/WAVE and filopodia through Cdc42 mediated activation of WASP (see Figure 1.8A). However, as discussed above, in dorsal closure it seems that the presence of both Rac and Cdc42 are required to assemble either lamellipodia or filopodia. The reasons for this could be either due to some form of structural limitations on the assembly of these actin protrusions or that the signalling controlling their assembly operates slightly differently from the parallel pathway model.

On a structural level it is possible to imagine that filopodia and lamellipodia might be reliant on each other for support, with, for example, the actin filaments which make up a filopodium being rooted in the lamellipodial network. This certainly appears to be the case in highly motile cultured melanoma cells, where specialised EM techniques reveal the actin network, with the parallel bundles of actin filaments which form filopodia emanating from the lamellipodial dendritic network (Svitkina et al., 2003). However an absolute structural dependency is not borne out in many cells, where one type of actin protrusions dominates, such as keratocytes whose leading edge is almost entirely composed of lamellipodia whilst, for example, some growth cones are dominated by

long filopodia with almost no lamellipodia. The filopodia produced by the leading edge during dorsal closure, especially late in the process, are quite different from the filopodia produced by many cell types, in particular they are much more dynamic than most. Therefore, it may be necessary for dorsal closure filopodia to have greater support, such that they cannot be built if the assembly of lamellipodia is prevented, by, for example, knocking out Rac activity. However, whilst this structural view of dorsal closure actin protrusions may have some merits, there are a couple of observations which indicate that it is unlikely to be the only explanation. Firstly, lamellipodia are only seen later in dorsal closure, but, in wild type embryos, filopodia begin to emerge from the leading edge early in the process. Secondly, it appears from my work with Myo10A that it is possible to get longer than normal filopodia with out any increase in lamellipodial protrusion size.

An alternative, although not mutually exclusive, explanation is that the signalling controlling actin protrusions during dorsal closure does not operate down two discrete pathways. In cultured *Drosophila* cells it appears that a cascade pathway may be operating to control the assembly of filopodia, with Scar being the major mediator of actin protrusion formation. In this model, Scar is activated by Rac, leading to the assembly of lamellipodia, with subsequent signals downstream of Cdc42 acting to transform lamellipodia into filopodia (Biyasheva et al., 2004). Such a cascade model of protrusion assembly definitely seems to fit in well with the complete eradication of protrusion assembly that I see when Rac function is knocked out. However, this model still does not explain how the filopodia seen early in dorsal closure can form in the absence of lamellipodia, perhaps the actin cable can provide an equivalent dendritic network at this point, but improved electron microscopy of the leading edge will be required to determine this.

6.3 ACTIN PROTRUSIONS PLAY THREE MAJOR ROLES IN DORSAL CLOSURE

The work presented in this thesis, along with previous live studies of dorsal closure, indicate that actin protrusions play three major roles during this process: two of these are sensory, as cells participate in segmental matching and in sensing "contact inhibition" cues and the third is an adhesion function as the two epithelial surfaces are zipped tightly together. The evidence and implications for each of these functions are explored below.

6.3.1 Segmental sensing

As discussed in the previous section, the expression of either dominant negative *Cdc42* (Jacinto et al., 2000) or *Rac1* in *engrailed* segmental stripes prevents expressing cells from assembling all but the most rudimentary of actin protrusions. A further consequence seen in both of these cases is that whilst these embryos do manage to close the hole, the cells of the leading edge are now unable to accurately find their correct partners on the opposing epithelial edge, resulting in frequent mis-matching of segments along the dorsal midline. Together these results indicate that one function of the leading edge actin protrusions is a sensing role, allowing cells to find their correct segmental partners on the opposing epithelial edge. Corroborating this finding, analysis of wild type closure also shows filopodia reaching out and interacting with incorrect segments and seemingly being repulsed, before retracting back (Jacinto et al., 2000).

A fascinating question, which requires further investigation, is how the actin protrusions perform this sensing role during dorsal closure, and, crucially, what molecules are required to mediate segmental matching? However, before speculating on the molecular components of segmental matching, it is important to consider another aspect that is likely to play an important part in keeping segments aligned: the actin cable. The actomyosin cable gives the leading edge structural rigidity and, coupled

with a limit on the maximum length which filopodia can grow, restricts the breadth of interactions that any single leading edge cell can make. When Rho activity is knocked out, either through expression of a dominant negative form or in a loss-of-function mutant, the actin cable is lost and the leading edge loses its tension and normal organisation. As a result, unrestrained leading edge cells can interact more freely, including with their adjacent neighbours, leading to a bunched, puckered midline, with no clear segmental alignment (Jacinto et al., 2002a; Magie et al., 1999). However, whilst the cable undoubtedly plays a key role in keeping the leading edge organised and preventing random interactions, it seems that the precise cell matching seen during wild type closure necessitates further "sensing machinery" to prevent errors.

As yet, there are very few clues as to what molecules may be involved in the segmental sensing seen during dorsal closure. It would seem likely that whatever is involved would be localised at the tips of the filopodia which explore the opposing epithelial edge as the hole closes. Any sensing molecule would, therefore, need to be carried to the filopodial tip and it is for this reason that the FERM domain myosins, investigated in Chapter 5, may provide a powerful first step in uncovering the sensing machinery. In other systems these myosins appear to be acting to transport crucial cargo to the tips of filopodia (Tokuo and Ikebe, 2004; Zhang et al., 2004). My investigations into Myo10A function during dorsal closure are still somewhat preliminary but the segmental mismatch phenotype I see with expression of a Myo10A RNAi snapback construct is tantalizing. It remains unclear whether this phenotype is a result of a change in the actin dynamics of the filopodia or a failure in the sensing machinery, but further investigation into this could yield some important findings. It is easy to begin to speculate what molecules could potentially play a role in segmental sensing; one possibility could be that cell-cell adhesion molecules are involved, with, perhaps, different cadherins being expressed by different cells along the leading edge. It is therefore, very intriguing that the Myo10A yeast two-hybrid screen, described in

Chapter 5, pulled out E-cadherin as a potential interactor with the myosin. Other strong candidates include the various axon guidance molecules such as semaphorins and robo/slit that may play related cell matching/guidance roles during the building of the nervous system (Tessier-Lavigne and Goodman, 1996), but, as yet, no evidence for a role of these molecules in dorsal closure has been uncovered.

6.3.2 Contact inhibition

Another function that the filopodia seem to be involved in, which may be related to the segmental matching role described above, is to sense, and react to, some form of "contact inhibition" cue as the two epithelial surfaces some together. This stops the two surfaces from over-running when they meet and also prevents interactions with adjacent neighbours. In wild type embryos, once the two epithelial fronts have met, the dynamics of the actin protrusions changes and their assembly by the leading edge is quickly quelled. An interesting consequence of expressing constitutively active *Rac1* in *engrailed* stripes is that these cells produce overly large lamellipodia, which seem unable to respond to these inhibitory cues appropriately and interact with their adjacent neighbours as if they were on the opposing epithelial edge. Whilst ideas of "contact inhibition" in dorsal closure are still extremely speculative, it is an exciting prospect that dorsal closure could provide a model to study this crucial cell biological question; as although contact inhibition was first outlined by Abercrombie in the 1950s (reviewed in Abercrombie, 1979), and has such obvious implications for cancer biology, there is still, as yet, no clear molecular mechanism.

6.3.3 Zippering

A final clear function for actin protrusions during dorsal closure is the zipping and fusion of the two epithelial surfaces. With *engrailed* expression of either dominant negative *Cdc42* or *Rac1*, the loss of actin protrusion assembly is followed by an inability of affected leading edge cells to fuse tightly at the midline during dorsal

closure, resulting in embryos which have small holes along the fusion seam. TEM studies of the zipping epithelial surfaces during dorsal closure clearly show the filopodia interdigitating and, ultimately, becoming sites for mature cell-cell adhesions (Jacinto et al., 2000). The fusion role of actin protrusions in dorsal closure is mirrored in other systems, such as ventral enclosure in the *C. elegans* embryo (Raich et al., 1999) and the fusion of keratinocytes in culture (Vasioukhin et al., 2000). Almost certainly this will turn out to be a general mode for fusion of epithelial sheets during embryogenesis. There is good evidence already for parallel mechanisms operating during eyelid closure (Zenz et al., 2003) and palate fusion (Taya et al., 1999) during mammalian embryogenesis and so the study of filopodia-primed adhesion may be of significant clinical importance with regard to congenital abnormalities.

6.4 NEW CANDIDATES FOR FILOPODIAL FUNCTION

With the multiple roles that actin protrusions appear to be playing during dorsal closure, the hunt is now on to find the molecules which mediate these functions. As discussed previously, the filopodial tip localising, FERM domain containing myosins may prove a particularly strong group of candidates. If such a myosin is found at the tips of filopodia during dorsal closure, discovering the cargos it is carrying could shed a great deal of light on how filopodia fulfil their dorsal closure roles.

In Chapter 5, I describe the early steps in beginning to address these questions. It certainly appears that the *Drosophila* Class XV myosin, Myo10A, localises to the tips of filopodia assembled by cultured fly S2R+ cells. So far, I have been unable to assess if Myo10A localises within dorsal closure filopodia *in vivo* and for this a fluorescent Myo10A fusion construct is really needed. However, the intriguing phenotype I see with the *Myo10A* RNAi snapback certainly seems to suggest that this myosin is involved in filopodial dynamics during dorsal closure. These results are only preliminary, and it will certainly be necessary to try driving expression of the snapback with a variety of GAL4

drivers and also to make more checks regarding the specificity of Myo10A knockdown by the snapback. But, these early indications of a role for Myo10A in dorsal closure certainly make the prospects that relevant molecules will be pulled out of the Myo10A yeast two-hybrid screen very good indeed. So far less than 20% of the positive interactors from the screen have been sequenced and already I have some interesting candidates. Perhaps the best candidate so far for a role in filopodial function is E-cadherin and, significantly, this is the first report of a direct interaction between this class of myosin and E-cadherin.

The Myo10A yeast two-hybrid screen has also pulled out α-tubulin and two microtubule binding proteins, EB1 and katanin-60. Whilst Myo10A may be interacting with microtubules and these factors in processes other than dorsal closure, all three could be interesting avenues to pursue. Certainly interactions between the actin and microtubule cytoskeletons are proving to be an important phenomenon that underlies a wide range of processes including cell migration, neuronal pathfinding and cellular wounding (reviewed in Rodriguez et al., 2003). In the case of cellular wounds in Xenopus oocytes, microtubules are carried to the wound edge by actin and appear to play a key role in the regulation of the actomyosin "purse-string" responsible for closing the wounds (Mandato and Bement, 2003). It seems likely that Myo10A may be mediating interactions between the two cytoskeletons, having as it does the ability to bind to both microtubules and actin. Very little is known about what role, if any, microtubules play in dorsal closure but Myo10A may provide a starting point for investigating this area.

To conclude, in this thesis I have presented a detailed live analysis of dorsal closure, focusing on the role of dynamic actin protrusions in this process. My investigations of wild type and *Rac* mutant embryos have suggested three roles for actin protrusions

during dorsal closure: segmental matching, "contact inhibition" and epithelial zippering. Understanding how the actin protrusions fulfil these functions and how this is linked to their assembly at the leading edge provides some exciting new research prospects. Finally, my preliminary investigations into the role of Myo10A in dorsal closure suggest that FERM domain containing myosins may prove to be a powerful tool to begin to address the molecular basis of filopodial function in dorsal closure.

References

Abercrombie, M. (1979). Contact inhibition and malignancy. *Nature* **281,** 259-62.

Adachi-Yamada, T., Fujimura-Kamada, K., Nishida, Y., and Matsumoto, K. (1999). Distortion of proximodistal information causes JNK-dependent apoptosis in Drosophila wing. *Nature* **400,** 166-9.

Adams, M. D., Celniker, S. E., Holt, R. A., Evans, C. A., Gocayne, J. D., Amanatides, P. G., Scherer, S. E., Li, P. W., Hoskins, R. A., Galle, R. F., George, R. A., Lewis, S. E., Richards, S., Ashburner, M., Henderson, S. N., Sutton, G. G., Wortman, J. R., Yandell, M. D., Zhang, Q., Chen, L. X., Brandon, R. C., Rogers, Y. H., Blazej, R. G., Champe, M., Pfeiffer, B. D., Wan, K. H., Doyle, C., Baxter, E. G., Helt, G., Nelson, C. R., Gabor, G. L., Abril, J. F., Agbayani, A., An, H. J., Andrews-Pfannkoch, C., Baldwin, D., Ballew, R. M., Basu, A., Baxendale, J., Bayraktaroglu, L., Beasley, E. M., Beeson, K. Y., Benos, P. V., Berman, B. P., Bhandari, D., Bolshakov, S., Borkova, D., Botchan, M. R., Bouck, J., Brokstein, P., Brottier, P., Burtis, K. C., Busam, D. A., Butler, H., Cadieu, E., Center, A., Chandra, I., Cherry, J. M., Cawley, S., Dahlke, C., Davenport, L. B., Davies, P., de Pablos, B., Delcher, A., Deng, Z., Mays, A. D., Dew, I., Dietz, S. M., Dodson, K., Doup, L. E., Downes, M., Dugan-Rocha, S., Dunkov, B. C., Dunn, P., Durbin, K. J., Evangelista, C. C., Ferraz, C., Ferriera, S., Fleischmann, W., Fosler, C., Gabrielian, A. E., Garg, N. S., Gelbart, W. M., Glasser, K., Glodek, A., Gong, F., Gorrell, J. H., Gu, Z., Guan, P., Harris, M., Harris, N. L., Harvey, D., Heiman, T. J., Hernandez, J. R., Houck, J., Hostin, D., Houston, K. A., Howland, T. J., Wei, M. H., Ibegwam, C., et al. (2000). The genome sequence of Drosophila melanogaster. *Science* **287,** 2185-95.

Affolter, M., Marty, T., Vigano, M. A., and Jazwinska, A. (2001). Nuclear interpretation of Dpp signaling in Drosophila. *Embo J* **20,** 3298-305.

Affolter, M., Nellen, D., Nussbaumer, U., and Basler, K. (1994). Multiple requirements for the receptor serine/threonine kinase thick veins reveal novel functions of TGF beta homologs during Drosophila embryogenesis. *Development* **120,** 3105-17.

Alifragis, P., Poortinga, G., Parkhurst, S. M., and Delidakis, C. (1997). A network of interacting transcriptional regulators involved in Drosophila neural fate specification revealed by the yeast two-hybrid system. *Proc Natl Acad Sci U S A* **94,** 13099-104.

Anderson, D. W., Probst, F. J., Belyantseva, I. A., Fridell, R. A., Beyer, L., Martin, D. M., Wu, D., Kachar, B., Friedman, T. B., Raphael, Y., and Camper, S. A. (2000). The motor and tail regions of myosin XV are critical for normal structure and function of auditory and vestibular hair cells. *Hum Mol Genet* **9,** 1729-38.

Ausubel, F. M., Brent, R., Kingston, R. E., Moore, D. D., Seidman, J. G., Smith, G. A. & Struhl, K. (1995). "Current Protocols in Molecular Biology." Wiley, New York.

Baum, B., and Kunda, P. (2005). Actin nucleation: spire - actin nucleator in a class of its own. *Curr Biol* **15,** R305-8.

Baum, B., and Perrimon, N. (2001). Spatial control of the actin cytoskeleton in Drosophila epithelial cells. *Nat Cell Biol* **3,** 883-90.

Baumgartner, S., Littleton, J. T., Broadie, K., Bhat, M. A., Harbecke, R., Lengyel, J. A., Chiquet-Ehrismann, R., Prokop, A., and Bellen, H. J. (1996). A Drosophila neurexin is required for septate junction and blood-nerve barrier formation and function. *Cell* **87,** 1059-68.

Bear, J. E., Svitkina, T. M., Krause, M., Schafer, D. A., Loureiro, J. J., Strasser, G. A., Maly, I. V., Chaga, O. Y., Cooper, J. A., Borisy, G. G., and Gertler, F. B. (2002). Antagonism between Ena/VASP proteins and actin filament capping regulates fibroblast motility. *Cell* **109,** 509-21.

Bement, W. M., Forscher, P., and Mooseker, M. S. (1993). A novel cytoskeletal structure involved in purse string wound closure and cell polarity maintenance. *J Cell Biol* **121,** 565-78.

Berg, J. S., and Cheney, R. E. (2002). Myosin-X is an unconventional myosin that undergoes intrafilopodial motility. *Nat Cell Biol* **4,** 246-50.

Berg, J. S., Powell, B. C., and Cheney, R. E. (2001). A millennial myosin census. *Mol Biol Cell* **12,** 780-94.

Biyasheva, A., Svitkina, T., Kunda, P., Baum, B., and Borisy, G. (2004). Cascade pathway of filopodia formation downstream of SCAR. *J Cell Sci* **117,** 837-48.

Blagg, S. L., Stewart, M., Sambles, C., and Insall, R. H. (2003). PIR121 regulates pseudopod dynamics and SCAR activity in Dictyostelium. *Curr Biol* **13,** 1480-7.

Brand, A. H., and Perrimon, N. (1993). Targeted gene expression as a means of altering cell fates and generating dominant phenotypes. *Development* **118,** 401-15.

Brennan, K., Baylies, M., and Arias, A. M. (1999a). Repression by Notch is required before Wingless signalling during muscle progenitor cell development in Drosophila. *Curr Biol* **9,** 707-10.

Brennan, K., Tateson, R., Lieber, T., Couso, J. P., Zecchini, V., and Arias, A. M. (1999b). The abruptex mutations of notch disrupt the establishment of proneural clusters in Drosophila. *Dev Biol* **216,** 230-42.

Brock, J., Midwinter, K., Lewis, J., and Martin, P. (1996). Healing of incisional wounds in the embryonic chick wing bud: characterization of the actin purse-string and demonstration of a requirement for Rho activation. *J Cell Biol* **135,** 1097-107.

Brown, N. H. (1994). Null mutations in the alpha PS2 and beta PS integrin subunit genes have distinct phenotypes. *Development* **120,** 1221-31.

Brown, N. H., Gregory, S. L., and Martin-Bermudo, M. D. (2000). Integrins as mediators of morphogenesis in Drosophila. *Dev Biol* **223,** 1-16.

Brummel, T. J., Twombly, V., Marques, G., Wrana, J. L., Newfeld, S. J., Attisano, L., Massague, J., O'Connor, M. B., and Gelbart, W. M. (1994). Characterization and relationship of Dpp receptors encoded by the saxophone and thick veins genes in Drosophila. *Cell* **78,** 251-61.

Bryant, P. J. (1999). Filopodia: fickle fingers of cell fate? *Curr Biol* **9,** R655-7.

Burbelo, P. D., Drechsel, D., and Hall, A. (1995). A conserved binding motif defines numerous candidate target proteins for both Cdc42 and Rac GTPases. *J Biol Chem* **270,** 29071-4.

Burridge, K., and Wennerberg, K. (2004). Rho and Rac take center stage. *Cell* **116,** 167-79.

Cadigan, K. M. (2002). Regulating morphogen gradients in the Drosophila wing. *Semin Cell Dev Biol* **13,** 83-90.

Chavez, V. M., Marques, G., Delbecque, J. P., Kobayashi, K., Hollingsworth, M., Burr, J., Natzle, J. E., and O'Connor, M. B. (2000). The Drosophila disembodied gene controls late embryonic morphogenesis and codes for a cytochrome P450 enzyme that regulates embryonic ecdysone levels. *Development* **127,** 4115-26.

Childs, S. R., Wrana, J. L., Arora, K., Attisano, L., O'Connor, M. B., and Massague, J. (1993). Identification of a Drosophila activin receptor. *Proc Natl Acad Sci U S A* **90,** 9475-9.

Colas, J. F., and Schoenwolf, G. C. (2001). Towards a cellular and molecular understanding of neurulation. *Dev Dyn* **221,** 117-45.

Conder, R., Yu, H., Ricos, M., Hing, H., Chia, W., Lim, L., and Harden, N. (2004). dPak is required for integrity of the leading edge cytoskeleton during Drosophila dorsal closure but does not signal through the JNK cascade. *Dev Biol* **276,** 378-90.

Cooper, L., Johnson, C., Burslem, F., and Martin, P. (2005). Wound healing and inflammation genes revealed by array analysis of 'macrophageless' PU.1 null mice. *Genome Biol* **6,** R5.

Coso, O. A., Chiariello, M., Yu, J. C., Teramoto, H., Crespo, P., Xu, N., Miki, T., and Gutkind, J. S. (1995). The small GTP-binding proteins Rac1 and Cdc42 regulate the activity of the JNK/SAPK signaling pathway. *Cell* **81,** 1137-46.

Cox, D., Berg, J. S., Cammer, M., Chinegwundoh, J. O., Dale, B. M., Cheney, R. E., and Greenberg, S. (2002). Myosin X is a downstream effector of PI(3)K during phagocytosis. *Nat Cell Biol* **4,** 469-77.

Cox, D., Tseng, C. C., Bjekic, G., and Greenberg, S. (1999). A requirement for phosphatidylinositol 3-kinase in pseudopod extension. *J Biol Chem* **274,** 1240-7.

Danjo, Y., and Gipson, I. K. (1998). Actin 'purse string' filaments are anchored by E-cadherin-mediated adherens junctions at the leading edge of the epithelial wound, providing coordinated cell movement. *J Cell Sci* **111 (Pt 22),** 3323-32.

De La Cruz, E. M., Ostap, E. M., Brundage, R. A., Reddy, K. S., Sweeney, H. L., and Safer, D. (2000). Thymosin-beta(4) changes the conformation and dynamics of actin monomers. *Biophys J* **78,** 2516-27.

Driessens, M. H., Hu, H., Nobes, C. D., Self, A., Jordens, I., Goodman, C. S., and Hall, A. (2001). Plexin-B semaphorin receptors interact directly with active Rac and regulate the actin cytoskeleton by activating Rho. *Curr Biol* **11,** 339-44.

Dutta, D., Bloor, J. W., Ruiz-Gomez, M., VijayRaghavan, K., and Kiehart, D. P. (2002). Real-time imaging of morphogenetic movements in Drosophila using Gal4-UAS-driven expression of GFP fused to the actin-binding domain of moesin. *Genesis* **34,** 146-51.

Eden, S., Rohatgi, R., Podtelejnikov, A. V., Mann, M., and Kirschner, M. W. (2002). Mechanism of regulation of WAVE1-induced actin nucleation by Rac1 and Nck. *Nature* **418,** 790-3.

Edwards, D. C., Sanders, L. C., Bokoch, G. M., and Gill, G. N. (1999). Activation of LIM-kinase by Pak1 couples Rac/Cdc42 GTPase signalling to actin cytoskeletal dynamics. *Nat Cell Biol* **1,** 253-9.

Ernest, S., Rauch, G. J., Haffter, P., Geisler, R., Petit, C., and Nicolson, T. (2000). Mariner is defective in myosin VIIA: a zebrafish model for human hereditary deafness. *Hum Mol Genet* **9,** 2189-96.

Eudy, J. D., and Sumegi, J. (1999). Molecular genetics of Usher syndrome. *Cell Mol Life Sci* **56,** 258-67.

Evangelista, M., Klebl, B. M., Tong, A. H., Webb, B. A., Leeuw, T., Leberer, E., Whiteway, M., Thomas, D. Y., and Boone, C. (2000). A role for myosin-I in actin assembly through interactions with Vrp1p, Bee1p, and the Arp2/3 complex. *J Cell Biol* **148,** 353-62.

Farge, E. (2003). Mechanical induction of Twist in the Drosophila foregut/stomodeal primordium. *Curr Biol* **13,** 1365-77.

Fehon, R. G., Dawson, I. A., and Artavanis-Tsakonas, S. (1994). A Drosophila homologue of membrane-skeleton protein 4.1 is associated with septate junctions and is encoded by the coracle gene. *Development* **120,** 545-57.

Franca-Koh, J., and Devreotes, P. N. (2004). Moving forward: mechanisms of chemoattractant gradient sensing. *Physiology (Bethesda)* **19,** 300-8.

Genova, J. L., Jong, S., Camp, J. T., and Fehon, R. G. (2000). Functional analysis of Cdc42 in actin filament assembly, epithelial morphogenesis, and cell signaling during Drosophila development. *Dev Biol* **221,** 181-94.

Giniger, E. (2002). How do Rho family GTPases direct axon growth and guidance? A proposal relating signaling pathways to growth cone mechanics. *Differentiation* **70,** 385-96.

Glise, B., Bourbon, H., and Noselli, S. (1995). hemipterous encodes a novel Drosophila MAP kinase kinase, required for epithelial cell sheet movement. *Cell* **83,** 451-61.

Glise, B., and Noselli, S. (1997). Coupling of Jun amino-terminal kinase and Decapentaplegic signaling pathways in Drosophila morphogenesis. *Genes Dev* **11,** 1738-47.

Grevengoed, E. E., Loureiro, J. J., Jesse, T. L., and Peifer, M. (2001). Abelson kinase regulates epithelial morphogenesis in Drosophila. *J Cell Biol* **155,** 1185-98.

Hakeda-Suzuki, S., Ng, J., Tzu, J., Dietzl, G., Sun, Y., Harms, M., Nardine, T., Luo, L., and Dickson, B. J. (2002). Rac function and regulation during Drosophila development. *Nature* **416,** 438-42.

Halsell, S. R., Chu, B. I., and Kiehart, D. P. (2000). Genetic analysis demonstrates a direct link between rho signaling and nonmuscle myosin function during drosophila morphogenesis. *Genetics* **156,** 469.

Harden, N. (2002). Signaling pathways directing the movement and fusion of epithelial sheets: lessons from dorsal closure in Drosophila. *Differentiation* **70,** 181-203.

Harden, N., Lee, J., Loh, H. Y., Ong, Y. M., Tan, I., Leung, T., Manser, E., and Lim, L. (1996). A Drosophila homolog of the Rac- and Cdc42-activated serine/threonine kinase PAK is a potential focal adhesion and focal complex protein that colocalizes with dynamic actin structures. *Mol Cell Biol* **16,** 1896-908.

Harden, N., Loh, H. Y., Chia, W., and Lim, L. (1995). A dominant inhibitory version of the small GTP-binding protein Rac disrupts cytoskeletal structures and inhibits developmental cell shape changes in Drosophila. *Development* **121,** 903-14.

Harden, N., Ricos, M., Ong, Y. M., Chia, W., and Lim, L. (1999). Participation of small GTPases in dorsal closure of the Drosophila embryo: distinct roles for Rho subfamily proteins in epithelial morphogenesis. *J Cell Sci* **112 (Pt 3),** 273-84.

Harden, N., Ricos, M., Yee, K., Sanny, J., Langmann, C., Yu, H., Chia, W., and Lim, L. (2002). Drac1 and Crumbs participate in amnioserosa morphogenesis during dorsal closure in Drosophila. *J Cell Sci* **115,** 2119-29.

Hariharan, I. K., Hu, K. Q., Asha, H., Quintanilla, A., Ezzell, R. M., and Settleman, J. (1995). Characterization of rho GTPase family homologues in Drosophila melanogaster: overexpressing Rho1 in retinal cells causes a late developmental defect. *Embo J* **14,** 292-302.

Hartenstein, V. (1993). "Atlas of Drosophila Development." Cold Spring Harbor Laboratory Press,

Hasson, T. (1999). Molecular motors: sensing a function for myosin-VIIa. *Curr Biol* **9,** R838-41.

Hasson, T., Heintzelman, M. B., Santos-Sacchi, J., Corey, D. P., and Mooseker, M. S. (1995). Expression in cochlea and retina of myosin VIIa, the gene product defective in Usher syndrome type 1B. *Proc Natl Acad Sci U S A* **92,** 9815-9.

Higashida, C., Miyoshi, T., Fujita, A., Oceguera-Yanez, F., Monypenny, J., Andou, Y., Narumiya, S., and Watanabe, N. (2004). Actin polymerization-driven molecular movement of mDia1 in living cells. *Science* **303,** 2007-10.

Higgs, H. N., and Pollard, T. D. (2000). Activation by Cdc42 and PIP(2) of Wiskott-Aldrich syndrome protein (WASp) stimulates actin nucleation by Arp2/3 complex. *J Cell Biol* **150,** 1311-20.

Hing, H., Xiao, J., Harden, N., Lim, L., and Zipursky, S. L. (1999). Pak functions downstream of Dock to regulate photoreceptor axon guidance in Drosophila. *Cell* **97,** 853-63.

Hollenberg, S. M., Sternglanz, R., Cheng, P. F., and Weintraub, H. (1995). Identification of a new family of tissue-specific basic helix-loop-helix proteins with a two-hybrid system. *Mol Cell Biol* **15,** 3813-22.

Hou, X. S., Goldstein, E. S., and Perrimon, N. (1997). Drosophila Jun relays the Jun amino-terminal kinase signal transduction pathway to the Decapentaplegic signal transduction pathway in regulating epithelial cell sheet movement. *Genes Dev* **11,** 1728-37.

Hu, H., Marton, T. F., and Goodman, C. S. (2001). Plexin B mediates axon guidance in Drosophila by simultaneously inhibiting active Rac and enhancing RhoA signaling. *Neuron* **32,** 39-51.

Hurd, D. D., and Saxton, W. M. (1996). Kinesin mutations cause motor neuron disease phenotypes by disrupting fast axonal transport in Drosophila. *Genetics* **144,** 1075-85.

Hutson, M. S., Tokutake, Y., Chang, M. S., Bloor, J. W., Venakides, S., Kiehart, D. P., and Edwards, G. S. (2003). Forces for morphogenesis investigated with laser microsurgery and quantitative modeling. *Science* **300,** 145-9.

Jacinto, A., Martinez-Arias, A., and Martin, P. (2001). Mechanisms of epithelial fusion and repair. *Nat Cell Biol* **3,** E117-23.

Jacinto, A., Wood, W., Balayo, T., Turmaine, M., Martinez-Arias, A., and Martin, P. (2000). Dynamic actin-based epithelial adhesion and cell matching during Drosophila dorsal closure. *Curr Biol* **10,** 1420-6.

Jacinto, A., Wood, W., Woolner, S., Hiley, C., Turner, L., Wilson, C., Martinez-Arias, A., and Martin, P. (2002a). Dynamic analysis of actin cable function during Drosophila dorsal closure. *Curr Biol* **12,** 1245-50.

Jacinto, A., Woolner, S., and Martin, P. (2002b). Dynamic analysis of dorsal closure in Drosophila: from genetics to cell biology. *Dev Cell* **3,** 9-19.

Jarecki, J., Johnson, E., and Krasnow, M. A. (1999). Oxygen regulation of airway branching in Drosophila is mediated by branchless FGF. *Cell* **99,** 211-20.

Jürgens, G., Wieschaus, E., Nüsslein-Volhard, C., and Kluding, H. (1984). Mutations affecting the pattern of the larval cuticle in Drosophila melanogaster II. Zygotic loci on the third chromosome. *Roux's archives of developmental biology* **193,** 283-295.

Kaiser, D. A., Vinson, V. K., Murphy, D. B., and Pollard, T. D. (1999). Profilin is predominantly associated with monomeric actin in Acanthamoeba. *J Cell Sci* **112 (Pt 21),** 3779-90.

Kalidas, S., and Smith, D. P. (2002). Novel genomic cDNA hybrids produce effective RNA interference in adult Drosophila. *Neuron* **33,** 177-84.

Kaltschmidt, J. A., Lawrence, N., Morel, V., Balayo, T., Fernandez, B. G., Pelissier, A., Jacinto, A., and Martinez Arias, A. (2002). Planar polarity and actin dynamics in the epidermis of Drosophila. *Nat Cell Biol* **4,** 937-44.

Kennerdell, J. R., and Carthew, R. W. (1998). Use of dsRNA-mediated genetic interference to demonstrate that frizzled and frizzled 2 act in the wingless pathway. *Cell* **95,** 1017-26.

Kidd, T., Bland, K. S., and Goodman, C. S. (1999). Slit is the midline repellent for the robo receptor in Drosophila. *Cell* **96,** 785-94.

Kiehart, D. P. (1999). The power of the purse string. *Curr Biol* **9,** R602-R605.

Kiehart, D. P., Franke, J. D., Chee, M. K., Montague, R. A., Chen, T. L., Roote, J., and Ashburner, M. (2004). Drosophila crinkled, mutations of which disrupt morphogenesis and cause lethality, encodes fly myosin VIIA. *Genetics* **168,** 1337-52.

Kiehart, D. P., Galbraith, C. G., Edwards, K. A., Rickoll, W. L., and Montague, R. A. (2000). Multiple forces contribute to cell sheet morphogenesis for dorsal closure in Drosophila. *J Cell Biol* **149,** 471-90.

Klepeis, V. E., Cornell-Bell, A., and Trinkaus-Randall, V. (2001). Growth factors but not gap junctions play a role in injury-induced Ca2+ waves in epithelial cells. *J Cell Sci* **114,** 4185-95.

Kockel, L., Zeitlinger, J., Staszewski, L. M., Mlodzik, M., and Bohmann, D. (1997). Jun in Drosophila development: redundant and nonredundant functions and regulation by two MAPK signal transduction pathways. *Genes Dev* **11,** 1748-58.

Kozlova, T., and Thummel, C. S. (2003). Essential roles for ecdysone signaling during Drosophila mid-embryonic development. *Science* **301,** 1911-4.

Krugmann, S., Jordens, I., Gevaert, K., Driessens, M., Vandekerckhove, J., and Hall, A. (2001). Cdc42 induces filopodia by promoting the formation of an IRSp53:Mena complex. *Curr Biol* **11,** 1645-55.

Kussel-Andermann, P., El-Amraoui, A., Safieddine, S., Nouaille, S., Perfettini, I., Lecuit, M., Cossart, P., Wolfrum, U., and Petit, C. (2000). Vezatin, a novel transmembrane protein, bridges myosin VIIA to the cadherin-catenins complex. *Embo J* **19,** 6020-9.

Lamb, R. S., Ward, R. E., Schweizer, L., and Fehon, R. G. (1998). Drosophila coracle, a member of the protein 4.1 superfamily, has essential structural functions in the septate junctions and developmental functions in embryonic and adult epithelial cells. *Mol Biol Cell* **9,** 3505-19.

Lechler, T., Shevchenko, A., and Li, R. (2000). Direct involvement of yeast type I myosins in Cdc42-dependent actin polymerization. *J Cell Biol* **148,** 363-73.

Lee, W. L., Bezanilla, M., and Pollard, T. D. (2000). Fission yeast myosin-I, Myo1p, stimulates actin assembly by Arp2/3 complex and shares functions with WASp. *J Cell Biol* **151,** 789-800.

Lehmann, R., and Tautz, D. (1994). In situ hybridization to RNA. *Methods Cell Biol* **44,** 575-98.

Letsou, A., Arora, K., Wrana, J. L., Simin, K., Twombly, V., Jamal, J., Staehling-Hampton, K., Hoffmann, F. M., Gelbart, W. M., Massague, J., and et al. (1995). Drosophila Dpp signaling is mediated by the punt gene product: a dual ligand-binding type II receptor of the TGF beta receptor family. *Cell* **80,** 899-908.

Li, G., Gustafson-Brown, C., Hanks, S. K., Nason, K., Arbeit, J. M., Pogliano, K., Wisdom, R. M., and Johnson, R. S. (2003a). c-Jun is essential for organization of the epidermal leading edge. *Dev Cell* **4,** 865-77.

Li, Z., Hannigan, M., Mo, Z., Liu, B., Lu, W., Wu, Y., Smrcka, A. V., Wu, G., Li, L., Liu, M., Huang, C. K., and Wu, D. (2003b). Directional sensing requires G beta gamma-mediated PAK1 and PIX alpha-dependent activation of Cdc42. *Cell* **114,** 215-27.

Liang, Y., Wang, A., Belyantseva, I. A., Anderson, D. W., Probst, F. J., Barber, T. D., Miller, W., Touchman, J. W., Jin, L., Sullivan, S. L., Sellers, J. R., Camper, S. A., Lloyd, R. V., Kachar, B., Friedman, T. B., and Fridell, R. A. (1999). Characterization of the human and mouse unconventional myosin XV genes responsible for hereditary deafness DFNB3 and shaker 2. *Genomics* **61,** 243-58.

Lu, Y., and Settleman, J. (1999). The Drosophila Pkn protein kinase is a Rho/Rac effector target required for dorsal closure during embryogenesis. *Genes Dev* **13,** 1168-80.

Luo, H. R., Huang, Y. E., Chen, J. C., Saiardi, A., Iijima, M., Ye, K., Huang, Y., Nagata, E., Devreotes, P., and Snyder, S. H. (2003). Inositol pyrophosphates mediate chemotaxis in Dictyostelium via pleckstrin homology domain-PtdIns(3,4,5)P3 interactions. *Cell* **114,** 559-72.

Luo, L., Liao, Y. J., Jan, L. Y., and Jan, Y. N. (1994). Distinct morphogenetic functions of similar small GTPases: Drosophila Drac1 is involved in axonal outgrowth and myoblast fusion. *Genes Dev* **8,** 1787-802.

Machesky, L. M., Atkinson, S. J., Ampe, C., Vandekerckhove, J., and Pollard, T. D. (1994). Purification of a cortical complex containing two unconventional actins from Acanthamoeba by affinity chromatography on profilin-agarose. *J Cell Biol* **127,** 107-15.

Machesky, L. M., and Insall, R. H. (1998). Scar1 and the related Wiskott-Aldrich syndrome protein, WASP, regulate the actin cytoskeleton through the Arp2/3 complex. *Curr Biol* **8,** 1347-56.

Magie, C. R., Meyer, M. R., Gorsuch, M. S., and Parkhurst, S. M. (1999). Mutations in the Rho1 small GTPase disrupt morphogenesis and segmentation during early Drosophila development. *Development* **126,** 5353-64.

Mandato, C. A., and Bement, W. M. (2003). Actomyosin transports microtubules and microtubules control actomyosin recruitment during Xenopus oocyte wound healing. *Curr Biol* **13,** 1096-105.

Mangeat, P., Roy, C., and Martin, M. (1999). ERM proteins in cell adhesion and membrane dynamics. *Trends Cell Biol* **9,** 187-92.

Maniak, M. (2001). Cell adhesion: ushering in a new understanding of myosin VII. *Curr Biol* **11,** R315-7.

Marchler-Bauer, A., and Bryant, S. H. (2004). CD-Search: protein domain annotations on the fly. *Nucleic Acids Res* **32,** W327-31.

Martin, P. (1997). Wound healing--aiming for perfect skin regeneration. *Science* **276,** 75-81.

Martin, P., D'Souza, D., Martin, J., Grose, R., Cooper, L., Maki, R., and McKercher, S. R. (2003). Wound healing in the PU.1 null mouse--tissue repair is not dependent on inflammatory cells. *Curr Biol* **13,** 1122-8.

Martin, P., Dickson, M. C., Millan, F. A., and Akhurst, R. J. (1993). Rapid induction and clearance of TGF beta 1 is an early response to wounding in the mouse embryo. *Dev Genet* **14,** 225-38.

Martin, P., and Lewis, J. (1992). Actin cables and epidermal movement in embryonic wound healing. *Nature* **360,** 179-83.

Martin, P., and Parkhurst, S. M. (2004). Parallels between tissue repair and embryo morphogenesis. *Development* **131,** 3021-34.

Martin, P., and Wood, W. (2002). Epithelial fusions in the embryo. *Curr Opin Cell Biol* **14,** 569-74.

Martin-Blanco, E., Gampel, A., Ring, J., Virdee, K., Kirov, N., Tolkovsky, A. M., and Martinez-Arias, A. (1998). puckered encodes a phosphatase that mediates a feedback loop regulating JNK activity during dorsal closure in Drosophila. *Genes Dev* **12,** 557-70.

McCluskey, J., and Martin, P. (1995). Analysis of the tissue movements of embryonic wound healing--DiI studies in the limb bud stage mouse embryo. *Dev Biol* **170,** 102-14.

McEwen, D. G., Cox, R. T., and Peifer, M. (2000). The canonical Wg and JNK signaling cascades collaborate to promote both dorsal closure and ventral patterning. *Development* **127,** 3607-17.

Mejillano, M. R., Kojima, S., Applewhite, D. A., Gertler, F. B., Svitkina, T. M., and Borisy, G. G. (2004). Lamellipodial versus filopodial mode of the actin nanomachinery: pivotal role of the filament barbed end. *Cell* **118,** 363-73.

Metzger, R. J., and Krasnow, M. A. (1999). Genetic control of branching morphogenesis. *Science* **284,** 1635-9.

Miki, H., Suetsugu, S., and Takenawa, T. (1998). WAVE, a novel WASP-family protein involved in actin reorganization induced by Rac. *Embo J* **17,** 6932-41.

Miki, H., Yamaguchi, H., Suetsugu, S., and Takenawa, T. (2000). IRSp53 is an essential intermediate between Rac and WAVE in the regulation of membrane ruffling. *Nature* **408,** 732-5.

Miller, J., Fraser, S. E., and McClay, D. (1995). Dynamics of thin filopodia during sea urchin gastrulation. *Development* **121,** 2501-11.

Millo, H., Leaper, K., Lazou, V., and Bownes, M. (2004). Myosin VI plays a role in cell-cell adhesion during epithelial morphogenesis. *Mech Dev* **121,** 1335-51.

Minden, A., Lin, A., Claret, F. X., Abo, A., and Karin, M. (1995). Selective activation of the JNK signaling cascade and c-Jun transcriptional activity by the small GTPases Rac and Cdc42Hs. *Cell* **81,** 1147-57.

Moon, S. Y., and Zheng, Y. (2003). Rho GTPase-activating proteins in cell regulation. *Trends Cell Biol* **13,** 13-22.

Morriss-Kay, G., and Tuckett, F. (1985). The role of microfilaments in cranial neurulation in rat embryos: effects of short-term exposure to cytochalasin D. *J Embryol Exp Morphol* **88,** 333-48.

Mullins, M. C., Rio, D. C., and Rubin, G. M. (1989). cis-acting DNA sequence requirements for P-element transposition. *Genes Dev* **3,** 729-38.

Narasimha, M., and Brown, N. H. (2004). Novel functions for integrins in epithelial morphogenesis. *Curr Biol* **14,** 381-5.

Narasimhulu, S. B., and Reddy, A. S. (1998). Characterization of microtubule binding domains in the Arabidopsis kinesin-like calmodulin binding protein. *Plant Cell* **10,** 957-65.

Nellen, D., Affolter, M., and Basler, K. (1994). Receptor serine/threonine kinases implicated in the control of Drosophila body pattern by decapentaplegic. *Cell* **78,** 225-37.

Newsome, T. P., Schmidt, S., Dietzl, G., Keleman, K., Asling, B., Debant, A., and Dickson, B. J. (2000). Trio combines with dock to regulate Pak activity during photoreceptor axon pathfinding in Drosophila. *Cell* **101,** 283-94.

Ng, J., Nardine, T., Harms, M., Tzu, J., Goldstein, A., Sun, Y., Dietzl, G., Dickson, B. J., and Luo, L. (2002). Rac GTPases control axon growth, guidance and branching. *Nature* **416,** 442-7.

Nobes, C. D., and Hall, A. (1995). Rho, rac, and cdc42 GTPases regulate the assembly of multimolecular focal complexes associated with actin stress fibers, lamellipodia, and filopodia. *Cell* **81,** 53-62.

Nolan, K. M., Barrett, K., Lu, Y., Hu, K. Q., Vincent, S., and Settleman, J. (1998). Myoblast city, the Drosophila homolog of DOCK180/CED-5, is required in a Rac signaling pathway utilized for multiple developmental processes. *Genes Dev* **12,** 3337-42.

Noselli, S. (1998). JNK signaling and morphogenesis in Drosophila. *Trends Genet* **14,** 33-8.

Noselli, S., and Agnes, F. (1999). Roles of the JNK signaling pathway in Drosophila morphogenesis. *Curr Opin Genet Dev* **9,** 466-72.

Nusslein-Volhard, C., and Wieschaus, E. (1980). Mutations affecting segment number and polarity in Drosophila. *Nature* **287,** 795-801.

Nüsslein-Volhard, C., Wieschaus, E. and Kluding, H. (1984). Mutations affecting the pattern of the larval cuticle in Drosophila melanogaster I. Zygotic loci on the second chromosome. *Roux's Arch Dev Biol* **193,** 267-282.

Oda, H., and Tsukita, S. (1999). Dynamic features of adherens junctions during Drosophila embryonic epithelial morphogenesis revealed by a Dalpha-catenin-GFP fusion protein. *Dev Genes Evol* **209,** 218-25.

Oliver, T. N., Berg, J. S., and Cheney, R. E. (1999). Tails of unconventional myosins. *Cell Mol Life Sci* **56,** 243-57.

Parkhurst, S. M., Bopp, D., and Ish-Horowicz, D. (1990). X:A ratio, the primary sex-determining signal in Drosophila, is transduced by helix-loop-helix proteins. *Cell* **63,** 1179-91.

Paunola, E., Mattila, P. K., and Lappalainen, P. (2002). WH2 domain: a small, versatile adapter for actin monomers. *FEBS Lett* **513,** 92-7.

Peng, J., Wallar, B. J., Flanders, A., Swiatek, P. J., and Alberts, A. S. (2003). Disruption of the Diaphanous-related formin Drf1 gene encoding mDia1 reveals a role for Drf3 as an effector for Cdc42. *Curr Biol* **13,** 534-45.

Penton, A., Chen, Y., Staehling-Hampton, K., Wrana, J. L., Attisano, L., Szidonya, J., Cassill, J. A., Massague, J., and Hoffmann, F. M. (1994). Identification of two bone morphogenetic protein type I receptors in Drosophila and evidence that Brk25D is a decapentaplegic receptor. *Cell* **78,** 239-50.

Pollard, T. D., and Borisy, G. G. (2003). Cellular motility driven by assembly and disassembly of actin filaments. *Cell* **112,** 453-65.

Poortinga, G., Watanabe, M., and Parkhurst, S. M. (1998). Drosophila CtBP: a Hairy-interacting protein required for embryonic segmentation and hairy-mediated transcriptional repression. *Embo J* **17,** 2067-78.

Pring, M., Weber, A., and Bubb, M. R. (1992). Profilin-actin complexes directly elongate actin filaments at the barbed end. *Biochemistry* **31,** 1827-36.

Quinlan, M. E., Heuser, J. E., Kerkhoff, E., and Mullins, R. D. (2005). Drosophila Spire is an actin nucleation factor. *Nature* **433,** 382-8.

Raftopoulou, M., and Hall, A. (2004). Cell migration: Rho GTPases lead the way. *Dev Biol* **265,** 23-32.

Raich, W. B., Agbunag, C., and Hardin, J. (1999). Rapid epithelial-sheet sealing in the Caenorhabditis elegans embryo requires cadherin-dependent filopodial priming. *Curr Biol* **9,** 1139-46.

Ramet, M., Lanot, R., Zachary, D., and Manfruelli, P. (2002). JNK signaling pathway is required for efficient wound healing in Drosophila. *Dev Biol* **241,** 145-56.

Ramirez-Weber, F. A., and Kornberg, T. B. (1999). Cytonemes: cellular processes that project to the principal signaling center in Drosophila imaginal discs. *Cell* **97,** 599-607.

Redd, M. J., Cooper, L., Wood, W., Stramer, B., and Martin, P. (2004). Wound healing and inflammation: embryos reveal the way to perfect repair. *Philos Trans R Soc Lond B Biol Sci* **359,** 777-84.

Reddy, A. S., Safadi, F., Narasimhulu, S. B., Golovkin, M., and Hu, X. (1996). A novel plant calmodulin-binding protein with a kinesin heavy chain motor domain. *J Biol Chem* **271,** 7052-60.

Reed, B. H., Wilk, R., and Lipshitz, H. D. (2001). Downregulation of Jun kinase signaling in the amnioserosa is essential for dorsal closure of the Drosophila embryo. *Curr Biol* **11,** 1098-108.

Richards, G. (1981). The radioimmune assay of ecdysteroid titres in Drosophila melanogaster. *Mol Cell Endocrinol* **21,** 181-97.

Ricos, M. G., Harden, N., Sem, K. P., Lim, L., and Chia, W. (1999). Dcdc42 acts in TGF-beta signaling during Drosophila morphogenesis: distinct roles for the Drac1/JNK and Dcdc42/TGF-beta cascades in cytoskeletal regulation. *J Cell Sci* **112 (Pt 8),** 1225-35.

Ridley, A. J., and Hall, A. (1992). The small GTP-binding protein rho regulates the assembly of focal adhesions and actin stress fibers in response to growth factors. *Cell* **70,** 389-99.

Ridley, A. J., Paterson, H. F., Johnston, C. L., Diekmann, D., and Hall, A. (1992). The small GTP-binding protein rac regulates growth factor-induced membrane ruffling. *Cell* **70,** 401-10.

Riesgo-Escovar, J. R., and Hafen, E. (1997a). Common and distinct roles of DFos and DJun during Drosophila development. *Science* **278,** 669-72.

Riesgo-Escovar, J. R., and Hafen, E. (1997b). Drosophila Jun kinase regulates expression of decapentaplegic via the ETS-domain protein Aop and the AP-1 transcription factor DJun during dorsal closure. *Genes Dev* **11,** 1717-27.

Riesgo-Escovar, J. R., Jenni, M., Fritz, A., and Hafen, E. (1996). The Drosophila Jun-N-terminal kinase is required for cell morphogenesis but not for DJun-dependent cell fate specification in the eye. *Genes Dev* **10,** 2759-68.

Ring, J. M., and Martinez Arias, A. (1993). puckered, a gene involved in position-specific cell differentiation in the dorsal epidermis of the Drosophila larva. *Dev Suppl,* 251-9.

Riveline, D., Zamir, E., Balaban, N. Q., Schwarz, U. S., Ishizaki, T., Narumiya, S., Kam, Z., Geiger, B., and Bershadsky, A. D. (2001). Focal contacts as mechanosensors: externally applied local mechanical force induces growth of focal contacts by an mDia1-dependent and ROCK-independent mechanism. *J Cell Biol* **153,** 1175-86.

Rodriguez, O. C., Schaefer, A. W., Mandato, C. A., Forscher, P., Bement, W. M., and Waterman-Storer, C. M. (2003). Conserved microtubule-actin interactions in cell movement and morphogenesis. *Nat Cell Biol* **5,** 599-609.

Rogers, S. L., Rogers, G. C., Sharp, D. J., and Vale, R. D. (2002). Drosophila EB1 is important for proper assembly, dynamics, and positioning of the mitotic spindle. *J Cell Biol* **158,** 873-84.

Rogers, S. L., Wiedemann, U., Hacker, U., Turck, C., and Vale, R. D. (2004). Drosophila RhoGEF2 associates with microtubule plus ends in an EB1-dependent manner. *Curr Biol* **14,** 1827-33.

Rogers, S. L., Wiedemann, U., Stuurman, N., and Vale, R. D. (2003). Molecular requirements for actin-based lamella formation in Drosophila S2 cells. *J Cell Biol* **162,** 1079-88.

Rohatgi, R., Ho, H. Y., and Kirschner, M. W. (2000). Mechanism of N-WASP activation by CDC42 and phosphatidylinositol 4, 5-bisphosphate. *J Cell Biol* **150,** 1299-310.

Roote, C. E., and Zusman, S. (1995). Functions for PS integrins in tissue adhesion, migration, and shape changes during early embryonic development in Drosophila. *Dev Biol* **169,** 322-36.

Rorth, P. (1998). Gal4 in the Drosophila female germline. *Mech Dev* **78,** 113-8.

Rorth, P., Szabo, K., Bailey, A., Laverty, T., Rehm, J., Rubin, G. M., Weigmann, K., Milan, M., Benes, V., Ansorge, W., and Cohen, S. M. (1998). Systematic gain-of-function genetics in Drosophila. *Development* **125,** 1049-57.

Rosenblatt, J., Peluso, P., and Mitchison, T. J. (1995). The bulk of unpolymerized actin in Xenopus egg extracts is ATP-bound. *Mol Biol Cell* **6,** 227-36.

Ruberte, E., Marty, T., Nellen, D., Affolter, M., and Basler, K. (1995). An absolute requirement for both the type II and type I receptors, punt and thick veins, for dpp signaling in vivo. *Cell* **80,** 889-97.

Rzadzinska, A. K., Schneider, M. E., Davies, C., Riordan, G. P., and Kachar, B. (2004). An actin molecular treadmill and myosins maintain stereocilia functional architecture and self-renewal. *J Cell Biol* **164,** 887-97.

Sabapathy, K., Jochum, W., Hochedlinger, K., Chang, L., Karin, M., and Wagner, E. F. (1999). Defective neural tube morphogenesis and altered apoptosis in the absence of both JNK1 and JNK2. *Mech Dev* **89,** 115-24.

Safer, D., and Nachmias, V. T. (1994). Beta thymosins as actin binding peptides. *Bioessays* **16,** 590.

Sagot, I., Klee, S. K., and Pellman, D. (2002). Yeast formins regulate cell polarity by controlling the assembly of actin cables. *Nat Cell Biol* **4,** 42-50.

Saiki, R. K., Gelfand, D. H., Stoffel, S., Scharf, S. J., Higuchi, R., Horn, G. T., Mullis, K. B., and Erlich, H. A. (1988). Primer-directed enzymatic amplification of DNA with a thermostable DNA polymerase. *Science* **239,** 487-91.

Sanders, L. C., Matsumura, F., Bokoch, G. M., and de Lanerolle, P. (1999). Inhibition of myosin light chain kinase by p21-activated kinase. *Science* **283,** 2083-5.

Satoh, S., and Tominaga, T. (2001). mDia-interacting protein acts downstream of Rho-mDia and modifies Src activation and stress fiber formation. *J Biol Chem* **276,** 39290-4.

Saxton, W. M., Hicks, J., Goldstein, L. S., and Raff, E. C. (1991). Kinesin heavy chain is essential for viability and neuromuscular functions in Drosophila, but mutants show no defects in mitosis. *Cell* **64,** 1093-102.

Schmidt, A., and Hall, A. (2002). Guanine nucleotide exchange factors for Rho GTPases: turning on the switch. *Genes Dev* **16,** 1587-609.

Scuderi, A., and Letsou, A. (2005). Amnioserosa is required for dorsal closure in Drosophila. *Dev Dyn* **233,** 249.

Self, T., Mahony, M., Fleming, J., Walsh, J., Brown, S. D., and Steel, K. P. (1998). Shaker-1 mutations reveal roles for myosin VIIA in both development and function of cochlear hair cells. *Development* **125,** 557-66.

Sells, M. A., Knaus, U. G., Bagrodia, S., Ambrose, D. M., Bokoch, G. M., and Chernoff, J. (1997). Human p21-activated kinase (Pak1) regulates actin organization in mammalian cells. *Curr Biol* **7,** 202-10.

Shah, M., Foreman, D. M., and Ferguson, M. W. (1992). Control of scarring in adult wounds by neutralising antibody to transforming growth factor beta. *Lancet* **339,** 213-4.

Shah, M., Foreman, D. M., and Ferguson, M. W. (1994). Neutralising antibody to TGF-beta 1,2 reduces cutaneous scarring in adult rodents. *J Cell Sci* **107 (Pt 5),** 1137-57.

Shah, M., Foreman, D. M., and Ferguson, M. W. (1995). Neutralisation of TGF-beta 1 and TGF-beta 2 or exogenous addition of TGF-beta 3 to cutaneous rat wounds reduces scarring. *J Cell Sci* **108 (Pt 3),** 985-1002.

Siemens, J., Lillo, C., Dumont, R. A., Reynolds, A., Williams, D. S., Gillespie, P. G., and Muller, U. (2004). Cadherin 23 is a component of the tip link in hair-cell stereocilia. *Nature* **428,** 950-5.

Sluss, H. K., and Davis, R. J. (1997). Embryonic morphogenesis signaling pathway mediated by JNK targets the transcription factor JUN and the TGF-beta homologue decapentaplegic. *J Cell Biochem* **67,** 1-12.

Sluss, H. K., Han, Z., Barrett, T., Davis, R. J., and Ip, Y. T. (1996). A JNK signal transduction pathway that mediates morphogenesis and an immune response in Drosophila. *Genes Dev* **10,** 2745-58.

Small, J. V., Isenberg, G., and Celis, J. E. (1978). Polarity of actin at the leading edge of cultured cells. *Nature* **272,** 638-9.

Snow, P. M., Bieber, A. J., and Goodman, C. S. (1989). Fasciclin III: a novel homophilic adhesion molecule in Drosophila. *Cell* **59,** 313-23.

Somogyi, K., and Rorth, P. (2004). Evidence for tension-based regulation of Drosophila MAL and SRF during invasive cell migration. *Dev Cell* **7,** 85-93.

Song, H., Golovkin, M., Reddy, A. S., and Endow, S. A. (1997). In vitro motility of AtKCBP, a calmodulin-binding kinesin protein of Arabidopsis. *Proc Natl Acad Sci U S A* **94,** 322-7.

Spradling, A. C. (1986). P element-mediated transformation. *In* "Drosophila, a Practical Approach" (D. B. Roberts, Ed.), pp. 175-97. IRL Press, Oxford.

Srinivasan, S., Wang, F., Glavas, S., Ott, A., Hofmann, F., Aktories, K., Kalman, D., and Bourne, H. R. (2003). Rac and Cdc42 play distinct roles in regulating PI(3,4,5)P3 and polarity during neutrophil chemotaxis. *J Cell Biol* **160,** 375-85.

Stark, K. A., Yee, G. H., Roote, C. E., Williams, E. L., Zusman, S., and Hynes, R. O. (1997). A novel alpha integrin subunit associates with betaPS and functions in tissue morphogenesis and movement during Drosophila development. *Development* **124,** 4583-94.

Stowers, R. S., Megeath, L. J., Gorska-Andrzejak, J., Meinertzhagen, I. A., and Schwarz, T. L. (2002). Axonal transport of mitochondria to synapses depends on milton, a novel Drosophila protein. *Neuron* **36,** 1063-77.

Stramer, B., Wood, W., Galko, M. J., Redd, M. J., Jacinto, A., Parkhurst, S. M., and Martin, P. (2005). Live imaging of wound inflammation in Drosophila embryos reveals key roles for small GTPases during in vivo cell migration. *J Cell Biol* **168,** 567-73.

Stronach, B., and Perrimon, N. (2002). Activation of the JNK pathway during dorsal closure in Drosophila requires the mixed lineage kinase, slipper. *Genes Dev* **16,** 377-87.

Strutt, D. I., Weber, U., and Mlodzik, M. (1997). The role of RhoA in tissue polarity and Frizzled signalling. *Nature* **387,** 292-5.

Svitkina, T. M., and Borisy, G. G. (1999). Arp2/3 complex and actin depolymerizing factor/cofilin in dendritic organization and treadmilling of actin filament array in lamellipodia. *J Cell Biol* **145,** 1009-26.

Svitkina, T. M., Bulanova, E. A., Chaga, O. Y., Vignjevic, D. M., Kojima, S., Vasiliev, J. M., and Borisy, G. G. (2003). Mechanism of filopodia initiation by reorganization of a dendritic network. *J Cell Biol* **160,** 409-21.

Takahashi, K., Matsuo, T., Katsube, T., Ueda, R., and Yamamoto, D. (1998). Direct binding between two PDZ domain proteins Canoe and ZO-1 and their roles in regulation of the jun N-terminal kinase pathway in Drosophila morphogenesis. *Mech Dev* **78,** 97-111.

Takenawa, T., and Miki, H. (2001). WASP and WAVE family proteins: key molecules for rapid rearrangement of cortical actin filaments and cell movement. *J Cell Sci* **114,** 1801-9.

Tautz, D., and Pfeifle, C. (1989). A non-radioactive in situ hybridization method for the localization of specific RNAs in Drosophila embryos reveals translational control of the segmentation gene hunchback. *Chromosoma* **98,** 81-5.

Taya, Y., O'Kane, S., and Ferguson, M. W. (1999). Pathogenesis of cleft palate in TGF-beta3 knockout mice. *Development* **126,** 3869-79.

Tepass, U., Fessler, L. I., Aziz, A., and Hartenstein, V. (1994). Embryonic origin of hemocytes and their relationship to cell death in Drosophila. *Development* **120,** 1829-37.

Tepass, U., Gruszynski-DeFeo, E., Haag, T. A., Omatyar, L., Torok, T., and Hartenstein, V. (1996). shotgun encodes Drosophila E-cadherin and is preferentially required during cell rearrangement in the neurectoderm and other morphogenetically active epithelia. *Genes Dev* **10,** 672-85.

Tepass, U., Tanentzapf, G., Ward, R., and Fehon, R. (2001). Epithelial cell polarity and cell junctions in Drosophila. *Annu Rev Genet* **35,** 747-84.

Tessier-Lavigne, M., and Goodman, C. S. (1996). The molecular biology of axon guidance. *Science* **274,** 1123-33.

Tokuo, H., and Ikebe, M. (2004). Myosin X transports Mena/VASP to the tip of filopodia. *Biochem Biophys Res Commun* **319,** 214-20.

Tuxworth, R. I., Weber, I., Wessels, D., Addicks, G. C., Soll, D. R., Gerisch, G., and Titus, M. A. (2001). A role for myosin VII in dynamic cell adhesion. *Curr Biol* **11,** 318-29.

Tzolovsky, G., Millo, H., Pathirana, S., Wood, T., and Bownes, M. (2002). Identification and phylogenetic analysis of Drosophila melanogaster myosins. *Mol Biol Evol* **19,** 1041-52.

Vadlamudi, R. K., Li, F., Adam, L., Nguyen, D., Ohta, Y., Stossel, T. P., and Kumar, R. (2002). Filamin is essential in actin cytoskeletal assembly mediated by p21-activated kinase 1. *Nat Cell Biol* **4,** 681-90.

Van Aelst, L., and D'Souza-Schorey, C. (1997). Rho GTPases and signaling networks. *Genes Dev* **11,** 2295-322.

Vasioukhin, V., Bauer, C., Yin, M., and Fuchs, E. (2000). Directed actin polymerization is the driving force for epithelial cell- cell adhesion. *Cell* **100,** 209-19.

Vasioukhin, V., and Fuchs, E. (2001). Actin dynamics and cell-cell adhesion in epithelia. *Curr Opin Cell Biol* **13,** 76-84.

Verkhusha, V. V., Tsukita, S., and Oda, H. (1999). Actin dynamics in lamellipodia of migrating border cells in the Drosophila ovary revealed by a GFP-actin fusion protein. *FEBS Lett* **445,** 395-401.

Vignjevic, D., Yarar, D., Welch, M. D., Peloquin, J., Svitkina, T., and Borisy, G. G. (2003). Formation of filopodia-like bundles in vitro from a dendritic network. *J Cell Biol* **160,** 951-62.

Vojtek, A. B., Hollenberg, S. M., and Cooper, J. A. (1993). Mammalian Ras interacts directly with the serine/threonine kinase Raf. *Cell* **74,** 205-14.

Weber, K. L., Sokac, A. M., Berg, J. S., Cheney, R. E., and Bement, W. M. (2004). A microtubule-binding myosin required for nuclear anchoring and spindle assembly. *Nature* **431,** 325-9.

Wei, L., Roberts, W., Wang, L., Yamada, M., Zhang, S., Zhao, Z., Rivkees, S. A., Schwartz, R. J., and Imanaka-Yoshida, K. (2001). Rho kinases play an obligatory role in vertebrate embryonic organogenesis. *Development* **128,** 2953-62.

Weigmann, K., Klapper, R., Strasser, T., Rickert, C., Technau, G., Jackle, H., Janning, W., and Klambt, C. (2003). FlyMove--a new way to look at development of Drosophila. *Trends Genet* **19,** 310-1.

Welch, H. C., Coadwell, W. J., Ellson, C. D., Ferguson, G. J., Andrews, S. R., Erdjument-Bromage, H., Tempst, P., Hawkins, P. T., and Stephens, L. R. (2002). P-Rex1, a PtdIns(3,4,5)P3- and Gbetagamma-regulated guanine-nucleotide exchange factor for Rac. *Cell* **108,** 809-21.

Wennerberg, K., and Der, C. J. (2004). Rho-family GTPases: it's not only Rac and Rho (and I like it). *J Cell Sci* **117,** 1301-12.

Werner, S., and Grose, R. (2003). Regulation of wound healing by growth factors and cytokines. *Physiol Rev* **83,** 835-70.

Whitby, D. J., and Ferguson, M. W. (1991). Immunohistochemical localization of growth factors in fetal wound healing. *Dev Biol* **147,** 207-15.

Widmann, C., Gibson, S., Jarpe, M. B., and Johnson, G. L. (1999). Mitogen-activated protein kinase: conservation of a three-kinase module from yeast to human. *Physiol Rev* **79,** 143-80.

Wieschaus, E., and Nüsslein-Volhard, C. (1986). Looking at embryos. *In* "Drosophila, a Practical Approach" (D. B. Roberts, Ed.), pp. 199-226. IRL Press, Oxford.

Wieschaus, E., Nüsslein-Volhard, C. and Jürgens, G. (1984). Mutations affecting the pattern of the larval cuticle in Drosophila melanogaster III. Zygotic loci on the X-chromosome and the fourth chromosome. *Roux's Arch Dev Biol* **193,** 296-307.

Williams-Masson, E. M., Malik, A. N., and Hardin, J. (1997). An actin-mediated two-step mechanism is required for ventral enclosure of the C. elegans hypodermis. *Development* **124,** 2889-901.

Wood, W., Jacinto, A., Grose, R., Woolner, S., Gale, J., Wilson, C., and Martin, P. (2002). Wound healing recapitulates morphogenesis in Drosophila embryos. *Nat Cell Biol* **4,** 907-12.

Ybot-Gonzalez, P., and Copp, A. J. (1999). Bending of the neural plate during mouse spinal neurulation is independent of actin microfilaments. *Dev Dyn* **215,** 273-83.

Young, P. E., Richman, A. M., Ketchum, A. S., and Kiehart, D. P. (1993). Morphogenesis in Drosophila requires nonmuscle myosin heavy chain function. *Genes Dev* **7,** 29-41.

Zebda, N., Bernard, O., Bailly, M., Welti, S., Lawrence, D. S., and Condeelis, J. S. (2000). Phosphorylation of ADF/cofilin abolishes EGF-induced actin nucleation at the leading edge and subsequent lamellipod extension. *J Cell Biol* **151,** 1119-28.

Zecchini, V., Brennan, K., and Martinez-Arias, A. (1999). An activity of Notch regulates JNK signalling and affects dorsal closure in Drosophila. *Curr Biol* **9,** 460-9.

Zeitlinger, J., Kockel, L., Peverali, F. A., Jackson, D. B., Mlodzik, M., and Bohmann, D. (1997). Defective dorsal closure and loss of epidermal decapentaplegic expression in Drosophila fos mutants. *Embo J* **16,** 7393-401.

Zenz, R., Scheuch, H., Martin, P., Frank, C., Eferl, R., Kenner, L., Sibilia, M., and Wagner, E. F. (2003). c-Jun regulates eyelid closure and skin tumor development through EGFR signaling. *Dev Cell* **4,** 879-89.

Zhang, H., Berg, J. S., Li, Z., Wang, Y., Lang, P., Sousa, A. D., Bhaskar, A., Cheney, R. E., and Stromblad, S. (2004). Myosin-X provides a motor-based link between integrins and the cytoskeleton. *Nat Cell Biol* **6,** 523-31.

Zheng, Y. (2001). Dbl family guanine nucleotide exchange factors. *Trends Biochem Sci* **26,** 724-32.

Zigmond, S. H., Evangelista, M., Boone, C., Yang, C., Dar, A. C., Sicheri, F., Forkey, J., and Pring, M. (2003). Formin leaky cap allows elongation in the presence of tight capping proteins. *Curr Biol* **13,** 1820-3.

Appendix

Movie Legends

Movie 1: Cell shape changes in the amnioserosa and epithelium characterise early dorsal closure

α-catenin-GFP expression is driven in the amnioserosa and epithelium using the *e22c-GAL4* driver. The embryo shown was just completing germ-band retraction as imaging was started. The movie shows a portion of the amnioserosa (top 70% of first frame) and epithelium (bottom 30% of first frame), with dorsal at the top of the picture. The large amnioserosa cells can be seen to shrink during the movie, whilst the cells of the epithelium elongate along their dorso-ventral axis. Together these cell shape changes help the epithelium to advance dorsally. During the course of the movie, the epithelial leading edge also resolves from a scalloped, disorganised edge to a taut surface.

Movie 2: Amnioserosa cell contraction in a wild type embryo

The *e22c-GAL4* driver is used to express α-catenin-GFP in the epithelium and amnioserosa of a wild type embryo. The amnioserosa cells contract during dorsal closure, pulling the two epithelial edges towards each other. Fully contracted cells are either extruded from the amnioserosal layer or disappear under the advancing epithelial edge.

Movie 3: Final zippering of wild type epithelium

GFP-actin is expressed in the epithelium using the *e22c-GAL4* driver. This movie shows the very final zippering events in a wild type embryo. Early in the movie the epithelium is brought together at the zipping canthi, just as occurs through the majority of dorsal closure. However, as the last epithelial cells approach the midline the leading edges are close enough in the centre of the hole to interact and close the epithelium.

Movie 4: Actin dynamics during dorsal closure in a wild type embryo

GFP-actin is expressed using *engrailed-GAL4* to visualise actin dynamics during dorsal closure in a wild type embryo. Movies such as this one were used to quantify wild type actin protrusion dynamics, as described in Chapter 3. During dorsal closure actin protrusions are formed by leading edge cells, with protrusion area increasing gradually as closure proceeds. The actin protrusions act to knit the two epithelial surfaces together, from zipping canthi at each end of the hole, and help the embryo to maintain segmental alignment as the hole closes.

Movie 5: Expression of constitutively active *Rac1* (*Rac1*^{V12}) induces the assembly of overly large lamellipodia

Rac1^{V12} is co-expressed in the embryonic epithelium along with GFP-actin using the *engrailed* driver. The *Rac1*^{V12} expressing cells assemble excessively large lamellipodia at the leading edge even from the very earliest stages of dorsal closure. The mutant cells are unrestrained, interacting with adjacent neighbours and eventually taking over portions of the leading edge.

Movie 6: Leading edge cells expressing dominant negative *Rac1* (*Rac1*^{N17}) assemble only the most cursory protrusions.

Rac1^{N17} expression is driven along with GFP-actin using the *engrailed-GAL4* driver. Leading edge cells expressing *Rac1*^{N17} fail to assemble wild type actin protrusions, forming only the most rudimentary protrusions. These embryos do eventually close but show segmental mismatching and small gaps at the midline.

Movie 7: Amnioserosal contraction in zygotic triple *Rac* mutants is delayed but does ultimately occur at a similar rate to wild type.

Expression of α-catenin-GFP is driven by *e22c-GAL4* in a $Rac1^{J11}$ *Rac2Δ mtlΔ* mutant. At the beginning of the movie there are large cells present in the amnioserosa. However, these cells are capable of contraction and do contract fully until they are extruded or disappear under the advancing leading edge.

Movie 8: Zygotic triple *Rac* mutants show a failure to assemble actin cable and protrusions in discrete stretches along the leading edge but are still able to close by continued amnioserosal contraction and the formation of new zipper fronts

Concurrent GFP-actin movies of a wild type embryo and a $Rac1^{J10}$ *Rac2Δ mtlΔ* mutant embryo, taken at the same magnification. The wild type embryo exhibits the characteristic eye-shaped dorsal hole that reduces in size as the epithelial edges are drawn together at zipping canthi at the anterior and posterior ends of the hole. In contrast, the $Rac1^{J10}$ *Rac2Δ mtlΔ* embryo has a long, thin, slit-shaped hole and possesses regions along the leading edge which fail to assemble either actin cable or protrusions. These actin-deficient stretches are bypassed, and the hole closed, by continued contraction of the amnioserosa and the formation of secondary zipping canthi.

Movie 9: Expression of a *Myo10A* RNAi snapback construct results in segmental mismatching during dorsal closure

The *Myo10A* RNAi snapback is co-expressed with GFP-actin using the *engrailed-GAL4* driver. For the majority of the process dorsal closure proceeds quite normally, but in the final stages, leading edge snapback expressing cells begin to interact and fuse with incorrect segmental partners, resulting in mismatched segments in the central region of the midline seam.

Movie 10: *Myo10A* RNAi snapback expressing cells extend excessively long protrusions

The *Myo10A* RNAi snapback is again co-expressed with GFP-actin in *engrailed* epithelial cells. Overly long filopodia are formed by the snapback expressing cells, in particular, observe the protrusions formed by cells of the top centre *engrailed* stripe in this movie. These long filopodia appear to persist for longer at their maximum length before retracting rapidly. The formation of these protrusions is also accompanied by segmental mismatch as the two epithelial surfaces come together. To allow for closer examination of the actin protrusions assembled in this embryo, the movie plays at almost half the speed of all other movies shown here.